Technische Universität München
TUM School of Life Sciences

TUM

Cancer-induced metabolic reprogramming dampens T cell function and contributes to wasting in cachexia

Julia Geppert

Vollständiger Abdruck der von der TUM School of Life Sciences der Technischen Universität München zur Erlangung einer

Doktorin der Naturwissenschaften (Dr. rer. nat.)

genehmigten Dissertation.

Vorsitz: Prof. Dr. Johann J. Hauner

Prüfer*innen der Dissertation:

     1.   Prof. Angelika Schnieke, Ph.D.

     2.   Prof. Dr. Stephan Herzig

     3.   Prof. Dr. Andreas Fischer

Die Dissertation wurde am 31.05.2022 bei der Technischen Universität München eingereicht und durch die TUM School of Life Sciences am 17.10.2022 angenommen.

>> Man muss das Unmögliche versuchen,
um das Mögliche zu erreichen. <<

Hermann Hesse

Abstract

Cancer cachexia is a multifactorial wasting disorder, accompanied by drastic weight loss and poor overall survival. Many of the negative effects mediated by cancer cachexia can be attributed to systemic inflammation, one of its most prominent hallmarks, with a strong rise of cytokines. However, therapeutic approaches, aiming to block these cytokines, were not or only in part able to improve cancer-associated tissue wasting. Hence, to date there is no efficient routine therapy available to counteract cachexia. Yet, chronic systemic inflammation as well as high glucocorticoid levels – as present in cachectic mice and patients – have previously been linked to compromised immune cell function. In line, a recent report has identified strong correlations between the numbers of specific immune cell subsets in the circulation and muscle strength in gastrointestinal cancer patients. Moreover, cancer cachexia was associated with a reduced efficacy of immune checkpoint inhibitors in cancer patients. However, the interplay between the immune system and cancer cachexia has still not been investigated in depth.

T cells are important mediators of anti-tumor immunity, as they secrete a variety of cytokines and effector molecules to fight tumor progression; yet, their specific role for cancer cachexia is not clear to date. Here I show that cachexia is associated with T cell lymphopenia – depletion of T cells from peripheral tissues, circulation and tumor – impaired T cell metabolism, reduced activation and dampened expression of T cell effector cytokines. Consequently, cytokine secretion from T cells did not contribute to the general inflammatory phenotype typically observed in cancer cachexia. Contrary, CD8+ T cell depletion from C26 tumor-bearing mice accelerated cachexia without affecting tumor size, implying that T cells act as systemic metabolic regulators.

Aging was shown to potentiate cachexia outcome in C57BL/6 mice, while it did not affect cachexia progression in BALB/c mice. Accelerated cachexia development in aged LLC tumor-bearing mice was associated with impaired *Il2* expression in T cells, indicating impaired proliferation and functionality of these cells, potentially worsening cachexia outcome.

Potential mechanisms mediating T cell repression in cachexia that were investigated in this thesis included elevated glucocorticoid signaling, central and local glucose deprivation and alterations of the cachectic plasma lipidome. Global transcriptional profiling highlighted and linked glucocorticoid signaling and glucose depletion to marked defects in T cell functionality. Strikingly, absence of T cell-intrinsic glucocorticoid signaling attenuated body weight and markedly improved T cell effector cytokine expression in pre-cachectic T cell-specific glucocorticoid receptor knockout *versus* control mice, strengthening the promising approach to improve T cell functionality and thereby prevent cachexia.

In this thesis the link between T cells and cachexia was investigated in depth, with the ultimate aim to identify novel regulators in cachectic T cells that can be manipulated to prevent T cell deterioration, and hence improve cancer-associated wasting.

Zusammenfassung

Krebskachexie ist eine multifaktorielle Auszehrungskrankheit, die mit einem drastischen Gewichtsverlust sowie einer schlechten Überlebensrate verbunden ist. Systemische Entzündung ist die Ursache vieler negativer Bestandteile der Krebskachexie, verbunden mit einem starken Anstieg verschiedener Zytokine. Therapeutische Ansätze, mit dem Ziel diese Zytokine zu inhibieren, waren leider nicht oder nur teilweise in der Lage, den krebsbedingten Gewebeschwund zu verbessern. Daher gibt es bis heute keine wirksame Routinetherapie zur Bekämpfung von Krebskachexie. Die für kachektische Mäuse und Patienten typische chronische systemische Entzündung, sowie hohe Glukokortikoidspiegel wurden bereits mit einer beeinträchtigten Funktion der Immunzellen in Verbindung gebracht. So wurde in einer kürzlich durchgeführten Studie ein starker Zusammenhang zwischen der Anzahl bestimmter Untergruppen von Immunzellen im Blutkreislauf und der Muskelkraft von Patienten mit Magen-Darm-Krebs festgestellt. Darüber hinaus wurde Krebskachexie mit einer verminderten Wirksamkeit von Immun-Checkpoint-Inhibitoren bei Krebspatienten in Verbindung gebracht. Nichtsdestotrotz gibt es bisher keine Studien, die den Zusammenhang des Immunsystems, speziell T-Zellen und Krebskachexie genauer untersucht haben.

T-Zellen sind wichtige Vermittler der Anti-Tumor-Immunität, da sie eine Vielzahl von Zytokinen und Effektormolekülen absondern, um das Fortschreiten des Tumors zu bekämpfen; doch ihre spezifische Rolle in der Kachexie ist bisher noch nicht klar. Diese Arbeit zeigt, dass Kachexie mit einer Lymphopenie der T-Zellen einhergeht, d. h. mit einer Verarmung der T-Zellen im peripheren Gewebe, im Blutkreislauf und im Tumor, sowie mit einer Verringerung des T-Zell-Stoffwechsels, der T-Zell-Aktivierung, und der Expression von T-Zell-Effektorzytokinen. Folglich hat die Zytokinsekretion von T-Zellen nicht zu dem entzündlichen Phänotyp beigetragen, der typischerweise bei Krebskachexie beobachtet wird. Im Gegensatz dazu beschleunigte die Depletion von CD8$^+$ T-Zellen aus C26 Tumor-Mäusen die Kachexie ohne Beeinflussung der Tumorgröße, was darauf hindeutet, dass T-Zellen als systemische Stoffwechselregulatoren wirken.

Hohes Alter beschleunigte die Kachexieentwicklung bei C57BL/6-Mäusen, während es keinen Einfluss in BALB/c-Mäusen hatte. Das beschleunigte Fortschreiten der Kachexie bei gealterten Mäusen, die einen LLC-Tumor trugen, wurde mit einer verminderten *Il2*-Expression in T-Zellen assoziiert, was auf eine geringere Proliferation und Funktionalität dieser Zellen hindeutet, und damit verbunden eventuell zur Verschlechterung von Kachexie beigetragen hat.

Zu den in dieser Arbeit untersuchten potenziellen Mechanismen, die die allgemeine Unterdrückung der T-Zellen bei Kachexie vermitteln, gehören erhöhte Glukokortikoid-Signale, zentraler und lokaler Glukoseentzug und Veränderungen des kachektischen Plasmalipidoms. Untersuchungen des globalen T-Zell-Transkriptoms haben Glukokortikoide sowie Glukose-Entzug in Zusammenhang mit deutlichen Defekten in der T-Zell-Funktionalität gebracht. In T-Zell-spezifischen Glukokortikoid-Knockout Mäusen konnte ich einen vielversprechenden Trend zu einer Verringerung des Körpergewichts und einer deutlichen Verbesserung der T-Zell-Effektorzytokinexpression bei Knockout-Mäusen im Vergleich zu Kontrollmäusen feststellen. Diese Ergebnisse stärken den vielversprechenden Ansatz, dass die Verbesserung der T-Zell Funktionalität mit der Verhinderung der Kachexie einhergehen kann.

In dieser Arbeit wurde der Zusammenhang zwischen T-Zellen und Kachexie eingehend untersucht, mit dem letztendlichen Ziel, neue Regulatoren in T-Zellen zu identifizieren, die zur Verhinderung der T-Zell-Dysfunktion eingesetzt werden können und damit verbunden zur Verbesserung von Krebskachexie.

1 INTRODUCTION

1.1 Cancer Cachexia

1.1.1 Epidemiology, Definition and Pathophysiology

Epidemiology - According to the International Agency for Research on Cancer, 19.3 million people worldwide were diagnosed with cancer in 2020 (Sung, 2021), with an especially high incidence in Europe, North America and Australia (Figure 1). About 50-80% of these cancer patients will develop a syndrome called cancer cachexia (Argiles, 2014), an underestimated comorbidity of many cancers, which has been previously linked to induce about 30% of all cancer-related deaths (von Haehling, 2010). Moreover, 50% of the remaining patients will die while simultaneously suffering from cachexia (von Haehling, 2010). The risk to develop cachexia is linked to the occurring tumor type: patients with pancreatic or gastric cancer have the highest incidence to develop cachexia with more than 80%, while around 50% of patients with lung, prostate or colon cancer are affected, and patients with breast tumors or leukemias show an incidence of approximately 40% (Dewys, 1980; Teunissen, 2007). Unfortunately, cancer cachexia incidence will likely increase in the future, as the world population is aging (Kanasi, 2016), and in line also cancer incidence will rise. For instance in the United States, cancer incidence between 2010 and 2030 in the elderly (> 65 years) is estimated to increase by 67% (Smith, 2009). Importantly, we have recently shown that aging affects cachexia-associated correlations of cytokines and bodyweight loss, underlining the importance of taking age into account when examining cancer patients and cachexia onset (Geppert, 2021). Unfortunately, systematic studies investigating cachexia development in the elderly are still limited to date.
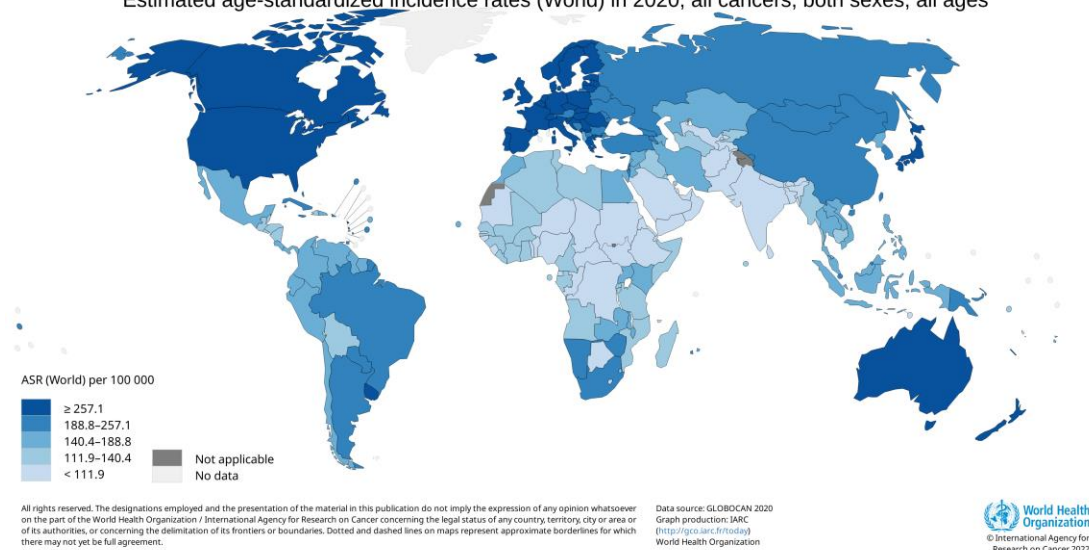
Figure 1. High cancer incidence as worldwide problem. Global distribution of cancer incidence per 100.000 individuals (age-standardized rate, ASR). From: Cancer Today, International Agency for Research on Cancer, WHO 2021.

Definition – The first mentioning of cachexia was already 400 years B.C. by Hippocrates who observed strong weight loss in combination with poor survival of patients (Katz, 1962). The term cachexia is led back to the Greek words "kakós" (bad) and "hexis" (condition), describing the overall severe condition of a patient. One of the first scientists linking the word cachexia to a chronic illness, was John Zachariah Laurence in 1855 by using the term "cancerous cachexia" (Laurence, 1855). However, it took another 150 years until the term "cancer-associated cachexia" was formally defined in 2011 in an International Consensus Statement, being approved by experts on the field of sarcopenia, cachexia and wasting disorders (SCWD) (K. Fearon, 2011). Thereby, cachexia was defined as "multifactorial

syndrome characterised by an ongoing loss of skeletal muscle mass (with or without loss of fat mass) that cannot be fully reversed by conventional nutritional support and leads to progressive functional impairment" (K. Fearon, 2011). Moreover, cancer patients were defined to be cachectic upon: 1) more than 5% weight loss over the past 6 months, 2) a BMI <20 kg/m^2 and proceeding weight loss >2%, or 3) sarcopenia and any degree of weight loss >2%. Patients with very mild weight loss up to 5% in combination with beginning anorexia and metabolic changes are staged as pre-cachectic, while disease progression ultimately leads to refractory cachexia with non-responsive anti-cancer treatment and a very low life expectancy (<3 months) (K. Fearon, 2011). Based on the global rise in bodyweight, in line with an increasing BMI of the elderly, the European Society of Clinical Nutrition and Metabolism (ESPEN) suggested a higher BMI cut-off value of 22 kg/m^2 in older individuals compared to 20 kg/m^2 in younger ones (Cederholm, 2015). Importantly, cachexia not only accompanies cancer evolvement, but also other chronic diseases such as acquired immune deficiency syndrome (Von Roenn, 1992), chronic obstructive pulmonary disease (Di Francia, 1994), chronic kidney disease (Cheung, 2010) and heart failure (Clark, 2017; Katz, 1962).

Pathophysiology – Cachexia is a multifactorial energy-wasting disorder leading to unintentional body weight loss, mostly reflecting adipose tissue and skeletal muscle wasting. Cancer cachexia development is accompanied and mediated by drastic systemic changes in the patient, which include chronic systemic inflammation (i.e. increased levels of Interleukin (IL) 6 or IL1β), anorexia, anemia, inhibition of anabolic pathways (Evans, 2008), as well as abnormal protein (Jeevanandam, 1984) and lipid metabolism (Morigny&Zuber, 2020; Rohm, 2016). Anorexia is a classical feature of cachexia, but nutritional approaches cannot fully reverse the strong imbalance between energy intake and expenditure in cachexia as metabolic dysfunction dominates the syndrome. Further important characteristics of cancer cachexia are proteolysis in cardiac and skeletal muscles, adipose tissue lipolysis, as well as futile energy wasting cycles within and between tissues (Rohm, 2019; Schmidt, 2018). All of the aforementioned effects are mediated by a complex multi-organ interplay, ultimately leading to a severe decrease in the patients' quality of life with individuals developing drastic weakness and fatigue. Additionally, cachexia implies a poor prognosis for the patient as it reduces the responsiveness and tolerance to anti-cancer therapies (Dewys, 1980; Miyawaki, 2020), thereby shortening overall survival (Tisdale, 2002).

1.1.2   Multi-organ interplay and mediators of cancer cachexia

Cancer cachexia onset and progression involve the interplay of several factors being responsible for the induction of drastic metabolic changes. Already in the beginnings of cachexia research, anorexia as sole cause for body wasting of cancer patients was refuted (Costa G, 1980). In line, it is not possible to fully reverse the cachexia-induced body composition changes by conventional nutritional support. Moreover, tumor burden is in most cases smaller than 1% of body mass, even upon enhanced cachexia; hence, an increased metabolic demand of tumors can also not explain the drastic energy disbalance observed in cachectic patients (K. C. Fearon, 2012).

Mediators – To date, it is known that cancer cachexia is arbitrated not only by tumor-derived but also by tumor-induced and subsequently host-derived humoral mediators, altogether they are termed cachexokines (K. C. Fearon, 2012; Norton, 1985). With respect to these cachexokines, inflammatory cytokines have gained lots of attention as classical markers and drivers of the disease (K. C. Fearon,

2012). These include interferon gamma (IFNγ) (Matthys, 1991), IL6 which is primarily secreted by the tumor (Rupert, 2021; Strassmann, 1992), tumor necrosis factor alpha (TNFα) (Oliff, 1987; Tracey, 1988), and IL1β (Strassmann, 1993). Indeed, the latter two mediators were initially named "cachectin" (TNFα) and "catabolin" (IL1β) due to their pronounced catabolic features. Despite their prominent role in cachexia progression, single or combinatorial antibody therapies targeting these inflammatory mediators, have not been successful to fully reverse body wasting in patients (Prado, 2019). Hence, further studies were initiated with the aim to identify novel regulators of cachexia that could be targeted to improve disease outcome. In this context, recent studies identified lipids as potentially harmful regulators of cancer cachexia (Morigny&Zuber, 2020; Riccardi, 2020).

The failure to establish functional routine therapies aiming to counteract cachexia, is likely dependent on the complex interplay of the disease. Hence, not only pro-inflammatory cytokines were found to be prominent mediators of wasting, but also additional humoral factors, secreted by the tumor have been identified as potent inducers of wasting. In this context, tumor-derived cachexokines that have been observed include lipid-mobilizing factor (LMF), also termed zinc-alpha-2-glycoprotein (ZAG) (Bing, 2004; Hirai, 1998; Hirai, 1997), parathyroid hormone-related protein (PTHrP) (Kir, 2016; Kir, 2014), proteolysis-inducing factor (PIF) (Lorite, 1998; Todorov, 1999), and secreted insulin/IGF antagonist (ImpL2) (Figueroa-Clarevega, 2015).

Overall, tumor-and host-derived molecules were shown to induce a cascade of detrimental effects on a variety of tissues (Figure 2), including adipose tissue, skeletal muscle, liver, brain, and the immune system.
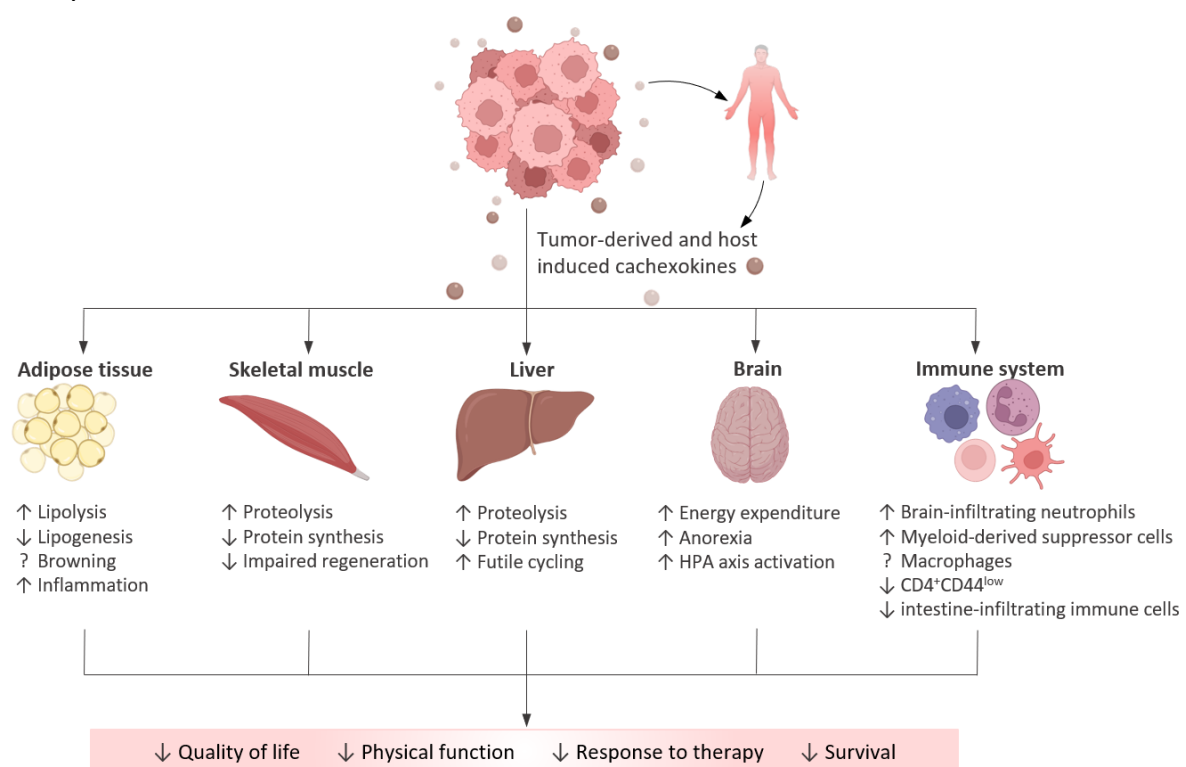
Figure 2. Tumor-derived and host-induced cachexokines induce detrimental effects on multiple tissues, leading to worsened disease outcome. Scheme adapted from (Schmidt, 2018). Created with BioRender.com.

Adipose Tissue – White adipose tissue (WAT) mainly consists of large spherical adipocytes, which are the major depot for triacylglycerol (TAG) storage, while keeping a dynamic homeostasis to balance lipolysis and lipogenesis (Klaus, 2004). In general, lipolysis is a consecutive process to hydrolyze triglycerides into free fatty acids (FFAs) and glycerol, followed by their secretion into the circulation.

Lipolysis is coordinated by three lipases: adipose triglyceride lipase (ATGL), hormone sensitive lipase (HSL) and monoglyceride lipase (MGL).

Wasting of adipose tissue is one of the most prominent hallmarks of cancer cachexia, generally preceding skeletal muscle wasting (Agustsson, 2007). Hereby, adipose tissue loss is predominantly driven by a combination of elevated lipolysis (Agustsson, 2007; Rydén, 2008) and inhibited lipogenesis (Tsoli, 2014), thereby dysregulating their functional balance, ultimately leading to lipid loss and a rise in resting energy expenditure (REE). Importantly, this event happens independently of malnutrition (Zuijdgeest-van Leeuwen, 2000). Lipolytic factors, such as IL6 (J. Han, 2018), LMF (Bing, 2004), or TNFα (Oliff, 1987) are important inducers of cachexia-associated lipolysis. For example, HSL was reported to be activated through the LMF-mediated induction of cyclic AMP (adenosine monophosphate), either derived from the tumor or induced by glucocorticoids (Russell, 2005; Tisdale, 1991; Todorov, 1998). Accordingly, elevated HSL activity and a rise in free fatty acids and glycerol has been noted in cachectic patients (Agustsson, 2007; Thompson, 1993). Also ATGL, which catalyzes the rate-limiting step of lipolysis, was shown to be induced by cancer cachexia (Das, 2011), while *Mgl* expression was reported to be unaltered (Geppert, 2021). In mice, knockout of HSL or ATGL partially prevented cancer-associated wasting (Das, 2011). Contrary to lipolysis, lipogenesis was reported to be reduced in adipocytes upon cachexia (Ishiko, 1999), as TNFα and IL6 were shown to hamper lipogenesis by mediating inhibition of the lipogenic enzyme lipoprotein lipase (LPL), subsequently leading to reduced lipid storage (Fried, 1989; Greenberg, 1992).

To date, the occurrence of WAT browning is still controversially discussed in the cachexia field. Kir and colleagues have shown that tumor-derived PTHrP stimulates *Ucp1* (Uncoupling protein 1) gene expression in white adipose tissue, which leads to a direct elevation of thermogenesis and REE, thereby contributing to tissue catabolism (Kir, 2014). A recent study demonstrated that the potential of PTHrP to induce browning is not mediated by direct stimulation of thermogenic gene expression but indirectly through the activation of immune cells, leading to elevated sympathetic activity, catecholamine synthesis and finally browning of white adipose tissue (Xie, 2022). Besides PTHrP, also micro RNAs and pro-inflammatory cytokines were observed to promote browning of white adipocytes upon cachexia (Di, 2021; J. Han, 2018). Nevertheless, Rohm *et al.* (Rohm, 2016) and others (Anderson, 2022; Michaelis, 2017) demonstrated that UCP1-mediated thermogenesis and increased REE in cachectic mice might be less pivotal than expected with respect to previous studies (Kir, 2014; Petruzzelli, 2014). In line, UCP1 knockout mice are neither protected from adipose tissue loss nor cachexia development, questioning the contribution of WAT browning to cancer-associated wasting (Rohm, 2016).

Skeletal Muscle – Cancer-induced wasting of muscle tissue is one of the most drastic and important hallmarks of cachexia and is known to be mediated by several distinct mechanisms. For instance, cachexia induces a futile energy-wasting cycle by elevating muscle proteolysis and amino acid secretion with the aim to support liver gluconeogenesis and tumor protein synthesis (Argilés, 2016; Argilés, 1991). Use of amino acids for energy production and subsequent elimination of nitrogen as a waste product of this process, is of very low efficiency, and hence likely to contribute to energy wasting in cachectic muscle (Friesen, 2015). However, the induction of energy-consuming futile cycles is likely to contribute to only a small extent of total muscle wasting that is observed upon cachexia. Instead, cancer-induced muscle atrophy is mediated by a repression of protein synthesis in combination with elevated protein breakdown. These effects are mediated by the interplay of two

major pathways, namely ubiquitin-mediated proteasome degradation (UPR) (L. Zhang, 2013) and autophagy (Penna, 2013).

Several factors were noted to induce a strong upregulation of the UPR system upon cancer cachexia, including PIF (Lorite, 1998), NFκB (nuclear factor 'kappa-light-chain-enhancer' of activated B-cells) (Cai, 2004; Wysong, 2011) and TNFα (Reid, 2001). Two E3-ligases were identified to be the essential drivers of muscle atrophy-related proteolysis, namely muscle RING finger 1 (MuRF1) and muscle atrophy F box (MAFbx, also termed Atrogin1). Both of them were shown to be drastically upregulated in all settings of muscle wasting and consequently also in several mouse models of cancer cachexia (Bodine, 2001; Geppert, 2021; Gomes, 2001; Lecker, 2004). Forkhead-box O (FoxO) transcription factors, which are controlled by the phosphatidylinositol 3 kinase (PI3K)/AKT pathway, regulate the expression of MuRF1 and Atrogin1 (Stitt, 2004). Importantly, lack of MuRF1 (Bodine, 2001) and Atrogin1 (Cong, 2011) partially prevents mice from developing denervation- and fasting-induced muscle wasting, respectively. Moreover, small-molecule chemical knockdown of MuRF1 improved muscle atrophy and dysfunction in cachectic mice (Adams, 2020).

Additionally, autophagy, which induces the recycling of intracellular components to maintain mitochondrial metabolic function and energy homeostasis, was noted to be involved in cancer-induced muscle wasting. In this context, it has been shown that autophagy plays an important role in several experimental models of cachexia, including APC$^{Min/+}$ (White, 2011), LLC (Lewis Lung Carcinoma) and C26 (Colon26) tumor-bearing mice (Penna, 2013). Moreover, the expression of autophagy markers in skeletal muscle was observed to be increased in cachectic patients suffering from different cancer types including pancreatic, gastric and esophageal cancer (Aversa, 2016; Stephens, 2015; Tardif, 2013).

Also excessive muscle fatty acid oxidation (FAO) has been shown to be involved in muscle atrophy in an experimental mouse model of kidney cancer (Fukawa, 2016). Fukawa *et al.* observed that cachectic kidney cancer cells secrete a cocktail of inflammatory factors, thereby inducing FAO in combination with an activation of the p38 MAPK stress-response signature in muscle. Interestingly, pharmacological blockage of FAO was able to protect mice from kidney cancer-induced muscle atrophy *in vitro* and *in vivo* (Fukawa, 2016).

Overall, cancer-associated muscle wasting is mediated by distinct mechanisms, of which the upregulation of the UPR system and autophagy are the most important.

Liver – High levels of pro-inflammatory cytokines such as IL6 and TNFα were noted to induce the production of acute phase proteins (APPs) by the liver and have previously been linked to decreased survival in cachectic pancreatic cancer patients. The liver-dependent production of these APPs is associated with the mobilization of amino acids from the periphery with skeletal muscles being the primary amino acid source, a process most likely contributing to muscle wasting upon cachexia (Moses, 2009). Additionally, upon cachexia the secretion of very low-density lipoproteins from the liver is inhibited by increased TSC22D4 (TSC22 domain family member 4) levels (Jones, 2013), subsequently leading to an accretion of lipids in the liver, promoting steatosis (Berriel Diaz, 2008). A main contributor to the negative energy balance in cancer cachexia is the liver-associated rise of futile cycles, being substrate cycles that misspend energy without anabolic or catabolic function. In cachexia, extensive amounts of lactate are produced by the tumor and are subsequently reconverted to glucose through hepatic gluconeogenesis in the highly energy-demanding cori cycle, thereby wasting a large proportion of energy (Friesen, 2015). Moreover, we recently observed increased

expression of enzymes involved in ceramide synthesis and degradation in cachectic livers of several cachexia mouse models, indicating an additional futile cycle contributing to cancer-associated energy wasting (Morigny&Zuber, 2020).

Brain – Contrary to mice, end-stage cancer patients are often affected by anorexia, mediated by several factors including TNFα, GDF15 (Growth differentiation factor 15), Lipocalin 2 and insulin-like 3 peptide (Olson, 2021). In this context, orexigenic hormones, such as ghrelin or neuropeptide Y (NPY) were observed to have appetite-stimulating characteristics, while anorexigenic neuropeptides like insulin, leptin, or glucagon-like peptide 1 were shown to inhibit food intake (Moran, 2011). Cachexia leads to the dysregulation of these hormones, thereby contributing to reduced food intake but also elevated energy expenditure. Importantly, high ghrelin levels in cachectic patients failed to induce orexigenic properties, implying the development of ghrelin resistance upon cachexia (Garcia, 2005). Altogether, abnormal hormonal signaling upon cachexia leads to anorexia and energy wasting.

The hypothalamic-pituitary-adrenal (HPA) axis is activated by many stressors that are also associated with cachexia, such as undernutrition, injury, or fear. Indeed, a recent report has also linked the activation of the HPA axis in cachectic animals to the well-known rise of glucocorticoids (GCs) (Martin, 2022). However, in their study, Martin *et al.* did not investigate the upstream activators that mediate HPA axis activation, although it is quite likely that increased cachexia-induced systemic inflammation might initiate the synthesis of corticotropin releasing hormone (CRH), which is the key regulator of the HPA axis in the hypothalamus (Besedovsky, 1991). GCs are secreted as systemic effector hormones from the adrenal cortex in response to stress. They are potent drivers of skeletal muscle catabolism, and in line exogenous GC supplementation was shown to drive muscle wasting (Braun, 2011). Importantly, absence of GCs or lack of the glucocorticoid receptor (GR) in muscle, inhibited cancer-induced muscle wasting (Braun, 2013).

Immune System – Chronic systemic inflammation as well as GCs have previously been shown to weaken the immune system (Cope, 2002; Elftman, 2007); thus, it is very likely that both of them also mediate immunologic repression upon cancer cachexia. However, despite this obvious connection, only a very limited number of studies has investigated the impact of cachexia development on the immune system to date. Hereby, both innate and adaptive immunity were linked to cachexia onset.
Innate Immunity – Burfeind *et al*. have recently identified elevated infiltration of neutrophils into brains of cachectic mice, targeting specific brain regions that are connected to feeding behavior and energy metabolism (Burfeind, 2020). Trafficking of those neutrophils to the brain was dependent on the expression of CCR2 (C-C motif chemokine receptor 2), and lack of CCR2 by pharmacological and genetic means prevented neutrophil recruitment to the brain and attenuated anorexia and muscle catabolism. In addition to neutrophils, also the occurrence of macrophages was linked to cancer-induced wasting in multiple tissues. Shuka *et al.* have observed a negative correlation between the amount of infiltrating macrophages and muscle-fiber cross sectional area in human PDAC patients (Shukla, 2020), and macrophage depletion in pancreatic tumor-bearing mice enhanced systemic inflammation and muscle wasting (Shukla, 2020). Moreover, a strong increase in the amount of CD68 immunoreactive macrophages has been observed in livers of cachectic pancreatic cancer patients, which was inversely correlated with weight loss, (Martignoni, 2009). Contrary to the aforementioned studies, defective myeloid cell activation in a hepatocellular carcinoma model of cachexia, was associated with reduced macrophage abundance in visceral adipose tissue but unexpectedly also

increased adipose tissue depletion (Erdem, 2019). In line, also Inaba and colleagues have observed a decline in muscle injury-induced infiltration of macrophages but also neutrophils and mesenchymal progenitors in cachectic C26 tumor-bearing mice (Inaba, 2018). In addition, myeloid-derived suppressor cells (MDSCs) are found in large numbers in tumors of several cachexia mouse models (Cuenca, 2014) and of gastric and pancreatic cancer patients (Khaled, 2014; Ohki, 2012), performing their strong immunosuppressive functions (Gabrilovich, 2009). In these different mouse models (4T1, LLC and C26), MDSC expansion was linked to an altered fat metabolism and the induction of the hepatic acute phase protein response (APPR), while a 4T1 subclone, which does not exhibit increased MDSC infiltration, did not induce elevated APPR (Cuenca, 2014). However, the direct link between cachexia development and MDSCs has not been proven yet, although the aforementioned study implies that tumor-infiltrating MDSCs play an important role.

Adaptive Immunity – The role of T cells in the context of oncology has been extensively studied, but whether or how they are influenced by cachexia development remains elusive to date. Immune checkpoint inhibitory therapy was noted to be less efficient in a cohort of cachectic patients with non-small cell lung carcinoma (Miyawaki, 2020), and muscle biopsies of cancer patients showed a strong positive correlation between muscle-infiltrating T cells and skeletal muscle mass (Anoveros-Barrera, 2019). Together these studies underline a possible connection of T cells and cancer-associated wasting. Additionally, Narsale *et al.* noted an association of circulating effector memory and recent thymic migrant (have diverse TCR repertoire and can respond to multiple antigens) CD8$^+$ T cells and increased muscle mass in cancer patients; however, cachexia was not examined in this study. Moreover, occurrence of regulatory T cells (Tregs) and central memory T cells was negatively correlated with muscle mass (Narsale, 2019). Hence, these data imply that robust T cell responses likely protect from cancer-induced muscle catabolism, while immune suppression (i.e., by Tregs or MSCDs) might have a contrary effect. In line, CD4$^+$CD44$^{v.low}$ precursor T cells were shown to be specifically depleted in cachectic non-obese diabetic mice (C. Zhao, 2008); and injection of CD4$^+$CD44$^{v.low}$ cells restored balanced numbers of naïve, memory and regulatory T cells and attenuated muscle mass loss (Z. Wang, 2008; C. Zhao, 2010; C. Zhao, 2015). Moreover, Bindels et al. reported a marked downregulation of immune cell-specific markers (i.e., Cd3, Tbet, Il17a, Foxp3, IL10, F4/80, Cd68, and Cd11c) in the intestine of cachectic mice (Bindels, 2016).

In infection-associated cachexia, virus-specific CD8$^+$ T cells were observed to induce adipose tissue depletion. Importantly, CD8$^+$ T cell null mice were demonstrated to be protected from infection-associated weight and adipose tissue loss (Baazim, 2019). Altogether, these studies highlight a potential link between cachexia development and T cell presence/ functionality. However, despite the strong associations between T cells and cachexia evolvement, no mechanistic studies elucidating the interaction of T cells, altered metabolism and cancer cachexia have been performed to date.

1.1.3   Therapeutic approaches to counteract cancer cachexia

Since blocking of cancer-induced anorexia as unimodal therapy via pharmacological or nutritional interventions was unsuccessful to prolong survival (Baldwin, 2012), therapeutic studies changed their focus to the manipulation of several cachexokines using primarily neutralizing antibodies or peptides.

TNFα – One of the most prominent wasting-inducing factors in cachexia is TNFα, mediating protein degradation through NFκB signaling (Y. P. Li, 1998). Importantly, TNFα inhibition by antibodies was

shown to prolong survival and weaken cancer-induced anorexia, protein degradation, hypertriglyceridemia and lipolysis in experimental rodent models of cachexia (B. C. Sheppard, 1990; Sherry, 1989; Torelli, 1999). In line, a recent meta-analysis investigated the link between administration of TNFα inhibitors and BMI and bodyweight in patients and found a positive correlation (Patsalos, 2020), underlining the potential therapeutic use of anti-TNFα as first-line cancer cachexia drug. However, despite the promising results of preclinical studies and the aforementioned meta-analysis, anti-TNFα treatment of cachectic cancer patients was not able to improve anorexia or prevent bodyweight loss (Goldberg, 1995; Jatoi, 2010; Wiedenmann, 2008). Hence, other mechanisms of TNFα inhibition were explored, such as blocking of TNFα synthesis by thalidomide to counteract cachexia in pancreatic and terminal cancer patients; but treatment led to contradictory results. While in a few studies thalidomide attenuated weight and lean mass depletion, and enhanced nutritional status and quality of life (Bruera, 1999; Gordon, 2005; Z. H. Khan, 2003), in another study, poor tolerability in combination with no benefit in cachectic cancer patients has been reported (Wilkes, 2011). These mixed results highlight that although thalidomide might be a promising approach in cachexia management, further investigations with respect to dosing and mechanism are needed to provide efficiency and safety for the patient.

IL6 – In the last decades, a variety of IL6 target tissues, including liver, gut, skeletal muscle and adipose tissue, has been identified (Flint, 2016; J. Han, 2018; Puppa, 2011; Strassmann, 1992). Some experimental mouse models of cachexia such as the APC$^{Min/+}$ or the C26 model, were reported to be dependent on high IL6 levels, and IL6 inhibition was shown to attenuate cachexia in these models (Strassmann, 1992). However, observations on the depencend of the well-known LLC cachexia model on IL6 have been equivocal. While we and others have demonstrated that LLC tumor-bearing mice develop cachexia independent of increased circulating IL6 levels (Geppert, 2021; Hetzler, 2015), Ohira and colleagues have demonstrated that only genetically modified LLC cells, overexpressing IL6 are capable to induce cancer-associated tissue wasting (Ohira, 1996). In line, Ando *et al.* reported that anti-IL6 therapy was not efficient in LLC tumor bearing mice (Au, 2016), unless LLC cells were genetically modified to overexpress IL6 (Ando, 2014). Nevertheless, advanced cancer patients show increased levels of plasma IL6, which are associated with anorexia, anemia and depression, and most importantly, correlate with bodyweight loss (Y. Guo, 2012). Moreover, monoclonal antibody treatment against IL6 reduced anemia, lean mass loss and fatigue in patients (J. R. Rigas 2010), while despite its potential to reduce muscle degradation and block cachexia progression, anti-IL6 treatment in APC$^{Min/+}$ mice was not sufficient to reverse the process (White, 2011).

In summary, IL6 is a promising target to counteract cancer-associated progression, but further investigations on possible adverse side effects and its influence on other tissues than muscle and fat are needed.

GDF15 – Circulating levels of GDF15, which is an important regulator of energy homeostasis, correlate with decreased survival and increased cancer-associated wasting in patients (Johnen, 2007; Lerner, 2015; C. Li, 2016; Staff, 2010). Intriguingly, blockage of GDNF receptor alpha-like (GFRAL) signaling, which is the corresponding receptor for GDF15, was able to prevent and restore body weight loss in mice carrying GDF15-expressing tumors (Suriben, 2020). Hence, inhibition of the GFRAL receptor by antagonistic antibody binding might be a promising, novel approach to counteract cachexia. However, further investigations are needed as GFRAL expression in human tissues is more

widespread compared to mice, which might hinder antibody specificity, thereby promoting unwanted side effects (Rohm, 2020).

The beneficial effects of all aforementioned studies underline that cachexia onset and progression are mediated by the interplay of a variety of factors. In line, Schäfer *et al.* have identified several cachexokines inducing cachexia-associated cardiomyocyte dysfunction in a combinatorial manner. Hence, individual knockout in an *in vitro* model was not sufficient to improve atrophy of cardiomyocytes, but simultaneous ablation was (Schäfer, 2016).

To date, removal of the tumor is the only reliable treatment to prevent and restore cancer-associated wasting (Norton, 1985), while despite efforts to find efficient therapeutic options, no defined standard of care is currently available to prevent cancer-associated tissue wasting. Multidisciplinary approaches combining nutritional and pharmacological treatment with exercise may be promising to delay cachexia progression and improve overall life quality of the patients (Solheim, 2012).

1.2   The immune system

Men are continually exposed to a myriad of exogenous invaders but also endogenous alterations that are potentially harmful to the body. The immune system, composed of lymphoid organs and cells, cytokines and humoral factors, recognizes and protects us from diseases of endogenous and exogenous origin. Its importance and essential function becomes even clearer by its dysfunction, as underactivity or repression lead to the development of tumors and severe infections, while overreaction of the immune system ends in autoimmune diseases. Upon appearance of an exogenous or endogenous stimulus conquering the body, a hierarchical immune response is initiated with the ultimate aim to eliminate the non-self target. Contrary to innate immunity, which uses a highly conserved pattern to provide immediate host defense but with a clear lack of specificity, T cell-mediated protection takes longer to develop, but is very precise as it executes its function in an antigen-specific manner. One central feature of adaptive immunity is the development of a memory after antigen exposure, which allows T cells to identify previously encountered antigens, leading to a more vigorous and rapid response upon re-exposure (Parkin, 2001).

1.2.1   T cells are important mediators of adaptive immunity

T cells develop from bone marrow-derived progenitors and migrate to the thymus, where T cell differentiation, including the expression of an antigen-specific T cell receptor (TCR) as well as negative and positive selection, are conducted, ensuring that T cells recognize non-self antigens, but not self antigens (Thapa, 2019). Antigen-specificity of T cells is their most important hallmark and is mediated by the development of specialized surface TCRs. Upon antigen presentation by antigen-presenting cells (APCs) in lymphoid organs, a myriad of signaling pathways is initiated in naïve T cells, leading to their proliferation and differentiation to effector cells, which can then traffic to diverse disease sites, where they execute their effector function. Dependent on the T cell subtype, diverse effector functions are mediated such as direct cellular cytotoxicity to tumor cells, support of a proper B cell function, and enhancement of inflammatory responses (Parkin, 2001).

Effector T cells – About 95% of T lymphocytes can be found within lymphoid tissues, such as spleen or lymph nodes, where they continuously traffic and bind transiently to several APCs to identify potential exogenous antigens. Those antigens are either directly brought to lymphoid organs via the

lymphatics or blood, or are transported within APCs such as dendritic cells or macrophages (Shen, 2010; Théry, 2001). Upon encounter of a T cell and its matching antigen, T cell activation is initiated, and T cells start to differentiate into multiple functional classes of effector T cells with specific tasks. In this context, two major classes of effector T cells can be distinguished, termed CD4$^+$ and CD8$^+$ T cells based on the surface expression of their hallmark receptors CD4 or CD8, respectively (Parkin, 2001) (Figure 3). Antigen recognition by the TCR is different between CD4$^+$ and CD8$^+$ lymphocytes, as CD4$^+$ T cells only recognize antigens that are presented with major histocompatibility complex (MHC) class II molecules (Kruisbeek, 1985), while CD8$^+$ T cells react to antigens with MHC class I (Norment, 1988). Since all nucleated cells express MHC class I molecules, any such cell which is producing abnormal tumor or virus-associated antigens, can present these peptide fragments on their surface within the MHC class I and will be subsequently killed by cytotoxic attack (Ljunggren, 1996). In contrast, MHC class II molecules are mostly expressed by professional APCs, such as dendritic cells (Roche, 2015).

Cytotoxic CD8$^+$ lymphocytes – Upon stimulation by MHC class I-bound antigen, naïve CD8$^+$ T cells differentiate into cytotoxic effector T cells with the potential to directly kill target cells, which is mainly mediated by the secretion of three types of preformed cytotoxic proteins: perforin, granzmyes, and granulysin, all of which are stored in membrane-bound secretory lysosomes in the cytosol of cytotoxic lymphocytes. Upon conjugation to a target cell, these cytotoxic granules, released by CD8$^+$ lymphocytes, traffic to the immunological synapse, where perforin inserts in the target cell membrane to form transient pores, through which granzymes can enter (Lopez, 2013). Granzymes subsequently mediate target cell death by their interaction with specific intracellular proteins such as pro-caspase3 (Darmon, 1995; Pardo, 2008) or BH3-interacting domain death agonist protein (Alimonti, 2001; Barry, 2000), leading to DNA fragmentation and mitochondrial cytochrome c release into the cytosol, respectively, and ultimately promoting apoptosis. The importance of perforin/granzyme-mediated direct killing was highlighted in perforin knockout mice, which lost a huge part of their killing activity (Kägi, 1994).

IFNγ is another secreted factor, essential for mediating CD8$^+$ T cell cytotoxicity (Tau, 2001). Autocrine IFNγ signaling promotes killing and enhances cytotoxic T cell motility (Bhat, 2017; Curtsinger, 2012). Moreover, IFNγ was also noted to inhibit viral replication (Karupiah, 1993), induce MHC class I expression (Zhou, 2009) and potentiate macrophage activation (Su, 2015).

Another pathway to induce target cell apoptosis, is the cross-linking of Fas ligand (FasL), expressed on cytotoxic CD8$^+$ and CD4$^+$ T cells, with the cell surface death receptor Fas in the target cell membrane, allowing also CD4$^+$ T cells to mediate cytotoxicity (Malyshkina, 2017). Upon a decrease of antigen load, perforin-granzyme mediated killing is diminished (Meiraz, 2009), and FasL-based cytotoxicity is enhanced as a complementary action, to ensure optimal cytotoxic attack throughout the whole immune response (Hassin, 2011).

Overall, cytotoxic CD8$^+$ T cells mediate immunity through a variety of mechanisms, thereby killing single target cells with great precision, preventing widespread tissue damage, which is crucial in non-regenerating tissues such as in neurons.

Following antigen clearance, cytotoxic effector T cells undergo rapid contraction through activation induced cell death, while concomitantly a small population of antigen-experienced CD8$^+$ T cells remains as memory CD8$^+$ T cells (Homann, 2001; Lau, 1994), a long-lived antigen-specific subpopulation that provides an enhanced immune response upon re-exposure to its specific antigen (Doherty, 1994). Memory T cells can be further subdivided into two broad subsets, namely central

memory (T$_{CM}$) and effector memory (T$_{EM}$) cells, by their expression of CCR7 (C-C motif chemokine receptor 7) and CD62L (Sallusto, 1999). T$_{EM}$ cells are more similar to effector T cells and are capable to traffic to inflamed tissues and display rapid effector function, while T$_{CM}$ lack immediate effector function, express lymph node homing receptors, but have elevated proliferative potential and produce higher amounts of IL2 (Sallusto, 2004; Sallusto, 1999). Recently, presence of CD8$^+$ memory T cells has been shown to be of positive prognostic value in immunotherapy for cancer patients. Additionally, occurrence of a third memory cell type, termed resident memory T cells (T$_{RM}$), which is present within a certain tissue, and in contrast to T$_{CM}$ and T$_{EM}$ does not recirculate through the blood, was associated with an improved outcome in several cancers (Edwards, 2018; Egelston, 2019; Komdeur, 2017).

CD4$^+$ helper T cells – CD4$^+$ T cells primarily provide anti-tumor immunity by supporting cytotoxic CD8$^+$ lymphocytes and antibody responses through secretion of effector cytokines. However, additionally, their cytotoxic potential to directly kill target cells has recently been observed in various diseases, including viral infection (Brown, 2016), autoimmune disorders (Peeters, 2017) and cancer (Cachot, 2021), but is still far from fully understood. Upon activation naïve CD4$^+$ lymphocytes can differentiate into distinct T helper (Th) subtypes depending on the strength of TCR signaling (Tao, 1997; van Panhuys, 2014) and cytokine milieu they are surrounded with at the moment of stimulation (Cote-Sierra, 2004; Lighvani, 2001). The categorization of these Th cells is based on their cytokine profiles, which currently distinguish between Tregs, Th1, Th2, Th9, Th17 and follicular helper T cells (Tfh) cells, with Th1, Th9 and Th17 being strongly linked to antitumor immunity (T. Li, 2020).

Th1 cells express high levels of their lineage-specific marker T-box transcription factor expressed in T-cells (T-bet) and INFγ and have been shown to mediate a robust anti-tumor response against multiple cancer types, including colorectal and breast cancer (T. Li, 2020). Th1-derived IFNγ can either inhibit tumor growth or thrust MHC class I and class II expression on tumor cells and APCs, thereby promoting antigen processing and presentation (Raval, 1998; Thelemann, 2014). Moreover, Th1 cells were recently reported to obtain cytotoxic features by expressing granzyme B (Śledzińska, 2020). Both, IL6 and transforming growth factor β (TGFβ) have previously been implicated in cachexia development (J. Han, 2018; Lima, 2019) and are potent suppressors of Th1 mediated anti-tumor immunity (Park, 2005; Tsukamoto, 2015). Furthermore, TGFβ but also PD1-PD-L1 (Programmed cell death 1/ Programmed cell death 1 ligand 1) interaction were observed to induce conversion of Th1 cells to a Treg phenotype by co-expression of T-bet and FOXP3 (forkhead box P3). These Th1-derived Treg cells were shown to display an immunosuppressive phenotype *in vitro* and *in vivo* (Amarnath, 2011; Kanamori, 2018; Stathopoulou, 2018).

Th9 cells are characterized by IL9 cytokine expression in combination with the expression of the transcription factor PU.1, being induced by T cell stimulation with TGFβ (Goswami, 2012). Th9 cells show robust anti-tumor functions with high cytolytic activity and superior resistance to exhaustion (Lu, 2018; Purwar, 2012).

Th17 cells produce high amounts of the cytokine IL17 and the lineage marker retinoic acid-related orphan receptor γt (RORγt) (Zou, 2010). Three major cytokines are necessary for the polarization of Th17, namely TGFβ, IL6 and IL1β (Chen, 2007; Mangan, 2006; Revu, 2018), all of which have been previously linked to cachexia (J. Han, 2018; Laird, 2021; Lima, 2019). Infiltration of Th17 cells into solid tumors is a widely observed phenomenon (Su, 2010; Tosolini, 2011), but their role is still not completely clear and rather ambiguous. For instance, Th17 cells are linked to a poor prognosis of

colorectal cancer patients (Tosolini, 2011) and inhibit tumor cell apoptosis, enhance tumor immune evasion and promote tumor angiogenesis and metastasis, but also were reported to recruit immune cells to the tumor, inhibit tumor cell invasion and promote the activation of cytotoxic T cells (Qian, 2017). Hence, more studies are needed to unravel the complex effects that Th17 cells mediate within tumors.

Tregs are the predominant cellular mediators of dominant tolerance, thereby preventing aberrant immune activation (Sakaguchi, 2008). They are characterized by high expression of IL2Rα (interleukin 2 receptor α chain) (Sakaguchi, 1995) and their lineage-defining transcription factor FOXP3 (Fontenot, 2003; Hori, 2003). Treg-specific immune suppression is mediated through multiple mechanisms, which are either contact-dependent like lysis of effector T cells via enzyme secretion (perforin, granzyme B) (Gondek, 2005) and inhibition of APCs (Misra, 2004), or mediated by the secretion of inflammatory cytokines (Asseman, 1999; Green, 2003), or by consumption and thereby depletion of essential cytokines for T cell functionality (Barthlott, 2005). Indeed, a pioneering study by Curiel *et al.* has associated intra-tumoral Tregs with poor survival in ovarian cancer, demonstrating the deleterious and immunosuppressive effects of Tregs (Curiel, 2004). Later on, additional reports supported this idea, and in line, high Treg infiltration into tumors has been linked to reduced survival in several cancer types (Bates, 2006; Fu, 2007). However, in contrast, multiple other analyses could not identify a link between Treg presence and patient survival upon cancer incidence (Grabenbauer, 2006; Hillen, 2008; Mahmoud, 2011; Mizukami, 2008). More recently, several studies have noted that Tregs can change their polarization towards an effector phenotype with anti-tumor characteristics, which might potentially explain the discrepancies in the aforementioned studies, as based on the predominant occurrence of either conventional Tregs or effector Tregs, clinical outcome is likely altered. Accordingly, Saito and colleagues (Saito, 2016) demonstrated that tumor-infiltrating FOXP3-positive Tregs can be classified into two types by their expression of FOXP3 (FOXP3^{hi} *versus* FOXP3^{lo}). They observed that colorectal cancer patients with abundant infiltration of non-suppressive FOXP3^{lo} Tregs displayed a remarkably better prognosis compared to patients with high suppression-competent FOXP3^{hi} cell-infiltration into their tumors. Hence, by specifically manipulating the distinct Treg subsets, tumor formation and patient outcome might be positively altered. Moreover, in contrast to murine lymphocytes, human activated T cells express intermediate levels of FOXP3, although they are not Tregs and do not have an immunosuppressive function (Allan, 2007; Morgan, 2005). Hence, a clearer differentiation between immunosuppressive CD4^{+}FOXP3^{hi} Tregs and activated CD4^{+}FOXP^{lo} T cells is necessary to elucidate the complex function of Tregs in anti-tumor immunity and enhance the patient's outcome with advanced knowledge. To this end, a clearer definition of human Tregs needs to be applied by the inclusion of additional markers. In line, several studies already identified a clear expression pattern to identify human Tregs as CD3^{+}CD4^{+}CD127^{lo}CD25^{hi}FOXP3^{hi} cells (Cossarizza, 2019; W. Liu, 2006).
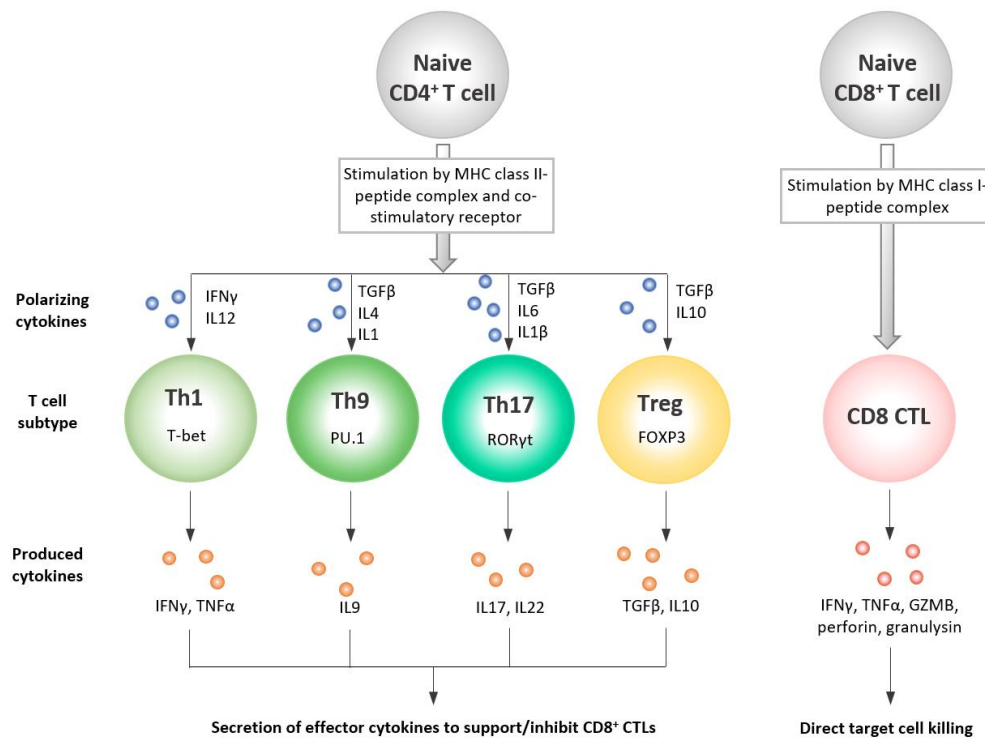
Figure 3. T cell differentiation. Naïve CD4^{+} and CD8^{+} T cells are activated by their respective MHC class-peptide complex and subsequently start to differentiate, aiming to gain effector function. Depending on the surrounding cytokine milieu, naïve CD4^{+} T cells can polarize into different subtypes. MHC= major histocompatibility complex; IFNγ= interferon gamma; IL12= interleukin 12; TNFα= tumor necrosis factor alpha; TGFβ= transforming growth factor beta 1; IL1β= interleukin 1 beta; IL6= interleukin 6; IL17= interleukin 17; IL10= interleukin 10; IL22= interleukin 22; GZMB= granzyme B.

Tissue-infiltrating T cells – Additionally to their presence in lymphoid organs, the occurrence of T cells in various non-lymphoid organs and tissues has been described in health and disease (Kälin, 2017; I. M. Khan, 2015; Rausch, 2008). Lean fat is predominantly populated by Tregs and macrophages, generating an anti-inflammatory environment and contributing to a balanced tissue homeostasis (Feuerer, 2009). However, with expanding lipid storage capacity and presence of adipocyte hypertrophy, quantitative and qualitative changes occur regarding immune cell infiltration, resulting in a decline of Tregs (Feuerer, 2009). Adipose tissue of obese individuals and mice has been demonstrated to be predominantly infiltrated by activated macrophages and effector T cells such as proinflammatory CD4^{+} T cells and cytotoxic CD8^{+} T cells, and more importantly this infiltration is associated with systemic metabolic dysfunction (Nishimura, 2009; Rausch, 2008; Strissel, 2010; H. Wu, 2007). Moreover, the presence of cytotoxic CD8^{+} T cells in adipose tissue precedes the development of insulin resistance, and depletion of CD8^{+} T cells resulted in improved insulin resistance (Nishimura, 2009). Unfortunately, so far researchers have not investigated in detail whether cachexia-induced adipose tissue wasting also affects immune cell populations in this tissue.

Also skeletal muscle wasting is one of the major hallmarks of cancer cachexia. Similar to adipose tissue, obesity also leads to increased macrophage and effector T cell infiltration of skeletal muscle with a simultaneous decline in Tregs (I. M. Khan, 2015). In this context, Khan and colleagues have reported that skeletal muscle-infiltrating immune cells are predominantly located in intermuscular and perimuscular fat depots, but not myotubes. Of note, myosteatosis has previously been shown to be a negative prognostic marker in patients with colon cancer (C. M. Lee, 2020). In cancer patients, T cell numbers in skeletal muscle correlated positively with muscle fiber size and especially CD8^{+} T cells were positively associated with muscle mass. Moreover, based on gene correlation analysis the authors suggested an inverse relationship of CD8^{+} T cell-related genes with several components of

muscle catabolic pathways, indicating that T cells might play a role in muscle mass preservation upon cancer (Anoveros-Barrera, 2019).

1.2.2   T cell activation and T cell receptor signaling

Activation of naïve T cells through their TCR is initiated by antigen/MHC complexes (Rosenthal, 1973; Shevach, 1973), and in case of CD4^{+} T cells, additional signaling of costimulatory receptors, such as CD28 (Linsley, 1991). This costimulatory signaling is of high importance, as its missing will result in a hyporesponsive state of the CD4^{+} T cell, termed anergy, leading to a lack of proliferation and low IL2 production (Schwartz, 2003). Co-stimulatory signals are mediated either by cross-linking of specific receptors on CD4^{+} T cells with their counterparts on APCs, or by provision of inflammatory cytokines, or a combination of both (Croft, 2017). Importantly, CD8^{+} T cells do not need these additional costimulatory signals to become properly activated (B. Wang, 2000). In general, TCR ligation with its respective MHC class molecule, will trigger a signal that is transmitted by CD3, being in a complex with the TCR, through FYN and LCK (Lymphocyte-specific protein tyrosine kinase)-mediated phosphorylation of immunoreceptor tyrosine based activation motifs (ITAMs) (Bu, 1995; Samelson, 1986) (Figure 4). Subsequently, phosphorylated ITAMs provide the binding site for Zeta-chain-associated protein kinase 70 (ZAP70), which directly becomes phosphorylated by LCK (A. C. Chan, 1992). ZAP70 activation triggers the recruitment of scaffold molecules such as SH2 domain containing leukocytes protein 76 kDa (SLP76) and linker of activated T cells (LAT). Both SLP76 and LAT mediate guanine nucleotide exchange factor 1 (VAV1)-dependent activation of phospholipase C γ1 (PLCγ1) (Yablonski, 2001), which in turn activates the production of diacylglycerol (DAG) and inositol triphosphate (IP3) from the hydrolysis of phosphatidylinositol 4,5-bisphosphate (PIP2). IP3 then promotes the downstream release of calcium ions (Ca^{2+}) from the endoplasmic reticulum, which promotes the entry of extracellular Ca^{2+} into the cell via calcium release-activated Ca^{2+} channels (CRAC). Altogether, this leads to the activation of calmodulin and subsequently calcineurin, followed by the nuclear translocation of the transcription factor nuclear factor of activated T cells (NFAT), thereby promoting IL2 gene transcription. Meanwhile, DAG recruits ras guanyl-releasing protein 1 (RasGRP1) and protein kinase C (PKCθ) to the cell membrane and thereby induces RasGRP1/Ras/ERK and PKCθ/IKK/NFκB signaling (Ebinu, 2000; Kane, 1999; Roose, 2005). Induction of MAPK/ERK signaling triggers the activation of adaptor-related protein complex 1 (AP1), which together with NFAT and NFκB orchestrates T cell activation, development and effector function. Moreover, SLP76 initiates a downstream cascade leading to cytoskeletal remodeling (Bubeck Wardenburg, 1998) and protein kinase B (AKT) activation, arbitrated by the direct interaction of SLP76 and the p85 subunit of PI3K. LAT was shown to be crucial in this process for mediating SLP76 localization (Shim, 2011). PI3K phosphorylates PIP2 to generate phosphatidylinositol-3,4,5-triphosphate (PIP3), which interacts with phosphoinositide-dependent protein kinase-1 (PDK-1) and AKT. Through its association with PDK1, PI3K triggers PKCθ activation, leading to NFκB translocation and activation (Kane, 1999), similar to DAG. Furthermore, PI3K/AKT signaling induces mechanistic target of rapamycin (mTOR) signaling, which orchestrates a variety of functions involved in cell cycle, survival, metabolism and growth pathways (Mills, 2009; Salmond, 2018). Importantly, CD28 co-stimulation was reported to enhance PI3K activity (Garçon, 2008). mTOR was also shown to link environmental signals such as glucose availability to different cellular fates of T cells (Chapman, 2014). In addition, the transcription factor FOXO1 was reported to integrate signals from mTOR and AKT signaling pathways in T cells, and to play an important role in proliferation (Stittrich, 2010), survival (Kerdiles, 2009), DNA repair (Ju, 2014) and glucose metabolism (W. Zhang, 2006).

Upon TCR stimulation, activated AKT mediates FOXO1 inhibition (Stahl, 2002). Importantly, T cells undergo metabolic reprogramming once they are being activated, which is crucial to adapt the distinct differentiation states. While naïve T cells mainly use oxidative phosphorylation of distinct nutrients such as glucose, lipids and amino acids to meet their energy demand, differentiating T effector cells – during antigen stimulation and activation – display elevated anabolic and bioenergetic needs. As described above, TCR stimulation leads to the PI3K-mediated induction of AKT signaling, which was shown to elevate the expression of glycolytic enzymes and nutrient transporters, thereby promoting increased glucose and amino acid utilization to facilitate T cell activation and proliferation (Barata, 2004; Edinger, 2002; Elstrom, 2004). When T cells then undergo clonal expansion, they predominantly perform aerobic glycolysis despite ample oxygen supply (T. Wang, 1976), similar to the well-known Warburg effect in cancer cells (Warburg, 1956). The switch to this rather insufficient metabolic state might be explained by simultaneous generation of cellular building blocks, such as fatty acids or amino acids as well as lactate, which can be shuttled into biosynthetic pathways. This re-use of building blocks is an efficient and fast mechanisms, thereby contributing to the rapid expansion of T cells and elimination of their target (Pearce, 2010).
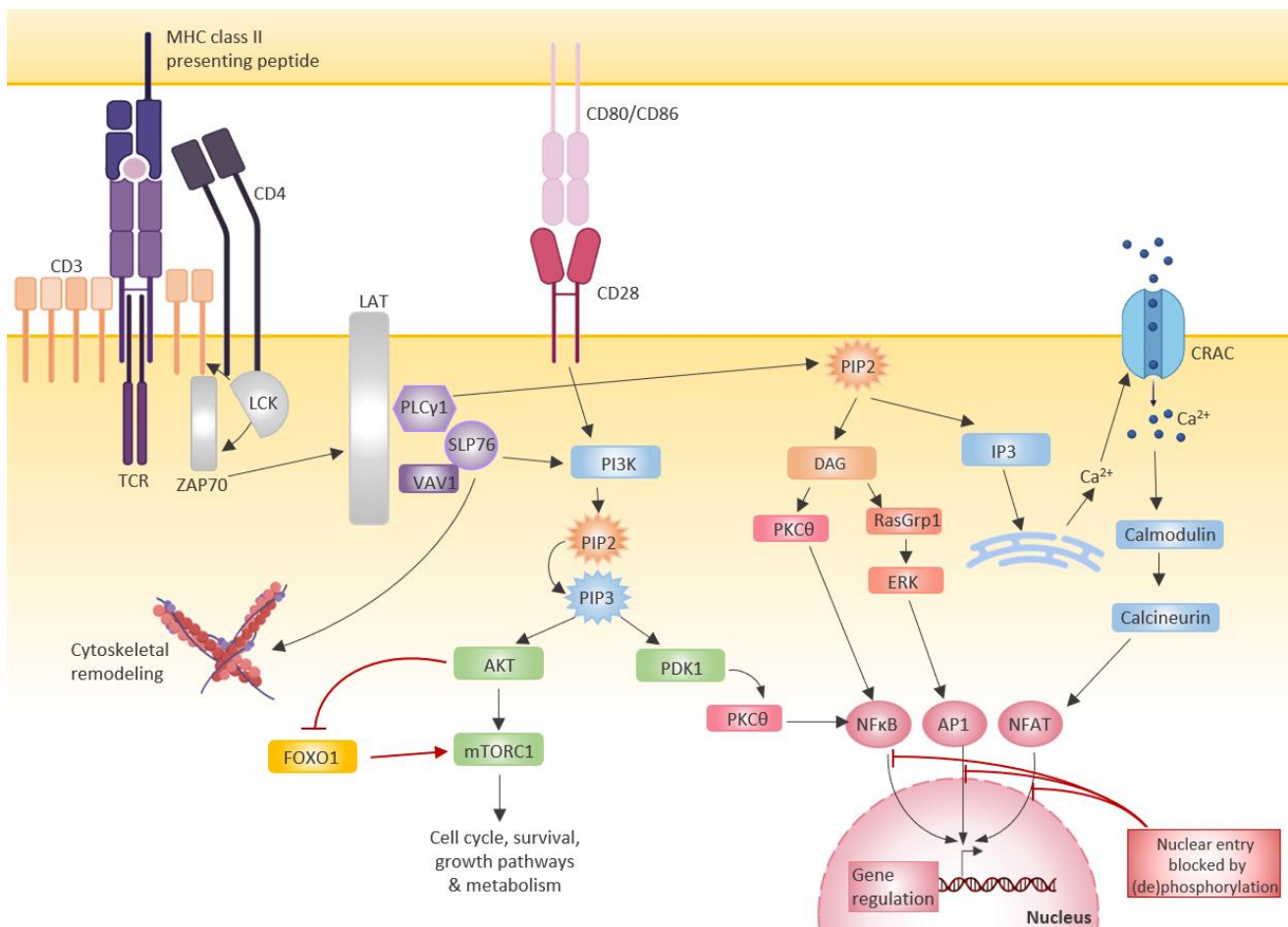
Figure 4. Activation of T cells. Following recognition of the MHC class II-peptide complex, a TCR signaling cascade is initiated, regulating proliferation, growth pathways, survival and metabolism, predominantly via AP1, NFκB, NFAT and mTOR. LCK= lymphocyte-specific protein tyrosine kinase; ZAP70= Zeta-chain-associated protein kinase 70; LAT= linker of activated T cells; PLCγ1= phospholipase C γ1; SPL76= SH2 domain containing leukocytes protein 76 kDa; VAV1= Guanine Nucleotide Exchange Factor 1; PI3K= Phosphatidylinositol 3-Kinase; PIP2= phosphatidylinositol 4,5-bisphosphate; PIP3= phosphatidylinositol-3,4,5-triphosphate; AKT= Protein kinase B; mTORC1= Mechanistic target of rapamycin; FOXO1= forkhead-Box-O-1; PDK1= Phosphoinositide-dependent protein kinase-1; PKCθ= Protein Kinase C θ; DAG= diacylglycerol; RasGrp1= Ras guanyl-releasing protein 1; ERK= extracellular-signal-regulated kinase; IP3= inositol triphosphate; NFκB= nuclear factor 'kappa-light-chain-enhancer' of activated B-cells; AP1= Adaptor-related Protein complex 1; NFAT= Nuclear

factor of activated T cells; CRAC= calcium release-activated Ca²⁺ channels; TCR= T cell receptor. Figure based on (Baniyash, 2004; Hedrick, 2012; Shyer, 2020). Created with BioRender.com.

1.2.3   T cell repression

In healthy individuals, T cell activation results in a strong induction of proliferation and effector function. However, there are multiple conditions that can dampen this activation cascade by either inhibitory receptor signaling or soluble inhibitory factors (Figure 5).
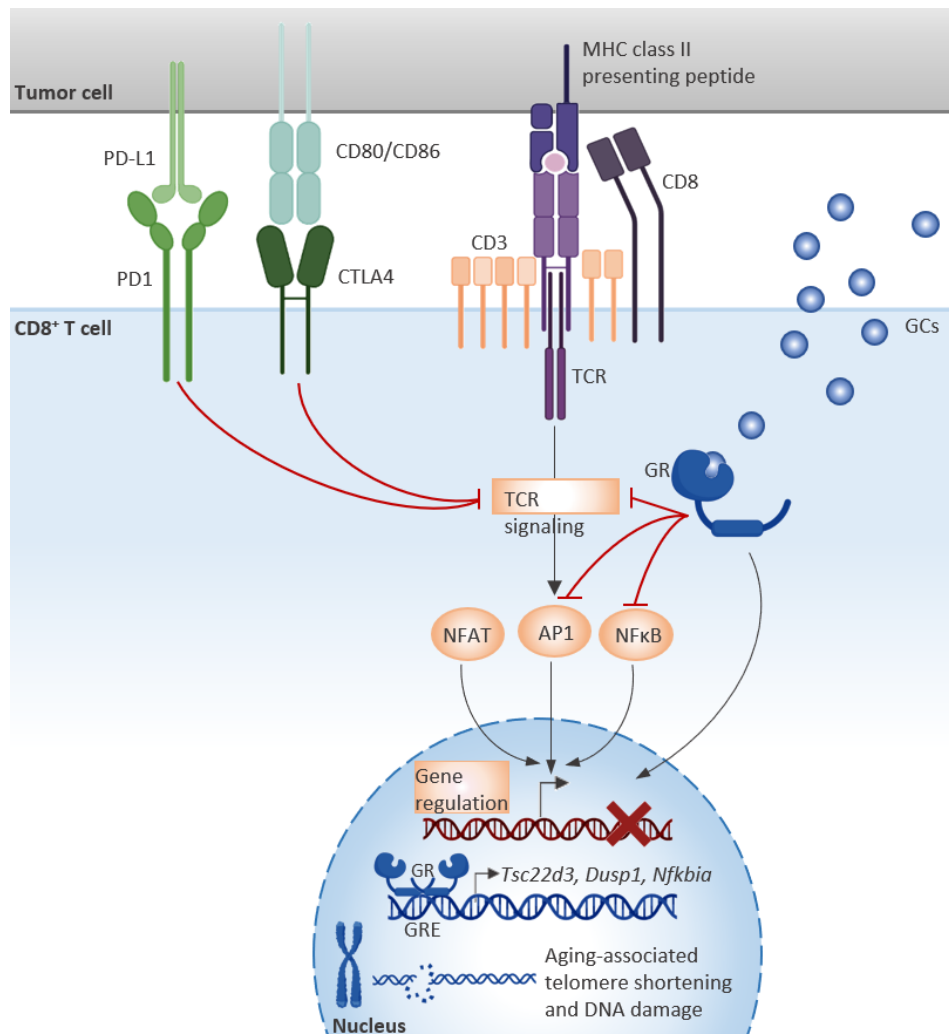
Figure 5. Mechanisms of T cell suppression. In general, there are two main dysfunctional states that T cells can adapt: exhaustion and senescence, which can be either age-or tumor-related or both. In addition, glucocorticoids were reported to induce T cell dysfunction. PD1= programmed cell death 1; PD-L1= PD ligand 1; CTLA4= cytotoxic T lymphocyte-associated antigen-4; TCR=T cell receptor; GCs= Glucocorticoids; GR= Glucocorticoid receptor; NFAT= Nuclear Factor of Activated T cells; AP1= Adaptor-related Protein complex 1; NFκB= nuclear factor 'kappa-light-chain-enhancer' of activated B-cells; GRE= glucocorticoid-responsive elements. Figure based on (Baniyash, 2004; Hedrick, 2012; Shyer, 2020). Created with BioRender.com.

Aging-mediated T cell senescence – Increasing age leads to the accumulation of damaged cells in many organs, and especially aging of the immune system has been linked to the onset of multiple diseases, including cancer (Thoma, 2021) and atherosclerosis (Childs, 2016). Moreover, independent of age, several studies have identified the occurrence of senescent T cells in various types of cancer (Montes, 2008; Ye, 2014; Ye, 2015). T cell senescence is triggered by DNA damage and telomer shortening, leading to the upregulation of p21, p53 and p16 in combination with a decrease of Cdk2, Cdk6 and cyclin D3 expression, altogether causing cell cycle arrest and a decline of cell proliferation

(Campisi, 2007). Senescence also impairs TCR signaling as identified by the loss of multiple key molecules that are part of the TCR signaling machinery, such as LCK, ZAP70, LAT and SLP76 (Lanna, 2014). More recently, additional mechanisms that are capable of triggering T cell senescence were reported. In this regard, naturally occurring but also tumor-derived Tregs were noted to repress naive and effector T cells via the induction of senescence (L. Li, 2019; X. Liu, 2018; Montes, 2008; Ye, 2012). Moreover, different tumor cell types *per se* were shown to mediate T cell senescence by increasing cAMP levels in corresponding T cells (Montes, 2008; Ye, 2014). These effects are mediated through the induction of DNA damage responses in the affected T cell, leading to cell cycle arrest and senescence (L. Li, 2019; X. Liu, 2018). Phenotypically, senescent T cells display a unique secretory phenotype, as they produce and secrete high amounts of inflammatory cytokines, i.e. IL2, IL6, TNFα, IFNγ, IL10 and TGFβ (Ye, 2012; Ye, 2013). Increased cytokine secretion by T cells might furthermore contribute to the aging-associated chronic low-grade inflammation, that is observed in aged individuals (Macaulay, 2013), which may promote tumor initiation and progression (Grivennikov, 2011).

Tumor-induced T cell exhaustion – Exhaustion is one of the best studied dysfunctional conditions that T cells can adapt. It describes a state in which T cells – as a response to chronic antigen stimulation – progressively lose their function. T cell exhaustion is often observed upon chronic viral infection (Quigley, 2010) or cancer incidence (Bense, 2017; C. Zheng, 2017). Exhausted T cells show impaired proliferation and cytotoxicity, as they lack proper production of cytokines such as TNFα, IL2 and IFNγ (Wherry, 2015). Mechanistically, both transcriptional and epigenetic alterations dominate T cell exhaustion. With respect to transcriptional reprogramming, exhausted T cells upregulate the expression of multiple inhibitory cell surface receptors such as PD1, TIGIT (T cell immunoglobulin and ITIM domain), CTLA4 (cytotoxic T lymphocyte-associated antigen-4), and LAG3 (lymphocyte activation gene 3), with NFAT, TOX (thymocyte selection-associated high mobility group box) and NR4A (nuclear receptor subfamily 4A) as central regulators of this process (O. Khan, 2019; Martinez, 2015; Mognol, 2017). Moreover, the zinc-finger transcription factor GATA3 (GATA binding protein 3) was demonstrated to be a crucial driver of T cell dysfunction in cancer (Singer, 2016). However, the precise mechanism controlling the induction of an exhausted state in T cells, remains poorly understood. Bringing a bit of enlightment, IL2 signaling has recently been reported to induce CD8^{+} T cell exhaustion by activation of a STAT5 pathway (Y. Liu, 2021).

In the healthy state, inhibitory receptors are transiently expressed to regulate the strength of the immune response and prevent autoimmunity, upon cancer burden, however, prolonged and high expression of several inhibitory receptors is a hallmark of T cell exhaustion (Wherry, 2015). The probably best-studied inhibitory receptor pathway in that context is PD1/PD-L1. PD-L1 on tumor cells activates PD1 on T cells, thereby preventing ZAP70 phosphorylation, leading to the downmodulation of TCR downstream signaling and attenuated IL2 production and T cell proliferation (K. A. Sheppard, 2004). Furthermore, PD1 was demonstrated to impair T cell activation by inhibiting CD28-induced signaling by blocking of PI3K activity. Another inhibitory receptor interfering with the CD28-mediated PI3K/AKT/mTOR signaling is CTLA4, but through a distinct mechanism involving protein phosphatase 2A (PP2A) to directly inhibit AKT (Parry, 2005). Modulating these dysregulated pathways by targeting inhibitory receptors using blockade therapies, is a revolutionary breakthrough in cancer immunotherapy. In a notable number of advanced-stage cancer patients, anti-PD1 and anti-CTLA4 treatment has shown promising results (Hodi, 2010; Motzer, 2015; Robert, 2015; Weber, 2015).

Importantly, co-administration of an anti-PD1 and anti-CTLA4 inhibitor has demonstrated a marked increase in the response rate and progression-free survival in metastatic melanoma patients (Postow, 2015). However, despite durable responses to anti-PD1 and anti-CTLA4 treatment, not all patients demonstrate tumor regression and hence fail to have clinical responses. Thus, it is important to identify additional pathways and inhibitory receptors that arbitrate T cell exhaustion upon cancer incidence. Recently, TIGIT has been demonstrated to be a promising target in cancer immunotherapy. Blockade of TIGIT alone was capable to impede tumor growth, and even more so when combined with additional checkpoint inhibitors such as PD1 or TIM3 (Kurtulus, 2015; X. Zhang, 2019). Interestingly, immune checkpoint inhibitory therapy was noted to be less efficient in a cohort of cachectic patients with non-small cell lung carcinoma (Miyawaki, 2020), implying that cachexia-induced immunologic abnormalities dampen treatment efficiency. Despite its strong benefits, the use of immune checkpoint inhibitory therapy is linked to a wide spectrum of side effects, so-called immune-related adverse events, characterized by general inflammation and immune activation in healthy tissue such as dermatitis (rash), enterocolitis or liver abnormalities (Fecher, 2013). In the future, further research is needed to identify next-generation inhibitory agents as well as treatment strategies to improve disease outcome while simultaneously decreasing adverse side effects.

Glucocorticoids – GCs are adrenal-derived steroid hormones, which are synthesized by metabolic breakdown of cholesterol. They are induced by the circadian rhythm, regulating metabolism and neural function (Dickmeis, 2009; Liston, 2013), as well as by stress, thereby enhancing neural function, cardiovascular output and mobilizing energy stores (Sapolsky, 2000). Synthesis of GCs is regulated by the HPA axis and its key regulator CRH, initiating the expression of several enzymes in the adrenal cortex to convert cholesterol into corticosterone (rodents) or cortisol (humans), which is subsequently secreted into the blood stream (Rice, 1991). In detail, various stressors, including inflammatory cytokines (TNFα, IL1, IL6, (Besedovsky, 1991)) cause the secretion of CRH from the hypothalamus to the anterior pituitary gland, where it stimulates the synthesis of POMC (proopiomelanocortin) (A. Slominski, 2000), leading to ACTH (adrenocorticotropic hormone) production and release. ACTH traffics then to the adrenal cortex, where it initiates the conversion of cholesterol into corticosterone/cortisol. Interestingly, CRH is also produced by a variety of peripheral tissues including immune cells (Karalis, 1997), gut (Kawahito, 1994), skin (A. T. Slominski, 2013), as well as placenta and testes (Kalantaridou, 2007). GCs bind intracellularly to the GR, which translocates subsequently into the nucleus to bind glucocorticoid-responsive elements, thereby regulating transcription of target genes (T. A. Johnson, 2021). The by far most potent effect of GCs is their repression of the immune system, particularly T cells. Importantly, lack of adrenal GC production leads to faster pathogen clearance, but at the same time increased mortality is observed as a result of uninhibited T cell responses and cytokine storm (Roggero, 2006; Ruzek, 1999). GCs mediate their powerful repression of T cells mostly by modifying transcription, thereby upregulating the expression of inhibitory receptors (CTLA4, PD1, LAG3), apoptotic genes, and immunoregulatory proteins, while they simultaneously decrease expression of co-stimulatory molecules, pro-inflammatory cytokines and cell cycle mediators (Taves, 2020). With respect to the transcription of immunoregulatory genes, GR mediates the induction of several immunosuppressive genes including *Tsc22d3, Dusp1* and *Nfkbia* (encoding GILZ, MKP1 and IκBα). GILZ (glucocorticoid-induced leucine zipper) arbitrates T cell suppression through direct interference with either AP1 and NFκB (Ayroldi, 2001; Mittelstadt, 2001) or RAS and RAF (Ayroldi, 2007), while MKP1 (MAP kinase phosphatase-1) and IκBα impair the ERK/MAPK pathway and NFκB signaling, respectively (Maneechotesuwan, 2009; Scheinman,

Cogswell, , 1995; Y. Zhang, 2009). Altogether, GCs induce an aberrant transcriptional profile interfering with TCR signaling, ultimately inhibiting T cell activation, cytokine expression and proliferation. Additionally, trans-repression via GR tethering to AP1 and NFκB (Heck, 1994; Ray, 1994) further promotes the dramatic T cell repression. Of note, defective T cell activation can also be arbitrated by reduced ability of Dendritic cells to prime naïve T cells due to GC-induced compromised Dendritic cell maturation (Elftman, 2007).

In a recent study, Acharya *et al.* noted the strong effect of a local GC rise in the tumor microenvironment on T cell effector differentiation, finally leading to CD8^{+} TIL dysfunction. Repeated activation of T cells in the presence of GCs has led to the upregulation of several dysfunction-associated genes (Acharya, 2020). Hence, GCs are another powerful mechanism to induce T cell dysfunction in both preclinical models and cancer patients (Acharya, 2020; H. Zhang, 2021).

1.3   Aim of the study

Cancer-induced body wasting represents an unmet clinical need and has been previously associated with unresponsiveness to immune checkpoint inhibitory therapy, suggesting suppressed T cell effector function caused by other means than classical T cell exhaustion. A combination of chronic systemic inflammation and increased glucocorticoid signaling - both hallmarks of cachexia – could possibly impair T cell functionality. Indeed, few studies have examined the interplay between cachexia and T cell function; however, no detailed mechanistic studies, elucidating the impact of cachexia on general T cell metabolism and functionality as well whether T cells contribute to disease progression, have been conducted to date. Hence, the aim of this thesis was to investigate this interconnection by using different experimental mouse models of cancer-cachexia in combination with *ex vivo* approaches. To this end, numerical, metabolic, and functional phenotyping of CD4^{+} and CD8^{+} T cells from spleen and tumor was conducted *ex vivo*, and *in vitro* studies were applied to elucidate whether the observed phenotype was dependent on tumor-derived factors or systemic changes. Cachexia-induced changes in the lipidome were assessed and the impact of aging on disease development was analyzed. Transcriptional profiling of splenic and tumor-derived T cells from cachectic mice, highlighted glucocorticoids as potent inducers of T cell suppression upon cachexia, and *in vitro* studies using dexamethasone were performed to mimic the cachectic T cell phenotype. As final proof of concept, T cell-specific glucocorticoid receptor knockout mice were generated, and cachexia was induced to assess whether absent glucocorticoid signaling in T cells can improve T cell functionality and finally disease outcome. Pilot studies were initiated to identify the translatability of preclinical results to the patient by comprehensive immune cell phenotyping of human peripheral blood mononuclear cells. Ultimately, our study identified T cells as novel metabolic regulators in cancer cachexia, and highlighted the attenuating effects of improving T cell functionality in cancer-associated wasting, thereby underlining that enhancing T cell effector function might be a promising strategy to counteract cachexia in cancer patients.

2   RESULTS

2.1   Mouse models capture systemic effects associated with human cancer cachexia

Due to their phylogenetic relation and physiological resemblance to humans (Bodenreider, 2005; Cheng, 2014; Yue, 2014), mouse models have a high potential to study human diseases. Thus, in the past decades, with the development of either pharmacological or genetic manipulation, researchers were able to gain more insight into the complexity of several diseases (Perlman, 2016; Vandamme, 2014). In cachexia research, mouse models are potent tools as they cover some of the systemic alterations of wasting, but still can be easily manipulated to identify genes and pathways contributing to cachexia development (Deboer, 2009). There are several commonly used mouse models in cancer cachexia research including genetic models such as the KPC (K-rasLSL.G12D/+; Trp53R172H/+; Pdx-1-Cre mutation) (Hingorani, 2005) or APC Min (adenomatous polyposis coli; multiple intestinal neoplasia) (Moser, 1990) models, as well as tumor implantation models like the Colon26 (C26) (Tanaka, 1990) or Lewis Lung Cancer (LLC) (Sherry, 1989), all capturing important systemic effects associated with cancer cachexia in patients. A schematic overview of the different mouse models used in this thesis is represented in Figure 6 and will be discussed in more detail in the following.
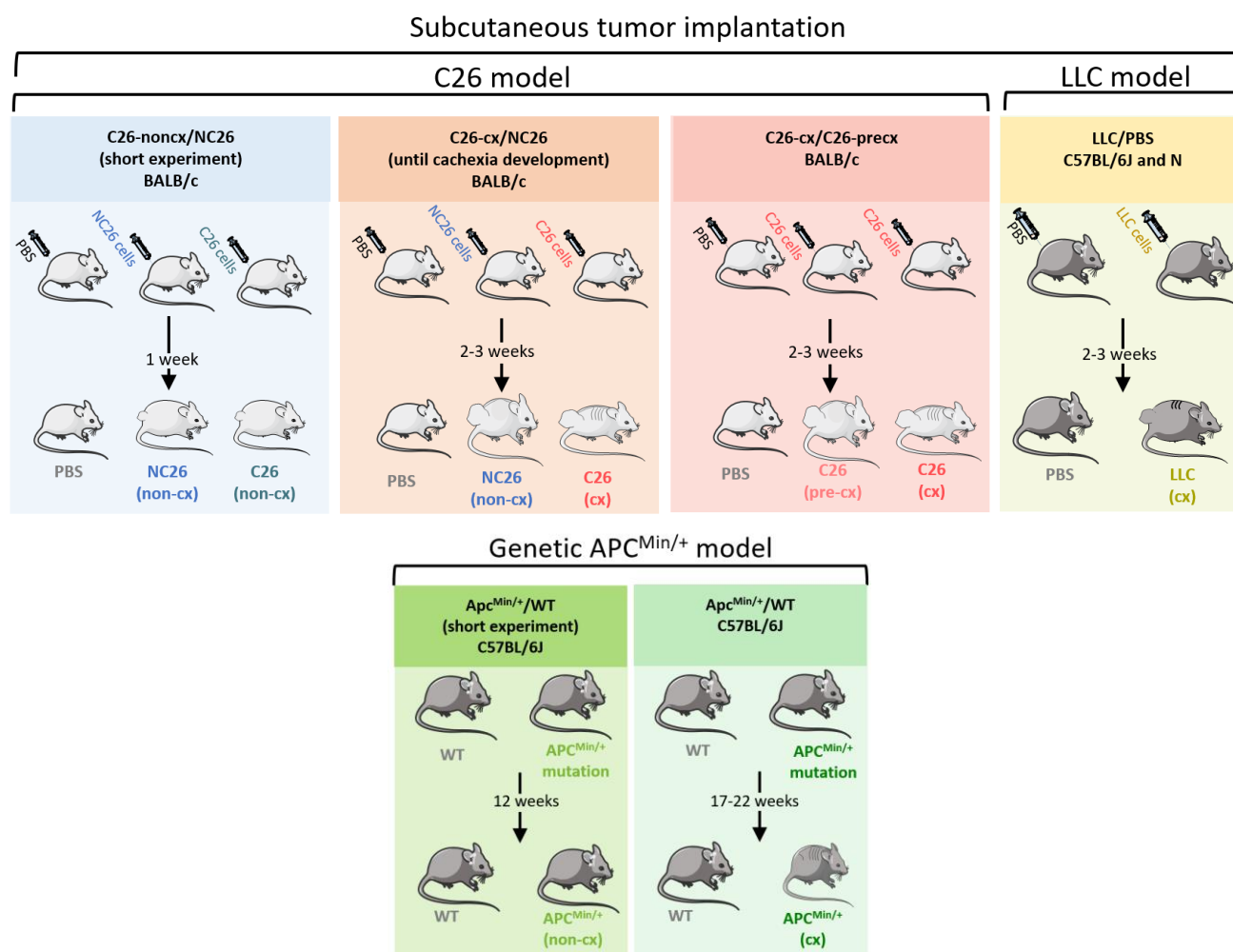
Figure 6. Schematic presentation of the different cachexia mouse models used in this study. Cancer cachexia was either induced by subcutaneous implantation of tumor cells (C26, LLC) or genetic modification of the APC locus in C57BL/6J mice (APC$^{Min/+}$ mice). Phosphate-buffered saline (PBS)-injected mice were used as healthy controls, while NC26-injected mice represented non-cachectic (non-cx) tumor-control mice. To investigate cancer cachexia (cx), C26 or LLC cells were injected into syngeneic mice, which were monitored over 2-3 weeks to develop cancer cachexia (highlighted in red and yellow, respectively). To adapt for the use of different cell lines and to check if the observed effects were truly and only based on cachexia presence, BALB/c mice injected with PBS, NC26 and C26 cells, were sacrificed one week post injection, when

cachexia was not present yet, to identify changes induced by the different tumor cell lines themselves (highlighted in blue). In addition, pre-cachexia (pre-cx) was analyzed to assess early changes upon disease onset (highlighted in orange). APC$^{Min/+}$ mutant mice developed cancer cachexia after 17-22 weeks, while young 12-week-old APC Min mice were sacrificed as a control before the onset of cancer cachexia (highlighted in green). Figure based on (Geppert, 2021; Morigny&Zuber, 2020).

2.1.1   Tumor implantation models of cancer cachexia

The most commonly used tumor implantation models of cancer cachexia research are the C26 and LLC model, in which these cell lines are implanted subcutaneously into syngeneic experimental mice, leading to tumor growth and cachexia development within 2-3 weeks (Sherry, 1989; Tanaka, 1990). To investigate the contribution of different factors and cell types to cachexia development, the injection of C26 or LLC tumor cells into genetically modified mice represents a fast and important tool. In this thesis, the contribution of T cells to cachexia development was investigated with the help of different mouse studies defined by various tumor entities, tumor sizes and stages of body wasting (Figure 6). To this end, mice were injected with either C26 or LLC cachexia-inducing tumor cells or non-cachexia-inducing NC26 control cells. PBS was used to adapt for changes due to the injection. To assess if the tumor cell lines themselves had an impact on systemic changes upon body wasting, a control experiment was performed, in which cachexia inducing C26 and NC26 control tumor cells were implanted. Mice were sacrificed one week later when tumors were only palpable, and no cachectic phenotype was present. In addition, early changes upon cachexia development were investigated in pre-cachectic mice (Figure 6).

Tumor growth is similar between cachexia-inducing and non-cachexia-inducing tumor cell lines
Monitoring of similar tumor growth between groups is of high importance in cancer cachexia research, as tumor size can influence cachexia onset and outcome via the tumor-dependent secretion of so-called cachexokines, factors, which were shown to actively promote tissue wasting (K. C. Fearon, 2012; Schäfer, 2016). Hence, to minimize variability and exclude effects based on different tumor sizes, tumor growth over time and final tumor weight were measured for all studies presented in this thesis. In the control C26 experiment, cachexia inducing C26 and control NC26 tumors were still small (Figure 7A) and just palpable at the time of sacrifice. Thus, no time course of tumor growth could be assessed for these groups. Approximately 7 days post injection, tumors started to be palpable, and growth was monitored in both cachexia implantation models over the course of the experiment (Figure 7). Pre-cachectic C26 tumor-bearing animals had a similar tumor size compared to the cachectic C26 mice (Figure 7A) but did not suffer from weight loss at the time of death (Figure 8D). C26 cachexia-inducing and NC26 control tumor cells grew to a similar size with comparable tumors at the end of the experiment (Figure 7A). Tumors of LLC-injected C57BL/6 mice grew steadily over the course of the experiment and reached a slightly bigger, but still comparable size to the NC26 and C26 tumors (Figure 7B). As there was no LLC-matching non-cachexia-inducing tumor control cell line available, LLC tumor-bearing mice were compared to PBS-injected controls.
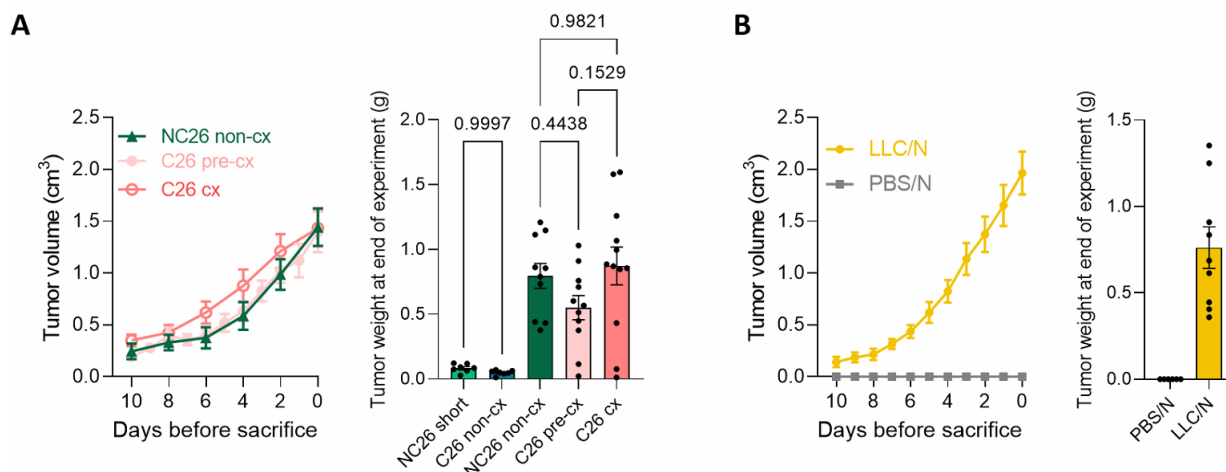
Figure 7. Tumor growth is similar between cachexia-and non-cachexia-inducing tumor cell lines. (A, B) Tumor growth over time and tumor weight at the end of the experiment in **(A)** NC26 and C26 tumor-bearing mice with different stages of tumor size and wasting and **(B)** C57BL/6N mice injected with PBS (PBS/N; grey; n=6) or LLC tumor cells (LLC/N; yellow; n=9). NC26 and C26 injected animals which were sacrificed 7 days post implantation, are displayed in light green (NC26 short; n=7) and dark turquoise (C26 non-cx; n=7), respectively. Cachectic C26 mice are displayed in dark red (C26 cx; n=12), while pre-cachectic animals are shown in light red (C26 pre-cx; n=11). NC26 tumor-bearing mice that had larger tumors (NC26 non-cx; n=10) are shown in dark green. Data are mean ± s.e.m. Statistical analyses were performed using unpaired *t*-test or one-way analysis of variance (ANOVA) with Tukey's multiple-comparison *post hoc* test.

Body wasting is a hallmark of cancer cachexia

Since tissue wasting is a prominent hallmark of cancer cachexia, bodyweight change of patients and mice is an important readout in cachexia research. Thus, the initial bodyweight between experimental groups of cachexia mouse experiments should not differ based on non-significant statistical analysis, as shown in Figure 8A and E. At the end of the experiment, tumor-subtracted bodyweight was only significantly reduced in the cachectic C26 tumor-bearing group (Figure 8B), but not in LLC tumor-bearing mice (Figure 8F), underlining the mild cachexia phenotype of this model, as previously shown (Geppert, 2021). To normalize for the differences in time to endpoint, a time course of bodyweight development was plotted starting 10 days prior to sacrifice (Figure 8C, G). PBS mice of all different experiments showed an increase in bodyweight over the course of the experiment, while cachectic C26 tumor-bearing mice showed a rapid and strong bodyweight drop starting two days prior to sacrifice (Figure 8C), in line with the severe phenotype of C26 cachectic mice that has already been reported by us (Geppert, 2021). Contrary, NC26 tumor control mice gained most weight over the course of the experiment, an effect most likely based on the continuous NC26 tumor growth (Figure 7A), as bodyweight change minus tumor was similar between NC26 and PBS injected mice (Figure 8D). Pre-cachectic C26 animals remained weight stable over the course of the experiment, while NC26 short and C26 non-cachectic mice, which were sacrificed 1 week post injection, gained similar weight (Figure 8C). This effect could also be observed when looking at the bodyweight change minus tumor at the end of the experiment (Figure 8D). All groups from the short experiment (PBS short, NC26 short and C26 non-cx), had equally increased their bodyweight independent of tumor presence, indicating that these mice were sacrificed before the onset of wasting and cachexia. All mice from the cachectic C26 group developed severe weight loss, while pre-cachectic mice showed no or only mild bodyweight loss (Figure 8D). Contrary to the C26 model, as already reported (Geppert, 2021), the LLC cachexia model shows only very weak signs of wasting, indicated by a non-significant, mild decrease of final bodyweight (Figure 8F), and an only slightly affected curve of bodyweight development over the course of the experiment (Figure 8G). Interestingly, LLC tumors induced mild bodyweight loss in

about 50% of the tumor-bearing animals with a very high variability, implying a high rate of non-responders (Figure 8H).
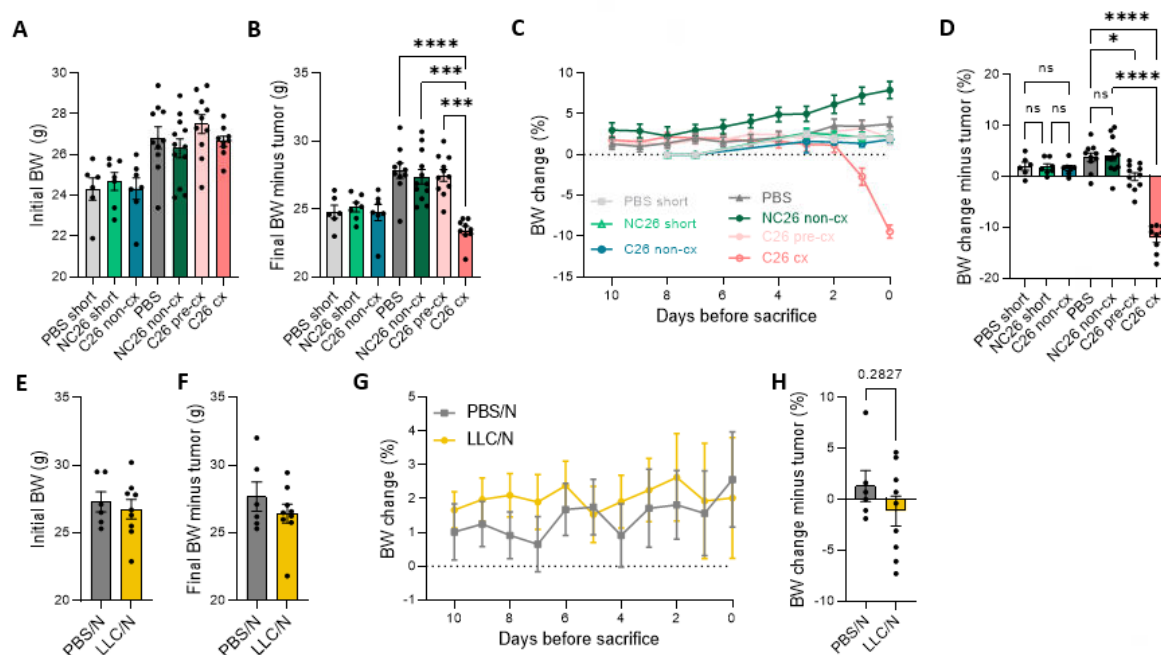
Figure 8. Body wasting is a hallmark of cancer cachexia. (A-H) Mice were injected with a cachexia-inducing tumor cell line (C26, LLC), a control tumor cell line (NC26) or PBS. Mice that were injected with PBS are depicted in grey (PBS short n=6, PBS n=10, PBS/N n=6). Numbers and color-coding of tumor-bearing mice is similar to Figure 7. **(A, E)** Initial bodyweight (BW) before PBS or tumor cell injection. **(B, F)** Final BW minus tumor at end of the experiment in PBS, NC26, C26 or LLC tumor-bearing mice. **(C, G)** Time course of bodyweight development starting 10 days prior to sacrifice (change in percentage compared to initial bodyweight before injection). **(D, H)** Bodyweight change minus tumor at the end of the experiment normalized to initial mass (expressed as percentage). Data are mean ± s.e.m. Statistical analyses were performed using unpaired *t*-test or one-way ANOVA with Tukey's multiple-comparison *post hoc* test. *p<0.05, ***p<0.001, ****p<0.0001.

Bodyweight loss in cachectic mice was also linked to adipose tissue and muscle wasting, as observed by Echo magnetic resonance imaging (EchoMRI) body composition analysis (Figure 9A, B). In line with the bodyweight data, cachectic C26 mice suffered from a severe decrease in lean mass and body fat (Figure 9A), while no changes in LLC/N mice were observed (Figure 9B). Interestingly, pre-cx mice also suffered from a decrease of fat mass, while lean mass was still unaffected, pointing out that adipose tissue wasting is initiated at a very early stage, while muscle wasting only occurs at very advanced cachexia stages. Likewise, inguinal (iWAT) and epididymal white adipose tissue (eWAT), and gastrocnemius muscle (GC) were reduced by long-term presence of C26 tumors (Figure 9C, D). Of note, PBS mice also displayed strong loss of body fat but with a high variability; probably a result of increased aggression and fighting only in one PBS cage, leading to elevated stress and reduced eating. As expected, no changes in the lean or fat mass were observed by short tumor presence in the control experiment (Figure 9A, C, D). Interestingly, despite an unchanged lean and fat mass as assessed by EchoMRI, LLC tumors induced a significant reduction of iWAT and GC mass and a non-significant reduction of eWAT (Figure 9C, D). Upon long-term tumor exposure (NC26 non-cx, C26 pre-cx, C26-cx, LLC), significant enlargement of the spleen was observed in all tumor-bearing mice, while short tumor cell exposure (NC26 short, C26 non-cx) did not affect spleen weight (Figure 9E). Interestingly, in a model of hepatocellular carcinoma, spleen weight correlated positively with tumor growth and an increase of certain immune cell types (Jiang, 2021), underlining the strong connection between the anti-tumor immune response, tumor size and spleen weight. Based on this study and the spleen

weight of cachectic and non-cachectic mice, NC26 and C26 tumors may induce a similar cellular immune response, while tumors in the short experiment were still too small to induce a proper cellular immune response.
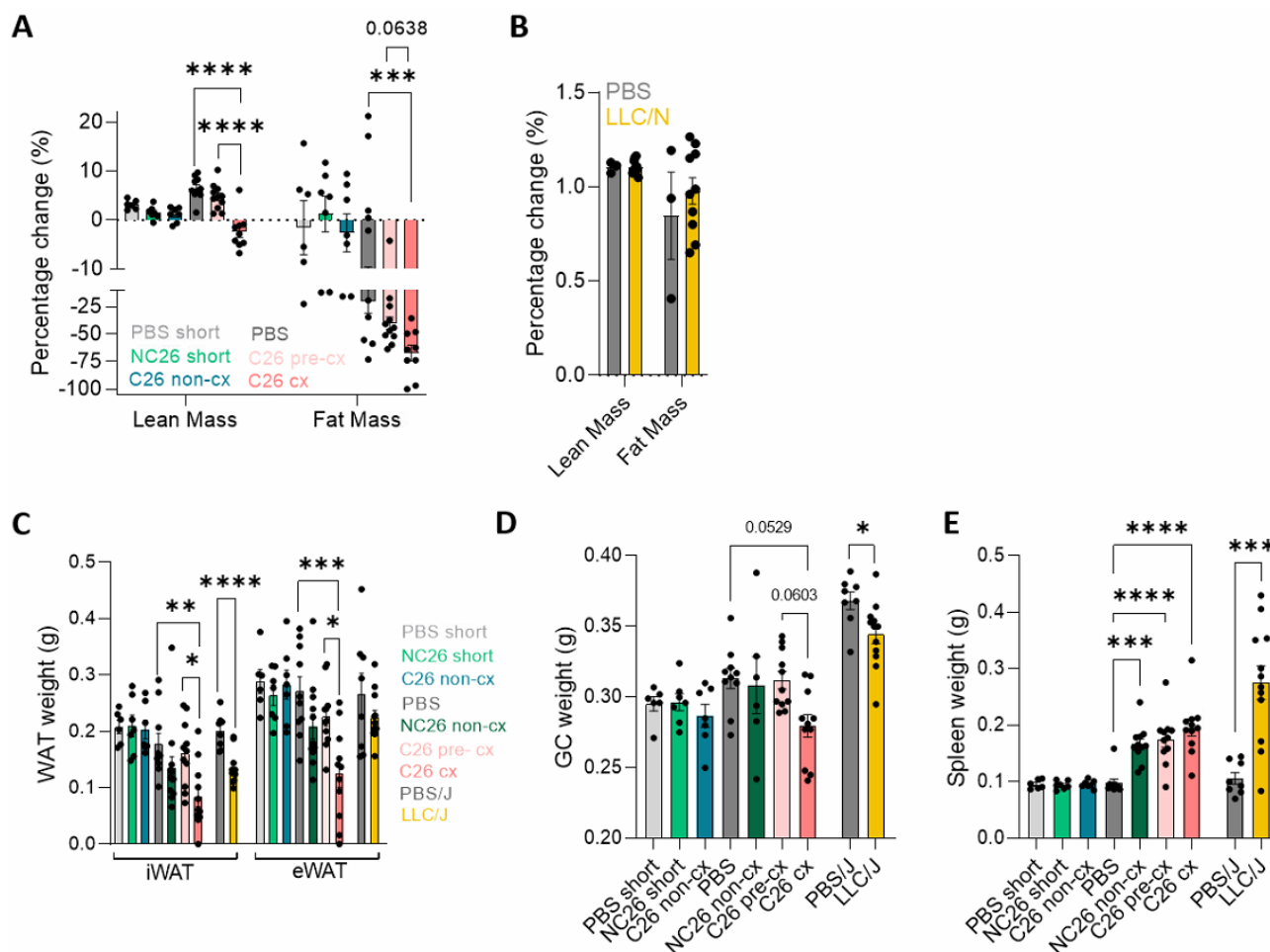

Figure 9. Cachexia is associated with tissue wasting. (A, B) Change in lean mass and body fat in **(A)** PBS short (n=6), NC26 short (n=7), C26 non-cx (n=7), PBS (n=10), C26 pre-cx (n=11) and C26 cx (n=9), and **(B)** PBS/N (n=3) and LLC/N (n=10) mice, as measured by EchoMRI. **(C, D, E)** Tissue weight of **(C)** iWAT and eWAT, **(D)** GC muscle and **(E)** spleen in PBS short (n=6), NC26 short (n=7), C26 non-cx (n=7), PBS (n=10), NC26 (n=12), C26 pre-cx (n=11) and C26 cx (n=11), and PBS/J (n=8) and LLC/J (n=12) mice. Data are mean ± s.e.m. Statistical analyses were performed using unpaired *t*-test or one-way ANOVA with Tukey's multiple-comparison *post hoc* test. *p<0.05, **p<0.01, ***p<0.001, ****p<0.0001.

Cancer cachexia influences circulating glucose and lipidome

In line with all previous results, C26 implantation had also the strongest effect on circulating glucose and lipid levels as assessed by plasma analysis (Figure 10). Cachectic C26 mice had significantly reduced circulating levels of glucose, while low density lipoprotein (LDL), cholesterol and non-esterified fatty acid (NEFA) levels were significantly elevated (Figure 10A, B, D, E). High density lipoprotein (HDL) and triglyceride (TG) levels were unchanged in all experiments (Figure 10C, F), inconsistent with already published data showing a decrease in TGs (Jones, 2013) and HDL (Dessí, 1992; Dessì, 1994) upon cancer cachexia. As expected, short-term presence of NC26 or C26 tumors did not alter any of the assessed circulating parameters (Figure 10), highlighting that solely cachexia onset and not tumor presence per se mediates alterations in circulating plasma parameters. Mice from the short control experiment had a general increase of TG levels (Figure 10F) compared to all other BALB/c mice. Interestingly, Chan *et al.* have shown that circulating TG levels are lower at the age of 20 weeks compared to 7 weeks (Y. K. Chan, 2012), and indeed, the mice from the short experiment were sacrificed at the age of 10 weeks, while all other BALB/c mice were between 16 and

18 weeks old at the moment of sacrifice. Circulating parameters behaved similarly in LLC tumor-bearing mice compared to the C26 model, except for NEFA levels which tended to be decreased upon LLC injection (Figure 10E).
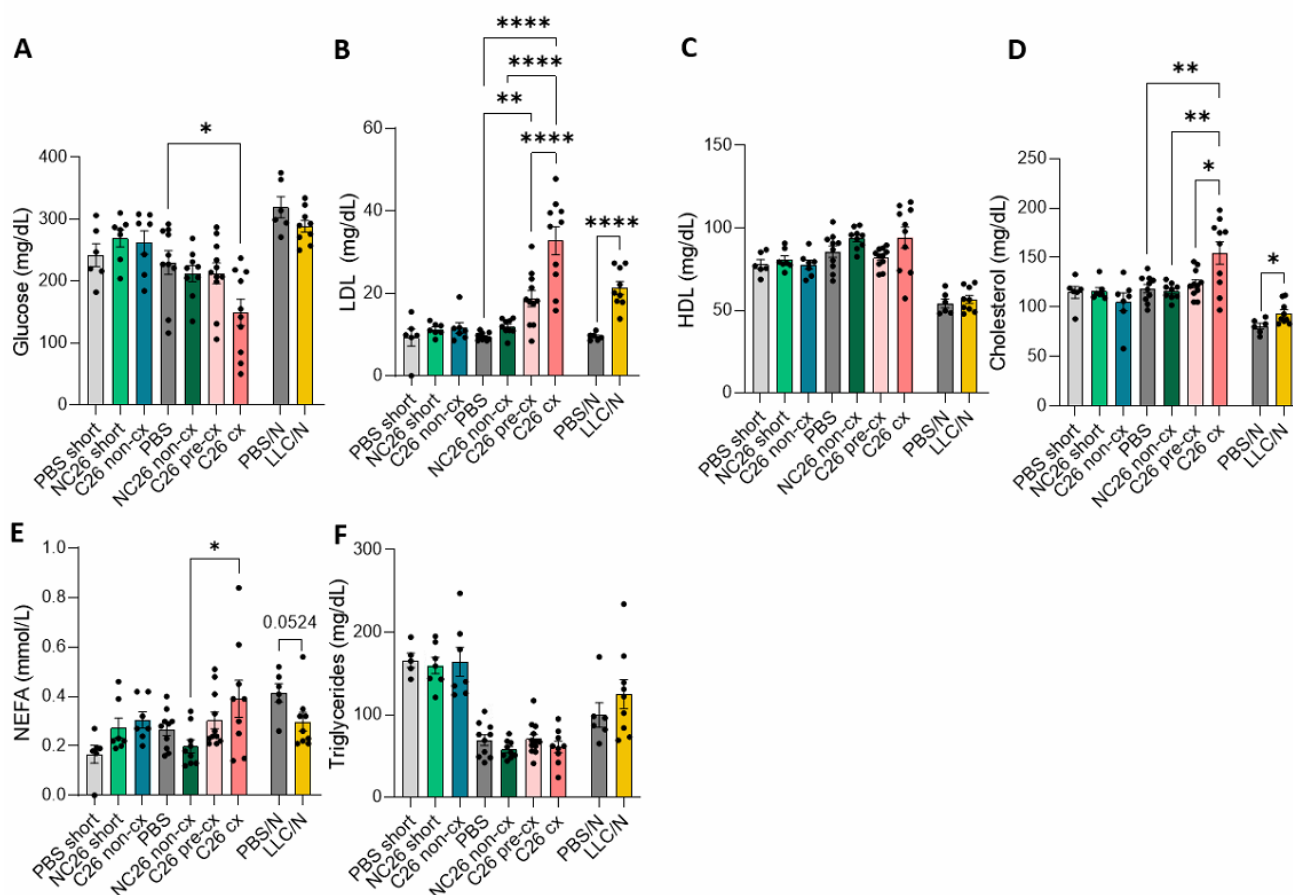
Figure 10. Cancer cachexia affects circulating levels of lipids and glucose. (A-F) Numbers of mice and color-coding same as in Figure 8. Circulating levels of **(A)** glucose, **(B)** low density lipoprotein (LDL), **(C)** high density lipoprotein (HDL), **(D)** Cholesterol, **(E)** non-esterified fatty acids (NEFAs), **(F)** triglycerides. Data are mean ± s.e.m. Statistical analyses were performed using unpaired *t*-test or one-way ANOVA with Tukey's multiple-comparison *post hoc* test. *p<0.05, **p<0.01, ****p<0.0001.

Food intake of cachectic C26 mice was increased at the end of the experiment and peaked before the final stages of cachexia (Figure 11A), in line with previous studies (Dwarkasing, 2014; Rohm, 2016). LLC tumor-bearing mice started to increase their food intake approximately 12 days post injection compared to PBS mice with an overall mild rise (Figure 11B).
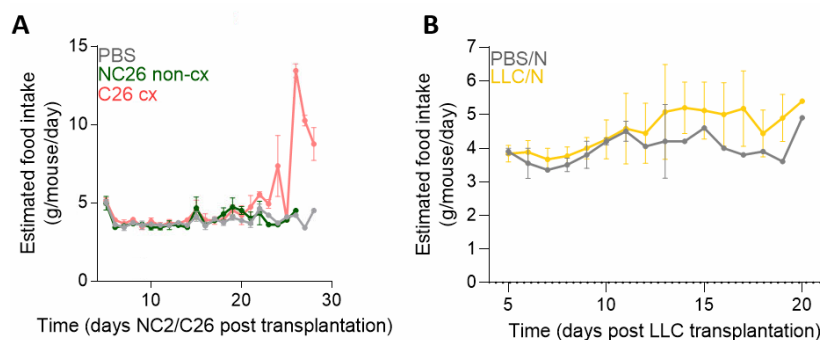

Figure 11. Estimated food intake of tumor-bearing mice is increased by cachexia. Same mice as in Figure 9. Estimated food intake in gram per mouse per day over the course of the experiment in **(A)** PBS, NC26 and C26 mice and **(B)** PBS and LLC mice.

2.1.2 The APC$^{Min/+}$ genetic model of cancer cachexia

The APC$^{Min/+}$ mouse, originally described as a model for colorectal cancer, has a heterologous mutation in the APC tumor suppressor gene predisposing these mice to the formation of intestinal polyps starting at the age of 4 weeks (Moser, 1990). APC$^{Min/+}$ mice suffer from a gradual bodyweight loss including muscle and adipose tissue wasting between 13 and 20 weeks of age, and thus were established as a model of cancer cachexia later on (Puppa, 2011). In combination with a stepwise increase in tumor burden, chronic inflammation and anemia, the progressive transition from a weight stable cancer condition to severe cachexia (Puppa, 2011), greatly mimics human cancer and cachexia burden, making the APC$^{Min/+}$ mouse a valuable model in cachexia research. In this study, cachexia was investigated in pre-cachectic and cachectic APC$^{Min/+}$ mice to identify early changes in disease development. In addition, young APC$^{Min/+}$ control mice were sacrificed between 11 and 13 weeks of age, prior to weight loss onset.

**The APC$^{Min/+}$ mouse is characterized by cancer-induced wasting**

APC$^{Min/+}$ mice grew in parallel with wildtype mice until the age of 15 weeks, when they started to progressively reduce weight gain compared to wildtype controls over a time course of about 6 weeks (Figure 12C). To calculate weight loss of APC$^{Min/+}$ mice, the highest bodyweight reached during the experiment was set as initial bodyweight to compensate for the continuous growth of the mice, whereas in wildtype mice the weight at 12 weeks of age was used as initial bodyweight. Pre-cachectic APC$^{Min/+}$ mice showed a reduced initial weight compared to age-matched wildtype or cachectic APC$^{Min/+}$ mice (Figure 12A). At the end of the experiment, cachectic and pre-cachectic mice had a significantly lower bodyweight compared to their wildtype controls, with strong bodyweight loss in cachectic APC$^{Min/+}$ mice, while pre-cachectic APC$^{Min/+}$ mice only suffered from mild weight loss (Figure 12A, B). Young control APC$^{Min/+}$ mice, sacrificed between 11 and 13 weeks showed a similar initial and final bodyweight, indicating that in this group cachexia was not present yet (Figure 12A, B). Figure 12D and E demonstrate that cachectic APC$^{Min/+}$ mice developed strong weight loss at the end of the experiment, while pre-cachectic APC$^{Min/+}$ mice only slightly altered their bodyweight, and age-matched wildtype mice increased their weight. Importantly, cachexia developed progressively over a time course of several days in APC$^{Min/+}$ mice (Figure 12D), resembling human cancer cachexia to a greater extent than the drastic C26 model.
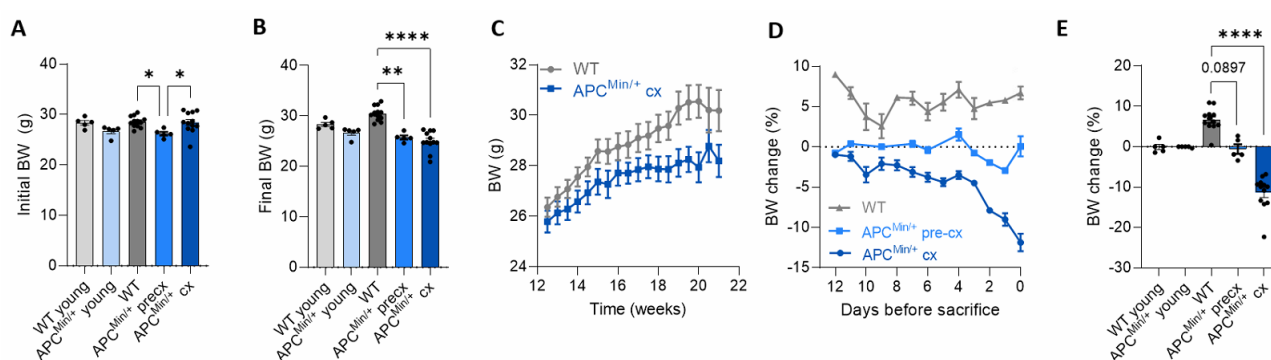
Figure 12. Cancer-induced wasting is a hallmark of the APC$^{Min/+}$ mouse model. (A) Initial and **(B)** final bodyweight of young (light blue, n=5), pre-cachectic (blue, n=5) and cachectic (dark blue, n=12) APC$^{Min/+}$ mice and their respective wildtype controls (young WT light grey, n=5; WT dark grey, n=12). **(C)** Time course of bodyweight development of WT (n=12) and APC$^{Min/+}$ (n=12) mice. **(D)** Bodyweight change in percentage starting 10 days prior to sacrifice in WT (n=12), APC$^{Min/+}$ pre-cx (n=5) and APC$^{Min/+}$ cx (n=12) mice. **(E)** Percentage of final bodyweight compared to initial/highest bodyweight in percentage. Same mice as in (A). Data are mean ± s.e.m. Statistical analyses were performed using unpaired *t*-test or one-way ANOVA with Tukey's multiple-comparison *post hoc* test. *p<0.01, **p<0.05, ****p<0.0001.

EchoMRI analyses confirmed these bodyweight changes, with APC[Min/+] mice developing significant adipose tissue wasting, while unexpectedly lean mass was unchanged (Figure 13A), strengthening that muscle wasting only appears at very late stages of cachexia development, in accordance with the C26 model. In line with these data, at the end of the experiment, APC[Min/+] mice showed significantly reduced iWAT and eWAT weight as well as GC muscle mass in both pre-cachectic and cachectic animals, with the strongest decrease in WAT in the latter (Figure 13B, C). As expected, young control mice did not show any differences in tissue weight mass (Figure 13B, C). As already shown (Lane, 2010), pre-cachectic and cachectic APC[Min/+] mice developed splenomegaly, probably due to increased extramedullary hematopoiesis (You, 2006) and elevated numbers of myeloid-derived suppressor cells (Gabrilovich, 2012), with spleens approximately 6-times bigger in size compared to wildtype controls (Figure 13D, E). Interestingly, spleen weight already started to non-significantly increase in young APC[Min/+] mice compared to age-matched wildtype mice (Figure 13D). This early onset of spleen enlargement might be explained by the potential impairment of stem cell differentiation in hematopoietic tissues due to the APC mutation. As stem cells exhibit a defect in their differentiation, they fail to mature, subsequently leading to extramedullary hematopoiesis in the spleen (You, 2006).
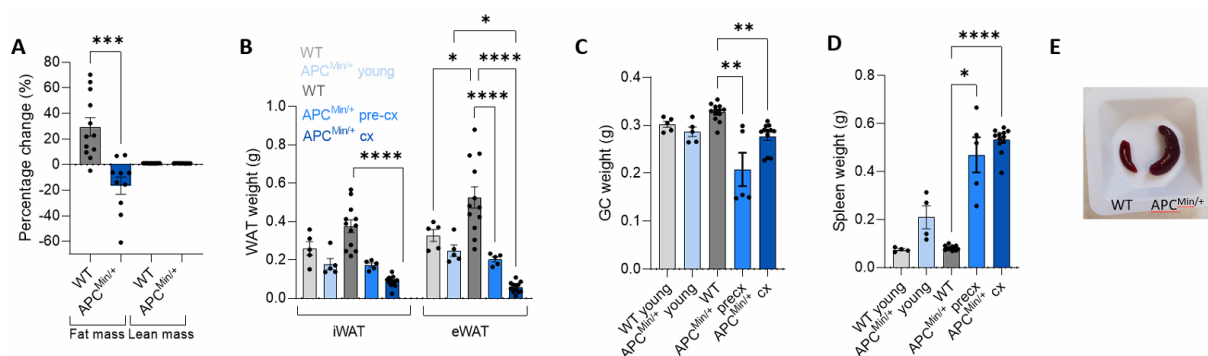
Figure 13. Tissue wasting is a hallmark of the APC[Min/+] mouse model. (A) Change in lean mass and body fat mass in percentage in WT (n=12) and APC[Min/+] (n=10) mice as measured by EchoMRI. **(B, C, D)** Tissue weights of **(B)** iWAT and eWAT, **(C)** gastrocnemius skeletal muscle and **(D)** spleen. Same mice as in Figure 12. **(E)** Exemplary picture of a WT and cachectic APC[Min/+] spleen. Data are mean ± s.e.m. Statistical analyses were performed using unpaired *t*-test or one-way ANOVA with Tukey's multiple-comparison *post hoc* test. *p<0.05, **p<0.01, ***p<0.001, ****p<0.0001.

Cachectic APC[Min/+] mice have altered circulating glucose and lipid levels

Pre-cachectic APC[Min/+] mice developed hypoglycemia (p=0.0966), which was worsened during the cachexia progression (Figure 14A). Additionally, cachectic mice showed elevated levels of LDL, Cholesterol, NEFAs and TGs, while HDL was decreased (Figure 14). Pre-cachectic APC[Min/+] mice displayed an intermediate state between wildtype and cachectic mice regarding LDL, cholesterol and triglyceride levels (Figure 14B, D, F), underlining the progressive transition of blood markers during cachexia development.

As expected, plasma parameters of young APC[Min/+] mice were not affected (Figure 14). In line with the strong increase in circulating lipids, plasma samples of APC[Min/+] mice showed a visible turbidity, called lipemia, as a result of a high concentration of lipoprotein particles (Farrell, 2016) (Figure 14G). Additionally, the severe anemia that APC[Min/+] mice were reported to develop over time (Lane, 2010) was observed by a decreased pellet of red blood cells when preparing plasma samples of these mice (Figure 14G).
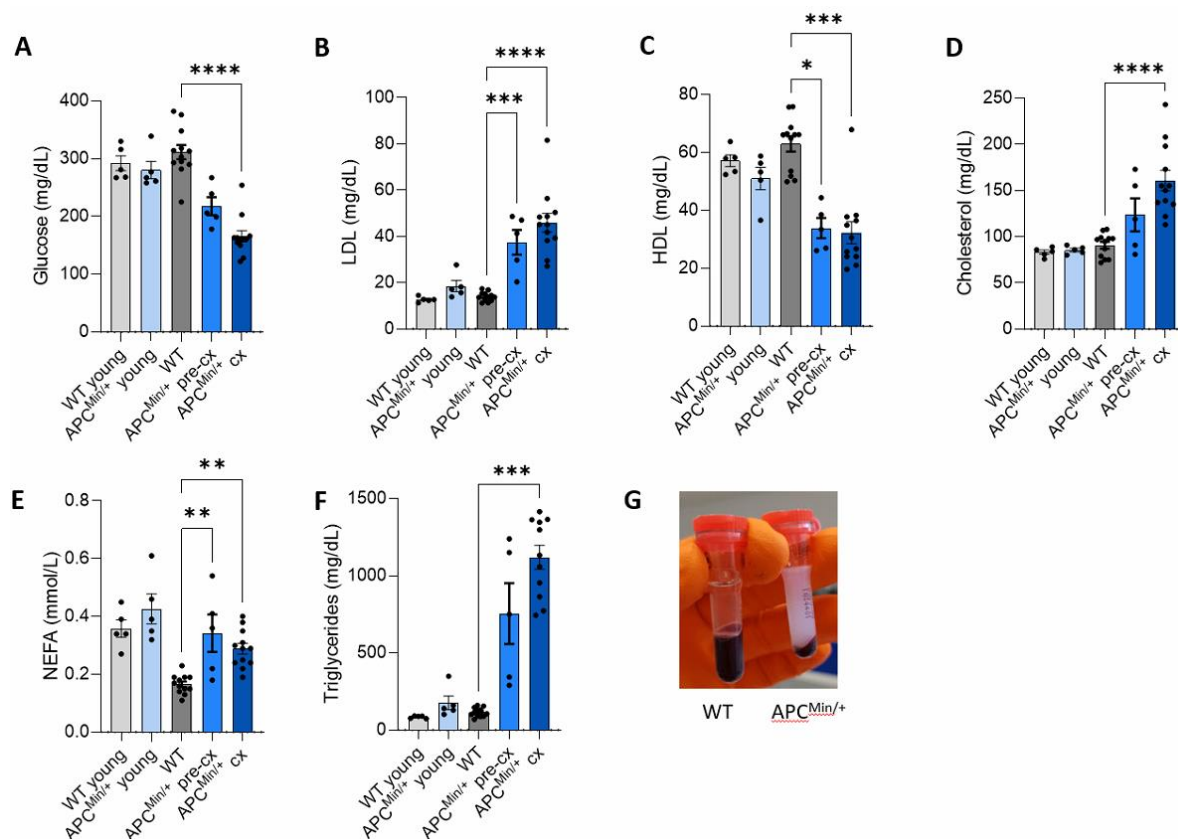
Figure 14. Plasma markers related to cachexia are altered in APC^Min/+ mice. (A-F) Numbers and color coding of mice is the same as in Figure 12. Plasma levels of **(A)** glucose, **(B)** LDL, **(C)** HDL, **(D)** Cholesterol, **(E)** NEFAs and **(F)** triglycerides. Data are mean ± s.e.m. Statistical analyses were performed using one-way ANOVA or Kruskal-Wallis test with Tukey's or Dunn's multiple-comparison *post hoc* test, respectively. *p<0.05, **p<0.01, ***p<0.001, ****p<0.0001.

2.2   Cachexia is associated with T cell lymphopenia in tissues

In the last decades, research on cancer immunotherapy has helped finding new and remarkably effective therapies for cancer treatment, including the use of immunological checkpoint inhibitors (Robert, 2020) or chimeric antigen receptor (CAR) T cells (June, 2018). In this context, low numbers of tumor-infiltrating lymphocytes (TILs) were noted to be a limiting factor for immunotherapy (Zappasodi, 2018), in line with a poor response to immunotherapy in melanoma patients with low T cell infiltration (Tumeh, 2014). Additionally, T cell infiltration into solid tumors was shown to be of high importance for a positive prognosis among different cancer types (Fridman, 2012). Regarding cachexia, a recent report showed that pre-treatment diagnosis of cancer cachexia strongly correlated with a reduced efficacy of PD1 or PD-L1 inhibitors in patients with advanced non-small cell lung cancer (Miyawaki, 2020). However, studies investigating the effect of cancer cachexia on TIL numbers are still scarce to date. Thus, I firstly aimed to assess if T cell infiltration into tissues was affected by cachexia onset.

T cell infiltration into cachectic tumors is reduced

Immunohistochemical analysis of cachectic (C26 cx, LLC) and non-cachectic (NC26 short, C26 non-cx, NC26 non-cx) tumors revealed a strong decrease in TILs upon cachexia, with especially reduced numbers of CD3+, CD4+ and FoxP3+ cells (Figure 15). Infiltrating CD8+ T cell numbers were unchanged in C26 cx tumors with a high variability compared to NC26 non-cx tumors and tended even to increase in C26 pre-cx tumors (Figure 15). CD4+ T cell infiltration into C26 tumors was increased upon pre-cachexia, while being strongly decreased in late-stage cachexia, also termed refractory cachexia,

underlining the still functional effector immune response in pre-cachectic mice, which seems to be diminished upon cachexia progression. LLC tumors revealed overall a very low infiltration of lymphocytes (Figure 15A). Tumors from the short experiment (NC26 short, C26 non-cx), showed increased infiltration of CD3^{+}, CD4^{+}, and FoxP3^{+} T cells compared to long-term tumor-bearing mice, possibly a result of increased infiltration shortly after implantation, and smaller tumor size with less necrotic tissue. In addition, T cell infiltration was similar between NC26 short and C26 non-cx tumors, indicating that reduced TIL numbers in cachectic C26 tumors were dependent on cachexia presence and not tumor-line specific (Figure 15).
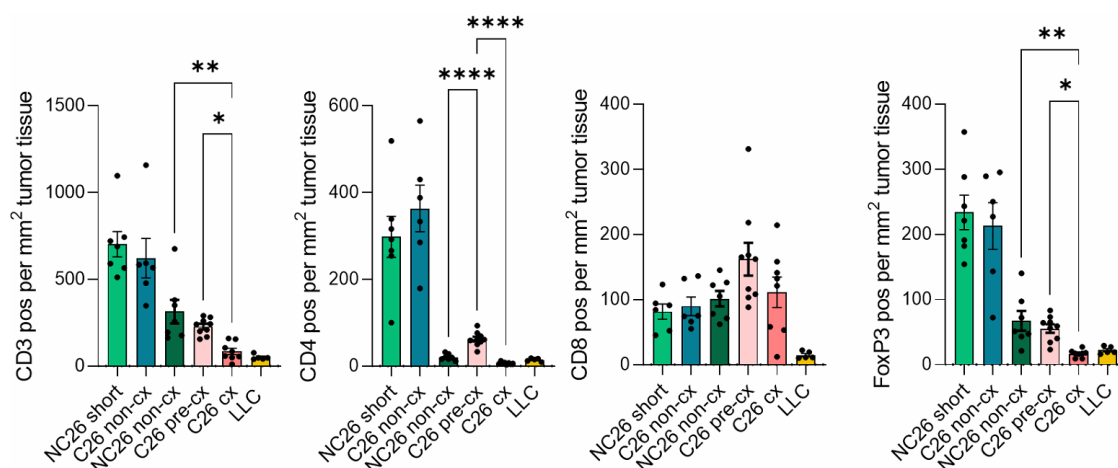
Figure 15. Reduced T cell numbers in cachectic tumors. Numbers of CD3-, CD4-, CD8- and FoxP3-positive cells in tumors of NC26 short (n=7), C26 non-cx (n=6), NC26 non-cx (n=7), C26 pre-cx (n=9), C26 cx (n=8) and LLC (n=5) mice. Data are mean ± s.e.m. Statistical analyses were performed using one-way ANOVA or Kruskal-Wallis test with Tukey's or Dunn's multiple-comparison *post hoc* test, respectively. To compare two groups to each other, unpaired *t*-test was conducted. *p<0.05, **p<0.01, ****p<0.0001.

The strong decrease in TILs by immunohistochemical analysis was verified using flow cytometry. Thereby, a trend towards a decrease in both CD4^{+} and CD8^{+} T cells was found in cachectic C26 compared to non-cachectic NC26 tumors (Figure 16A). There was a strong positive correlation between the number of CD3^{+} cells and bodyweight change, meaning the higher the bodyweight loss the less T cells were present in tumor tissue (Figure 16B), in line with the important role of TILs for patient outcome (Fridman, 2012). This correlation was not observed in the short-term presence of NC26 and C26 tumors (Figure 16B), again implying that cancer cachexia solely impairs T cell infiltration. In patients, a non-significant reduction of *CD3E* gene expression was observed in weight losing (CCx) *vs.* weight stable cancer (WSC) patients (Figure 16C), implying translational potential of the data collected in our mouse models of cancer cachexia. Of note, there was a mild trend for a correlation of CD3E expression and bodyweight change in colon cancer patients (p= 0.1068).
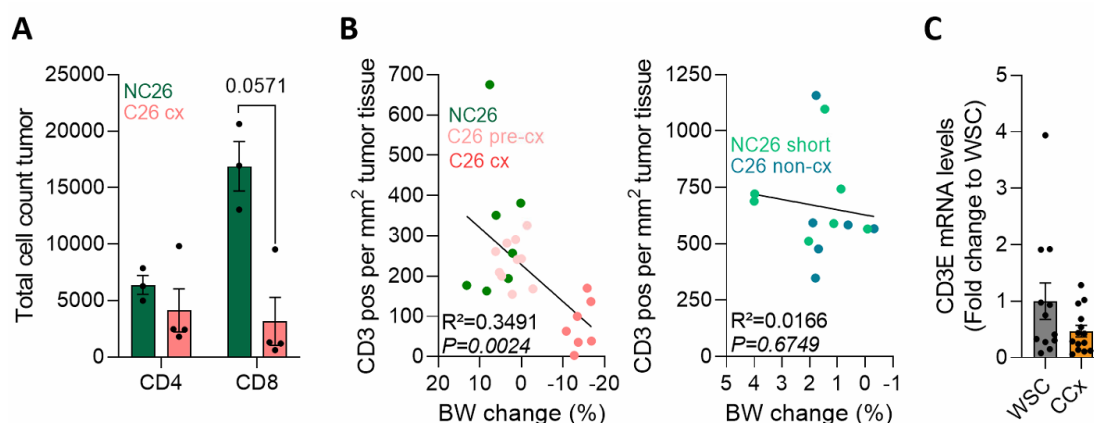
Figure 16. TIL numbers positively correlated with bodyweight change, and murine data show translational potential to humans. (A) Total cell count of CD4$^+$ and CD8$^+$ cells in NC26 non-cx (n=3) and C26 cx (n=4) tumors, assessed by flow cytometry. **(B)** Correlations of CD3$^+$ cells and bodyweight change in NC26 non-cx (n=7), C26 pre-cx (n=10), C26 cx (n=7), NC26 short (n=7) and C26 non-cx (n=7) mice. **(C)** Expression of *CD3E* in weight-stable cancer (WSC, n=12) and cachectic cancer (CCx, n=14) patients. Data are mean ± s.e.m. Statistical analyses were performed using unpaired *t*-test. Correlations were analyzed using linear regression analysis.

Decreased numbers of CD3$^+$ T cells in cachectic tumors of mice were shown to be a result of reduced proliferation, as indicated by less CD3$^+$Ki67$^+$ double positive cells in C26 cachectic tumors (Figure 17A). A reduction of TILs in cachectic tumors due to increased apoptosis could be excluded by terminal deoxynucleotidyl transferase dUTP nick end labeling (TUNEL) staining (Figure 17B). Using the TUNEL assay, apoptotic cells can be detected by labeling double-strand DNA breaks that occur during the late stages of apoptosis (Kyrylkova, 2012). Thus, co-staining of TUNEL and the general T cell marker CD3, led to the identification of a similar number of apoptotic T cells in NC26 and C26 tumors (Figure 17B). In addition, chemokines play an important role by regulating recruitment of immune cells into tumors (Allavena, 2011). Upon cancer cachexia, altered gene expression levels related to chemokines were found in cachectic C26 tumors compared to pre-cachectic C26 and non-cachectic NC26 tumors (Figure 17C). *Cxcl9* and *Cxcl11*, both involved in CXCR3-dependent T cell chemotaxis, were decreased in cachectic compared to pre-cachectic C26 tumors, in line with a previous report by Flint and colleagues (Flint, 2016). *Ccl4* gene expression was significantly downregulated in C26 cx *vs.* C26 pre-cx tumors, while being unchanged compared to NC26 tumors. Interestingly, the presence of both Cxcl9 and Ccl4 has been linked to the presence of CD8$^+$ TILs in melanoma biopsies (Harlin, 2009), underlining the potential relation between reduced T cell infiltration and chemokine expression in cachectic C26 tumors. Cachectic tumors showed a significant increase in *Cx3cl1* gene expression (Figure 17C), an important TIL-recruiting chemokine that was associated with positive outcome upon different tumor onsets (Conroy, 2020). In summary, these data show that the reduction of TILs in cachectic tumors might be a result of reduced T cell infiltration into cachectic tumors due to altered chemokine levels, in combination with reduced proliferation.
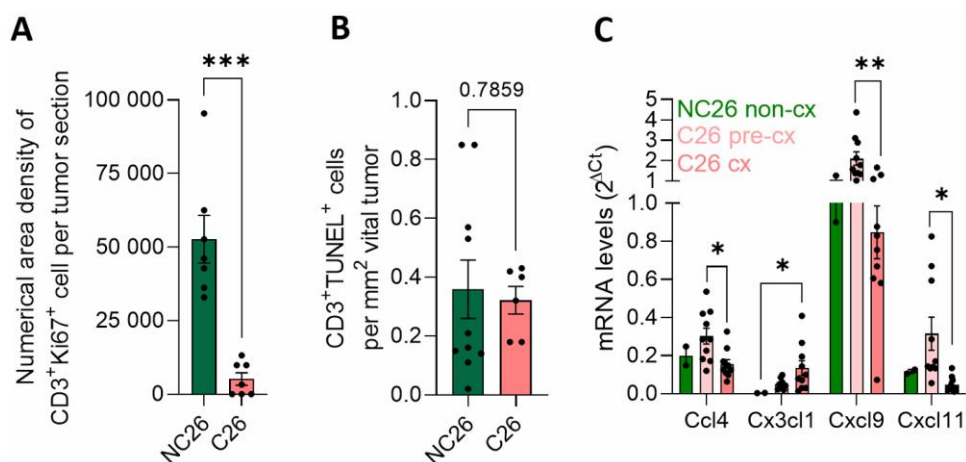
Figure 17. Proliferation and altered chemokine levels potentially mediate reduction of T cell numbers in cachectic tumors. (A) Quantification of CD3$^+$Ki67$^+$ double-positive cells in NC26 (n=7) and C26 (n=7) tumors, measured by immunohistochemical staining. **(B)** Numbers of CD3$^+$TUNEL$^+$ cells in NC26 (n=10) and C26 (n=6) tumors. **(C)** mRNA levels of different chemokines in tumors of NC26 (n=2), C26 pre-cx (n=10), and C26 cx (n=10) mice. Data are mean ± s.e.m. Statistical analyses were performed using one-way ANOVA or Kruskal-Wallis test with Tukey's or Dunn's multiple-comparison *post hoc* test, respectively. To compare two groups to each other, unpaired *t*-test was conducted. *p<0.05, **p<0.01, ***p<0.001.

**T cell infiltration into metabolic tissues is decreased**

Systemic inflammation is a major hallmark of cancer cachexia (Webster, 2020), affecting not only the circulation but also tissues, such as muscle and adipose tissue (Batista, 2016; Webster, 2020). As T cells are known to be involved in controlling tissue inflammation in obesity (R. Liu, 2019), we hypothesized that T cells might be potent, targetable regulators of tissue inflammation in cachexia, worsening the pro-inflammatory state and metabolic dysfunction. To this end, T cell infiltration and characteristics were investigated in adipose tissues and skeletal muscle of cachectic and non-cachectic tumor-bearing mice using flow cytometry and gene expression analysis. Opposite to our hypothesis, gene expression analysis of eWAT and GC muscles revealed a reduction in T cell-related marker genes (Figure 18A). Hereby, *Cd8* and *Foxp3* were significantly downregulated in cachectic eWAT, while *Cd4* was only non-significantly reduced. Expression in GC muscles was of high variability, but all three genes *Cd8*, *Cd4* and *Foxp3* were non-significantly decreased in cachectic compared to non-cachectic NC26 tumor-bearing or healthy PBS control mice, in agreement with a previously published report (Berardi, 2008). Recently published data reported strong positive correlations between numbers of muscle-infiltrating T cells and muscle mass in cancer patients (Anoveros-Barrera, 2019), underlining the possible link between T cell numbers and muscle wasting upon cachexia. Gene expression results were verified by flow cytometric analysis of eWAT, iWAT and GC muscles to assess the total count of CD4^{+} and CD8^{+} cells (Figure 18B). CD4^{+} T cell numbers were significantly reduced in eWAT and GC of cachectic mice, while being unchanged in iWAT. CD8^{+} tended to be decreased in GC muscle and to a lower extent in iWAT and eWAT.
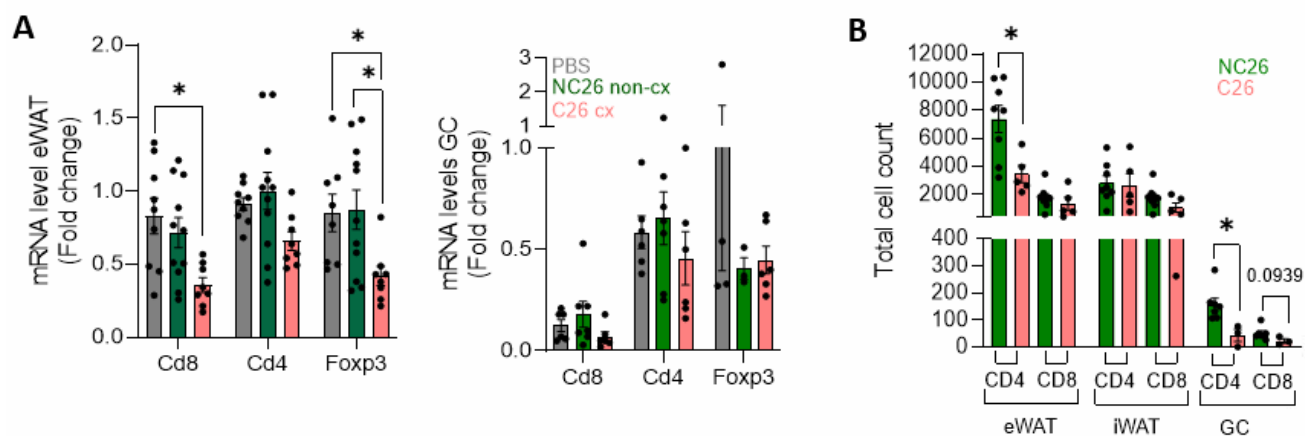
Figure 18. Reduced T cell infiltration into metabolic tissues. (A) Gene expression levels of T cell marker genes in eWAT of PBS (n=10), NC26 (n=11) and C26 cx (n=8) mice, and GC muscle in PBS (n=6), NC26 (n=7) and C26 cx (n=6) mice. **(B)** Total cell count of CD4^{+} and CD8^{+} cells in eWAT, iWAT (NC26 n=8, C26 cx n=5) and GC (NC26 n= 7, C26 cx n=3), as assessed by flow cytometry. Data are mean ± s.e.m. Statistical analyses were performed using one-way ANOVA or Kruskal-Wallis test with Tukey's or Dunn's multiple-comparison *post hoc* test, respectively. To compare two groups to each other, unpaired *t*-test was conducted. *p<0.05.

Proliferative status of CD4^{+} and CD8^{+} T cells in WAT and GC of non-cachectic NC26 and cachectic C26 tumor-bearing mice was investigated by staining of Ki67^{+} T cells and subsequent flow cytometric analysis. To confirm that staining was not affected and still functional despite collagenase treatment of tissue samples, non-draining lymph nodes (ndLNs) were used as positive staining controls as they were not treated with collagenase. The percentage of Ki67^{+}CD4^{+} T cells was unaltered in eWAT, iWAT and GC, while interestingly the percentage of Ki67^{+}CD8^{+} cells tended to be non-significantly increased in WAT and GC, indicating elevated proliferation of CD8^{+} T cells upon cachexia. CD62L, a marker for naïve T cells, playing an important role in T cell migration and homing to lymph nodes (Arbonés, 1994; Kahn, 1994), showed significantly elevated expression on CD8^{+} T cells from WAT and GC (Figure 19B),

indicating an increase in naïve CD8^{+} T cells, and thus a decrease in effector CD8^{+} T cells. As expected, almost 100% of CD4^{+} and CD8^{+} T cells were CD62L-positive, as CD62L is of high importance for lymphocyte homing to lymph nodes (Ley, 2004). CD62L expression was unaltered on CD4^{+} tissue-infiltrating T cells (Figure 19B). An additional way to assess immune health, is the calculation of the CD4/CD8 ratio as a substitute marker for immune senescence (Bruno, 2017). To this end, I thus analyzed the CD4/CD8 ratio in several metabolic tissues including eWAT, iWAT and GC (Figure 19C). I observed an increase in the CD4/CD8 ratio in cachectic WAT, while GC was unaffected. The percentage of FoxP3^{+}CD4^{+} regulatory T cells (Tregs) was unchanged in WAT and GC of C26 tumor-bearing mice (Figure 19D).
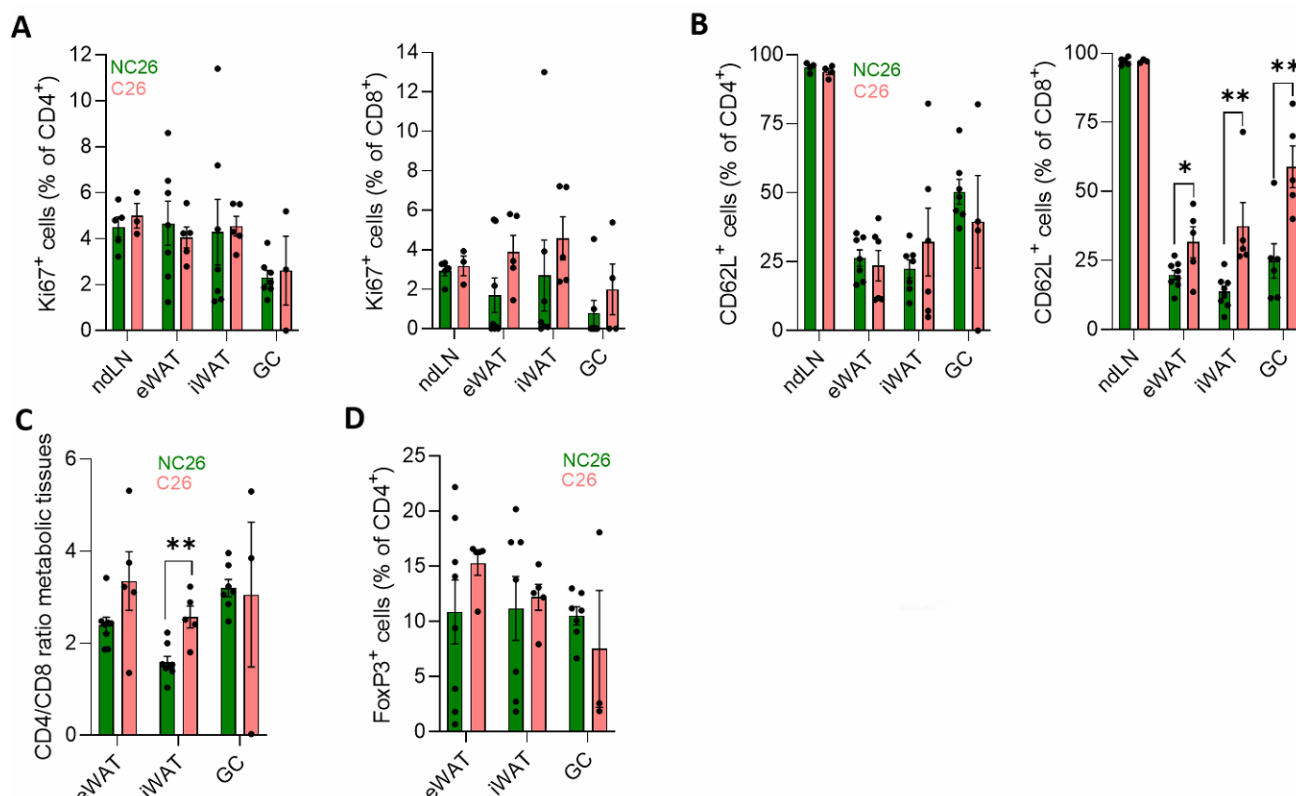
Figure 19. T cells in metabolic tissues are less activated and display a higher percentage of regulatory T cells. Numbers of individual mice used for each experiment are indicated by single plotted dots. **(A)** Ki67^{+} cells as percentage of CD4^{+} or CD8^{+} T cells in non-draining lymph nodes (ndLNs), eWAT, iWAT and GC in NC26 and C26 cx mice. **(B)** Naïve CD62L^{+} cells as percentage of CD4^{+} and CD8^{+} T cells in ndLNs, eWAT, iWAT and GC, assessed by flow cytometry. **(C)** CD4/CD8 ratio of T cells in metabolic tissues (eWAT, iWAT, GC). **(D)** FoxP3^{+} regulatory T cells as percentage of CD4^{+} T cells in eWAT, iWAT and GC of NC26 and C26 tumor-bearing mice, data were collected by flow cytometric analyses. Data are mean ± s.e.m. Statistical analyses were performed using unpaired *t*-test. *p<0.05, **p<0.01.

To assess the relevance and cachexia-specificity of the tissue-infiltrating T cell depletion, I correlated TIL numbers with the bodyweight change and weight of several organs. There was a strong positive correlation between tumor-infiltrating T cell numbers, especially CD4^{+} and FoxP3^{+} T cells and weight of cachexia-associated organs such as eWAT, iWAT, and GC muscle in the experiment with cachectic C26 and non-cachectic NC26 mice (Figure 20C, red squares). Thus, higher bodyweight change (meaning no bodyweight loss), as well as eWAT, iWAT and GC weight correlated strongly with higher numbers of TILs, while contrary, increased TIL numbers were associated with reduced tumor weight. Importantly, these correlations were already present in pre-cachectic/cachectic C26 mice (Figure 20B), while not being present in non-cachectic C26/NC26 tumor-bearing mice (Figure 20A). To control for the quality of the correlations, I had a closer look at bodyweight change and its relation to the different organs among cachexia. As expected, I found a strong positive correlation between

bodyweight loss and organ wasting upon cachexia (Figure 20C, blue square), and to lesser extent in pre-cachexia (Figure 20B), while there was no correlation in non-cachectic mice (Figure 20A).
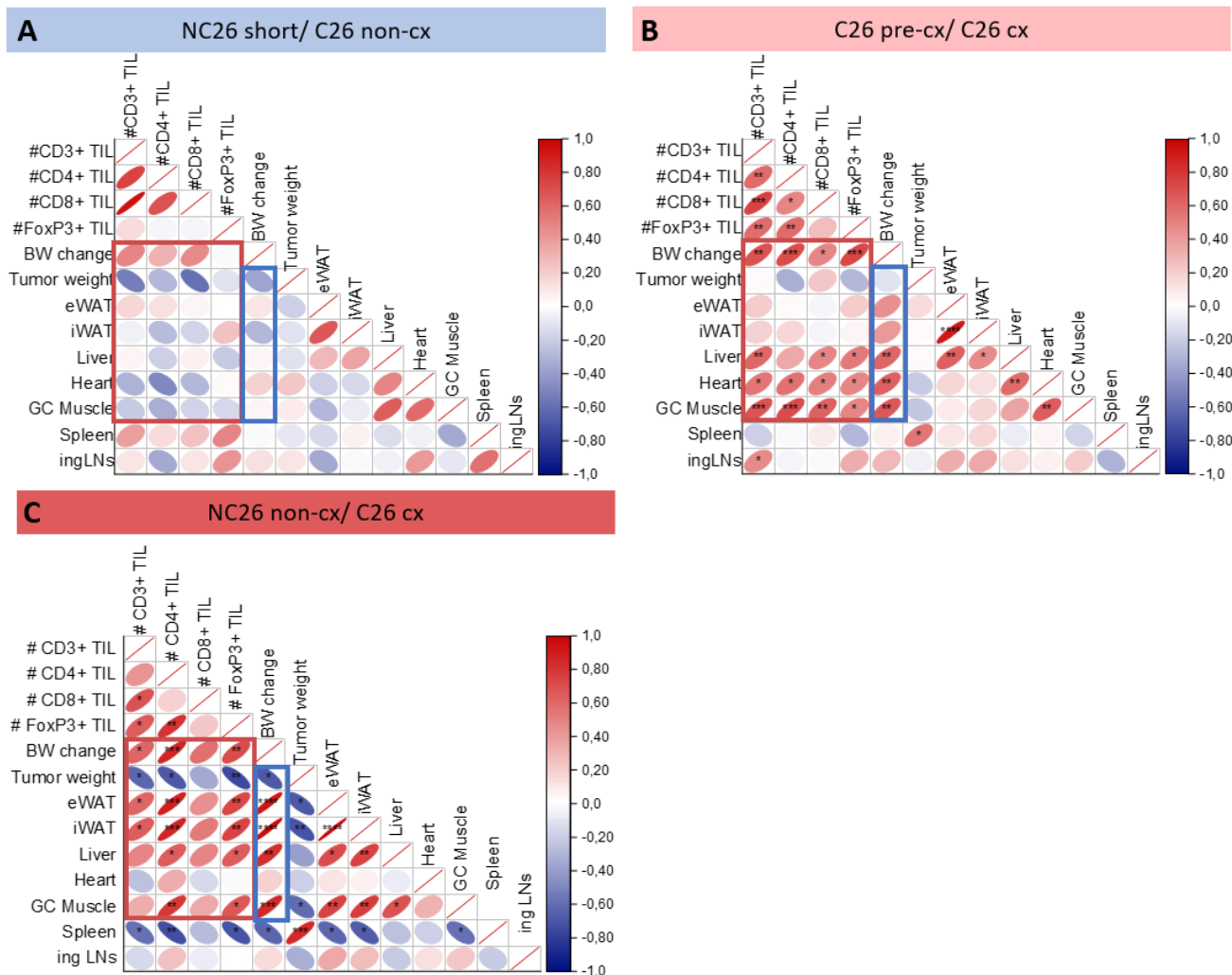
Figure 20. Numbers of tumor-infiltrating T cells strongly correlate with weight of metabolic organs. Pearson correlation matrices of TIL numbers, bodyweight change (in percentage) and tissue weights in **(A)** non-cachectic C26 and NC26 mice from the short-term study, **(B)** pre-cachectic and cachectic C26 mice and **(C)** cachectic C26 and non-cachectic NC26 mice. The angle of the ellipse indicates whether the correlation is positive (1.0) or negative (-1.0) and in addition, the size of the ellipse is associated with the Pearson coefficient. The smaller the width of the ellipse, the closer the Pearson coefficient was to 1.0/-1.0. Color coding can be looked up at the color scale ranging from -1.0 (blue) to 1.0 (red). Red squares highlight correlations between numbers of TILs and important cachexia-associated organs, while blue squares highlight the association between bodyweight change (in percentage) and organ weight. Significances of the correlations are indicated using *p<0.05, **p<0.01, ***p<0.001, ****p<0.0001.

Next, tissue infiltration of other immune cell types from innate and adaptive immunity was assessed to investigate cachexia-mediated alterations. Gene expression analyses of *Adgre1* (encoding F4/80) and *Cd68*, both macrophage marker genes, revealed no changes in eWAT, but a significant decrease in GC muscles of pre-cachectic and cachectic C26 mice (Figure 21A), in line with Inaba *et al.* (Inaba, 2018). Of note, in collaboration with the HMGU core facility for Pathology & Tissue Analytics we also stained tumor sections of NC26 and C26 tumors with F4/80 and CD68 for immunohistochemical detection of macrophages. However, due to cross-immunoreactivity of tumor cells, quantification by digital image analysis was not possible (data not shown). Expression of *Cd161* and *Cd335*, both related to Natural Killer (NK) cells, was downregulated in pre-cachectic and cachectic eWAT and GC, while being increased in non-cachectic NC26 tumor-bearing mice compared to PBS injected animals (Figure 21B), implying elevated NK cell infiltration into NC26 and decreased numbers in C26 metabolic

tissues. *Cd19* gene expression levels, indicating B cell presence, were decreased in eWAT and GC of NC26 tumor-bearing mice compared to pre-cachectic C26 and PBS-injected animals, and tended to be decreased as well in cachectic mice (Figure 21C). *Cd205*, a marker for Dendritic cells, was unchanged between all groups (Figure 21D).
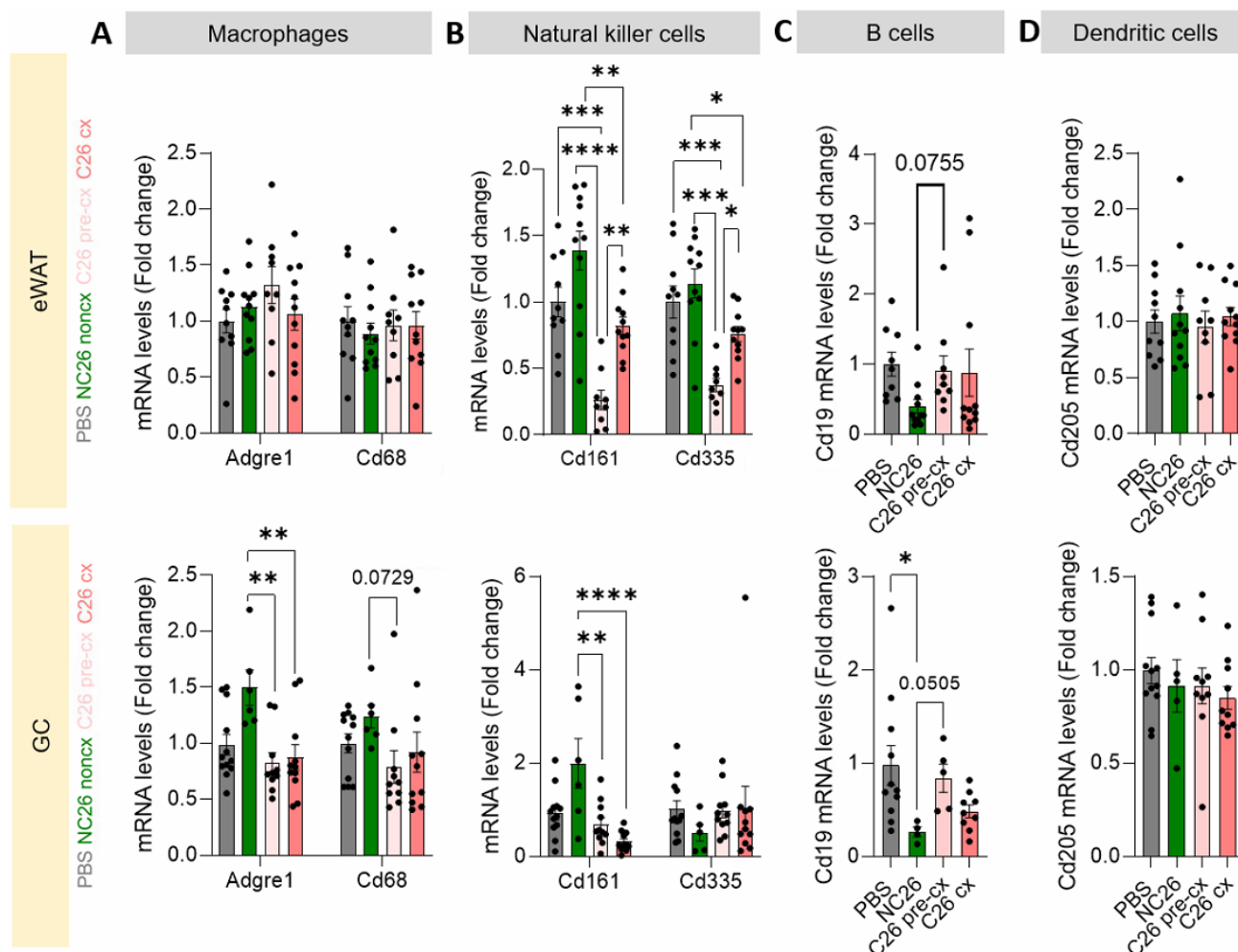
Figure 21. Expression levels of markers associated with innate and adaptive immunity are altered in C26 tumor-bearing mice. Gene expression in eWAT (PBS n=10; NC26 n=11; C26 pre-cx n=9; C26 cx n=11) and GC (PBS n=12; NC26 n=4-6; C26 pre-cx n=5-11; C26 cx n=9-11) of markers associated with **(A)** macrophages (*Adgre1, Cd68*), **(B)** natural killer cells (*Cd161, Cd335*), **(C)** B cells (*Cd19*) and **(D)** dendritic cells (*Cd205*). Data are mean ± s.e.m. Statistical analyses were performed using one-way ANOVA or Kruskal-Wallis test with Tukey's or Dunn's multiple-comparison *post hoc* test, respectively. *p<0.05, **p<0.01, ***p<0.001, ****p<0.0001.

Splenic T cell numbers tend to be reduced in cachectic mice

Numbers of splenic T cells tended to be decreased in cachectic C26 compared to non-cachectic PBS and NC26 control mice, as indicated by immunohistochemical analysis of CD3^{+} cells in the spleen (Figure 22). While the occurrence of CD8^{+} T cells was unchanged, CD4^{+} T cells were strongly decreased, thereby probably in part accounting for the decreased numbers of CD3^{+} splenocytes. FoxP3^{+} Tregs were unaltered between all three groups.
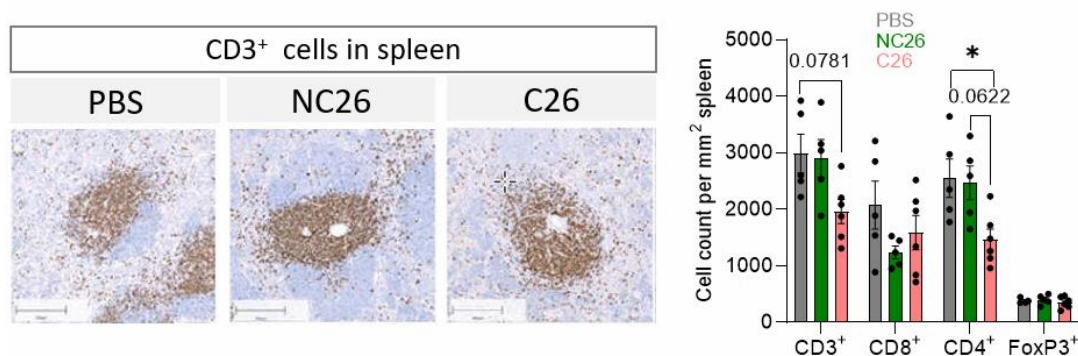
Figure 22. Splenic T cell numbers tend to be decreased in cancer cachexia. Representative images of immunohistochemical staining of CD3-positive cells in spleen sections of PBS (n=5), NC26 (n=4) and C26 (n=6) mice. Quantification of CD3$^+$, CD8$^+$, CD4$^+$ and FoxP3$^+$ cells per mm^2 tissue. Immunohistochemical stainings were assessed by the core facility Pathology & Tissue Analytics at the Helmholtz Center Munich. Data are mean ± s.e.m. Statistical analyses were performed using one-way ANOVA or Kruskal-Wallis test with Tukey's or Dunn's multiple-comparison *post hoc* test, respectively. **p<0.01.

2.3 Modified ceramides are elevated in cancer cachexia

The presence of immune cells in adipose tissue has been investigated extensively in the past, with its main focus on obesity (Duffaut, 2009; Nishimura, 2009; Rausch, 2008; H. Wu, 2007). In this context, the potential contribution of immune cells to diseases such as metabolic dysfunction has been appreciated (Mauro, 2012; Rocha, 2009). On the molecular level, Han and colleagues have shown that a pathogen-dependent increase of the immune defense in WAT alters adipose tissue function by suppression of pathways linked to lipid metabolism (S. J. Han, 2017). Since I have noted altered immune cell infiltration of WAT upon cachexia, we hypothesized subsequent changes in lipid metabolism, specifically the plasma lipidome. To this end, together with Pauline Morigny, I performed several cancer cachexia mouse studies, including PBS and NC26, pre-cachectic and cachectic C26 animals, mice with short-term presence of tumors (PBS short, NC26 short, C26 non-cx), as well as LLC, wildtype and APC$^{Min/+}$ mice (similar to Figure 6). Additionally, plasma of cachectic *versus* weight stable cancer patients was analyzed. Using plasma, a broad range lipidomic analysis was performed in collaboration with the core facility Metabolomics & Proteomics. Plasma lipids were analyzed using FIA-MS/MS and the Lipidyzer^{TM} platform, in which a total of 13 lipid classes and more than 1100 lipid species were analyzed. A detailed description of the study can be found in Morigny and Zuber *et al.* (Morigny&Zuber, 2020).

The circulating lipidome alters upon cancer cachexia

Using PLS-DA analysis, we investigated the separation of the different cx and non-cx groups in each experiment based on their circulating lipid profile (Figure 23A). C26 cx, non-cachectic NC26 and PBS control mice groups were separated in the PLS-DA analysis. NC26 and PBS mice had a rather similar lipid profile as suggested by the overlap of their ellipses in the PLS-DA analysis. Interestingly, C26 pre-cx mice showed an intermediate lipid profile between cachectic C26 and healthy PBS mice, indicating that the stepwise development of cancer cachexia is accompanied by a gradual change of the circulating lipid profile. As expected, there was no difference between the groups from the short experiment, as indicated by the strong overlap of PBS short, NC26 short and C26 non-cx mice (Figure 23A), underlining that changes in the cachectic lipid profile solely rely on cachexia development and are not tumor cell line dependent. Additionally, the profound impact of cachexia on the plasma lipidome as assessed in cachectic C26 mice was confirmed in the implantation LLC mouse model and the genetic APC$^{Min/+}$ model, which both developed markedly altered lipid profiles associated with

cachexia (Figure 23A). To assess alterations in the quality and quantity of the circulating lipid species in non-cachectic and cachectic mice, volcano plots were used to highlight differences (Figure 23B). Thereby, we detected commonly regulated lipid species in cachectic mice among the different mouse models used, such as an increase in sphingolipid species, like sphingomyelines (SMs), ceramides (CERs), hexosyl-ceramides (HCERs) and a decrease in lysophosphatidylcholines (LPCs). Importantly, these lipid classes were largely non-regulated in non-cachectic C26 mice from the short experiment, implying the specific dysregulation of these lipids by cachexia.
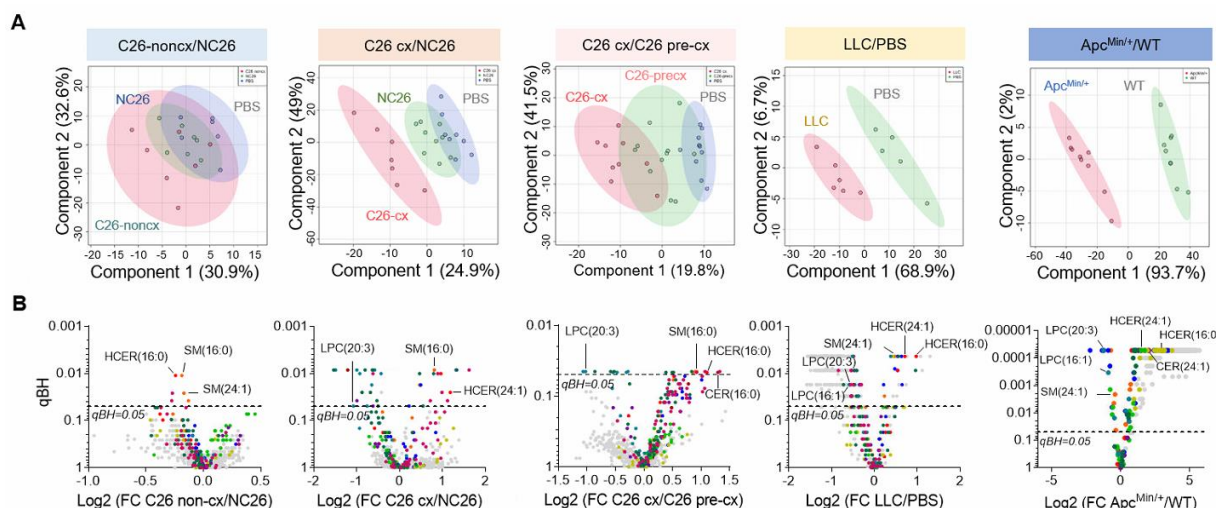
Figure 23. Circulating lipid profile is altered in cancer cachexia. (A) Partial least squares-discriminant analysis (PLS-DA) scoreplots of plasma lipid species show similarities and dissimilarities between different groups (PBS short n= 6, NC26 short n=7, C26 non-cx n= 7; PBS n=8-10, NC26 n=9, C26 cx n=7-9; C26 pre-cx n=11; C57BL/6 PBS n=5, LLC n= 6; wildtype n=9, APC[Min/+] n=9). PLS-DAs were applied using MetaboAnalyst4.0 and ellipses show 95% confidence intervals for the individual group. **(B)** Same mice than in (A). Changes in lipid species between indicated groups are shown as volcano plots, and are represented by Log2 fold change (FC). The adjusted P value (qBH) of 0.05 is indicated by the dashed lines. Statistical analyses were performed using two-sided Wilcoxon rank sum tests and p values were adjusted for multiple testing using the Benjamini-Hochberg correction method. This study was conducted in collaboration with Pauline Morigny and data collection and analysis were shared equally between us. Figure based on (Morigny&Zuber, 2020).

Next, changes in all lipid classes, potentially altered by cancer cachexia, were assessed. (Figure 24A-D). In total, 13 lipid classes were covered by the Lipidyzer™ platform and a detailed analysis of each of them can be found in (Morigny&Zuber, 2020), however, the focus of this thesis will be on the most strongly cachexia-regulated lipid classes. LPCs were mainly decreased in the plasma of cachectic C26 and LLC mice, while being unchanged in C26 non-cx and NC26 mice (Figure 24A), in accordance with the previously published decrease of LPC plasma levels in cachectic cancer patients (Cala, 2018). In addition, we found SMs, CERs and HCERs, all belonging to the sphingolipid family, to be elevated in practically all cachexia models, while being unchanged in C26 non-cx mice (Figure 24A-D). Importantly, similar to the PLS-DA analysis, C26 pre-cx mice again displayed an intermediate state between PBS and C26 cx animals, with a gradual rise of circulating sphingolipids as cachexia progressed. Interestingly, in a very comprehensive metabolomic analysis, O'Connell and colleagues have recently observed similar changes in cachectic C26 tumor-bearing mice, including a strong reduction in LPC species and an increase in lipid classes related to the sphingolipid family (O'Connell, 2021).
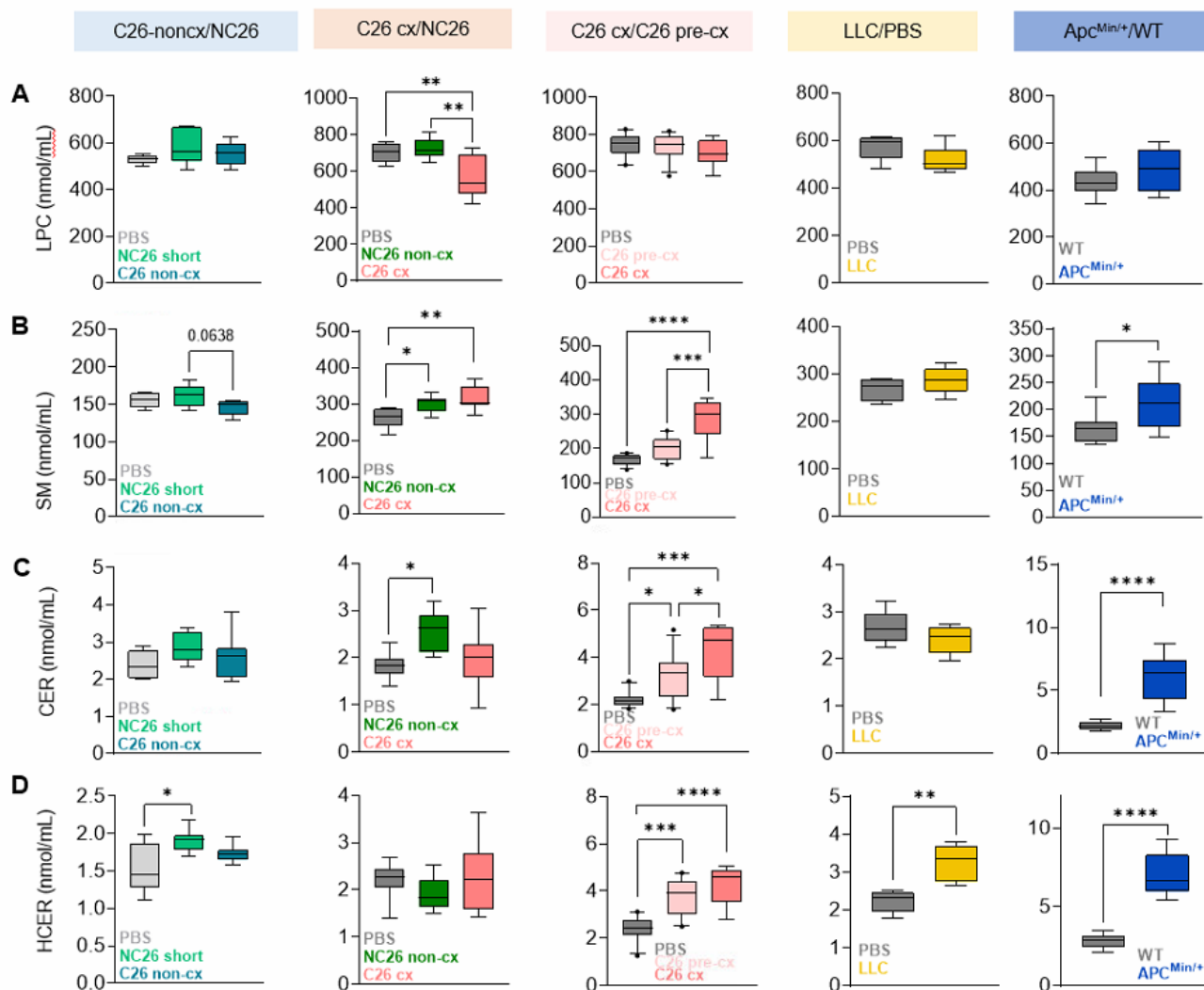
Figure 24. Cachexia alters lysophosphatidylcholine and sphingolipid classes in cachectic tumor-bearing mice. (A-D) Lipid class sum concentrations are shown for **(A)** lysophosphatidylcholine (LPC), **(B)** sphingomyelins (SM), **(C)** ceramides (CERs) and **(D)** hexosyl-ceramides (HCER) in same mice than Figure 23. Data are plotted as median 10-90 percentile. One-way ANOVA or Kruskal-Wallis test with Tukey's or Dunn's multiple-comparison post hoc test, respectively, were performed to compare lipid class sum concentrations in experiments with three groups, while unpaired t test or Mann-Whitney test were conducted to compare two groups. Tests were two sided. *p<0.05, **p<0.01, ***p<0.001, ****p<0.0001. This study was conducted in collaboration with Pauline Morigny and data collection and analysis were shared equally between us. Figure based on (Morigny&Zuber, 2020).

Lipid species are mutually regulated in mice and cancer patients suffering from cachexia

To finally explore the translatability of the lipidomics data assessed in experimental models, we investigated changes in the cachectic plasma lipidome of gastrointestinal cancer patients. Importantly, lipid classes were similarly regulated between patients and mice in cachexia development. We found a total of 81 lipid species commonly regulated between at least one mouse model of cancer cachexia and cachectic patients. 11 of these 81 lipid species were upregulated, and only 6 of those were consistently altered in both mouse models and patients, all of them being related to the sphingolipid family, including SM(16:0), SM(24:1), CER(16:0), CER(24:1), HCER(16:0), and HCER(24:1) (Figure 25A). Contrary, the two most commonly downregulated lipid species were LPC(16:1) and LPC(20:3), both significantly decreased upon cachexia in mice and patients (Figure 25A). None of these lipid species being commonly increased or reduced upon cachexia were changed in C26 non-cx mice, underlining that their dysregulation is probably closely related to cachexia. In addition, the concentration of these lipid species closely correlated with bodyweight change in mice

and patients. Representative correlations of one of the lipid species, namely HCER(24:1), and bodyweight change are shown in Figure 25B for all different experiments. As expected, non-cachectic C26 tumor-bearing mice did not show alterations in any of these 8 commonly regulated lipid species, and also correlations of the lipids with bodyweight change were non-significant (Figure **25**B). We found a gradual rise of some of these lipid species in line with the progressive transition from a weight stable cancer condition to severe cachexia, implying their potential role as biomarkers in cancer cachexia.
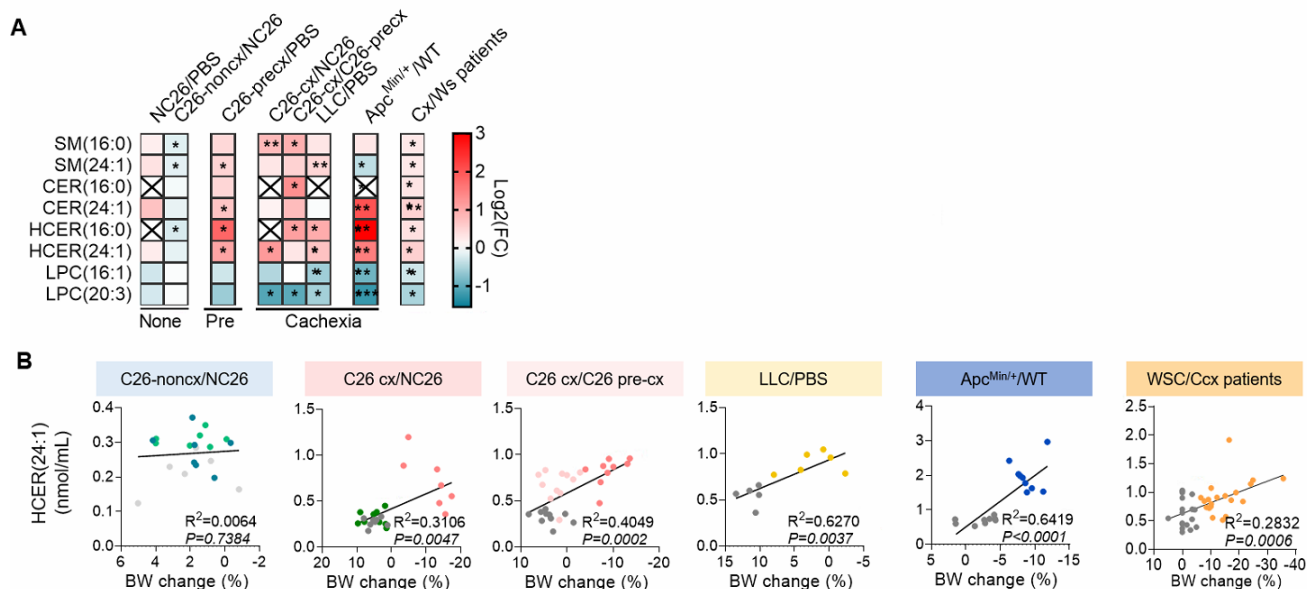
Figure 25. Lipid species are commonly regulated in mice and cancer patients upon cachexia. (A) Heat map representing the fold change of lipid species that were uniformly affected in various mouse models of cachexia (same mice as in Figure 23) and cachectic cancer patients (Ccx, n= 20; WSC n=19). Patient characteristics can be found in more detail in the methods section. **(B)** Correlations showing the concentration of HCER(24:1) and the percentage of bodyweight change in mouse models of cancer cachexia and cachectic cancer patients. Same mice and patients as in (A). Statistical analysis was performed using two-sided Wilcoxon rank sum tests and p values were adjusted for multiple testing using the Benjamini-Hochberg correction method. Correlations were analyzed using linear regression analysis. *p<0.05, **p<0.01, ***p<0.001. This study was conducted in collaboration with Pauline Morigny and data collection and analysis were shared equally between us. Figure based on (Morigny&Zuber, 2020).

Coming back to our initial hypothesis, investigating if altered immune cell infiltration into WAT might change adipose tissue metabolism, finally leading to an altered plasma lipidome, we were keen to identify the primary source of elevated sphingolipid levels in cachectic mice. Importantly, adipose tissue has previously been shown to contribute to circulating ceramide levels (Flaherty, 2019). To this end, we analyzed the gene expression profile of enzymes related to sphingolipid metabolism, including ceramide synthesis and degradation, in eWAT of non-cachectic PBS and NC26 tumor-bearing mice, as well as in pre-cachectic and cachectic C26-injected mice (Figure 26). Contrary to what was expected, we found decreased gene expression levels of enzymes involved in the different ceramide synthesis pathways (Figure 26A). *Sptlc1* (serine palmitoyl transferase 1)*, Kdsr* (3-ketosphinganine reductase)*, Cers5, Cers6, Cers2* (ceramide synthases 5, 6 and 2)*, Degs1* and *Degs2* (dihydroceramide desaturases 1 and 2), all belonging to the *de novo* ceramide synthesis pathway, and *Smpd1* (sphingomyelin phosphodiesterase 1) as part of the salvage pathway (Gault, 2010), were either unchanged or significantly downregulated in epidydimal white adipose tissue of pre-cachectic or cachectic mice (Figure 26A). Additionally, ceramide degradation seemed to be unchanged as well between cachectic C26 and PBS-injected mice, as indicated by *Asah1* (N-acylsphingosine amidohydrolase 1) expression levels (Figure 26A), altogether suggesting a general decrease in

ceramide metabolism in cachectic eWAT. Thus, immune infiltration into adipose tissue is likely not the driver of elevated ceramide levels in cachectic mice. Instead, we found most of the aforementioned enzymes being increased in cachectic livers (Figure 26B), indicating that liver might be the major source of elevated circulating ceramides (Morigny&Zuber, 2020). Interestingly, Watt *et al.* have demonstrated that *de novo* generated ceramides are not stored in the liver, but rather secreted into the circulation (Watt, 2012), again underlining the potential impact of high amounts of liver-synthesized ceramides to high circulating levels in cachectic animals.
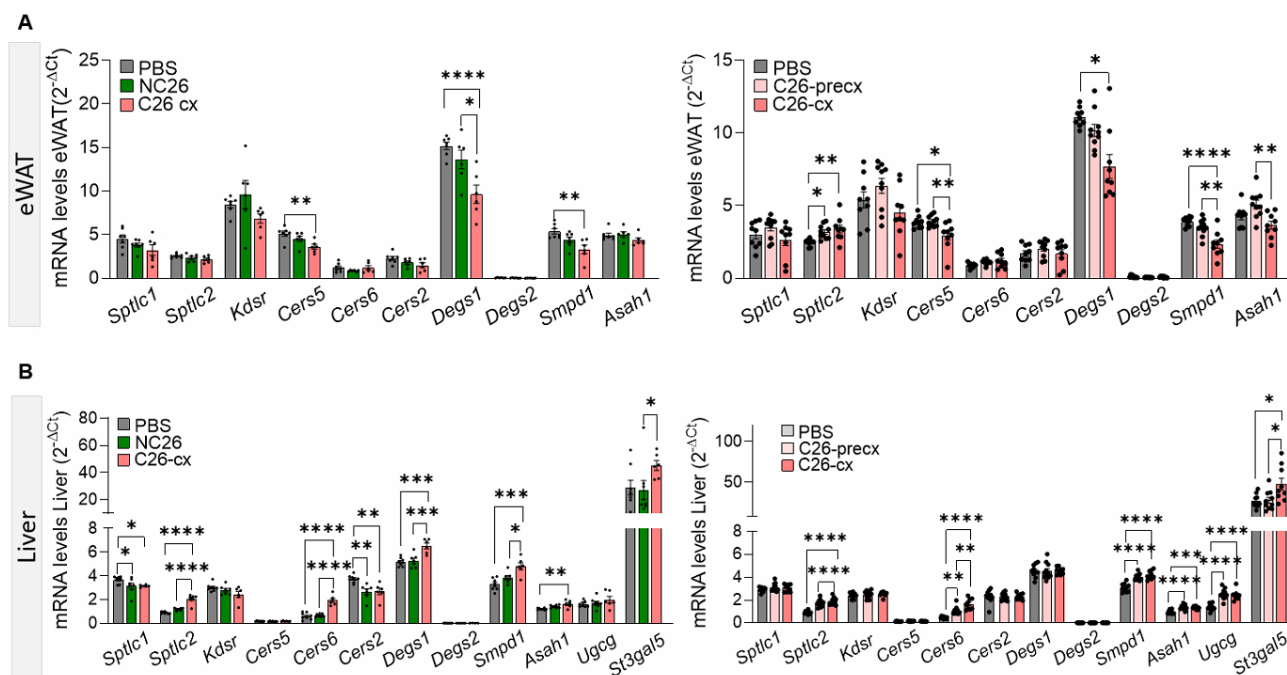
Figure 26. Liver as primary source of increased circulating ceramide levels in cachectic mice. (A-B) mRNA levels of same mice as in Figure 23. Expression of enzymes related to ceramide de novo synthesis (*Sptlc1*, serine palmitoyl transferase 1; *Kdsr,* 3-ketosphinganine reductase; *Cers5, Cers6, Cers2*, ceramide synthases; *Degs1, Degs2*, dihydroceramide desaturases) and the salvage pathway (*Smpd1*, sphingomyelin phosphodiesterase). HCER and glycosphingolipid synthesis are measured by gene expression of *Ugcg* (UDP-Glucose Ceramide Glucosyltransferase) and *St3gal5* (ST3 Beta-Galactoside Alpha-2,3-Sialyltransferase 5), respectively. Ceramide degradation is indicated by expression of *Asah1* (N-acylsphingosine amidohydrolase 1). **(A)** Gene expression levels in eWAT and **(B)** Liver. Statistical analysis was performed using unpaired one-way ANOVA or Kruskal–Wallis tests with Bonferroni or Dunn's post-hoc tests. Tests were two sided. Data are mean ± SEM. *p<0.05, **p<0.01, ***p<0.001, ****p<0.0001. This study was conducted in collaboration with Pauline Morigny and data collection and analysis were shared equally between us. Figure based on (Morigny&Zuber, 2020).

2.4   T cell metabolism and function are impaired in cancer cachexia

2.4.1   T cell metabolism is affected by cancer cachexia

Fatty acids (FA) are potent players in cancer development due to their role as signaling molecules and building blocks for membrane biosynthesis (Koundouros, 2020). Additionally, cancer cells can hijack fatty acid metabolism (Tang, 2018), thereby increasing tumor growth. Moreover, T cell function, especially in the tumor microenvironment, can be impaired due to an increased uptake of long chain fatty acids (Manzo, 2020) and oxidized low density protein mediated by CD36 (Endemann, 1993; Xu, 2021). Other lipid classes such as sphingomyelin and ceramides have also been linked to T cell dysfunction in cancer (Tallima, 2021; Vaena, 2021). Therefore, we hypothesized that the observed T cell dysfunction in cancer cachexia might be mediated by elevated levels of circulating free FAs (FFAs) and sphingolipids, including ceramides and sphingomyelin, as noted in our lipidomics study (see chapter 2.3), possibly conveyed by CD36. Of note, all experiments in this chapter (chapter 2.4) were conducted using T cells isolated from the spleen, unless stated otherwise. Thus, I first assessed

Cd36 gene expression in T cells isolated from the spleen of non-cachectic and cachectic mice of different mouse strains (Figure 27). In CD8^{+} splenocytes, *Cd36* expression was increased in all long-term tumor-bearing BALB/c mice (non-cx and cx) in a similar manner, independent of cachexia presence, while it was unchanged in CD4^{+} T cells (Figure 27A). Surprisingly, *Cd36* gene levels also tended to be elevated in CD8^{+} T cells from non-cachectic short-term C26 tumor-bearing mice. In line with the C26 data, CD8^{+} T cells from pre-cachectic and cachectic APC$^{Min/+}$ animals also revealed a significant increase of *Cd36* compared to WT mice, while cachectic LLC tumor-bearing mice displayed slightly upregulated *Cd36* expression in both CD4^{+} and CD8^{+} T cells (Figure 27A, B). Together, the significant *Cd36* upregulation in NC26 non-cx and pre-cachectic mice (C26, APC$^{Min/+}$), but also the non-significant increase in C26 non-cx mice suggests that *Cd36* expression on CD8^{+} T cells increases in a tumor-dependent but not cachexia-specific manner, underlining that CD36-mediated elevated uptake of lipids cannot be the underlying cause for T cell impairment in cachexia.
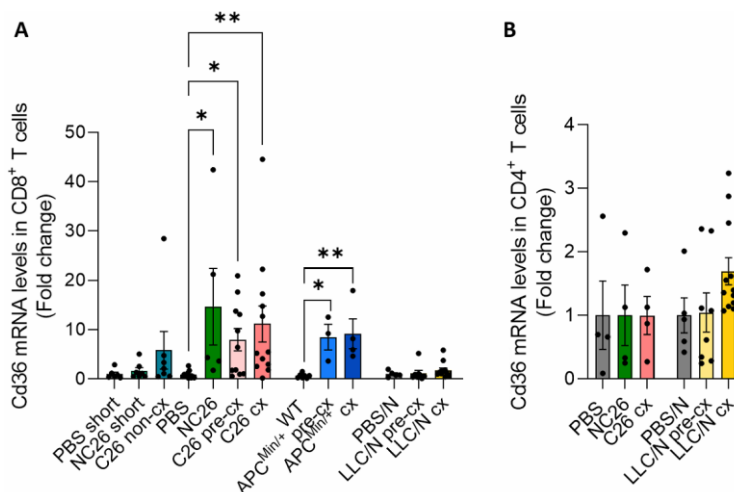
Figure 27. *Cd36* gene expression in T cells is not affected by cachexia. mRNA levels of *Cd36* were assessed in CD8^{+} and CD4^{+} T cells isolated from the spleen of PBS short (n=6), NC26 short (n=7), C26 non-cx (n=7), PBS (n=12), NC26 (n=5), C26 pre-cx (n=11) and C26 cx (n=12) mice; as well as PBS/N (n=5), LLC/N pre-cx (n=8) and LLC/N cx (n=12) animals. In addition, expression of *Cd36* was analyzed in wildtype (n=7), APC$^{Min/+}$ pre-cx (n=3) and APC$^{Min/+}$ cx (n=4) CD8^{+} splenocytes. Data are mean ± s.e.m. Statistical analyses were performed using unpaired *t* test and one-way ANOVA or Kruskal-Wallis test with Tukey's or Dunn's multiple-comparison *post hoc* test, respectively. *$p<0.05$, **$p<0.01$.

Gene expression of enzymes related to T cell metabolism is altered upon cancer cachexia

Cancer cachexia is known to induce systemic inflammation accompanied by an increase in many circulating cytokines (Webster, 2020), while at the same time, it has become increasingly clear that cytokines can regulate T cell metabolism (Bishop, 2021). Thus, we hypothesized that elevated cytokine appearance in the circulation but also in the tissue microenvironment might influence T cell metabolism in cancer cachexia. Hence, I determined expression levels of metabolic genes, including *Abca1* (ATP Binding Cassette Subfamily A Member 1), *Cpt1a* (Carnitine palmitoyltransferase 1A), *Slc2a1* (Solute Carrier Family 2 Member 1, encoding GLUT1) and *Ldha* (Lactate Dehydrogenase A) in T cells from cachectic mice (Figure 28). Interestingly, a marked rise in the expression of *Abca1* was only found in CD8^{+} T cells from short-term NC26 and C26 tumor-bearing mice but not (pre-)cachectic C26 mice (Figure 28A), while it was unchanged in cachectic LLC tumor-bearing (Figure 28B) and APC$^{Min/+}$ (Figure 28C) mice. Since ABCA1 is known to mediate efflux of phospholipids and cholesterol (Castella, 2017), T cells might also contribute to altered circulating levels of phospholipids and cholesterol during the early development of cachexia, as observed by lipidomic analyses. CPT1A is the limiting and rate-controlling factor for long chain fatty acid oxidation within mitochondria (Raud, 2018). In cachectic CD8^{+} T cells, *Cpt1a* expression was strongly increased in all tumor-bearing animals

(NC26, C26, LLC) independent of their cachectic status (Figure 28A, B). In line, a non-significant increase in *Cpt1a* was also noted in cachectic APC^Min/+ mice (Figure 28C).

Antigen stimulation mediates a switch of T cell metabolism to favoring aerobic glycolysis despite ample oxygen supply, which is accompanied by an increase in LDHA converting pyruvate to lactate (Peng, 2016). CD8+ T cells from short-and long-term NC26 and non-cachectic C26 mice showed a strong increase in *Ldha* gene expression (Figure 28A), further underlining proper activation of these cells by NC26 and C26 tumor antigens. Also pre-cachectic C26 CD8+ T cells showed a significant upregulation of *Ldha*, which was abolished upon cachexia progression (Figure 28A), implying the transition to a dysfunctional state in which T cells cannot react properly to tumor-antigen stimulation. Contrary, cachectic APC^Min/+ and (pre-) cachectic LLC CD8+ T cells showed an increase of *Ldha* (Figure 28B, C).
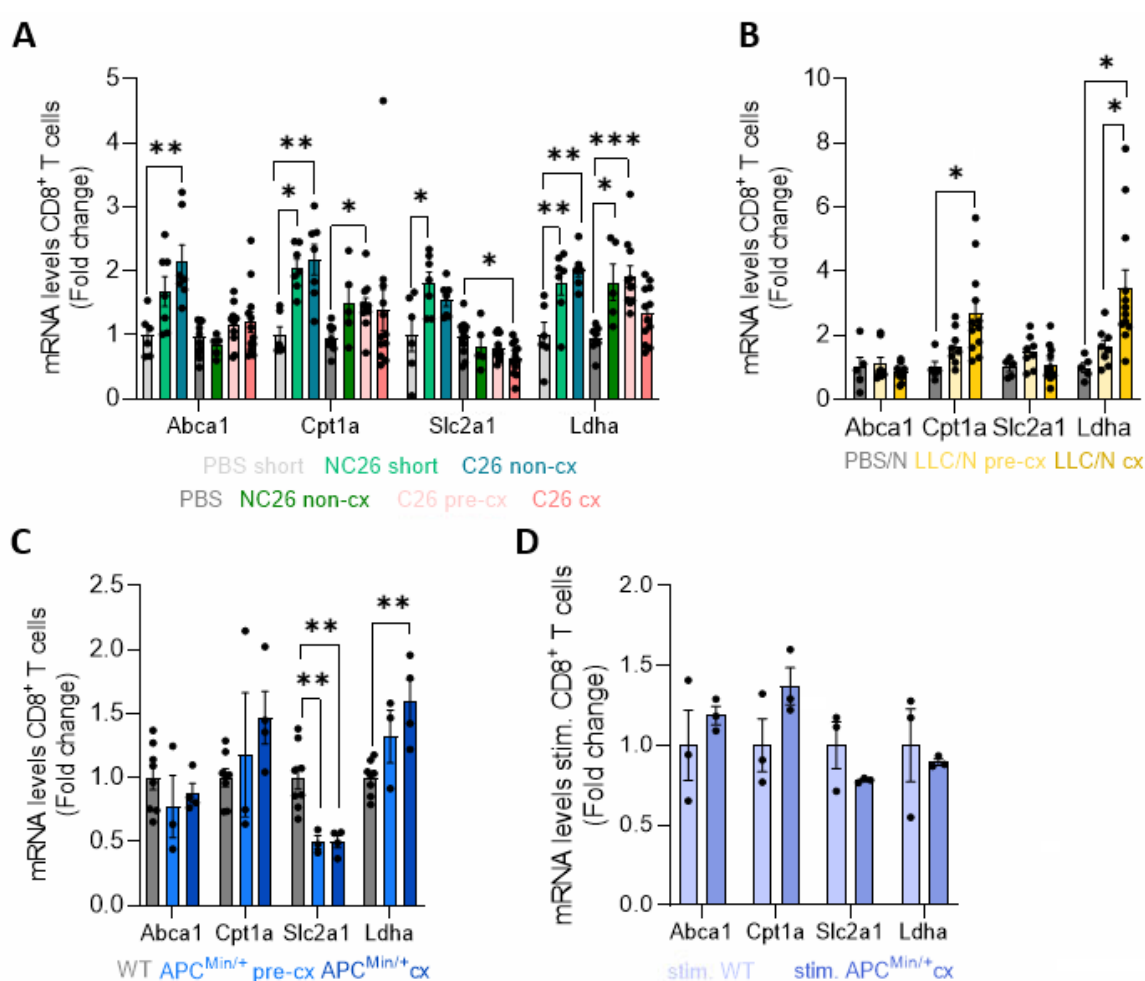
Figure 28. Expression levels of metabolic enzymes are altered in circulating CD8+ T cells isolated from the spleen upon cancer cachexia. (A-D) Expression of *Abca1, Cpt1a, Slc2a1* and *Ldha* in CD8+ T cells from **(A)** PBS short (n=6), NC26 short (n=7), C26 non-cx (n=7), PBS (n=12), NC26 (n=5), C26 pre-cx (n=11) and C26 cx (n=12) mice, **(B)** PBS/N (n=5), LLC/N pre-cx (n=8) and LLC/N cx (n=12), **(C)** WT (n=8), APC^Min/+ pre-cx (n=3) and APC^Min/+ cx (n=4). **(D)** Expression in CD8+ T cells of WT (n=3) and APC^Min/+ cx (n=3) mice after overnight stimulation with CD3/CD28 antibodies. Data are mean ± s.e.m. Statistical analyses were performed using one-way ANOVA or Kruskal-Wallis test with Tukey's or Dunn's multiple-comparison *post hoc* test, respectively. *p<0.05, **p<0.01.

Gene expression levels of *Slc2a1*, encoding the major glucose transporter GLUT1 in T lymphocytes (Cretenet, 2016), were significantly decreased in CD8+ T cells from cachectic C26, as well as cachectic APC^Min/+ animals (Figure 28A, C), while being upregulated in pre-cachectic LLC mice, which was blunted upon cachexia (Figure 28B). Strikingly, there was a significant increase of *Slc2a1* in non-

cachectic C26 and short-term NC26 mice (Figure 28A), indicating proper functioning of T cells upon stimulation by tumor-presence. Antigen stimulation of T cells in general leads to T cell activation, increased glucose uptake via GLUT1, and subsequently upregulation of T cell effector function (Jacobs, 2008; Macintyre, 2014; C. S. Palmer, 2015). Hence, the consistent repression of Slc2a1 in cachectic T cells, suggests a progressive inhibition of glucose uptake in line with cachexia development in different mouse strains. Importantly, when stimulating CD8+ T cells overnight using anti-CD3 and anti-CD28 antibodies, gene expression of metabolic enzymes was to some extent restored to normal levels (Figure 28D), implying that dampened T cell glucose uptake upon tumor-antigen stimulation in cachexia is not related to intrinsic, developmental changes, but rather dependent on inhibiting factors or nutrient depletion in the microenvironment or problems with antigen stimulation.

Accordingly, also CD4+ T cells from cachectic C26 and LLC tumor-bearing animals showed an altered gene expression profile upon cachexia (Figure 29). CD4+ T cells from LLC tumor-bearing mice showed stronger changes compared to C26 mice, which displayed an overall high variability. As in CD8+ T cells, I observed a marked upregulation of *Cpt1a* and *Ldha* in cachectic LLC CD4+ T cells, while *Abca1* and *Slc2a1* were unaltered (Figure 29B). Intriguingly, pre-cachectic LLC mice highlighted the progressive upregulation of *Ldha* and *Cpt1a*, while they showed even a significant upregulation of *Abca1* compared to PBS mice in CD4+ T cells, indicating the progressive loss of metabolic integrity with cachexia development. In contrast to the strong alterations in CD8+ T cells from C26 (pre-)cx mice, I did not observe any changes in CD4+ T cells from NC26 or C26 mice.
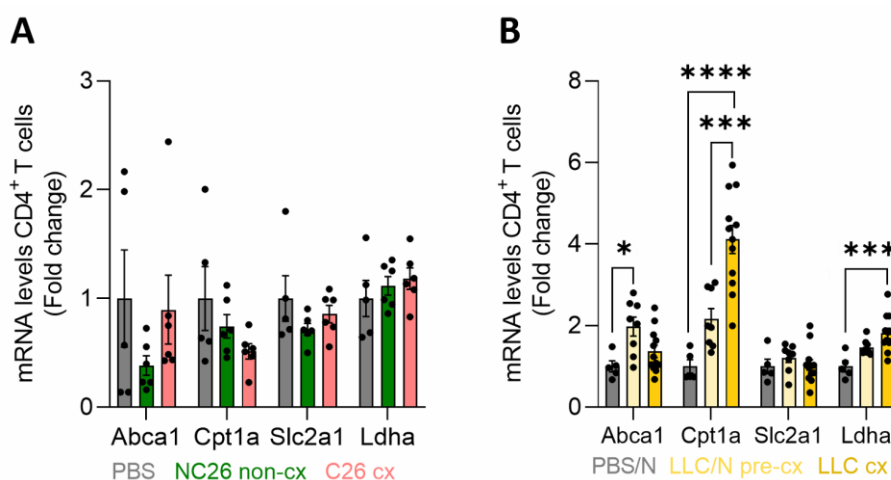
Figure 29. CD4+ T cells display altered expression levels of metabolic enzymes. Expression of *Abca1*, *Cpt1a*, *Slc2a1* and *Ldha* in CD4+ T cells from **(A)** PBS (n=5), NC26 (n=6) and C26 cx (n=6) or **(B)** PBS/N (n=5), LLC/N pre-cx (n=8) and LLC/N cx (n=12) mice. Data are mean ± s.e.m. Statistical analyses were performed using one-way ANOVA or Kruskal-Wallis test with Tukey's or Dunn's multiple-comparison *post hoc* test, respectively. *p<0.05, ***p<0.001, ****p<0.0001.

CD8+ T cells from cachectic mice have an altered mitochondrial metabolic profile

Since the expression of enzymes related to T cell metabolism was altered upon cancer cachexia, I next sought to determine if the energy demand of CD8+ T cells isolated from non-cachectic and cachectic mice was also changed, based on their oxygen consumption rate (OCR). To this end, a comprehensive metabolic analysis was conducted using various mitochondrial inhibitors to identify metabolic changes using a Seahorse XFe96 Bioanalyzer, on CD8+ T cells isolated from spleens of cachectic *vs*. non-cachectic animals. CD8+ T cells from cachectic C26 tumor-bearing mice tended to have a reduced general energy demand and oxidative phosphorylation (OXPHOS) compared to non-cachectic NC26 mice, as measured by basal and maximal respiration (Figure 30A). Additionally, a trend for a decreased basal respiration of cachectic C26 CD8+ T cells *vs.* pre-cachectic C26 CD8+ T cells was

observed (Figure 30B), underlining the progressive transition from a functional to an impaired T cell metabolism upon cancer cachexia development. Despite expressional changes of metabolic enzymes due to short-term tumor implantation (Figure 28A), neither basal nor maximal respiration of NC26 short and non-cachectic C26 CD8$^+$ T cells was altered (Figure 30C).

Figure 30. Oxygen consumption rate (OCR) of CD8$^+$ T cells is reduced in cachectic C26 mice. (A-C) OCR of CD8$^+$ T cells over time, challenged by injections of 1 µM oligomycin, 1.5 µM FCCP, 1 µM Antimycin and 1 µM Rotenone, and 100 mM 2-deoxyglucose (2-DG). Calculations of basal and maximal respiration are based on OCR levels and can be looked up in detail in the methods section. Measurements with CD8$^+$ T cells from **(A)** PBS (n=10), NC26 (n=11) and C26 cx (n=10) mice, **(B)** PBS (n=4), C26 pre-cx (n=9) and C26 cx (n=5) mice, and **(C)** PBS short (n=6), NC26 short (n=7) and C26 non-cx (n=6 OCR over time, n=7 bar graphs) mice. Data are mean ± s.e.m. Statistical analyses were performed using two-way ANOVA with Tukey's multiple-comparison *post* hoc test, as well as one-way ANOVA or Kruskal-Wallis test with Tukey's or Dunn's multiple-comparison *post hoc* test, respectively. *p<0.05, **p<0.01, ***p<0.001.

An unchanged basal and maximal respiration could be observed in LLC-tumor bearing animals, but with very high variability (Figure 31A), in line with the high variability of LLC mice to develop cachexia (as previously discussed, (Geppert, 2021). CD8$^+$ T cells from pre-cachectic and cachectic APC$^{Min/+}$ mice exhibited a reduced maximal respiration compared to their wildtype controls, while basal respiration in cachectic APC$^{Min/+}$ mice was not changed (Figure 31B). Importantly, CD8$^+$ T cell energy metabolism from cachectic APC$^{Min/+}$ mice was restored by *ex vivo* CD3/CD28 co-stimulation (Figure 31C), implying that the intrinsic potential for activation was largely unchanged by cachexia.
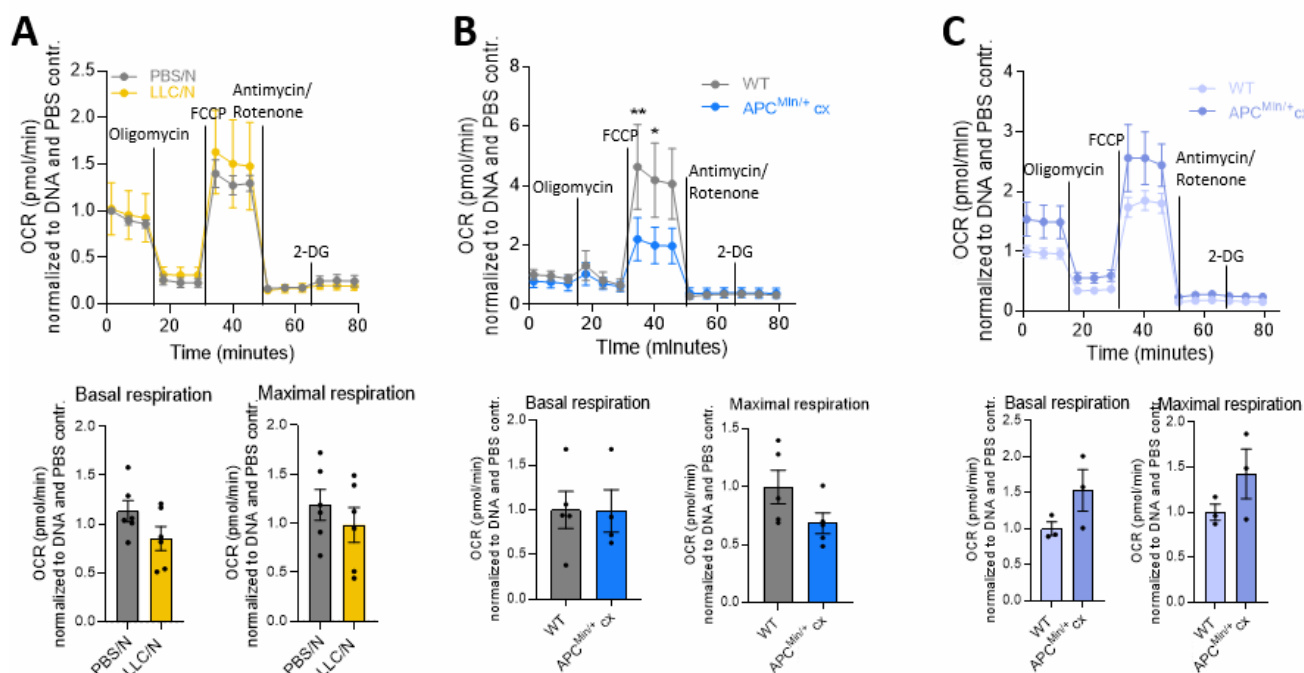
Figure 31. Oxygen consumption rate (OCR) of CD8+ T cells is affected in cachectic LLC and APC^Min/+ mice. (A-C) OCR in CD8+ T cells over time, being challenged by 1 µM oligomycin, 1.5 µM FCCP, 1 µM Antimycin and 1 µM Rotenone, and 100 mM 2-DG injections. Calculations of basal and maximal respiration were based on measured OCR levels. Calculation is described in detail in methods section. Measurements in CD8+ T cells from **(A)** PBS (n=6) or LLC/N (n=7) mice, **(B)** WT (n=5), APC^Min/+ cx (n=5) mice and **(C)** after CD3/CD28 co-stimulation in CD8+ T cells from WT (n=3) and APC^Min/+ cx (n=3) mice. Data are mean ± s.e.m. Statistical analyses were performed using two-way ANOVA with Tukey's multiple-comparison *post* hoc test, unpaired *t* test, as well as one-way ANOVA or Kruskal-Wallis test with Tukey's or Dunn's multiple-comparison *post hoc* test, respectively. **p<0.01.

CD8+ T cell glycolysis is affected by cancer cachexia

Upon T cell activation, T cell metabolism rapidly switches from mitochondrial respiration to aerobic glycolysis (Menk, 2018), enabling proper activation of effector function (Pearce, 2013). CD8+ T cell glycolysis was assessed by challenging T cells with different metabolic inhibitors and subsequent analysis of the extracellular acidification rate (ECAR) using a Seahorse XFe96 Bioanalyzer. Thereby, a reduction of glycolysis in CD8+ T cells, as measured by ECAR, was observed in cachectic C26, LLC and APC^Min/+ mice (Figure 32A, B, D, E). Intriguingly, CD8+ T cells from pre-cachectic C26 tumor-bearing animals showed an in-between stage of PBS and cachectic C26 mice (Figure 32B), implying a gradual impairment of T cell metabolism in cachexia.

Short-term tumor-bearing NC26 and non-cachectic C26 CD8+ T cells showed no changes in glycolysis compared to PBS mice (Figure 32C). Reduced glycolysis in cachectic APC^Min/+ mice was revoked upon overnight stimulation using anti-CD3/anti-CD28 antibodies (Figure 32F), indicating that cachectic T cells do not suffer from a stimulation/metabolism defect per se, but rather an immunosuppressive environment must be the underlying cause for the alterations in T cell metabolism upon cachexia.
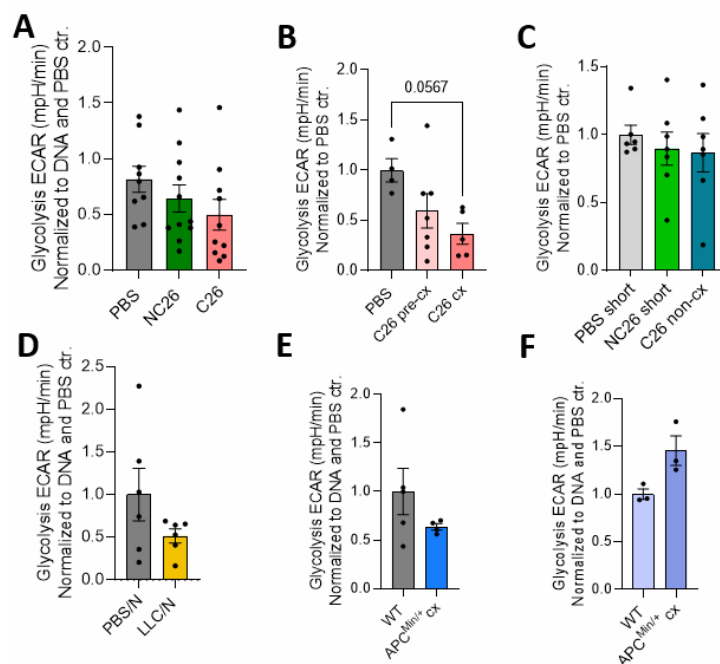
Figure 32. CD8$^+$ T cell glycolysis is affected by cancer cachexia. Calculations of glycolysis were based on ECAR data measured using the Seahorse XFe96 Flux Analyzer. **(A-E)** Glycolysis rates as a measure of ECAR were assessed in CD8$^+$ T cells from **(A)** PBS (n=9), NC26 (n=11), C26 cx (n=10), **(B)** PBS (n=4), C26 pre-cx (n=7), C26 cx (n=5), **(C)** PBS short (n=6), NC26 short (n=7), C26 short (n=7), **(D)** PBS/N (n=6), LLC/N (n=7), and **(E)** WT (n=5) and APC$^{Min/+}$ cx (n=4) mice. **(F)** CD8$^+$ T cells from WT (n=3) and APC$^{Min/+}$ cx (n=3) mice were stimulated overnight using anti-CD3/anti-CD28 antibodies. Data are mean ± s.e.m. Statistical analyses were performed using unpaired *t* test as well as one-way ANOVA or Kruskal-Wallis test with Tukey's or Dunn's multiple-comparison *post hoc* test, respectively.

2.4.2   CD8+ T cell effector function is compromised in cachexia

T cell activation is tightly coupled to T cell metabolism as upon stimulation T cells underlie the Warburg effect switching their metabolism from oxidative phosphorylation to aerobic glycolysis, while similarly upregulating important effector cytokines, such as Interferon gamma (IFNγ) (Kouidhi, 2017). Since the metabolic profile of CD8$^+$ T cells was strongly altered upon cancer cachexia (Figure 27-Figure 32), I next sought to determine changes in T cell effector function. To this end, mRNA levels of effector cytokines were characterized in CD8$^+$ splenocytes (Figure 33). A marked repression of effector cytokine expression, including *Il2* (interleukin 2), *Tnfα* (Tumor necrosis factor alpha), and *Ifnγ*, indicating reduced T cell activation, was specifically associated with cachexia in different mouse models (Figure 33). Interestingly, this was specific to cancer cachexia and tumor presence, as mice carrying a non-cachexia-inducing tumor, such as NC26, or mice carrying tumors only for a short time, e.g. NC26 short or C26 non-cx, showed an unaltered or enhanced inflammatory effector profile compared to PBS or WT mice (Figure 33). Pre-cachectic C26, APC$^{Min/+}$ and LLC mice highlighted the gradual progression of cancer cachexia as they often displayed an intermediate stage between cachectic and control mice (Figure 33). CD8$^+$ T cells from NC26 short and C26 non-cx mice upregulated *Pdcd1*, encoding programmed cell death 1 (PD1), significantly compared to PBS short mice (Figure 33A) and also *ex vivo* CD3/CD28 co-stimulation of CD8$^+$ splenocytes from APC$^{Min/+}$ mice strongly induced *Pdcd1* expression. Interestingly, PD1 has previously been reported to be increased on naïve T cells upon TCR antigen stimulation (Chikuma, 2009), explaining its strong upregulation in CD8$^+$ T cells challenged by short-term tumor presence or overnight stimulation. However, in combination with other markers such as Thymocyte Selection Associated High Mobility Group Box (TOX) (O. Khan, 2019) or T Cell Immunoreceptor With Ig And ITIM Domains (TIGIT) (X. Zhang, 2019), PD1 expression can remain high and be a sign of T cell exhaustion, upon long-term stimulation by tumor antigens

(Dolina, 2021). Gene expression of *Pdcd1*, was slightly increased in CD8$^+$ splenocytes from (pre-) cachectic C26 tumor-bearing mice compared to PBS and NC26 control mice (Figure 33A), while being unchanged in LLC (Figure 33B) and APC$^{Min/+}$ (Figure 33C) animals. Moreover, mRNA levels of TOX were unchanged in CD8$^+$ T cells from cachectic C26 animals, but strongly decreased in pre-cachectic and cachectic LLC (Figure 33B) and APC$^{Min/+}$ (Figure 33C) mice. In combination, these data suggest that dampening of T cell effector function in cachexia was not mediated by T cell exhaustion. Strikingly, CD3/CD28 co-stimulation of CD8$^+$ splenocytes from APC$^{Min/+}$ mice led to a strong, but similar induction of effector cytokine gene expression in all groups and restored mRNA levels of cachectic CD8$^+$ T cells (Figure 33C), implying a largely unchanged intrinsic potential for T cell activation in cancer cachexia.
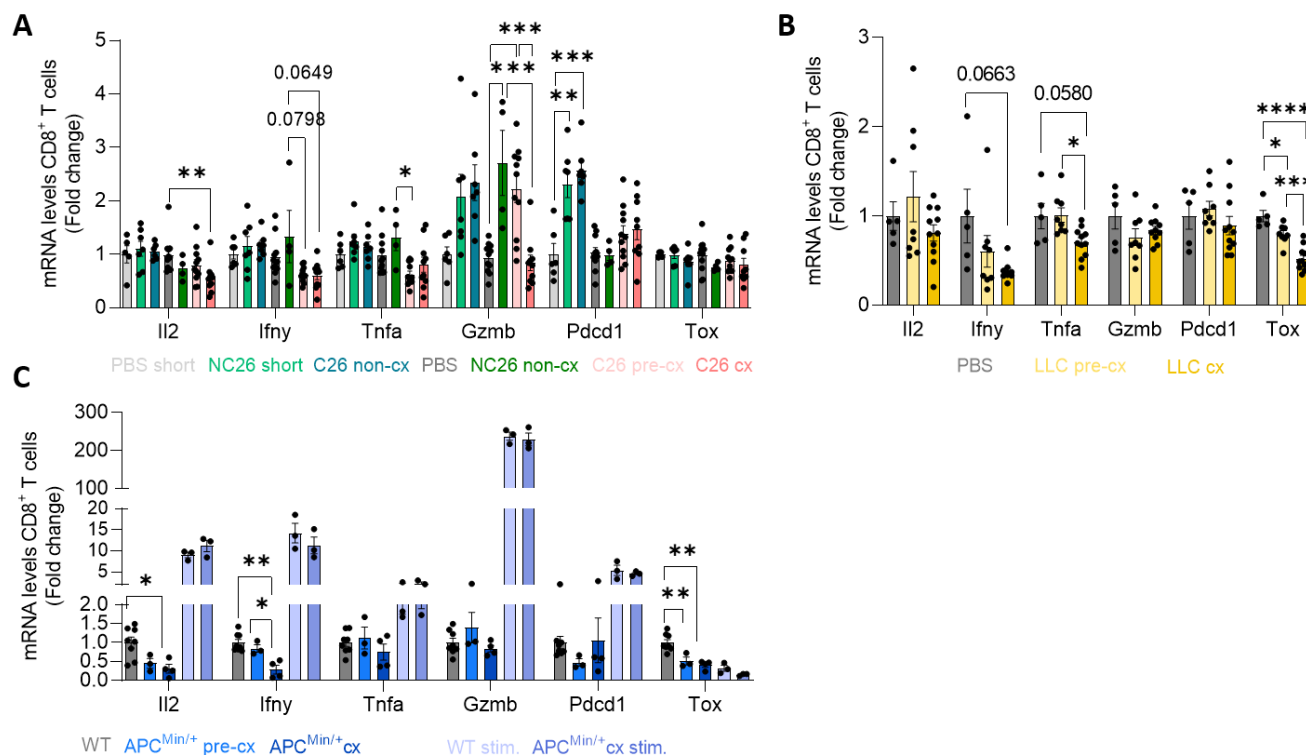
Figure 33. Impaired effector cytokine expression in CD8$^+$ T cells in cancer cachexia. (A-C) mRNA expression of T cell activation marker genes in CD8$^+$ splenocytes from **(A)** PBS short (n=6), NC26 short (n=7), C26 non-cx (n=7), PBS (n=11), NC26 (n=4), C26 pre-cx (n=11) and C26 cx (n=10) mice, **(B)** PBS C57BL/6N (n=5), LLC pre-cx (n=8) and LLC cx (n=11) mice, **(C)** WT (n=8), APC$^{Min/+}$ pre-cx (n=3), APC$^{Min/+}$ cx (n=4), as well as activated WT (n=3) and APC$^{Min/+}$ cx (n=3) by CD3/CD28 co-stimulation. Data are mean ± s.e.m. Statistical analyses were performed using one-way ANOVA or Kruskal-Wallis test with Tukey's or Dunn's multiple-comparison *post hoc* test, respectively. *p<0.05, **p<0.01, ***p<0.001, ****p<0.0001.

In line with CD8$^+$ T cells, CD4$^+$ splenocytes from cachectic C26 and LLC tumor-bearing mice seemed to be dysfunctional based on their effector gene regulation (Figure 34). Accordingly, cachexia induced a downregulation of *Ifnγ* and *Tnfα* in cachectic C26 and LLC mice (Figure 34A, B). Interestingly, *Pdcd1* expression was unaltered in CD4$^+$ splenocytes from cachectic mice, while *Tox* was downregulated, suggesting reduced T cell exhaustion upon cachexia, in accordance with the CD8$^+$ T cell expression levels. Together, these data suggest that exhaustion is likely not involved in T cell repression upon cachexia.

CD4$^+$ T cells are also often termed helper T cells (Th cells) and can be divided into different subtypes, having different roles in the immune system. Interestingly, the two predominant classes Th1 and Th2 cells both have been previously analyzed regarding their immunotherapeutic role in cancer. Th1 cells are characterized by IFNγ production, while Th2 cells secrete IL-4, IL-10 and IL-13, and express Gata binding protein 3 (GATA3) as their subtype-specific transcription factor (Bradley, 1996; W. Zheng,

1997). CD4+ T cells from cachectic LLC mice displayed strongly reduced levels of *Gata3, Il4* and *Il10*, indicating reduced presence of Th2 circulating T cells upon cachexia (Figure 34B).

These data were in line with a marked reduction of *Gata3* and *Il13* expression in C26 cx mice compared to PBS-injected animals. However, *Il4* and *Il10* levels were not altered in cachectic C26 mice (Figure 34A). Additionally, also *Ifnγ* levels were downregulated in CD4+ splenocytes from cachectic mice (Figure 34), implying reduced amounts of Th1 cells. Altogether, these results indicate that cancer cachexia might induce a defect in helper T cell differentiation, and thereby an accumulation of naïve CD4+ T cells (as already discussed in 2.2.).
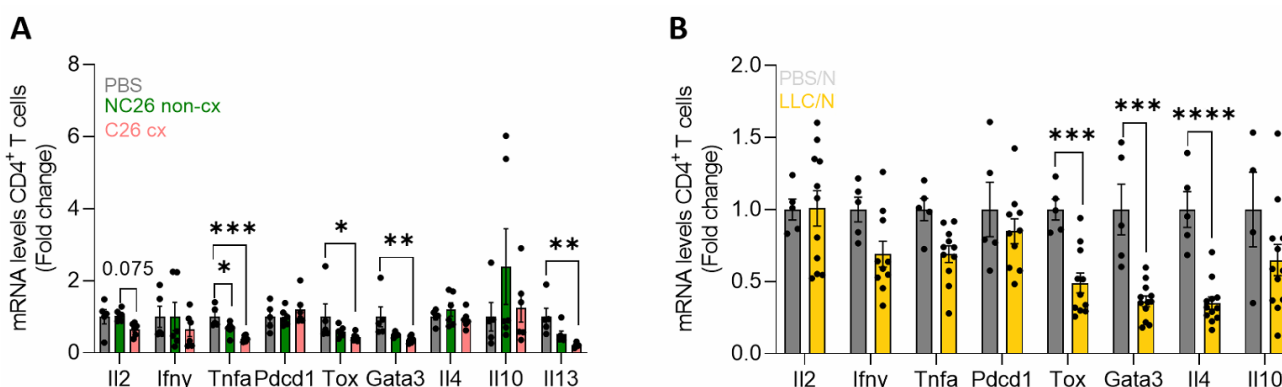
Figure 34. CD4+ T cell effector and subtype marker gene expression is dysregulated in cachexia. (A-B) Gene expression of T cell activation and subtype specific marker genes in CD4+ splenocytes from **(A)** PBS (n=5), NC26 (n=6) and C26 cx (n=6) mice, and **(B)** PBS/N (n=5) and LLC/N (n=11) animals. Data are mean ± s.e.m. Statistical analyses were performed using one-way ANOVA or Kruskal-Wallis test with Tukey's or Dunn's multiple-comparison *post hoc* test, respectively. *p<0.05, **p<0.01, ***p<0.001, ****p<0.0001.

Strikingly, dysregulated effector gene expression was not limited to circulating T cells but was also present in tumor-infiltrating lymphocytes (TILs), with a downregulation of *Il2, Ifnγ, Tnfα* and *Gzmb* in both CD4+ and CD8+ TILs in cachectic C26 compared to non-cachectic NC26 tumor-bearing mice (Figure 35). These data further highlight the extensive systemic impact cachexia has on T cells in different tissues.
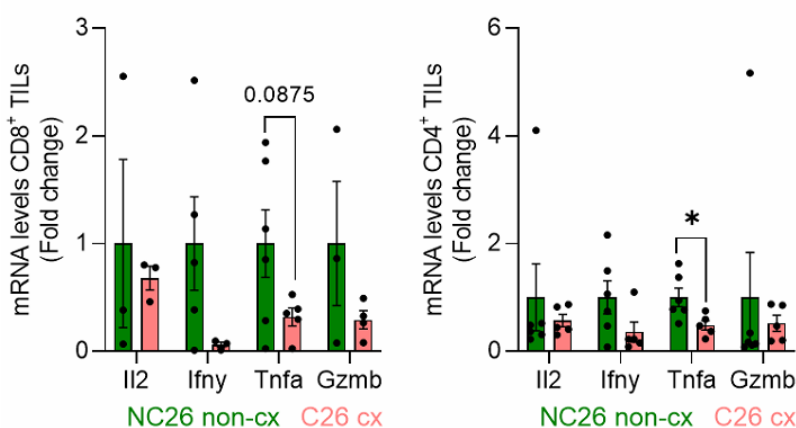
Figure 35. Cachexia reduces effector gene expression of tumor-infiltrating lymphocytes (TILs). Expression levels of T cell effector genes in CD8+ and CD4+ TILs from non-cachectic NC26 (n=5) and cachectic C26 (n=5) mice. Data are mean ± s.e.m. Statistical analyses were performed using unpaired t test or Mann-Whitney test. *p<0.05.

2.5   T cell impairment is mediated by systemic alterations and not tumor- secreted factors

2.5.1   Phenotype of cachectic T cells cannot be mimicked *in vitro* by conditioned tumor cell medium treatment

Tumors actively promote cancer cachexia by secreting so-called cachexokines, factors that were shown to arbitrate numerous effects on organs and metabolic tissues (He, 2014; Kir, 2014; Petruzzelli, 2014; Schäfer, 2016). To determine the impact of tumor-derived factors on specific cell types in greater detail, conditioned medium (CM) can be used to mimic the secretion of tumor-derived factors into the circulation (J. Guo, 2017). To investigate if the attenuation of T cell metabolism and effector function was directly mediated by tumor-secreting factors in cancer cachexia, I isolated CD4$^+$ and CD8$^+$ splenocytes from wildtype C57BL/6 mice and cultured them for 48 h in tumor cell (C26, NC26) or no cell (NC) control conditioned medium (CM). Expression of genes involved in metabolism (Figure 36A, D) and effector function (Figure 36B, D) was largely unaffected by conditioned media treatment or revealed tumor-specific but not cachexia-specific effects. In detail, only *Cd36* was non-significantly upregulated in naïve CD8$^+$ T cells treated with C26 CM and to lesser extent in NC26 CM cultured cells, while all other metabolic markers, including *Cpt1a*, *Slc2a1* and *Ldha* were unaltered (Figure 36A). Similarly, *Slc2a1* expression was unchanged in naïve CD4$^+$ circulating T cells between the three treatment groups (Figure 36D). *Il2, Ifnγ,* and *Tnfα* mRNA levels were largely unchanged in both CD8$^+$ and CD4$^+$ splenocytes treated with NC CM, NC26 CM and C26 CM (Figure 36B, D). *Pdcd1*, encoding PD1, expression was strongly increased in naïve CD8$^+$ and CD4$^+$ T cells treated with NC26 or C26 CM (Figure 36B, D), highlighting a tumor- but not cachexia-specific effect. Similarly, *Gzmb* mRNA levels were significantly downregulated in a tumor-related but not cachexia-specific manner in naïve CD8$^+$ T cells (Figure 36B). *Tox* expression was unchanged in naïve CD8$^+$ T cells (Figure 36B).
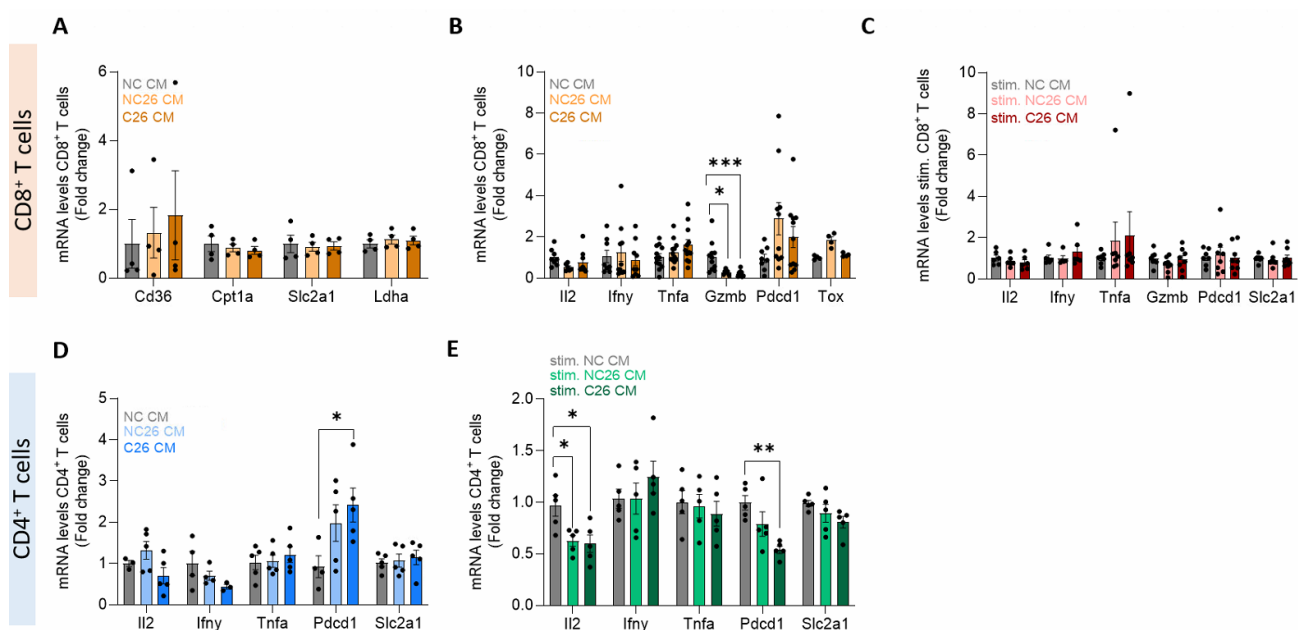
Figure 36. Cachexia-mediated alterations in the expression of genes associated with metabolism or effector function cannot be mimicked *in vitro* by conditioned tumor cell medium. (A-B) CD8$^+$ splenocytes from wildtype C57BL/6 mice were treated with control no-cell (NC) conditioned medium (CM) (n=4-12), NC26 CM (n=4-12) or C26 CM (n=4-12) for 48 h. **(A)** mRNA levels of metabolic genes, including *Cd36, Cpt1a, Glut1* and *Ldha*. **(B)** Gene expression of genes associated with T cell effector function, such as *Il2, Ifnγ, Tnfα, Gzmb, Pdcd1* and *Tox*. **(C)** Expression of metabolic and effector function genes in CD8$^+$ T cells seeded on CD3/CD28 coated plates and treated for 48 h with NC CM (n=6-8), NC26 CM (n=5-8) and C26 CM (n=6-8). **(D)** CD4$^+$ splenocytes were isolated from wildtype C57BL/6 mice and cultured for 48 h in NC CM (n=3-5), NC26 CM (n=4-5) or C26 CM (n=3-5), subsequently mRNA levels of different effector (*Il2, Ifnγ, Tnfα, Pdcd1*) and metabolic (*Glut1*) genes were assessed. **(E)** Circulating CD4$^+$ T cells were cultured for 48 h in anti-CD3/ anti-CD28 coated plates and treated with NC CM (n=5), NC26 CM (n=5) and C26 CM (n=5). Experiments were conducted by me and with help of

Madleen Biggel as part of her internship (supervision by me). n= biological replicates with at least two technical replicates. Data are mean ± s.e.m. Statistical analyses were performed using one-way ANOVA or Kruskal-Wallis test with Tukey's or Dunn's multiple-comparison *post hoc* test, respectively. *p<0.05, **p<0.01, ***p<0.001.

In their physiological environment, upon tumor burden, T cells are stimulated by peptide antigens that are loaded onto major histocompatibility complex (MHC) class I or II molecules (Rossjohn, 2015). In combination with co-stimulation of the CD28 receptor, this leads to T cell activation and subsequent adaptations in metabolism and effector function (Hwang, 2020; R. Wang, 2011). To mimic T cell activation by MHC-presented tumor peptides *in vitro*, I stimulated isolated CD4$^+$ and CD8$^+$ T cells with anti-CD3/anti-CD28 treatment, and cultured those cells in combination with conditioned media for 48 h. Importantly, also in this setting neither CD8$^+$ nor CD4$^+$ T cell mRNA levels of metabolic and effector genes were largely affected by CM treatment (Figure 36C, E). I noted no alterations in *Il2, Ifnγ, Gzmb, Pdcd1* and *Slc2a1* levels in stimulated CD8$^+$ splenocytes treated with NC CM, NC26 CM or C26 CM (Figure 36C), while *Tnfα* was non-significantly upregulated in a tumor-dependent manner (Figure 36C). In stimulated CD4$^+$ T cells, *Il2* was significantly downregulated upon presence of NC26, or C26 CM compared to NC CM (Figure 36E). Additionally, also *Pdcd1* mRNA levels were significantly decreased upon C26 CM treatment in stimulated CD4$^+$ T cells (Figure 36E), both being regulated in rather a tumor- instead of cachexia-dependent manner. Overall, the phenotype of cachectic CD4$^+$ or CD8$^+$ splenocytes could not be mimicked by treatment of naïve or stimulated cells with CM of cachexia inducing *vs.* non-cachexia inducing tumor cells, as either no or only tumor-specific effects were observed. These data suggest that the attenuation of T cell metabolism and effector function in cancer cachexia relies on systemic changes involving for instance nutrient depletion or immunosuppressive conditions rather than the presence of certain tumor-derived factors.

Tumor-secreted factors do not mediate metabolic alterations of T cells in cancer cachexia
T cells isolated from cachectic mice were metabolically impaired as measured by Seahorse analyses (see chapter 2.4.1). To test if these effects were mediated by tumor-derived factors, despite unchanged expression levels of metabolic genes, CD8$^+$ T cells were isolated from wildtype C57BL/6 mice and cultured for 48 h in CM with or without CD3/CD28 mediated co-stimulation. Subsequent metabolic phenotyping using a Seahorse XFe96 Bioanalyzer revealed no differences between the OCR of naïve or stimulated CD8$^+$ splenocytes upon NC26 or C26 CM treatment (Figure 37A, C). In line, basal and maximal respiration were largely unaffected by treatment with tumor cell CM, with a trend towards increased maximal respiration in a tumor cell-specific manner (Figure 37B, D). Glycolysis as measured by ECAR was not altered by NC26 or C26 CM compared to NC CM (Figure 37B, D).
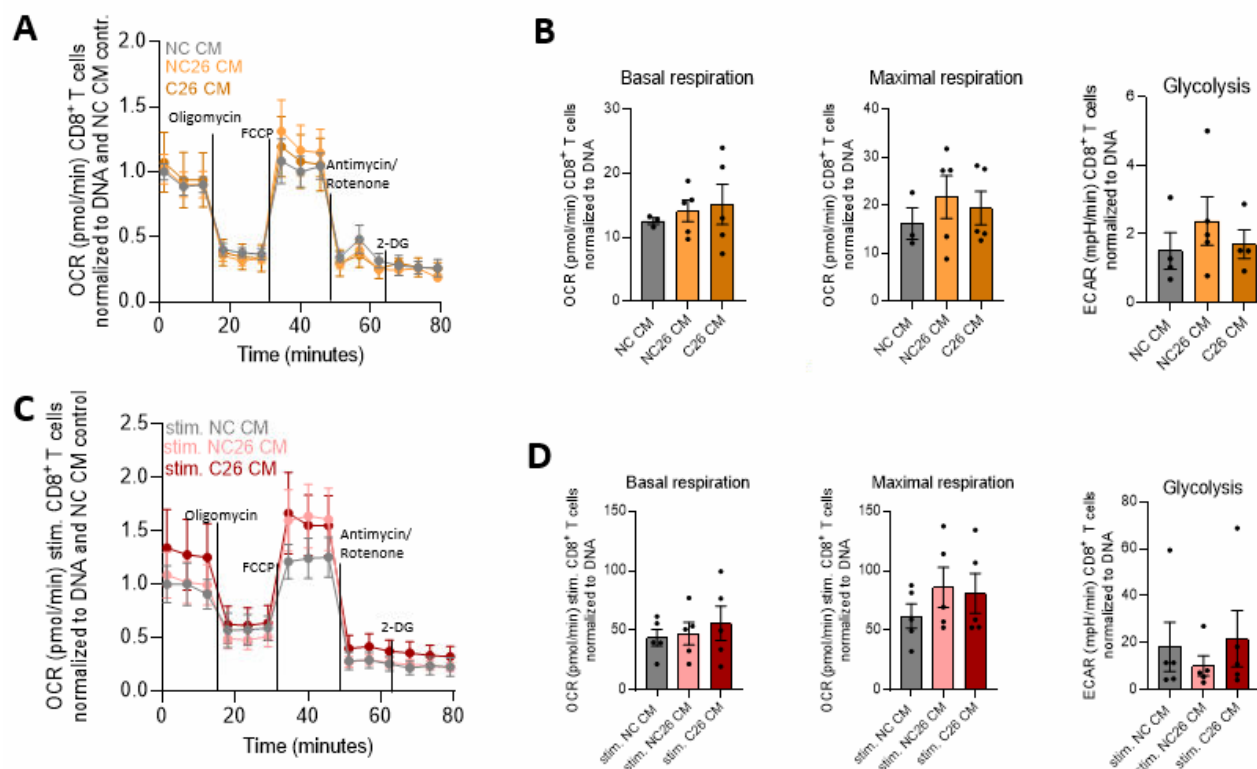
Figure 37. Conditioned media treatment of CD8+ splenocytes cannot recapitulate metabolic changes upon cachexia. (A-B) CD8+ T cells, isolated from the spleen of wildtype C57BL/6 mice, were treated with CM from NC26 (n=5) or C26 tumor cells (n=5), or as a control no-cell (NC) CM (n=4) was used. **(A)** OCR of CM treated CD8+ T cells across time, challenged by injections of oligomycin, FCCP, Antimycin and Rotenone, and 2-DG. **(B)** Calculations of basal and maximal respiration are based on OCR levels and can be looked up in detail in the methods section. Glycolysis rate as a measure of ECAR was assessed in CD8+ T cells treated with NC CM, NC26 CM and C26 CM. **(C-D)** CD8+ splenocytes were isolated from wildtype C57BL/6 mice, stimulated using anti-CD3/anti-CD28 antibodies, and incubated with NC CM (n=5), NC26 CM (n=5) or C26 CM (n=5) for 48 h. **(C)** OCR of stimulated and treated CD8+ T cells across time, challenged by injections of oligomycin, FCCP, Antimycin and Rotenone, and 2-DG. **(D)** Calculations of basal and maximal respiration based on OCR levels. Glycolysis rate as a measure of ECAR was assessed in CD8+ T cells treated with NC CM, NC26 CM and C26 CM. Experiments were planned by me and conducted together with Madleen Biggel as part of her internship with my help and supervision. Data are mean ± s.e.m. Statistical analyses were performed using two-way ANOVA with Tukey's multiple-comparison *post hoc* test, as well as one-way ANOVA or Kruskal-Wallis test with Tukey's or Dunn's multiple-comparison *post hoc* test, respectively.

Circulating naïve CD4+ T cells also displayed no alterations of OCR (Figure 38A), basal and maximal respiration as well as glycolysis (Figure 38B) upon NC26 or C26 CM treatment, in line with the results of CD8+ T cells described above. Upon stimulation, OCR over time and maximal respiration were unchanged in CD4+ T cells treated with CM (Figure 38C, D), while there was a trend for decreased basal respiration in tumor cell CM-treated T cells (Figure 38D). Contrary to CD8+ T cells, glycolysis was strongly decreased in stimulated CD4+ splenocytes treated with NC26 or C26 tumor cell CM.
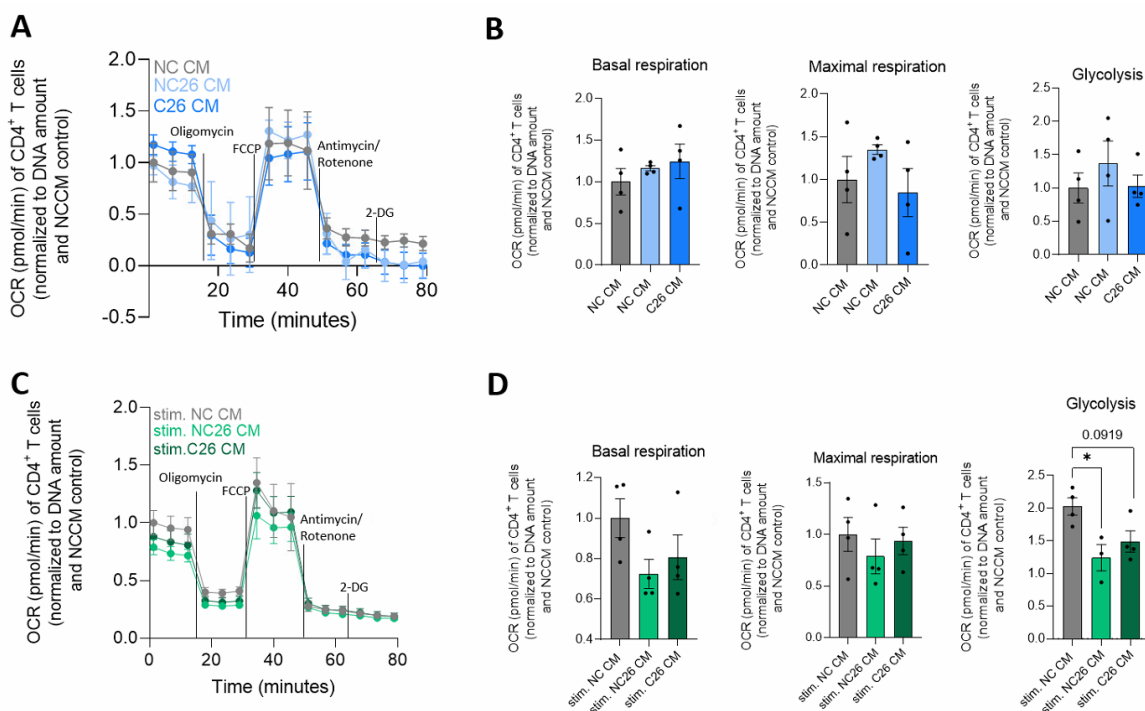
Figure 38. Conditioned media treatment of circulating CD4$^+$ T cells does not mimic metabolic changes upon cachexia. (A-B) CD4$^+$ T cells, isolated from the spleen of wildtype C57BL/6 mice, were treated with CM from NC26 (n=4) or C26 tumor cells (n=4), or as a control no-cell (NC) CM (n=4) was used. **(A)** OCR of CM treated CD4$^+$ T cells across time, challenged by injections of oligomycin, FCCP, Antimycin and Rotenone, and 2-DG. **(B)** Calculations of basal and maximal respiration are based on OCR levels. Glycolysis rate is based on ECAR measurements. **(C-D)** CD4$^+$ splenocytes were isolated from wildtype C57BL/6 mice, stimulated using anti-CD3/anti-CD28 antibodies, and supplied with NC CM (n=4), NC26 CM (n=4) or C26 CM (n=4) for 48 h. **(C)** OCR of stimulated and treated CD4$^+$ T cells across time, challenged by injections of oligomycin, FCCP, Antimycin and Rotenone, and 2-DG. **(D)** Calculations of basal and maximal respiration based on OCR levels and measurement of glycolysis based on ECAR levels. Experiments were planned by me and conducted together with Madleen Biggel as part of her internship with my help and supervision. Data are mean ± s.e.m. Statistical analyses were performed using two-way ANOVA or one-way ANOVA with Tukey's multiple-comparison *post hoc* test. *p<0.05.

Reduced numbers of tumor-infiltrating T cells could be in part explained by decreased proliferation, as assessed by reduced CD3-Ki67 co-expression (see chapter 2.2). Contrary, analysis of *Ki67* and *Pcna* (Proliferating Cell Nuclear Antigen) mRNA levels revealed no changes in naïve CD8$^+$ T cells treated with tumor cell CM (Figure 39A). CD3/CD28 co-stimulated CD8$^+$ cells showed a trend for increased *Ki67* gene expression in a tumor-dependent context, while *Pcna* was unaffected (Figure 39B).
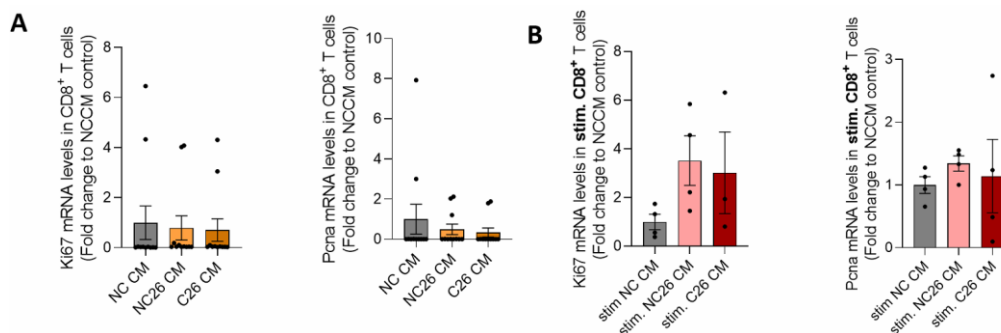
Figure 39. Proliferation of CD8$^+$ splenocytes is likely unaffected by treatment with NC26 or C26 tumor cell CM. (A-B) Circulating CD8$^+$ T cells were isolated from the spleen, and cultured in NC, NC26 or C26 CM for 48h. Ki67 and Pcna mRNA levels of **(A)** naïve CD8$^+$ T cells treated with NC (n=11), NC26 (n=11), C26 (n=11) CM or **(B)** stimulated CD8$^+$ splenocytes treated with NC (n=4), NC26 (n=3) or C26 (n=3-4) CM. Data are mean ± s.e.m. Statistical analyses were performed using one-way ANOVA or Kruskal-Wallis test with Tukey's or Dunn's multiple-comparison *post hoc* test, respectively.

Altogether, these results suggest that dampened T cell metabolism and function are mediated by systemic alterations and not tumor- secreted factors.

2.6   CD8+ T cell depletion aggravates cachexia

To prove the direct and causal relationship between cancer cachexia and T cell function, CD4+ and CD8+ T cells were depleted alone or in combination in PBS or C26 tumor-bearing mice using antibodies. Antibody injections were initiated 8 days post C26 cell injection, once tumors were palpable, and repeated every third day (Figure 40). The experiment was ended after 18 days, when all mice of one group had developed cancer cachexia. Thereby, survival of the different groups in combination with a mechanistic study could be investigated.
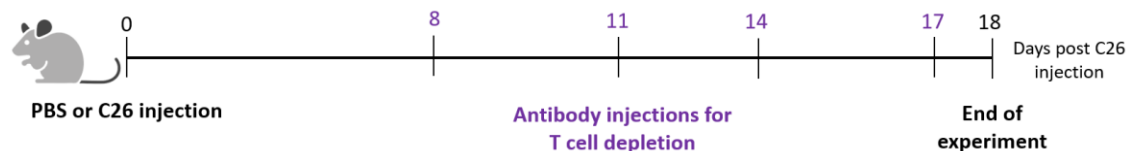
Figure 40. Illustration of antibody injections for T cell depletion in PBS and C26 tumor-bearing mice. Anti-CD4 and anti-CD8 depletion antibodies were intraperitoneally (i.p.) injected every third day, starting 8 days post tumor cell injection. The experiment was ended after 18 days, when all mice of one group had developed cancer cachexia.

Circulating CD4+ and CD8+ T cells were successfully depleted by antibody injections

The near-complete depletion of CD4+ and/or CD8+ T cells in the circulation was confirmed at multiple timepoints throughout the experiment by flow cytometric analyses of blood samples (Figure 41, results are exemplary shown for C26 tumor-injected mice, complete depletion was also confirmed in PBS mice, data not shown). To control for any harmful effects mediated by antibody treatment per se, isotype control antibodies were used.
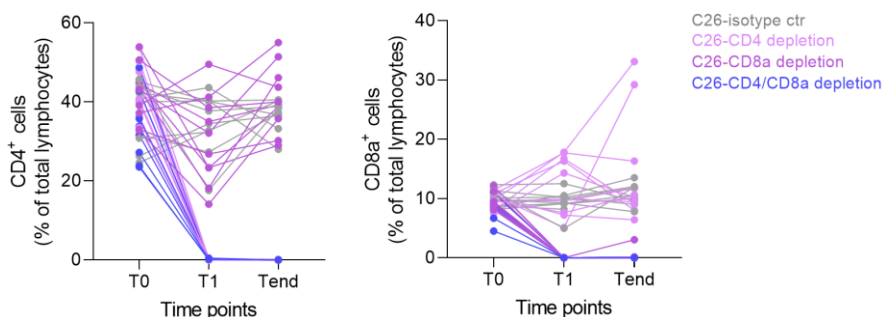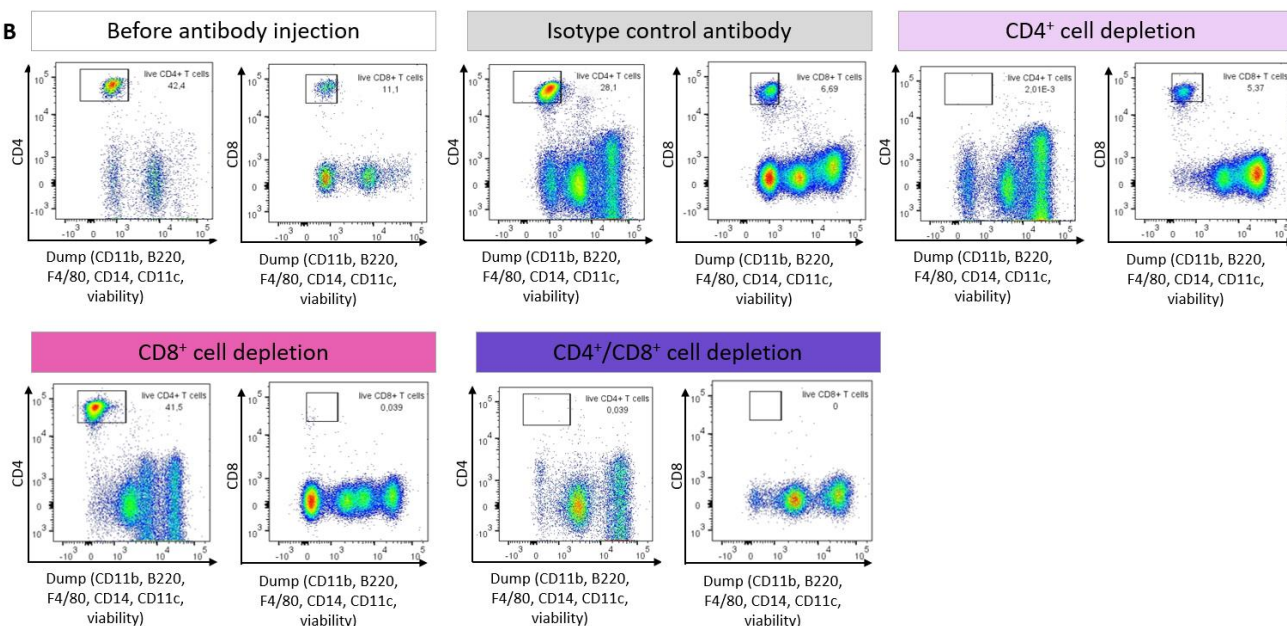
Figure 41. Near-complete CD4$^+$ and CD8$^+$ T cell depletion in the circulation of C26 tumor-bearing mice using antibodies. (A) Percentage of CD4$^+$ and CD8$^+$ T cells from all lymphocytes was measured in the blood by flow cytometry. Percentages were assessed before antibody injections (T0), during the experiment (T1) and at the day of sacrifice (Tend) in C26 animals injected with isotype control (n=10), CD4 depletion (n=10), CD8 depletion (n=10), or a combination of CD4 and CD8 depletion (n=9) antibodies. **(B)** Representative flow cytometric analysis of CD4$^+$ and CD8$^+$ T cells in antibody-depleted mice. T cells were gated as live single cells from total lymphocytes, which were CD11b$^-$B220$^-$F4/80$^-$CD14$^-$CD11c$^-$.

CD8$^+$ but not CD4$^+$ T cell depletion in C26 tumor-bearing mice accelerates cachexia development

Initial bodyweight of C26- and PBS-injected mice was similar, as assessed by non-significant statistical analysis, shown in Figure 42A. Depletion of CD8$^+$, but not CD4$^+$ cells from C26 mice accelerated weight loss and worsened cachexia (Figure 42B, D), underlining the importance of functional cytotoxic T cells to counteract cancer-induced wasting. Depletion of both CD8$^+$ and CD4$^+$ T cells only mildly accelerated cachexia development compared to the isotype control group. Hence, at the end of the experiment all mice from the CD8$^+$ depletion group had developed cachexia, while contrary, 60% of the mice from the CD4$^+$ depletion group were still cachexia-free (Figure 42D). Since all mice were sacrificed once all mice from one group had developed cachexia, a similar percentage of weight loss was observed between isotype control, CD8$^+$ depleted and CD4$^+$/CD8$^+$ depleted mice, while mice depleted of CD4$^+$ T cells showed significantly less body wasting due to decelerated cachexia development(Figure 42C, D). CD4$^+$ T cell depletion decelerated cachexia progression (Figure 42B, D), but simultaneously significantly decreased tumor growth (Figure 43). Importantly, healthy control mice, injected with the different depletion antibodies, remained weight-stable during the course of the experiment (Figure 42B, C, green color coding).
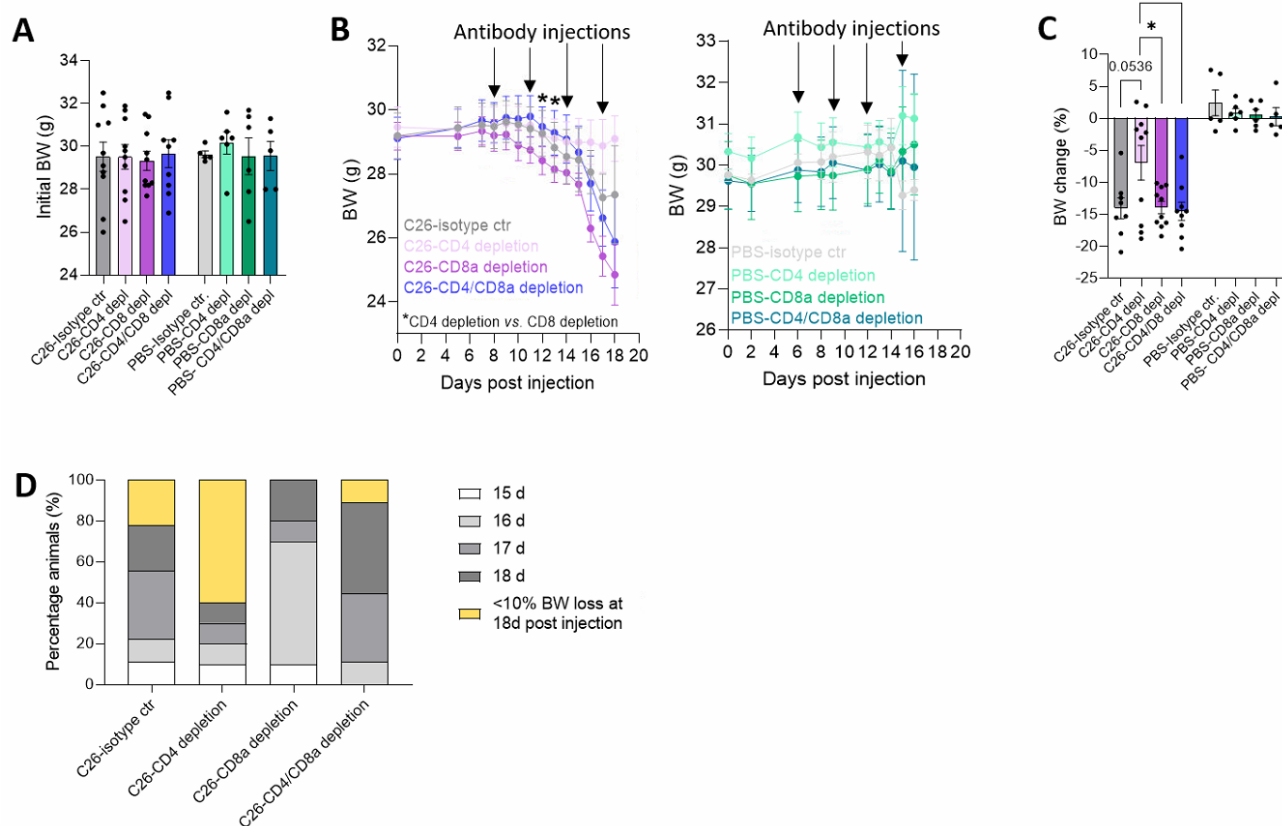
Figure 42. CD8$^+$ T cell depletion in C26 tumor-bearing mice speeds up cachexia development. CD4$^+$ and/or CD8$^+$ T cells were depleted from C26 tumor-bearing or PBS control mice. Same C26 tumor-bearing mice as in Figure 41. PBS mice, n=5/6 per group. Mice were sacrificed upon 10% bodyweight loss or latest on day 18 (C26) or 16 (PBS). **(A)** Initial bodyweight in gram. **(B)** Bodyweight in gram plotted against days post injection. Antibodies against CD4, CD8, both or an isotype control antibody were injected on day 8, 11, 14, and 17 post C26 injection, and on day 6, 9, 12, and 15 post PBS injection, indicated by black arrows. Only significances compared to isotype control were highlighted. **(C)** Bodyweight

changes in percentage. **(D)** Percentage of animals sacrificed due to cachexia on different days, indicated by white and grey color, or at the end of the experiment without any weight loss (yellow). Data are mean ± s.e.m. Statistical analyses were performed using two-way ANOVA or one-way ANOVA with Tukey's multiple-comparison *post hoc* test. *p<0.05.

CD4+ but not CD8+ T cell depletion affects tumor growth in C26 tumor-bearing mice

Tumor growth over the course and at the end of the experiment was similar between C26 mice injected with isotype control, anti-CD8, or a combination of anti-CD4/CD8 antibodies (Figure 43). In contrast, CD4^{+} depletion significantly decreased tumor growth around 13 days post C26 injection, as measured by tumor volume, shortly after the second antibody injection (Figure 43). This was probably due to the depletion of CD4^{+} regulatory T cells (Tregs), leading to an increased amount of cytotoxic T cells within the tumor as a compensatory effect (data not shown).
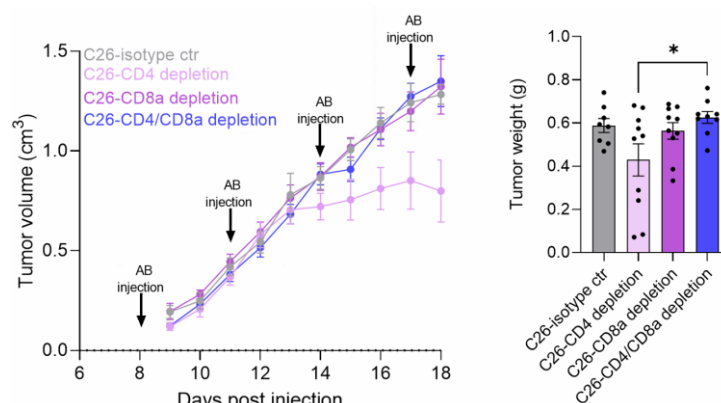
Figure 43. CD4^{+} but not CD8^{+} T cell depletion affects tumor growth in C26 tumor-bearing mice. Same mice as in Figure 42. **(A)** Tumor volume of mice during the course of the experiment, assessed by caliper measurements. **(B)** Tumor weight in gram at the end of the experiment. Data are mean ± s.e.m. Statistical analyses were performed using two-way ANOVA or one-way ANOVA with Tukey's multiple-comparison *post hoc* test. *p<0.05.

So far, a strong causal connection between CD8^{+} T cells and cachexia development could be assessed using T cell depletion antibodies. However, the similar weight loss between the groups, resulting from the study design, and the significantly reduced tumor sizes in the CD4^{+} depleted group, prohibited further mechanistic investigations on the strong effect of CD8^{+} T cells, as well as the influence of CD4^{+} T cells on cachexia development. To verify the first experiment and additionally gain more insight into underlying mechanisms, I conducted a second experiment with a modified experimental design. To this end, similar to the first experiment, C26 tumor-bearing mice were injected with different depletion antibodies, but this time the experiment was ended once the majority of one group had developed cachexia. This ensured that at this time point some mice already were cachectic, while others were still weight stable, enabling further mechanistic studies on organs and tissues of mice with different degrees of cachexia. In addition, I included a second CD4^{+} depletion group, which received their first anti-CD4 injection at a later timepoint to reduce interference of CD4^{+} T cell absence with tumor growth (Figure 44).
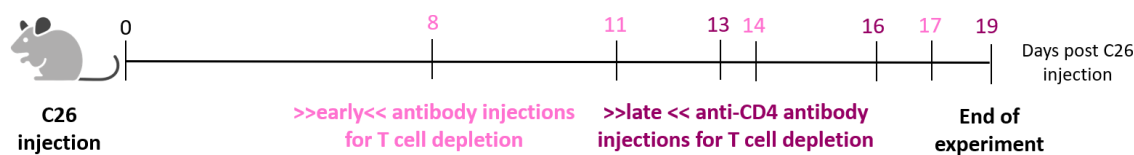

Figure 44. Illustration of antibody injections for T cell depletion in C26 tumor-bearing mice. CD4 and CD8 depletion antibodies were intraperitoneally (i.p.) injected every third day, starting 8 days post tumor cell injection. The experiment was ended after 19 days, when the majority of the CD8^{+} T cell depleted group had developed cancer cachexia. A >>late<<

anti-CD4 depletion group was included to reduce effects of the CD4+ T cell depletion on tumor growth, being injected for the first time five days later (at day 13) compared to all other groups.

Both, CD8+ and CD4+/CD8+ depletion accelerate and worsen cancer cachexia

Indeed, also the second experiment verified the strong causal relationship between CD8+ T cells and cachexia development. Both groups challenged with a CD8+ T cell depletion (CD8+ single and CD4+/CD8+ combi depletion), developed severe bodyweight loss over the time course of the experiment (Figure 45B, C), despite similar tumor growth over time (Figure 45D). In contrast to the first experiment, not only depletion of CD8+ T cells on their own, but also in combination with CD4+ T cells led to severe accelerated weight loss in the second study. Importantly, initial bodyweight of all groups was comparable at the beginning of the experiment, indicated by non-significant statistical analysis (Figure 45A). Again, early anti-CD4 injections interfered with tumor growth, as indicated by a reduced increase in tumor volume from day 15 on and a decreased tumor weight at the end of the experiment (Figure 45D). This effect could be avoided by delayed anti-CD4 injections, resulting in similar tumor volume during the experiment and potentially even a trend for slightly increased tumor weight at the end of the experiment compared to isotype control mice (Figure 45D). Moreover, the late CD4+ depletion tended to increase wasting compared to isotype control mice, as measured by the percentage of bodyweight change (Figure 45C), suggesting that upon similar tumor growth CD4+ T cell absence worsens cachexia, but to a lesser extent compared to CD8+ T cell depletion,

Overall, this second experiment confirmed the previously made observations about the importance of functional T cells to counteract cachexia, solved the problem of smaller sized tumors induced by CD4+ T cell depletion and built the basis for further mechanistic studies, described in more detail in the following.
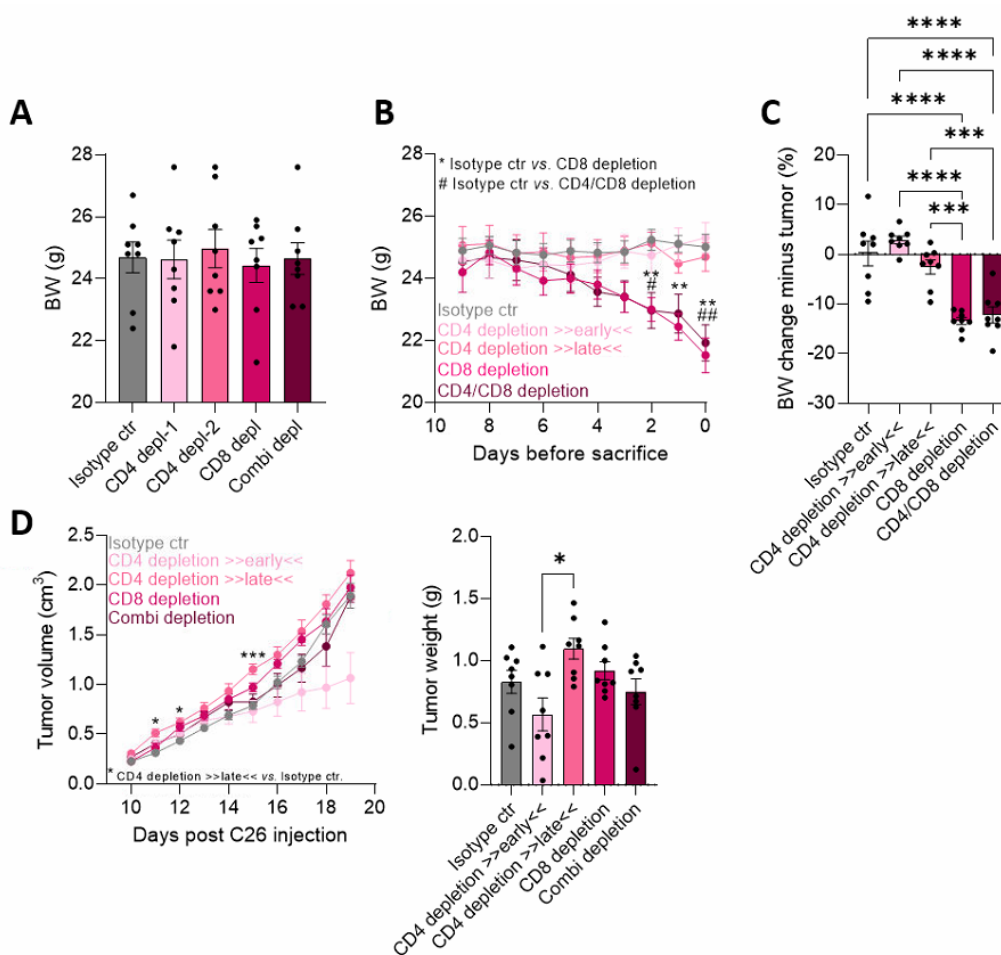
Figure 45. CD8⁺ and CD4⁺/CD8⁺ depletion accelerate and worsen body wasting. (A-C) C26 tumor-bearing mice were injected with isotype control (n=8), anti-CD4 at an early (n=8) and late (n=8) timepoint, anti-CD8 (n=8) and a combination of anti-CD4/anti-CD8 (n=8) antibodies. **(A)** Initial bodyweight before tumor implantation or antibody injection. **(B)** Bodyweight development over the course of the experiment. Only significances compared to isotype control were highlighted. **(C)** Bodyweight change minus tumor weight at the end of the experiment in percentage. **(D)** Tumor volume and weight during the course and at the end of the experiment. Only significances compared to isotype control were highlighted. Data are mean ± s.e.m. Statistical analyses were performed using two-way ANOVA or one-way ANOVA with Tukey's multiple-comparison *post hoc* test or Kruskal-Wallis test with Dunn's multiple-comparison *post hoc* test. *p<0.05, **p<0.01, ***p<0.001, ****p<0.0001.

CD8⁺ T cell depletion worsens wasting upon cancer cachexia

In line with the significant weight loss of C26 tumor-bearing mice accelerated by CD8⁺ or CD4⁺/CD8⁺ depletion, weight of metabolic tissues, including iWAT, eWAT and skeletal muscle, was strongly reduced (Figure 46A, B, C), indicating aggravated tissue wasting. Interestingly, splenomegaly was not decreased by antibody injections (Figure 46D). Contrary, CD4⁺ and CD8⁺ cell depletion, alone or in combination, resulted in significantly smaller draining lymph nodes (Figure 46E), implying that the antibody treatment was especially successful at this site, most likely due to the close distance to the injection site (i.p. injection).
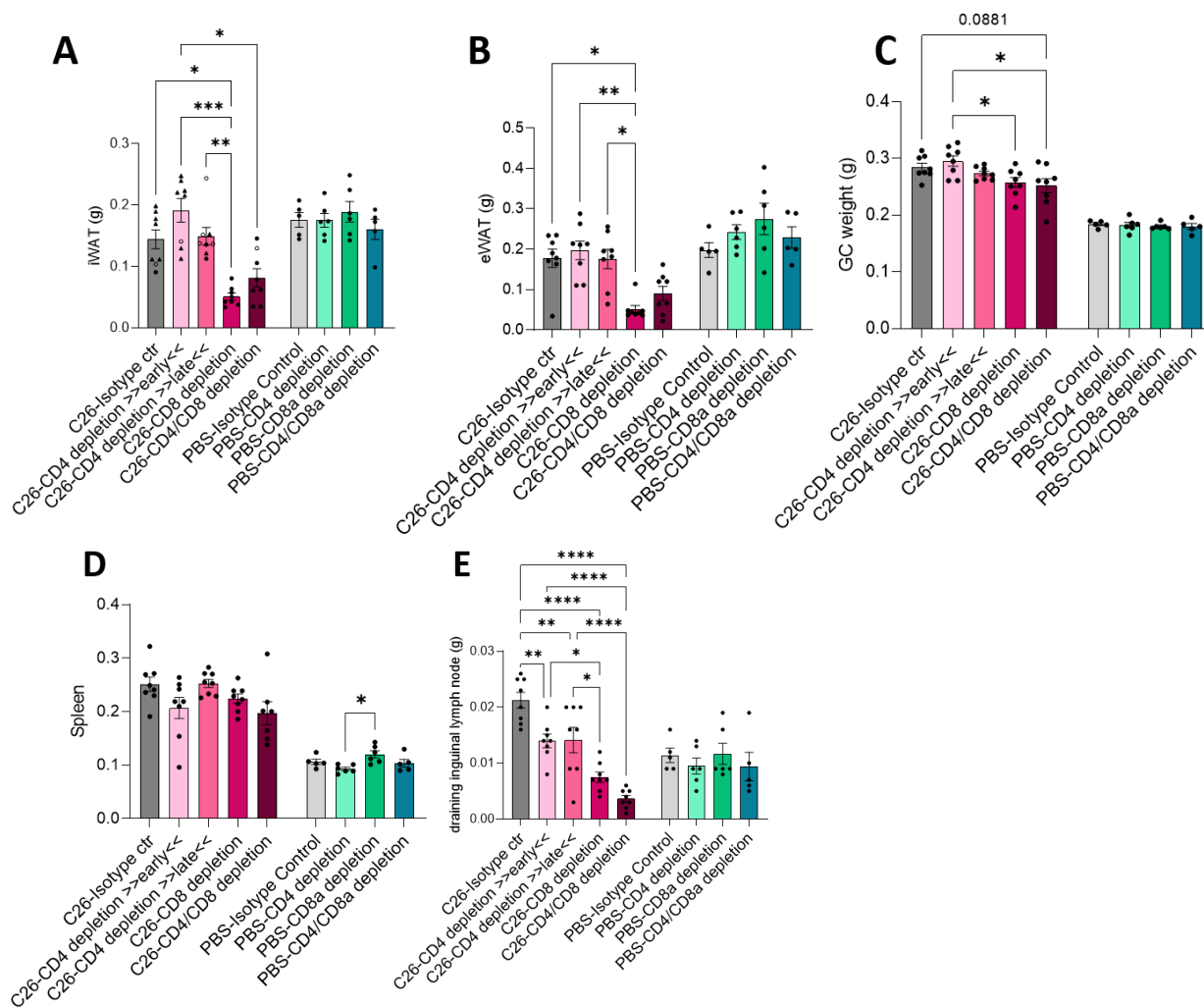
Figure 46. CD8⁺ T cells are involved in wasting upon cancer cachexia. (A-E) Organ weights of C26 tumor-bearing or healthy PBS mice, injected with isotype control (C26 n=8, PBS n=5), anti-CD4 early (C26 n=8, PBS n=6) or late (C26 n=8), anti-CD8 (C26 n=8, PBS n=6) or a combination of anti-CD4/anti-CD8 (C26 n=8, PBS n=5) antibodies. Weights of **(A)** iWAT, **(B)** eWAT, **(C)** skeletal muscle (GC), **(D)** spleen and **(E)** draining inguinal lymph nodes in C26 or both inguinal lymph nodes in PBS mice. Data are mean ± s.e.m. Statistical analyses were performed using one-way ANOVA with Tukey's multiple-

comparison *post hoc* test or Kruskal-Wallis test with Dunn's multiple-comparison *post hoc* test. *p<0.05, **p<0.01, ***p<0.001, ****p<0.0001.

Cachexia in CD8+-depleted C26 tumor-bearing mice alters circulating lipids

We and others have previously determined essential changes in the circulating lipidome in cancer cachexia (Cala, 2018; Morigny&Zuber, 2020; Riccardi, 2020; L. A. Taylor, 2007). In line with these data, cachexia in CD8+ and CD4+/CD8+-depleted C26 tumor-bearing animals resulted in a strong increase of cholesterol, HDL, and LDL levels, while triglycerides were decreased in CD8+-depleted mice and unaltered in all other groups. Plasma NEFA and glucose levels were unchanged between all groups, but glucose tended to be slightly decreased in groups with a high cachexia incidence (Figure 47). Importantly, circulating parameters were largely unaffected in PBS-injected mice treated with T cell depletion antibodies, implying that the observed changes were mostly cachexia-dependent and not specific to T cell depletion. However, plasma triglycerides were significantly reduced in healthy CD4+/CD8+ depleted mice compared to animals treated with an early injection of anti-CD4 antibodies (Figure 47D), indicating a functional connection between T cells and lipid metabolism, as already shown by others (Gisterå, 2018; Klingenberg, 2013).
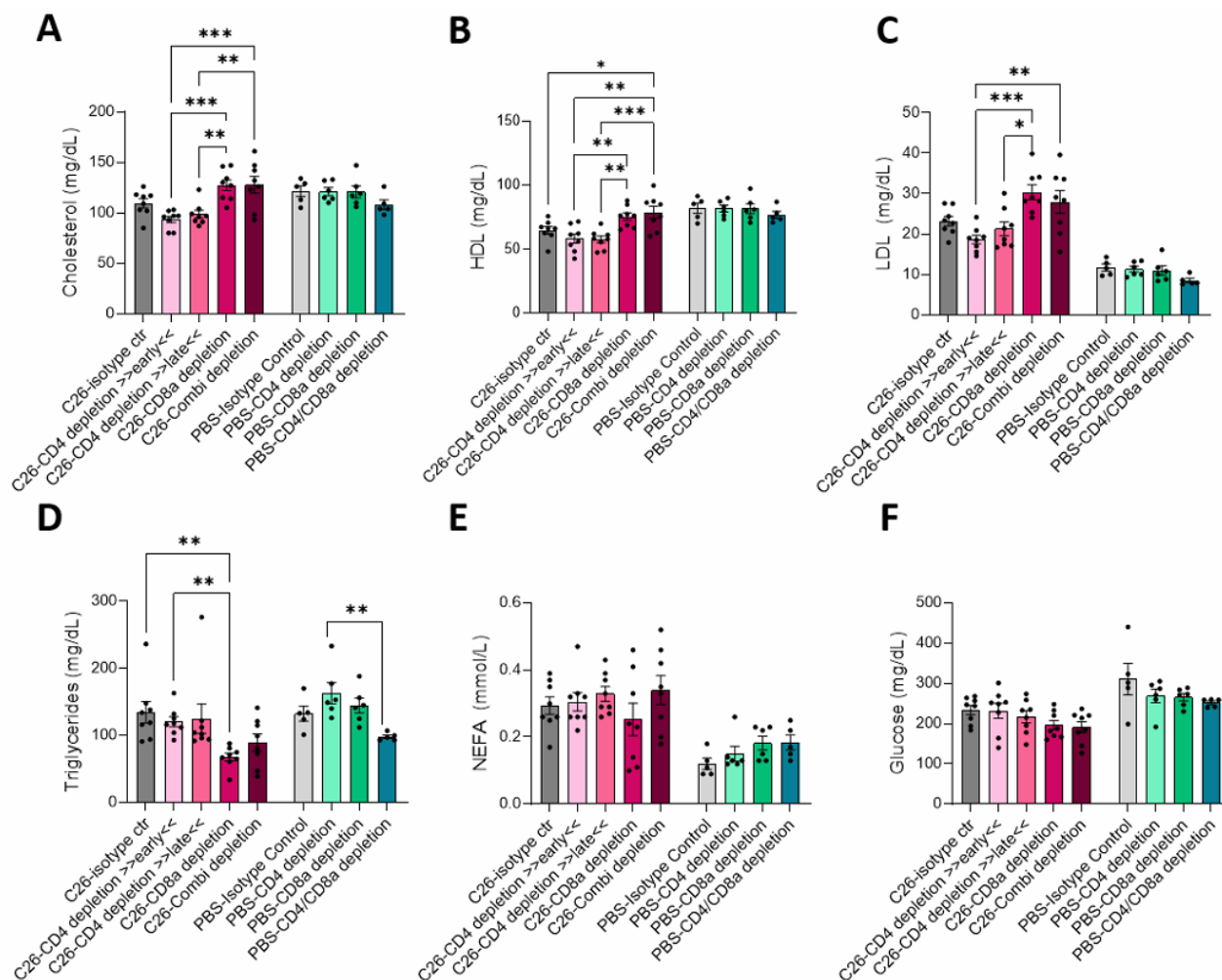
Figure 47. Levels of circulating lipids are altered in cachectic C26 tumor-bearing mice. Same mice as in Figure 46. Circulating levels of **(A)** cholesterol, **(B)** HDL, **(C)** LDL, **(D)** Triglycerides, **(E)** NEFAs, and **(F)** Glucose in C26- or PBS-injected mice, treated with anti-CD4 or anti-CD8 depletion antibodies, measured using a chemical analyzer. Data are mean ± s.e.m. Statistical analyses were performed using one-way ANOVA with Tukey's multiple-comparison *post hoc* test or Kruskal-Wallis test with Dunn's multiple-comparison *post hoc* test. *p<0.05, **p<0.01, ***p<0.001.

C26-induced expression of wasting markers is enhanced upon CD8+ and CD4+/CD8+ cell depletion

Tissue wasting in cancer cachexia is often determined by assessing muscle atrogenes, including Atrogin 1 (F-Box Protein 32/Fbxo32), MuRF1 (Muscle-specific RING Finger Protein 1, also called Tripartite Motif Containing 63/Trim63), FoxO3a (Forkhead-Box-Protein O3) and Ctsl (Cathepsin-L) (Rohm, 2019; Webster, 2020). To determine if T cell depletion affected C26-induced expression of wasting markers, I evaluated gene expression of Trim63, Fbxo32, FoxO3a and Ctsl in skeletal muscle of C26- and PBS-injected mice treated with T cell depleting antibodies (Figure 48). In line with body and organ weight loss, CD8+ and CD4+/CD8+ T cell depletion strongly induced atrogene expression in C26 tumor-bearing animals (Figure 48A), with particularly high expression in cachectic animals (filled circles), while pre-cachectic (empty circles) and non-cachectic (triangle) mice showed low expression. This indicates that high atrogene marker expression is more specific to cachexia-development, which was accelerated in CD8 depletion groups, than dependent on T cell depletion. Although GC muscle mass was not altered in T cell depleted PBS mice, significant downregulation of atrogene expression was observed in CD4+/CD8+ depleted mice (Figure 48B), suggesting a rather positive effect of the absence of CD4+ and CD8+ T cells on skeletal muscles of PBS mice, which – to my knowledge – has not been reported so far in healthy mice.
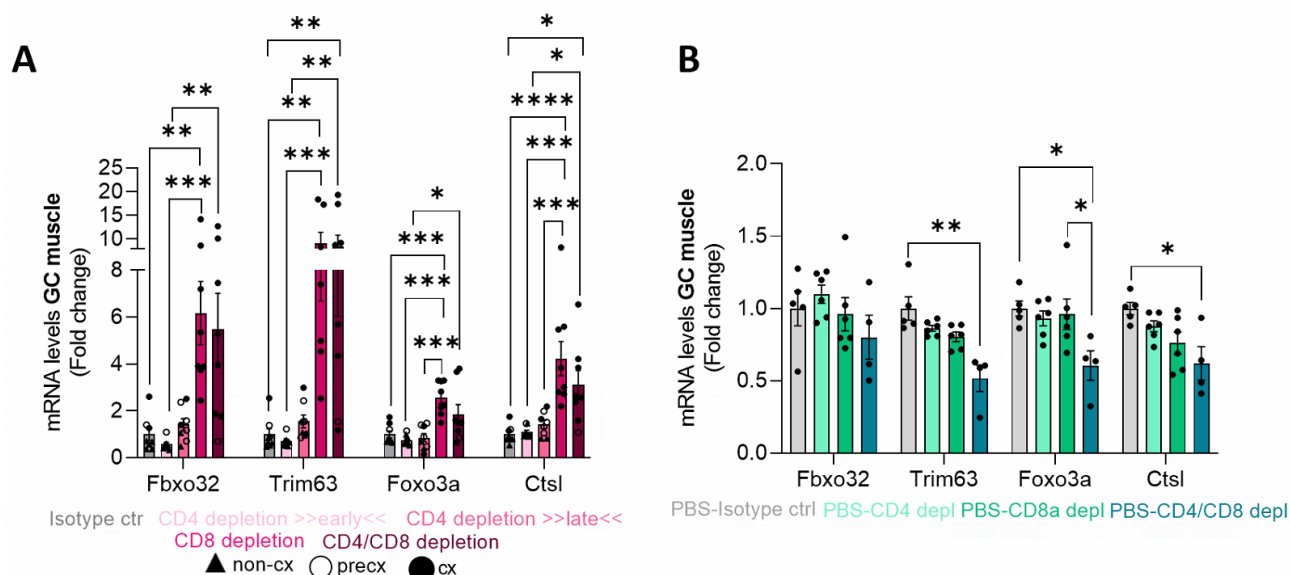
Figure 48. C26-induced expression of muscle wasting markers is enhanced upon cachexia in CD8+ and CD4+/CD8+ cell depletion. Same mice as in Figure 46. Expression of different cachexia-associated genes in in gastrocnemius (GC) muscle of **(A)** C26 tumor-bearing mice and **(B)** PBS injected mice, depleted with CD4 and/or CD8 antibodies. Data are mean ± s.e.m. Statistical analyses were performed using one-way ANOVA with Tukey's multiple-comparison *post hoc* test or Kruskal-Wallis test with Dunn's multiple-comparison *post hoc* test. *p<0.05, **p<0.01, ***p<0.001.

Adipose tissue is drastically affected by cachexia development, leading to major changes in the expression of genes involved in several metabolic and inflammation-related pathways, as already reported by us (Geppert, 2021). To check if AT wasting, which was accelerated by the depletion of CD8+ T cells, was also present at the molecular level, expression of key enzymes of lipolysis, including *Atgl* (adipose triglyceride lipase), *Mgl* (monoacylglycerol lipase), *Plin4* (Perilipin 4), *Hsl* (hormone-sensitive lipase), and *Cpt1a* (Carnitine Palmitoyltransferase 1A) was investigated. Contrary to our hypothesis, a significant reduction of *Mgl* and *Plin4* was observed in CD8+ T cell depleted iWAT of C26 tumor-bearing mice, while *Atgl*, *Hsl* and *Cpt1a* levels were unchanged between all groups (Figure 49A). This indicates a protective effect of the CD8+ depletion, alone or in combination, on the molecular mechanisms of adipose tissue lipolysis in cancer cachexia, despite the significant organ

wasting observed on tissue level (Figure 46A, B). Interestingly, *Mgl* and *Plin4* downregulation seemed to be dependent on CD8^{+} T cell depletion, as pre-cachectic (empty circles) and cachectic (filled circles) mice from the isotype control or CD4 depletion group showed higher gene expression levels, independent of cachexia onset (Figure 49A). Surprisingly, CD4^{+}/CD8^{+} depletion also significantly downregulated expression of *Atgl*, *Mgl*, *Plin4* and *Hsl* in healthy mice compared to isotype control mice (Figure 49B), underlining the strong connection between T cells and adipose tissue metabolism. However, despite improved gene expression of wasting markers on the molecular level, AT loss was worsened in CD8 and CD4/CD8 depleted C26 tumor-bearing mice, indicating that potential post-transcriptional/translational changes predominate these molecular changes.
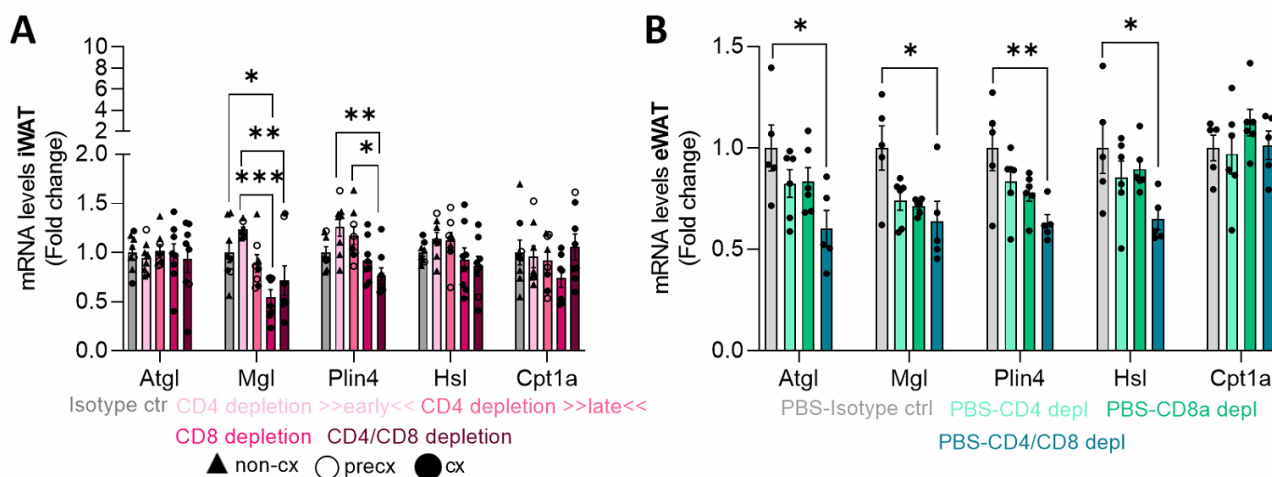
Figure 49. C26-induced expression of adipose tissue wasting markers is ameliorated by CD8^{+} and CD4^{+}/CD8^{+} cell depletion. Same mice as in Figure 46. Gene expression of adipose tissue wasting markers related to cancer cachexia in **(A)** iWAT of C26 tumor-bearing or **(B)** PBS injected mice, depleted of CD4^{+} and/or CD8^{+} T cells. Data are mean ± s.e.m. Statistical analyses were performed using one-way ANOVA with Tukey's multiple-comparison *post hoc* test or Kruskal-Wallis test with Dunn's multiple-comparison *post hoc* test. $*p < 0.05$, $**p < 0.01$, $***p < 0.001$.

Obesity-associated WAT inflammation may in part be triggered by cytotoxic CD8^{+} T cells (Q. Wang, 2018), which is why we sought to determine if adipose tissue inflammation upon cachexia was affected by T cell depletion, thereby enhancing wasting. To this end, key markers of inflammation, namely *Il6*, *Tnfα*, *Il2* and *Ifnγ* were assessed in WAT of C26 tumor-bearing T cell depleted mice (Figure 50A). No common signature of altered inflammatory markers could be observed, despite the fact that cachectic mice showed a largely lowered expression of inflammatory markers compared to pre-cachectic or healthy mice (exclusive *Il6*) (Figure 50A). I found a strong reduction of the effector cytokines *Tnfα* and *Ifnγ* in iWAT from CD8^{+} and to a smaller extent CD4^{+}/CD8^{+} T cell-depleted C26 tumor-bearing mice. Interestingly, both *Tnfα* and *Ifnγ* were also reduced in healthy mice upon CD4^{+}/CD8^{+} and to a smaller degree in CD4^{+} or CD8^{+} depleted mice (Figure 50B). Together, these results suggest that T cell derived *Tnfα* and *Ifnγ* cytokine expression might be an important contributor to elevated proinflammatory cytokine levels in WAT. Moreover, low levels of *Ifnγ* in iWAT of cachectic *versus* non-cachectic mice, were especially prominent in the early CD4^{+} depletion group in C26 tumor-bearing mice. Here, the CD4^{+} depletion, including the depletion of Tregs, possibly led to an increase of cytotoxic CD8^{+} T cells (as assessed by *Cd8* gene expression in iWAT, Figure 51), which are known to secrete high amounts of pro-inflammatory cytokines (Mosmann, 1997), thereby explaining the increased *Ifnγ* expression in non-cachectic mice (Figure 50A). Probably, this effect was abolished in cachectic mice due to very low numbers of tissue infiltrating CD8^{+} T cells (see chapter 2.2). *Il2* gene expression seemed to be downregulated in healthy mice receiving T cell depletion antibodies (Figure 50B), while it tended to be increased in CD4 early depletion and CD4/CD8 depletion

in C26 tumor-bearing mice (Figure 50A). Gene expression of *Il6*, a potent mediator of cancer cachexia in the C26 mouse model (Geppert, 2021; Strassmann, 1992; Zaki, 2004), was reduced upon CD4^{+} T cell depletion, alone or in combination, in healthy animals, while it tended to increase upon CD8^{+} cell depletion (Figure 50A, B). Interestingly, upon C26 tumor cell-injection, CD4^{+} and CD4^{+}/CD8^{+} T cell depletion led to a non-significant increase of *Il6* expression in iWAT, independent of cancer cachexia. Importantly, *Il6* expression was regulated *vice versa* in PBS-injected animals, with high *Il6* levels in eWAT of CD8^{+} T cell depleted mice, while CD4^{+} and CD4^{+}/CD8^{+} T cell depletion led to a reduction of *Il6* expression compared to isotype control mice (Figure 50B).
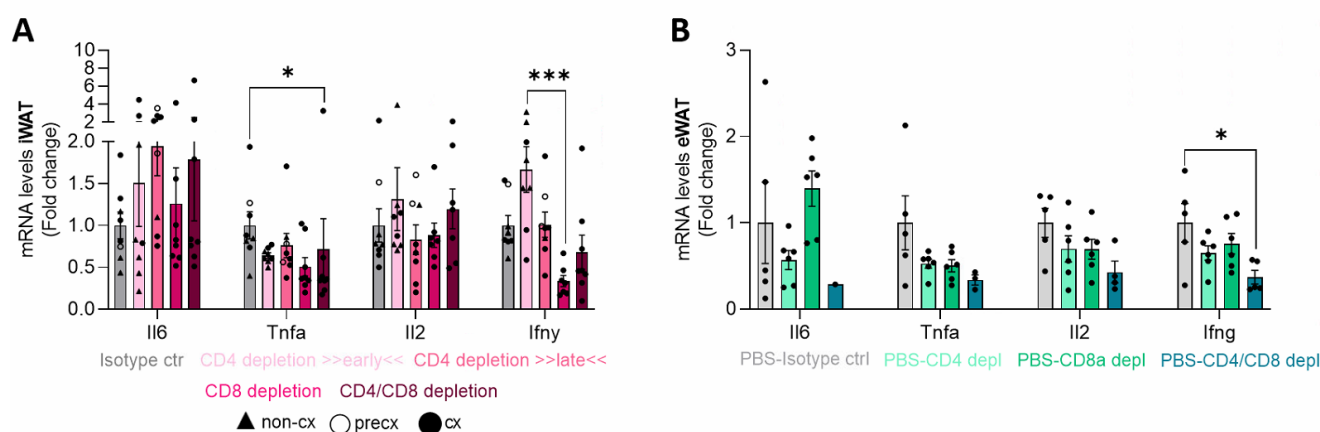
Figure 50. Expression of inflammatory markers in adipose tissue is altered by depletion of different T cell subsets. Same mice as in Figure 46. Gene expression of inflammatory genes in **(A)** iWAT of C26 tumor-bearing and **(B)** eWAT of PBS-injected mice, depleted of different T cell subsets. Data are mean ± s.e.m. Statistical analyses were performed using one-way ANOVA with Tukey's multiple-comparison *post hoc* test or Kruskal-Wallis test with Dunn's multiple-comparison *post hoc* test. *p<0.05, ***p<0.001.

Successful CD8^{+} T cell depletion in metabolic tissues and tumor

Complete T cell depletion in the circulation was continuously checked during the course of the experiment using flow cytometry. However, T cells are also known to infiltrate peripheral tissues (T. D. Wu, 2020), exerting their functions on a local base. Therefore, I assessed if T cell depletion antibodies also successfully depleted adipose and muscle tissue- specific as well as tumor infiltrating lymphocytes. To this end, I analyzed the expression of T cell marker genes, including *Cd3, Cd8, Cd4, Foxp3* and the CD8^{+} T cell effector cytokine *Gzmb*. Both, CD4^{+} and CD8^{+} single depletion nicely reduced *Cd4* and *Cd8* expression in GC muscles from C26 tumor-bearing mice by approximately 50%, while combi CD4^{+}/CD8^{+} T cell depletion resulted only in a proper *Cd8* reduction and contrary an increase in *Cd4* gene expression (Figure 51A). In healthy animals, single CD4^{+} T cell depletion did not reduce *Cd4* expression in GC muscles, while in combination with a CD8^{+} T cell depletion, also *Cd4* expression levels were reduced (Figure 51B).

 Depletion of CD8^{+} T cells in healthy mice reduced *Cd8* expression strongly, as expected (Figure 51B). *Foxp3* expression in GC muscles was reduced in CD4 depleted C26 tumor-bearing mice, in line with a decreased *Cd4* gene expression, but also CD4/CD8 combi-depleted C26 animals showed a strong reduction of *Foxp3* levels, despite increased *Cd4* expression (Figure 51), implying a reduction in FoxP3^{+} Tregs, in combination with a general increase of CD4^{+} helper T cells. Additionally, C26 animals being depleted of CD8^{+} T cells showed a reduction of *Foxp3* in GC muscles as well, likely rather a result of low tissue-infiltrating T cell numbers due to cachexia than the CD8^{+} depletion itself (Figure 51). Surprisingly, *Foxp3* levels were not altered in healthy mice treated with T cell depletion antibodies (Figure 51B). In both C26- and PBS-injected mice, CD4^{+} T cell depletion led to a high expression of *Cd8* in skeletal muscle, especially in non-cachectic animals (Figure 51A, B), probably as a result of

decreased numbers of regulatory CD4^{+} cells, mediating a suppressive effect on cytotoxic CD8^{+} T cells (Hasenkrug, 2011). In iWAT, T cell depletion treatment resulted in an even stronger decrease in *Cd8* and *Cd4* expression compared to GC muscles (60-100%), with a particularly robust reduction of *Cd8* expression in CD8^{+} and CD4^{+}/CD8^{+} depleted C26 mice (Figure 51C). *Foxp3* and *Gzmb* expression in iWAT behaved comparably to GC muscles, with the exception that *Gzmb* levels were unchanged upon CD4^{+} T cell depletion in iWAT (Figure 51C). In healthy mice, anti-CD8 treatment led to significant downregulation of *Cd8*, and anti-CD4 treatment to a less strong decrease of *Cd4* (Figure 51D). Combi-treatment resulted in a prominent reduction of *Cd8*, while *Cd4* was not affected. Interestingly, *Gzmb* levels tended to increase upon CD8^{+} and CD4^{+}/CD8^{+} cell depletion (Figure 51D) in healthy control mice, contrary to what was expected. Overall, T cell depletion was largely successful in adipose and muscle tissue, with a stronger effect of anti-CD8 treatment compared to anti-CD4.
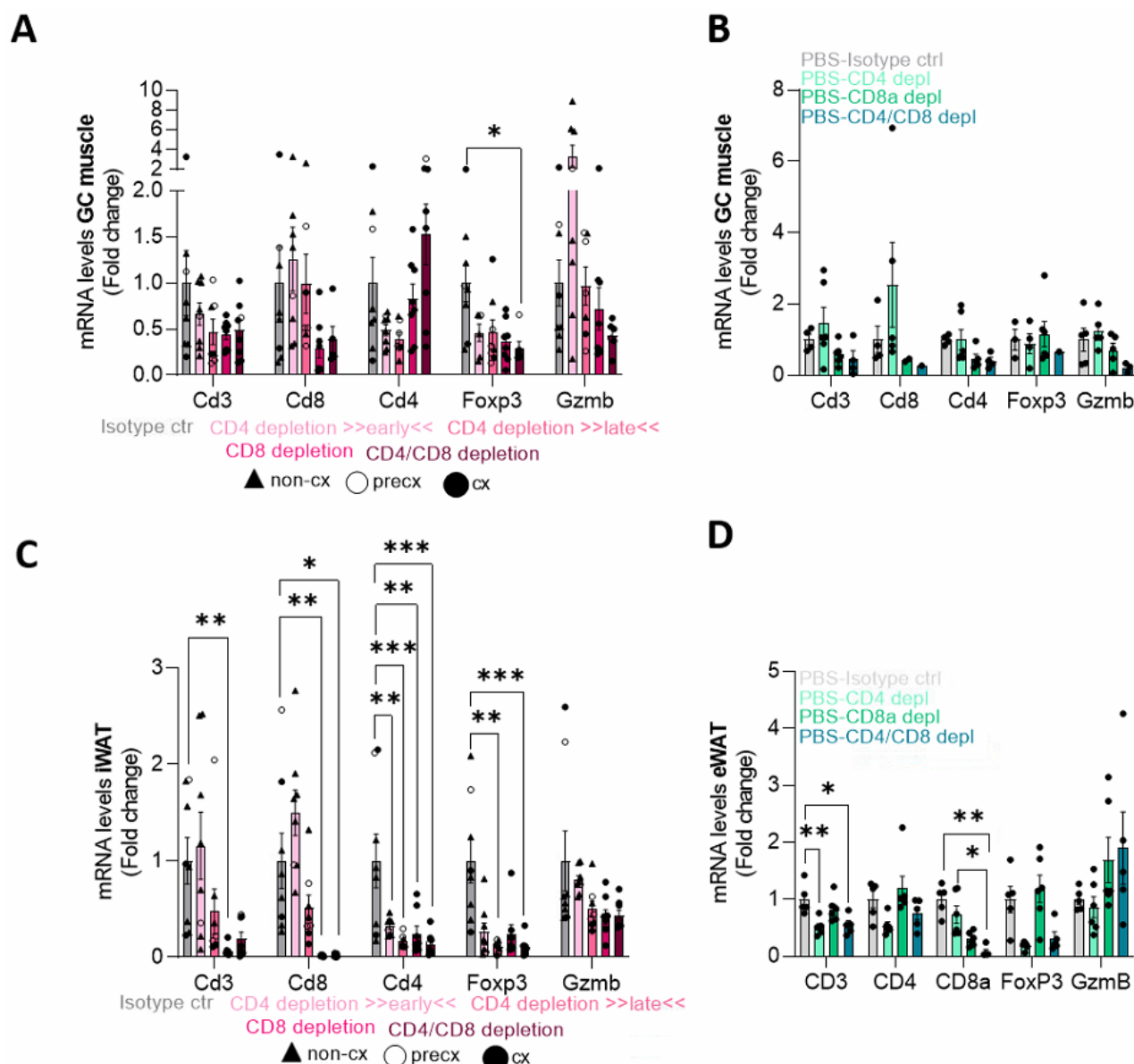
Figure 51. T cell depletion altered immune cell marker expression in metabolic tissues. Same mice as in Figure 46. **(A-D)** mRNA levels of immune cell marker genes, namely *Cd3, Cd8, Cd4, Foxp3* and *Gzmb* in **(A)** GC muscle of C26 tumor-bearing mice, **(B)** GC muscle of PBS mice, **(C)** iWAT of C26 tumor-bearing mice and **(D)** iWAT of PBS mice. Filled triangles represent non-cachectic, empty circles pre-cachectic and filled circles cachectic C26 tumor-bearing mice. Only significances compared to isotype control were highlighted. Data are mean ± s.e.m. Statistical analyses were performed using one-way ANOVA or Kruskal-Wallist test with Tukey's or Dunn's multiple-comparison *post hoc* test, respectively. *p<0.05, **p<0.01, ***p<0.001.

In tumor tissue, expression levels of immune marker genes were regulated similarly to iWAT and GC muscle. In brief, CD8+ and CD4+/CD8+ depletion resulted in a very strong reduction of *Cd8* expression, while anti-CD4 treatment only partly downregulated *Cd4* in the late CD4 and combi depletion group (Figure 52). Interestingly, high expression of T cell markers (*Cd4, Cd8, Gzmb*) in tumors was particularly evident in mice which had not developed cachexia (triangles and empty circles *vs.* full circles, Figure 52), thus especially in the anti-CD4 depletion group.
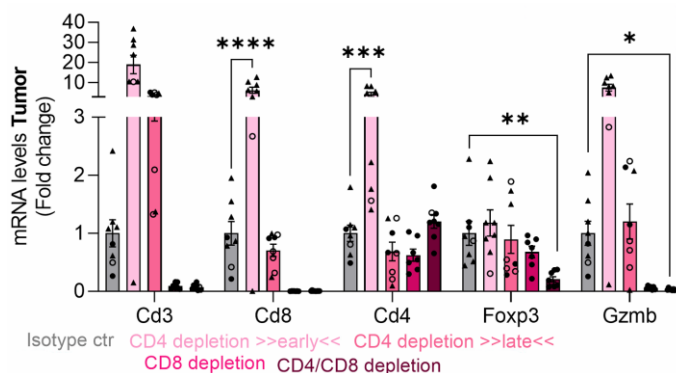
Figure 52. Expression of immune cell markers in C26 tumors of T cell depleted mice. Same mice as in Figure 46. Gene expression of immune marker genes, including *Cd3, Cd8, Cd4, Foxp3* and *Gzmb* was assessed in C26 tumor-bearing mice treated with T cell depletion antibodies. Filled triangles represent non-cachectic, empty circles pre-cachectic and filled circles cachectic C26 tumor-bearing mice. Only significances compared to isotype control were highlighted. Data are mean ± s.e.m. Statistical analyses were performed using one-way ANOVA or Kruskal-Wallist test with Tukey's or Dunn's multiple-comparison *post hoc* test, respectively. *p<0.05, **p<0.01, ***p<0.001, ****p<0.0001.

As previously described in this thesis, I have already found altered chemokine expression in cachectic tumors, possibly leading to less tumor infiltration and thus reduced T cell numbers in cachectic tumors (chapter 2.2). Hence, I sought to determine if by systemic T cell depletion chemokine expression in C26 tumors was altered, as assessed by gene expression analysis. In line with previously observed data, non-cachectic animals had high expression levels of Ccl4, Cx3cl1, Cxcl9 and Cxcl11 (Figure 53), indicating increased T cell attraction, resulting in elevated T cell infiltration, as also suggested by elevated expression of T cell marker genes in non-cachectic T cell depleted mice (Figure 52). Tumors from CD8 depleted mice, alone or in combination with CD4 depletion, had a strongly reduced CD8+ T cell infiltration (Figure 52), in combination with a significant reduction of chemokine marker expression (Figure 53), again underlining that chemokine levels in tumors are important attractors for T cells, which seem to be blunted in cancer cachexia.
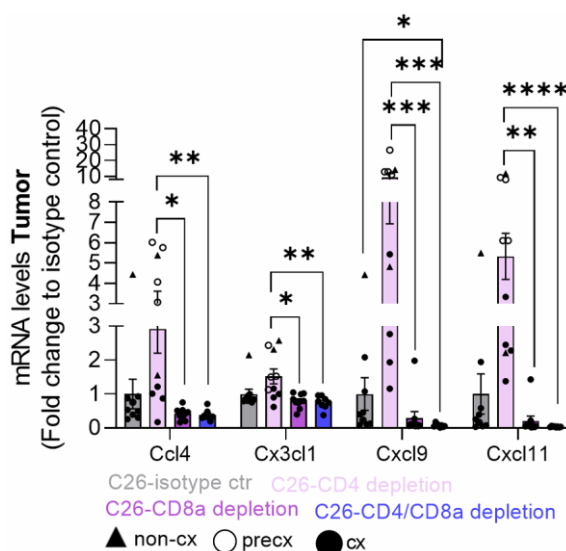
Figure 53. Altered chemokine levels in cachectic C26 tumor-bearing mice. Same mice as in Figure 42. Gene expression levels of chemokines, in detail Ccl4, Cxc3cl1, Cxcl9 and Cxcl11 in C26 tumor-bearing mice treated with T cell depletion antibodies. Filled triangles represent non-cachectic, empty circles pre-cachectic and filled circles cachectic C26 tumor-bearing mice. Data are mean ± s.e.m. Statistical analyses were performed using one-way ANOVA or Kruskal-Wallist test with Tukey's or Dunn's multiple-comparison *post hoc* test, respectively. *p<0.05, **p<0.01, ***p<0.001, ****p<0.0001.

2.7 Transcriptional remodeling of T cells in cancer cachexia

So far, T cell activity seemed blunted upon cancer cachexia, based on reduced tissue-infiltrating T cell numbers, decreased proliferation, dampened gene expression of effector cytokines, and altered metabolism (chapters 2.2 and 2.4.) Moreover, a direct functional relationship between T cell presence and cachexia development was observed (chapter 2.6). To unravel now functional mechanisms underlying the dysregulated T cell function, transcriptional profiling was performed.

To this end, BALB/c mice were injected with C26 cachexia-inducing tumor cells or as a control, PBS or NC26 non-cachexia-inducing tumor cells (Figure 54). Once C26 mice developed cachexia, CD4^{+} and CD8^{+} T cells were enriched from spleen and tumor using fluorescence-activated cell sorting (FACS) and sent for RNA sequencing. Due to very low cell numbers, TILs were sequenced using SMARTer sequencing, while circulating T cells were sequenced using low-input sequencing.
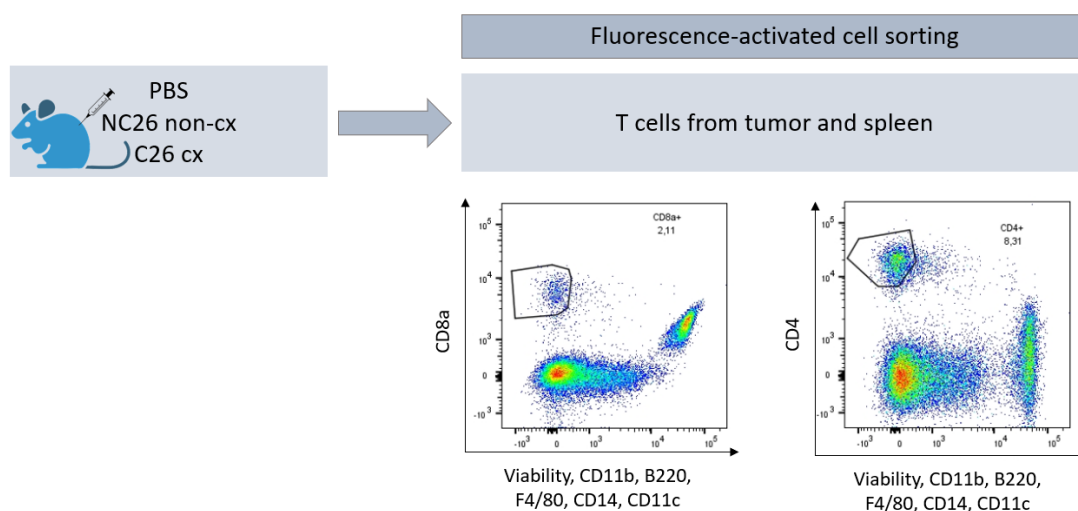
Figure 54. Experimental setup for RNA sequencing of T cells from cachectic and non-cachectic mice. Experimental setup showing subcutaneous injection of PBS, NC26 and C26 cells into BALB/c mice, followed by CD4^{+} and CD8^{+} T cell enrichment from spleen and tumor using fluorescence-activated cell sorting (FACS).

2.7.1 Distinct gene expression profiles of cachectic T cells

Principal component analysis (PCA) revealed a strong discrimination between cachectic and non-cachectic T cells from spleen and tumor (Figure 55). Both, circulating CD4^{+} and CD8^{+} T cells from cachectic C26 mice (red and green circled) showed a distinct gene profile compared to T cells from non-cachectic NC26- or PBS-injected mice (blue and purple circled) (Figure 55A). Interestingly, T cells from PBS and NC26 mice clustered strongly together, indicating a relatively similar T cell gene expression profile, again highlighting the deep impact of cachexia – but not tumor presence itself – on T cells. In addition, there was also a good separation between CD4 and CD8 T cells (Figure 55A). CD4^{+} TILs from cachectic mice could also be discriminated from CD4^{+} TILs isolated from NC26 tumor-bearing mice, while CD8^{+} TILs mostly showed a discrimination between cachectic and non-cachectic mice, but with a high variability of CD8^{+} TILs from non-cachectic mice, as one mouse showed a closer gene expression profile to cachectic mice compared to non-cachectic (Figure 55B). The higher

variability in the CD8+ TILs in comparison to the other groups likely results from the relatively small number of isolated and sequenced cells in this group.
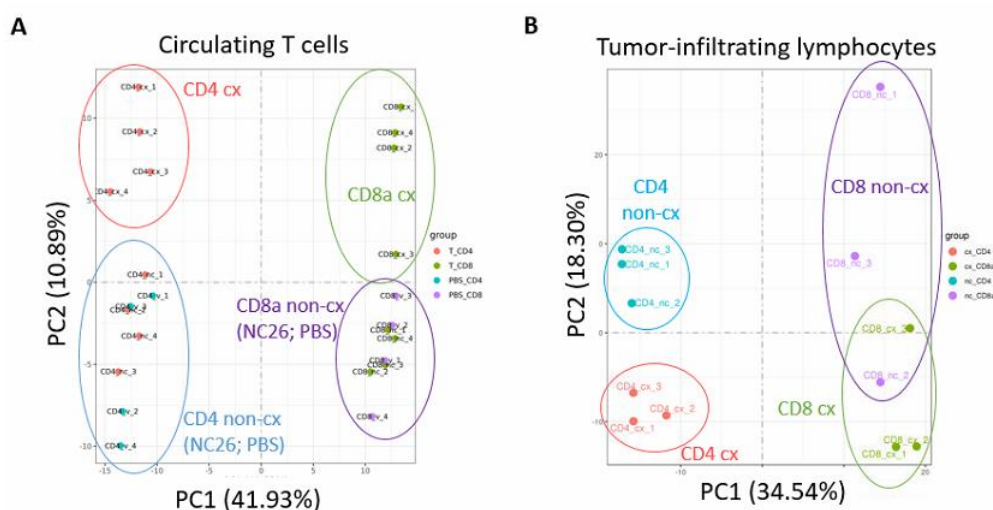
Figure 55. Circulating and tumor-infiltrating T cells from cachectic mice have a distinct gene expression profile. Principal component analysis (PCA) from CD4+ and CD8+ T cells isolated from **(A)** spleen and **(B)** tumor. The different groups are highlighted in distinct colors.

Heat maps showing the gene profile of CD4+ and CD8+ T cells from spleen and tumor, support the data presented in the PCA plots in greater detail (Figure 56). Overall, comparison of CD4+ and CD8+ T cells in both spleen and tumor shows a mostly contrary gene expression, as indicated by red and blue colour coding, respresenting up- or downregulation, respectively. In the circulation, several genes are regulated differently between T cells from cachectic mice compared to non-cachectic NC26 or PBS mice, while again, T cells from non-cachectic mice (NC26, PBS) behave similarly based on their gene expression profiles, implying, a strong dysregulation of genes by cachexia in T cells (Figure 56A). Similar to circulating T cells, also the CD4+ and CD8+ T cell expression profile in cachectic C26 tumors was clearly different to NC26 TILs (Figure 56B).
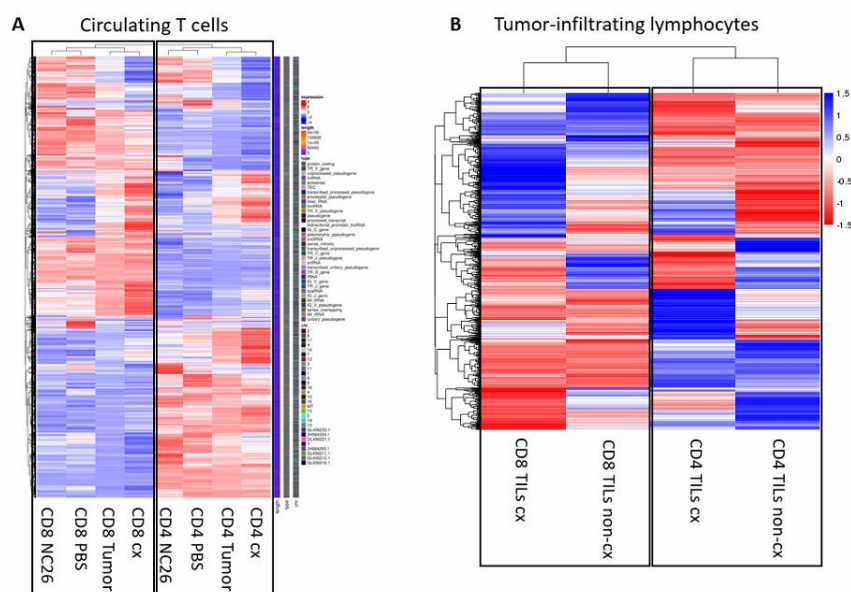
Figure 56. T cells from cachectic mice show altered gene expression profiles. Heat maps showing gene expression changes detected in RNA sequencing experiments from T cells isolated from **(A)** spleen or **(B)** tumor. **(A)** Circulating CD8+ and CD4+ T cells from C26 cachectic mice are named CD8 cx and CD4 cx, respectively. The group named CD8 Tumor combines gene expression analysis of CD8+ T cells from all tumor-bearing mice (C26 and NC26). Similarly, the CD4 Tumor group combines CD4+ circulating T cell gene expression from C26 and NC26 mice. **(B)** T cells termed TIL cx refer to cachectic C26 tumor-bearing mice, while non-cx refers to NC26 tumor-bearing mice.

Altogether, PCA and heatmap analyses showed clear alterations of the gene expression profiles of CD4$^+$ and CD8$^+$ T cells from spleen and tumor, mediated by cancer cachexia.

Comparing circulating T cells from C26 (cx) and NC26 (non-cx) tumor-bearing mice, almost 2500 (1214 up in cx, 1242 down in cx) and 3000 (1406 up in cx, 1420 down in cx) significantly regulated genes in CD4$^+$ and CD8$^+$ T cells were detected, respectively (Figure 57A). Interestingly, approximately half of the genes being regulated by C26 were shared by CD4$^+$ and CD8$^+$ circulating T cells with 99% of the genes being regulated in the same direction, implying that the strong modulation by cancer cachexia is not limited to a certain T cell type, but instead leads to a strong impairment of both T cell subtypes in a similar manner (Figure 57C). When I compared TILs from C26 and NC26 tumors, nearly 4000 genes (1811 up in cx, 1858 down in cx) were being regulated in CD4$^+$ TILs. Comparison of CD8$^+$ TILs revealed almost 1500 genes being altered (727 up in cx, 871 down in cx). Due to the much lower presence of CD8+ T cells within the tumors, the overall RNA yield was also low in these samples, likely leading to lower gene counts and higher variability between samples (see Table 1).
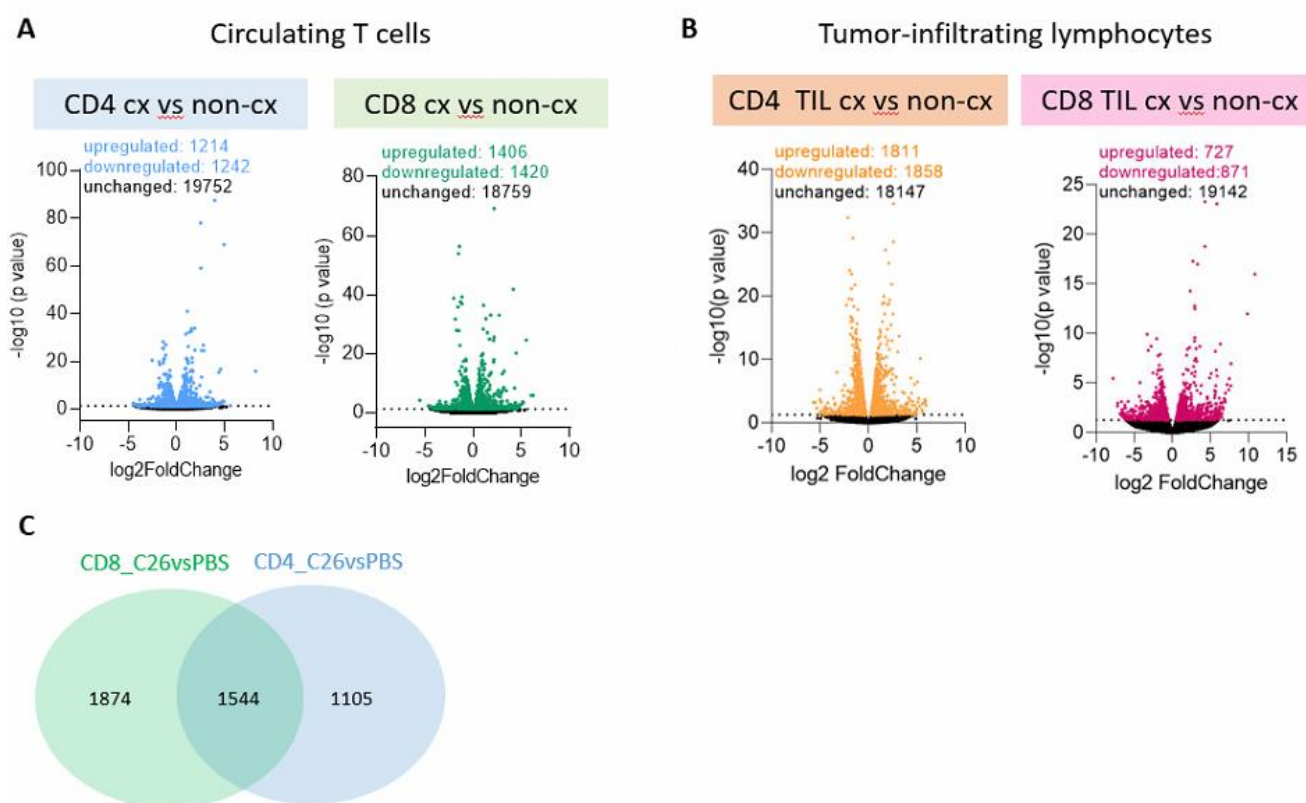
Figure 57. Gene expression of T cells from spleen and tumor is altered by cachexia presence. C26 mice developed cachexia, while PBS- and NC26-injected mice were used as a control. T cells were enriched using FACS and analyzed using RNA sequencing. Volcano plots display differentially expressed genes (DEGs) from **(A)** circulating and **(B)** tumor-infiltrating T cells. **(C)** Venn diagram presenting overlap of DEGs from circulating CD8$^+$ and CD4$^+$ T cells of C26 *vs*. PBS mice.

Table 1. Numbers of sorted cells for RNA sequencing using flow cytometry. The amount of isolated TILs for sequencing was much lower compared to splenic T cells. Displayed are total numbers of isolated T cells per cell type and group. CD4$^+$ and CD8$^+$ T cells are gated as live CD3$^+$CD11b-B220-F4/80-CD14-CD11c$^-$ CD4$^+$ or CD8$^+$ cells, respectively.

Tissue	Cell Type	Group	Number sorted cells
Tumor	CD4$^+$ TIL	NC26	9109, 8040, 3850
	CD8$^+$ TIL	NC26	8939, 10266, 3092
	CD4$^+$ TIL	C26	2460, 12911, 9963, 11320
	CD8$^+$ TIL	C26	700, 7973, 5833, 11787
Spleen	CD4$^+$ spleen	PBS	1674390, 2000000, 2000000, 2000000
	CD8$^+$ spleen	PBS	512882, 500000, 500000, 50000
	CD4$^+$ spleen	NC26	2000000, 1703178, 2000000, 2000000
	CD8$^+$ spleen	NC26	502556, 500000, 500000, 500000
	CD4$^+$ spleen	C26	1514603, 2000000, 2000000, 2000000
	CD8$^+$ spleen	C26	500000, 500000, 500000, 500000,

2.7.2 Strong inhibition of T cell activation pathways in T cells from cachectic mice

Reduced proliferation and effector function as assessed by flow cytometry and qPCR (outlined in chapters 2.2 and 2.4.2) already implied functional impairments in T cell activation, and indeed ingenuity pathway analysis (IPA) linked pathways related to T cell activation and effector function to cachexia onset (Figure 58). Interestingly, almost all of the top 20 regulated canonical pathways, as identified by IPA, were being decreased (blue color) in both CD4$^+$ and CD8$^+$ T cells from spleen and tumor of cachectic C26 *vs.* non-cachectic NC26 mice, implying a strong repression of T cells upon cachexia. Pathways being related to T cell activation and effector function were all decreased in T cells from cachectic mice, except for STAT3 signaling, which was increased in cachectic CD8$^+$ TILs (Figure 58B). However, STAT3 has already been associated with impaired T cell function, and STAT3 ablation from adoptively transferred CD8$^+$ T cells has previously been shown to improve T cell infiltration into tumors, proliferation and anti-tumor effector function (Kujawski, 2010). Accordingly, elevated STAT3 signaling in cachectic CD8$^+$ TILs, as assessed by RNA sequencing (Figure 58B), could in part mediate reduced tumor infiltration.

Decreased activation and effector function pathways are highlighted in yellow and include phosphoinositide 3-kinase (PI3K)/AKT signaling, Janus kinase/Signal Transducer and Activator of Transcription (JAK/STAT) signaling, nuclear factor 'kappa-light-chain-enhancer' of activated B-cells (NF-κB) signaling, CD28 signaling, T cell receptor (TCR) signaling, interferon signaling and Programmed cell death protein 1/ programmed death-ligand 1 (PD1/PD-L1) signaling (Figure 58), implying a strong repression and reduced activation status of T cells in cancer cachexia. Surprisingly, the EIF2 pathway was the most activated pathway in CD4$^+$ T cells from C26 cachectic mice, implying increased translation (Kleijn, 2002), which paired with reduced proliferation as assessed by staining, might indicate an increased stress response.
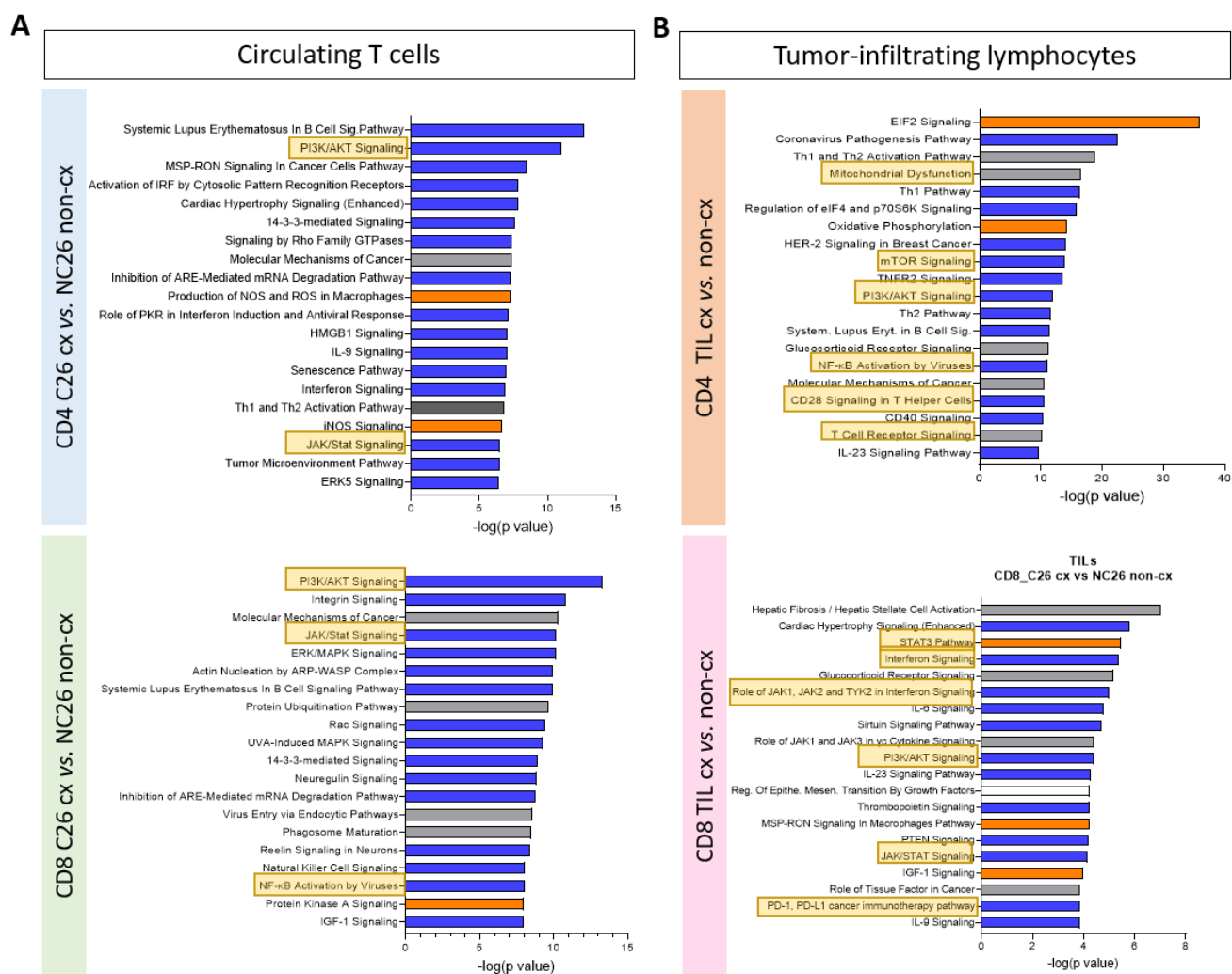
Figure 58. Cachexia represses activation and effector function of CD4+ and CD8+ T cells. Ingenuity pathway analysis (IPA) of CD4+ and CD8+ T cells from cachectic C26 and non-cachectic NC26 mice revealed a strong reduction of most pathways being detected in a canonical pathway analysis. Regulated pathways related to activation status or effector function are highlighted in yellow. Upregulated pathways are displayed in orange, downregulated pathways blue and if no clear regulation pattern was available, pathways were colored grey. T cells were isolated from **(A)** spleen or **(B)** tumor.

Indeed, also by performing Kyoto Encyclopedia of Genes and Genomes (KEGG) pathway analysis, I found that almost all significantly regulated pathways in both CD4+ and CD8+ T cells from tumor and spleen, were downregulated upon cancer cachexia (Figure 59), strengthening the results of the IPA analysis. Strikingly, many pathways that were detected in circulating CD4+ or CD8+ T cells were commonly regulated in C26 cx/NC26 non-cx and C26 cx/PBS mice (indicated by yellow arrows; Figure 59A), emphasizing that the strong repression of T cells is likely not mediated by tumor presence *per se*, but rather relies on cachexia development. In addition, there was also an overlap between circulating CD8+ cells and CD4+ T cells from C26 cx *vs.* NC26 mice, as indicated by orange arrows (Figure 59A), indicating a general effect mediating T cell repression irrespective of the T cell subtype. Also, KEGG pathways being regulated in CD4+ TILs overlapped with circulating CD4+ T cells from C26 cx *vs.* NC26 non-cx mice (highlighted by green arrows; Figure 59B), emphasizing a systemic T cell inhibition and not tissue specific effects. Overall, these data suggest a strong downregulation of several pathways associated with T cell activation and function by cancer cachexia in both major T cell subtypes (CD4+ and CD8+ T cells) and two different sites of the body (circulation and tumor). Comparison of gene profiles from CD4+ and CD8+ splenocytes from NC26 *vs.* PBS mice revealed minor changes in the KEGG pathway analysis with only three and two pathways being significantly altered

due to tumor occurrence, respectively (Figure 59A). These data highlight the strong regulation in T cells that is induced by cachexia development, irrespective of tumor occurrence.
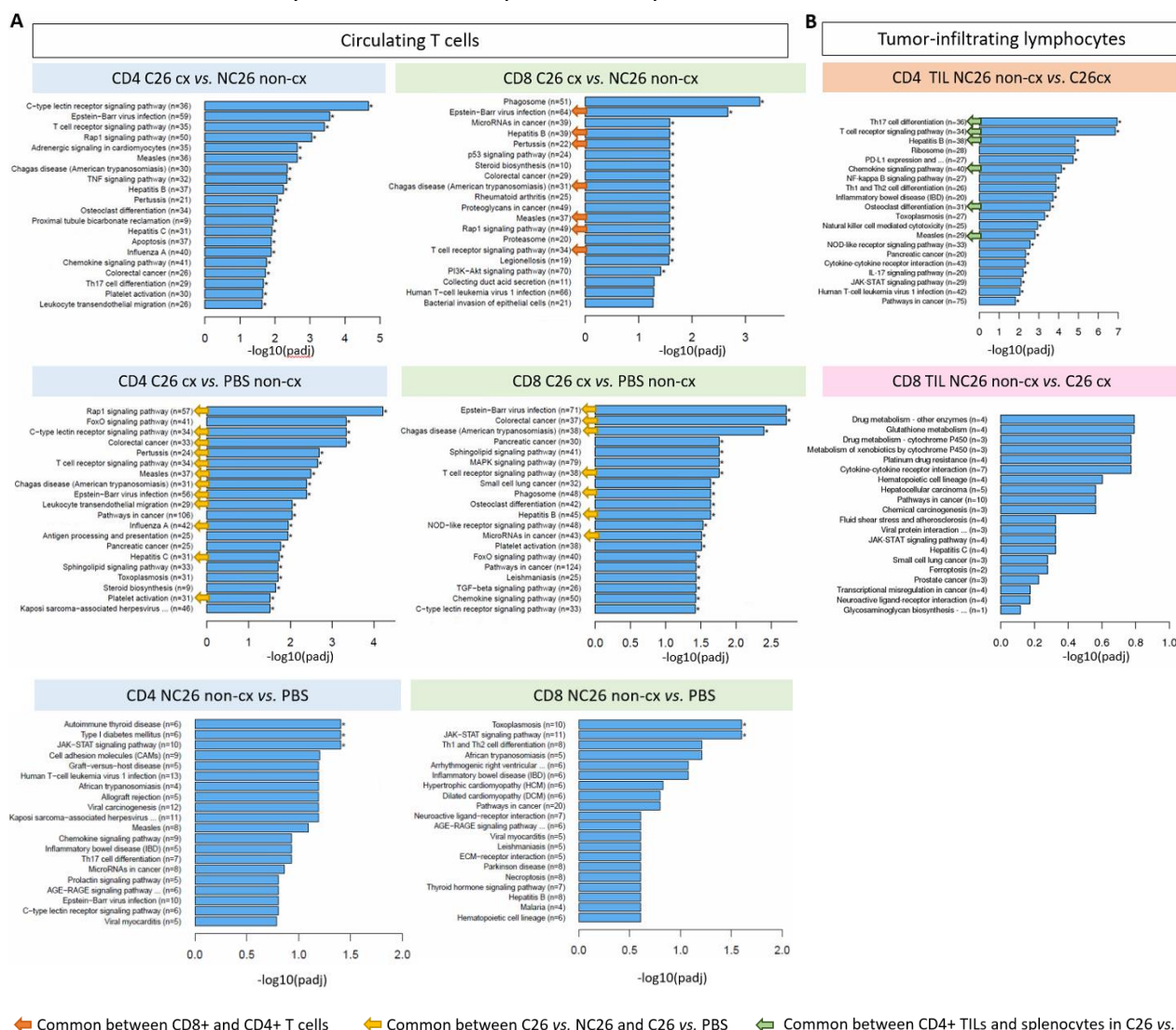
Figure 59. Impairment of T cell activation pathways by cancer cachexia based on Kyoto Encyclopedia of Genes and Genomes (KEGG) pathway analysis. KEGG pathway analysis of CD4^{+} and CD8^{+} T cells from cachectic C26 and non-cachectic NC26 or PBS mice revealed a strong reduction of almost all pathways. T cells were isolated from **(A)** spleen or **(B)** tumor. **(A)** Yellow arrows highlight commonly regulated pathways between T cells from C26 *vs*. NC26 and C26 *vs.* PBS mice. Orange arrows highlight common regulation between CD8^{+} and CD4^{+} T cells from cx *vs*. non-cx NC26 mice. KEGG pathway analysis in CD4^{+} and CD8^{+} splenocytes in NC26 *vs*. PBS mice. **(B)** Green arrows highlight similar regulation between CD4^{+} TILs and circulating CD4^{+} T cells from C26 *vs.* NC26 mice.

2.7.3   Cachectic T cells display markers of exhaustion and senescence simultaneously

In order to escape the immune system, malignant tumors can trick T cells into different dysfunctional states, namely exhaustion or senescence, both leading ultimately to T cell dysfunction but differing regarding their metabolic and molecular regulation (Y. Zhao, 2020). Interestingly, a canonical pathway analysis using IPA revealed senescence amongst the top 20 regulated pathways in circulating CD4^{+} T cells (Figure 58A). Thus, we were interested if dysfunctional cachectic T cells might display features of senescence or exhaustion, with the ultimate goal to identify certain pathways that could be specifically targeted in T cells to improve T cell functionality and thereby cachexia outcome in the future. To this end, I compared our RNA sequencing data sets to different markers that were specific for either exhausted or senescent T cells (Y. Zhao, 2020). Table 2 displays the different markers and their regulation upon exhaustion and senescence, as published by Zhao and colleagues (Y. Zhao,

2020), with yellow indicating an increase in the distinct state (exhaustion, senescence, cachexia) and blue showing a decrease. Interestingly, based on the expression of surface markers, their cytokine and transcriptional profile, as well as metabolic and functional alterations, both CD4^{+} and CD8^{+} T cells from spleen and tumor of cachectic mice (C26 vs. NC26) did not follow a distinct pattern, meaning they displayed neither a classically exhausted nor fully senescent state. This analysis implies that the repression that T cells undergo during cachexia development displays features of both cell senescence and exhaustion, involving different pathways and molecular changes (Y. Zhao, 2020).

Table 2. Cachectic T cells display features of exhaustion and senescence. Markers for T cell exhaustion and senescence are from (Y. Zhao, 2020). Increased gene expression levels of surface markers, TCR signaling machinery, cytokines and transcriptional levels, as well as metabolic and functional alterations were highlighted in yellow (increased upon senescence, exhaustion or cachexia), while blue showed a decrease of the aforementioned. Unaltered gene expression in our RNA sequencing data as indicated by white color. Significant alterations in the gene expression levels of T cells from C26 cx mice, were specified by stars. *p<0.05, **p<0.01, ***p<0.001, ****p<0.0001.

Category	Marker	Exhaustion	Senescence	CD8 spleen	CD4 spleen	CD8 TILs	CD4 TILs
Typical feature	Proliferative activity						
Surface marker	PD-1						
	CTLA4			*	***		****
	TIM3						
	LAG3						
	BTLA				**		
	TIGIT				*		***
	CD244						
	CD160			*		***	****
	CD39						
	4-1BB						
	CD27				*		****
	CD28			****	***		
	CD57						
	KLRG1			*	**		
	CD45RA						
TCR signaling machinery	LCK						**
	ZAP70						
	DLG1						
	Lat			***	**		
	SLP-76			****	****		
Cytokine Profile	IL-2 (early stage)						****
	TNF (intermediate)			****	****		****
	IFNg (late stage)						****
	ßChemokines				*		****
	SASP						
	IL6						
	IL8						
	IL10				***		
	TGFß			*	*	****	****
Transcriptional profile	NFAT			**	**		****
	Nr4a			***	****	****	****
	Blimp-1						
	BATF					****	****
	FoxP3						
Metabolic alteration	Glycolysis						
	Mitochondrial biogenesis						
	Reactive oxygen species						
Functional alteration	Cytotoxic activity						
	Gzmb			Gzma***		Gzma,c,d,e,f,g	***
	Perforin				***		**

2.8   Aging aggravates cachexia in tumor-bearing mice

It has been well studied that the functionality of the adaptive immune system declines with age, including T cells developing a state called senescence, leading to an accumulation of terminally differentiated effector T cells (Foster, 2011). In line, age potentiates cancer incidence dramatically (Berben, 2021), which is likely accompanied by an increased onset of cancer cachexia. This idea is supported by an elevated prevalence of cachexia in cancers of older age, such as pancreatic cancer (Dunne, 2019). Additionally, upon cancer cachexia, T cells partially display a senescent state, which is why we sought to assess the impact of aging (accompanied by a decline in immune function) on cancer cachexia development. To this end, different mouse models (LLC and C26) were used to investigate cancer cachexia development upon aging. In addition, two different substrains of C57BL/6 mice were used for the LLC studies, as it has previously been reported that C57BL/6J and C57BL/6N mice have developed genotypic and phenotypic differences over time that could potentially affect cachexia development, such as insulin sensitivity or body composition (Simon, 2013). Hence, young adult mice of an age of 2-4 months and aged animals at the age of 15-20 months were injected with cachexia-inducing tumor cells and characterized in terms of cachexia development.

2.8.1   Effects of aging on tumor growth and body wasting in tumor-bearing mice

Approximately 7 days after subcutaneous injection of LLC cells into C57BL/6J and C57BL/6N mice, and C26 cell injection into BALB/c mice, tumors started to be palpable and grew to a similar size over time. At the end of the experiment, younger mice of all groups developed larger tumors with even significant differences in LLC/J and C26 mice (Figure 60A, B, C), in accordance with (Beheshti, 2015).
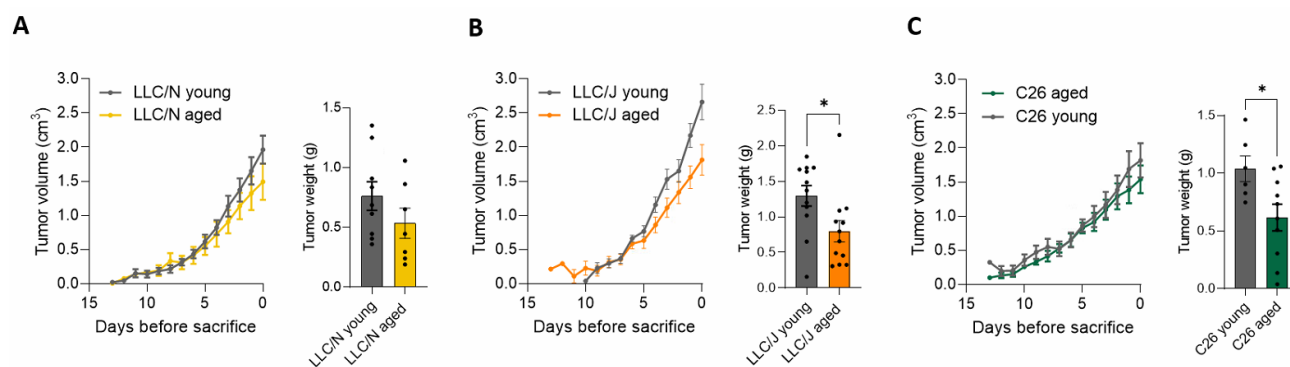
Figure 60. Age has a mild effect on tumor growth. (A-C) C57BL/6 and BALB/c mice were injected with LLC or C26 tumor cells, respectively. Shown is tumor growth over time and tumor weight at the end of the experiment. **(A)** Young C57BL/6N mice were 2 months at start of the experiment (grey, LLC/N young, n=9), while aged C57BL/6N mice were 16 months (yellow, LLC/N aged, n=7). **(B)** Comparison of C57BL/6J animals injected with LLC cells. Young mice were 3 months at experiment start (grey, LLC/J young, n=12), aged C57BL/6J mice were 20 months old (orange, LLC/J aged, n=12). **(C)** Young BALB/c mice were injected with C26 cells at an age of 4 months (grey, C26 young, n=6), while aged C26-injected BALB/c mice were 15 months old (dark green, C26 aged, n=10). Data are mean ± s.e.m and statistical analyses were performed using unpaired t-test or Mann–Whitney test. Figure based on (Geppert, 2021). * p<0.05.

Cachexia is defined by severe bodyweight loss over time (Roeland, 2020). Hence, bodyweight development was investigated during the course of the experiment to assess the influence of age on cancer cachexia and plotted starting 10 days prior to sacrifice to adjust for the difference in time to human endpoint. Bodyweight evolution was consistent with only minor changes in aged PBS-injected animals, while young PBS mice of all groups strongly gained bodyweight over time (Figure 61A). Upon tumor injection, aged mice developed severe bodyweight loss over the course of the experiment, with LLC/J showing the earliest and highest degree of loss (Figure 61A). In contrast, only young C26 tumor-bearing mice suffered from strong body wasting, while young LLC/N and LLC/J mice still gained

weight over time (Figure 61A). Interestingly, both young and aged LLC/J mice dropped stronger in bodyweight compared to LLC/N mice (Δ bodyweight in aged: 7.3% *vs.* 5.8% and in young: 5.0% *vs.* 2.4%; Figure 61B), reflecting the serious impact of the genotypic and phenotypic differences between these two substrains on cachexia development. In young LLC tumor-bearing mice, bodyweight loss was induced with a very high variability, with some mice developing strong weight loss, while others were non-responders (Figure 61B). Contrary to LLC tumor-bearing mice in which wasting was potentiated by age, young C26 tumor-bearing mice developed significantly higher bodyweight loss compared to aged C26 mice (8.2% in aged *vs.* 18.5% in young mice; Figure 61B). Overall, higher age caused weight loss in LLC/N mice, worsened cachexia in LLC/J animals, and did not affect weight loss in the C26 model (Figure 61).

Figure 61. Cancer cachexia is affected by age and strain. (A-B) Young and aged mice were injected with PBS as a control or tumor cells (LLC, C26) to induce cachexia. Young mice injected with PBS are shown in light grey color (PBS/N young, n=6; PBS/J young, n=8; PBS/BALB/c young, n=5), while young adult mice injected with tumor cells are depicted in dark grey (LLC/N young, n=9; LLC/J young, n=12; C26 young, n=6). Light colors refer to aged PBS-injected animals (PBS/N aged, light yellow, n=5; PBS/J aged, light orange, n=10; PBS/BALB/c aged, light green, n=5). Aged tumor-bearing mice are depicted in dark colors (LLC/N aged, yellow, n=7; LLC/J aged, orange, n=12; C26 aged, green, n=10). **(A)** Bodyweight change over time in percentage (compared to initial mass before injection) starting 10 days prior to sacrifice. **(B)** Bodyweight change minus tumor in percentage (compared to initial bodyweight) at the end of the experiment. Data are mean ± s.e.m and statistical analyses were conducted using two-way analysis of variance (ANOVA) with Tukey's multiple-comparison post hoc test. Figure based on (Geppert, 2021). *p<0.05, **p<0.01, ***p<0.001, ****p 0.0001.

In line, aged LLC/N mice displayed significant wasting of GC muscles upon LLC injection, while young LLC tumor-bearing C57BL/6N mice did not show significant differences, highlighting an age-and tumor-dependent effect (Figure 62). In C57BL/6J mice only age-related changes of iWAT and eWAT were observed, while LLC injection did not alter organ weight in neither young nor aged mice (Figure

62). These data emphasize again strain-dependent differences on C57BL/6 background. C26- injection induced a strong wasting phenotype of WAT and GC in BALB/c mice mostly independent of age (Figure 62).
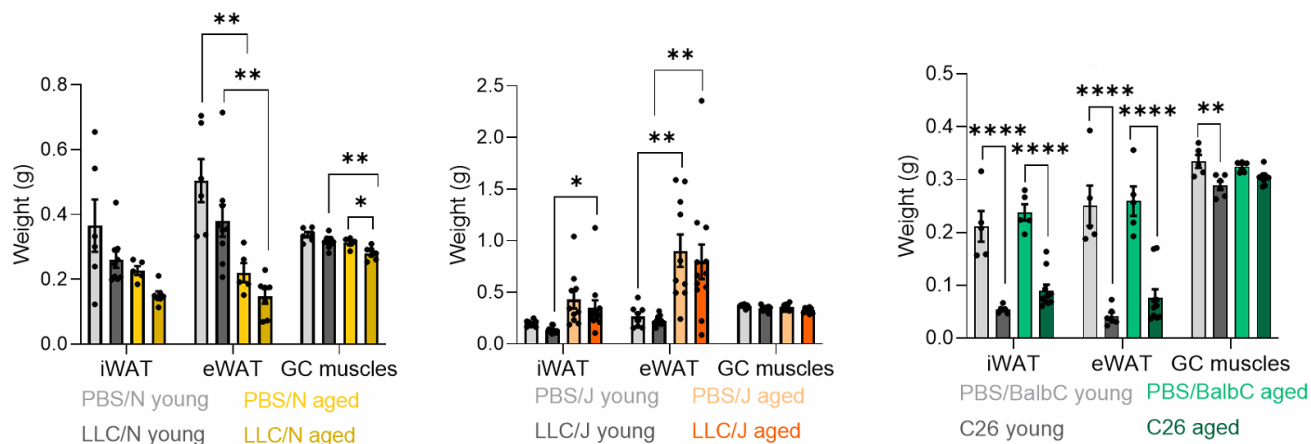
Figure 62. Cachexia induces tissue-wasting in an age- and strain-dependent manner. Same mice as in Figure 61. Tissue weights of iWAT, eWAT and GC muscles in mice of different ages, injected with different tumor cell lines or PBS. Data are mean ± s.e.m and statistical analyses were conducted using two-way ANOVA with Tukey's multiple-comparison post hoc test. Figure based on (Geppert, 2021). *p<0.05, **p<0.01, ****p<0.0001.

2.8.2 Changes in T cell subtype composition are not likely drivers of cachexia in aged mice

During the course of aging, the functionality of the adaptive immune system including T cells declines, resulting in a state termed senescence (Foster, 2011). In mice developing cancer cachexia, markers associated with T cell senescence were induced with cachexia development, indicating accelerated aging of the immune system. Hence, we were interested if upon aging, a state in which T cell senescence is predominantly occurring, T cell dysfunction upon cachexia might be accelerated, thereby worsening cachexia development and disease outcome in aged mice and individuals.

In this context, weight of draining and non-draining inguinal lymph nodes was increased in all tumor-bearing mice irrespective of age, indicating a strong immune response to tumors (Märkl, 2012), while spleen weight was more elevated upon tumor injection in young compared to old tumor-bearing mice (Figure 63A), indicating a stronger upregulation of the immune system (Jiang, 2021). To investigate the functional status and the state of senescence in T cells of aged PBS-or tumor cell-injected mice, their CD4$^+$/CD8$^+$ T cell ratio was determined (Figure 63B), with a low ratio being indicative of aging (J. E. Turner, 2016). As previously shown (Sim, 1998), BALB/c mice displayed a much higher CD4$^+$/CD8$^+$ ratio than C57BL/6N mice. Apart from that, the ratio of circulating CD4$^+$/CD8$^+$ T cells was unchanged in BALB/c mice, despite tumor presence or high age of the mice (Figure 63B). Aged C57BL/6N mice showed a significantly declined CD4$^+$/CD8$^+$ T cell ratio, which tended to be further reduced but with a high variability by tumor presence (Figure 63B).

Regulatory T cells (Tregs) play a central role in immune self-tolerance, thereby preventing auto-immune diseases. However, upon cancer incidence, Tregs can inhibit immune surveillance against tumor cells, hence hampering an effective anti-tumor response (Togashi, 2019). In line with previous studies (Garg, 2014), FoxP3$^+$ Tregs were increased in aged C57BL/6N and BALB/c mice, while tumor presence did not affect circulating Treg levels in addition (Figure 63C).

In summary, contrary to our hypothesis, a general decline and change of subtype composition of T cells might not be linked to the age-related acceleration of cachexia in C26 or LLC tumor-bearing mice. Furthermore, the presence of FoxP3$^+$ Tregs was only increased in aged LLC/N mice and did not seem to be affected by tumor cell injection.
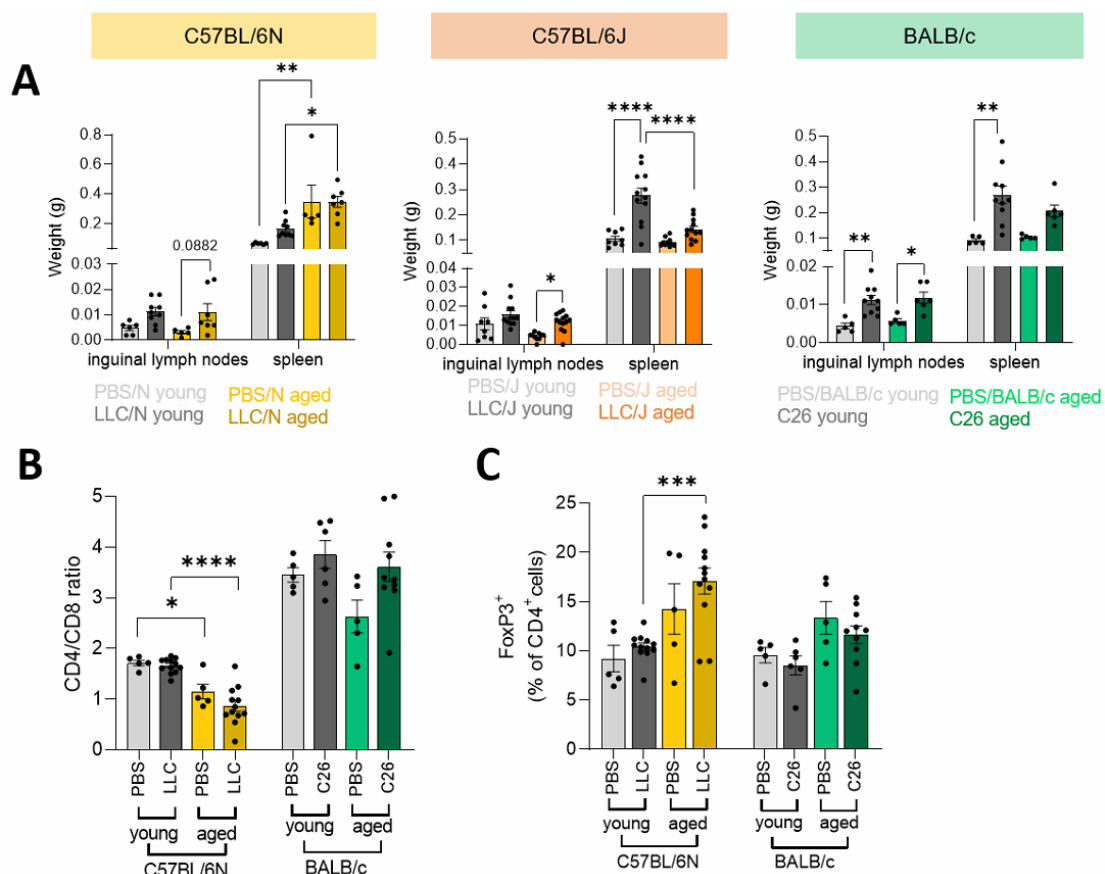
Figure 63. Immune cell decline might not influence accelerated cachexia development upon aging. (A-C) Same mice as in Figure 61. **(A)** Weight of inguinal lymph nodes and spleen. **(B)** CD4$^+$/CD8$^+$ ratio of circulating T cells, based on flow cytometric analysis. **(C)** Percentage of FoxP3$^+$ regulatory T cells (% of CD4$^+$ T cells) in blood, as measured by flow cytometry. Data are mean ± s.e.m and statistical analyses were performed using two-way ANOVA with Tukey's multiple-comparison post hoc test. Figure based on (Geppert, 2021). *p<0.05, **p<0.01, ***p<0.001, ****p<0.0001.

Additionally, I investigated T cell effector function based on molecular changes to assess if cachexia acceleration in aged mice did alter anti-tumor T cell functionality. In CD8$^+$ T cells, effector function based on expression of genes related to T cell functionality, was non-significantly increased in C57BL/6N mice, while high age led to the age-related reduction of some genes, such as *Ifnγ, Tnfα* or *Tox* in BALB/c mice (Figure 64A). *Il2* tended to be elevated in CD4$^+$ and CD8$^+$ T cells from aged PBS/N and PBS- BALB/c mice compared to young mice, but with a very high variability, while C26 and LLC injection decreased *Il2* expression again in aged mice (Figure 64A, B). Interestingly, reduced *Il2* expression implies an impaired effector differentiation and clonal expansion of CD4$^+$ and CD8$^+$ splenocytes (Bachmann, 2007), in line with the more severe phenotype of aged *vs*. young LLC/N tumor-bearing mice, which show no alterations of *Il2* expression upon LLC injection. *Tnfα* and *Ifnγ* expression tended to be increased by age in C57BL/6N and BALB/c mice, with the exception of CD8$^+$ T cells from BALB/c mice, where I saw rather a downregulation. Interestingly, this increase of effector cytokine expression by high age was dampened again by cachexia onset, as LLC and C26 tumor-bearing mice displayed reduced levels of *Ifnγ* and *Tnfα* compared to their age-matched controls (Figure 64), indicating a repressed T cell function dependent on age and tumor presence. *Gzmb* was non-significantly upregulated in aged LLC/N mice, while being unchanged in young LLC and all BALB/c mice. Interestingly, expression of *Pdcd1*, encoding PD1, was strongly increased in CD4$^+$ and CD8$^+$ T cells from aged C57BL/6N mice, suggesting in combination with elevated *Tox* levels in CD4$^+$ T cells of aged animals increased T cell exhaustion upon aging (Figure 64B). This phenomenon could also be

observed in CD4⁺ T cells from aged BALB/c mice, but not CD8⁺ T cells which behaved quite the opposite way.
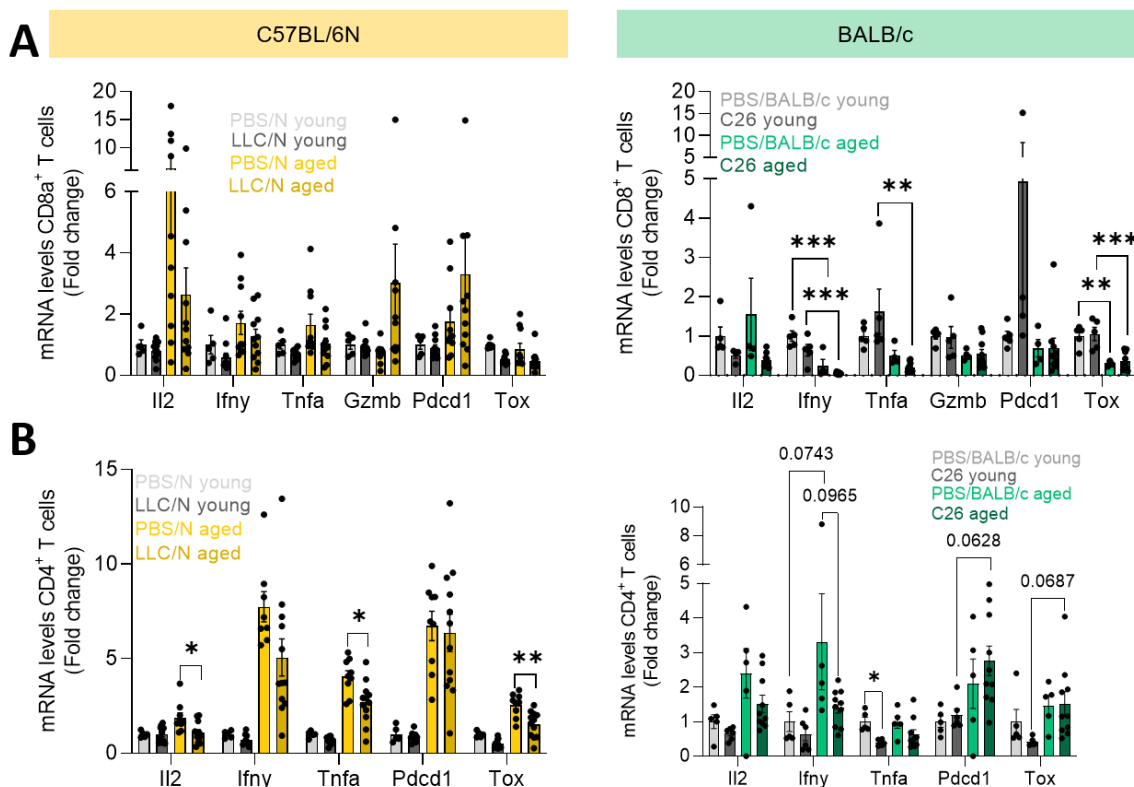
Figure 64. Expression of genes associated with T cell effector function is largely unaltered by age. (A-B) mRNA levels of genes related to T cell effector function in PBS/N young (n=5), LLC/N young (n=11), PBS/N aged (n=10), LLC/N aged (n=11) and PBS/BALB/c young (n=6), C26 young (n=5), PBS/BALB/c aged (n=4) and C26 aged (n=10) **(A)** CD8⁺ T cells isolated from the spleen. **(B)** CD4⁺ T cells isolated from the spleen. Data are mean ± s.e.m and statistical analyses were performed using two-way ANOVA with Tukey's multiple-comparison post hoc test. *p<0.05, **p<0.01, ***p < 0.001.

In summary, changes in the subtype composition of T cells, meaning an imbalance in the percentage of CD4⁺ and CD8⁺ cells, is unlikely to mediate accelerated cachexia onset upon high age. However, an increased percentage of Tregs in combination with elevated exhaustion could potentially be linked and contribute to accelerated and worsened cachexia in aged LLC tumor-bearing mice, despite an overall higher expression of inflammatory cytokines, which is a common feature of T cell senescence, termed inflammaging (Macaulay, 2013). The cachexia-induced dampening of effector function as assessed by gene expression of *Il2* and *Ifny* was observed to even greater extent CD4⁺ and CD8⁺ T cells from aged LLC and C26 tumor-bearing mice.

2.8.3   Aging increases the induction of atrophy markers in tumor-bearing mice

Wasting of skeletal muscle is a hallmark of cancer cachexia (Rohm, 2019), which on the molecular level is often assessed by the expression of atrogenes, including MuRF1, Atrogin 1, FoxO3a, and Ctsl (Deval, 2001; Rohm, 2019; Sandri, 2004). In order to investigate the effect of aging on atrophy markers upon cancer cachexia, the expression of Trim63, Fbxo32, FoxO3a, and Ctsl was measured in Gastrocnemius (GC) muscles from young and old C57BL/6 and BALB/c mice (Figure 65A). Remarkably, LLC-induced skeletal atrophy was only present in aged C57BL/6N mice, but not LLC/N young mice, reflecting the induction of bodyweight loss along with cachexia development upon aging. In LLC/J mice, age potentiated atrogene expression strongly (Figure 65A), again highlighting the aggravation of cachexia severity by age in C57BL/6 mice. C26 injection led to a strong upregulation of atrogenes

in young BALB/c mice, which was blunted by age (Figure 65A), as previously reported (Talbert, 2014), These observations were also in line with smaller weight loss in old compared to young C26 tumor-bearing mice.

Myosteatosis, which has recently been shown to be a negative prognostic marker in patients with colon cancer (C. M. Lee, 2020), was determined by assessing mRNA levels of Atgl (adipocyte triglyceride lipase) and Plin4 (perilipin 4) in GC muscles (Figure 65B). Especially young C26 tumor-bearing mice were shown to have a significant increase in *Atgl* and *Plin4*, which was dampened by age (Figure 65B), underlining the strong phenotype of the young C26 cachexia model. Expression of *Plin4* was also significantly elevated in aged LLC/J mice and tended to be upregulated in aged LLC/N mice, again highlighting increased cachexia severity in line with elevated bodyweight loss upon aging. Accordingly, also *Atgl* tended only to be increased in aged LLC tumor-bearing mice, but not young (Figure 65B).
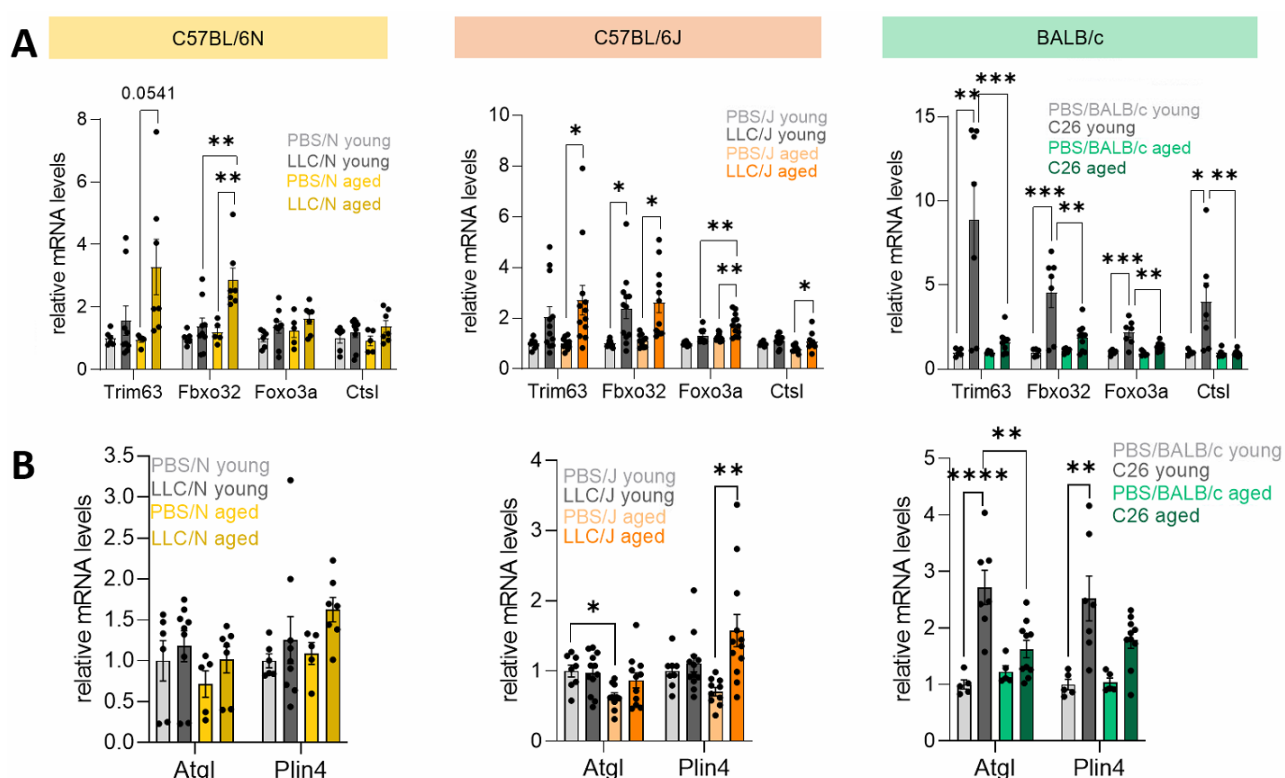
Figure 65. Tumor-dependent gene expression of atrogene markers in cachectic skeletal muscle is affected by age. (A-B) Same mice as in Figure 61. **(A)** mRNA levels of several atrogenes associated with cancer cachexia in GC muscles **(B)** *Atgl* and *Plin4* mRNA levels. Data are mean ± s.e.m and statistical analyses were performed using two-way ANOVA with Tukey's multiple-comparison post hoc test. Figure based on (Geppert, 2021). *p<0.05, **p<0.01***, p<0.001, ****p<0.0001.

2.8.4   Cachexia markers in mouse models and patients behave differently upon aging

Interleukin 6 (IL6) has been identified as central cachexokine and extensively studied in the past (Baltgalvis, 2008; Strassmann, 1992). Hence, we hypothesized that altered IL6 levels could potentially mediate the age-and strain-related effects that were observed in cachexia development. To this end, I measured circulating IL6 levels in C57BL/6 and BALB/c mice and correlated them to the bodyweight change of the mice (Figure 66). Interestingly, there was a significant increase in young and a trend in aged C26 tumor-bearing mice for an increase of circulating IL6 upon cachexia (Figure 66A), as already shown (Talbert, 2014). Surprisingly, circulating IL6 levels were largely unaffected by age or tumor in C57BL/6 mice, except for aged LLC/N mice which tended to have elevated plasma IL6. Correlations of circulating IL6 levels and bodyweight change revealed substantial strain-dependent differences, with positive correlations in C57BL/6N and BALB/c mice, and a negative correlation in C57BL/6J mice

(Figure 66B). Hence, caution is warranted when choosing mouse models for cachexia research as strong strain-related differences might impact the outcome of the experiment. Interestingly, when mice were separated into groups according to their age, only young animals showed a significant correlation of IL6 and bodyweight change (p=0.0018), which was lost upon aging (p=0.5672) (Figure 66C), indicating a strong impact on age-related changes on IL6 levels in tumor-bearing mice that should be taken into account when investigating IL6-dependent cachexia.
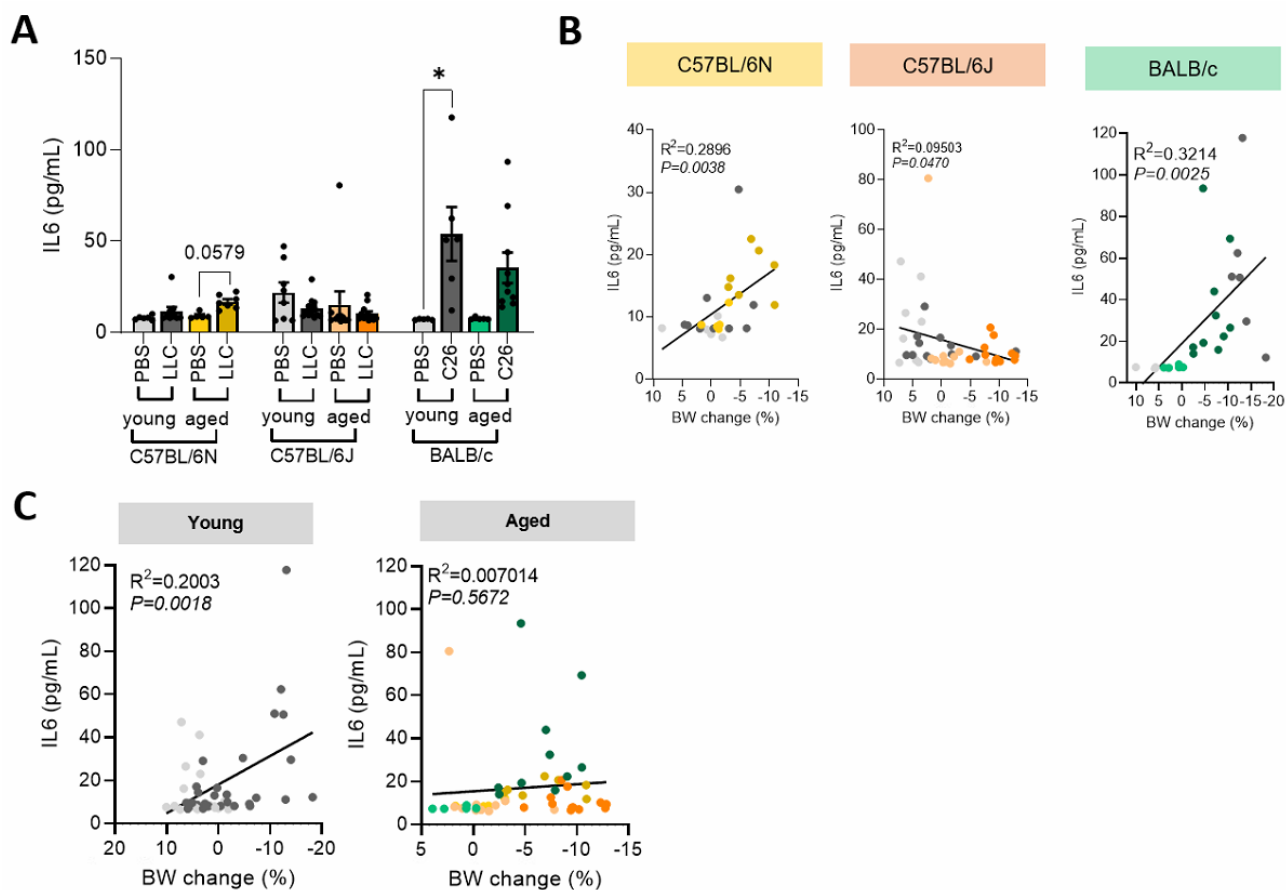
Figure 66. Circulating IL6 levels are changed in a strain-and tumor-dependent manner. (A-C) Same mice as in Figure 61. **(A)** Circulating IL6 levels in different mouse strains in young and aged mice. **(B)** Correlations between plasma IL6 and bodyweight change (final bodyweight minus tumor *vs.* initial bodyweight). **(C)** Correlations comparing circulating IL6 with bodyweight change in young or aged mice across all mouse models. Data are mean ± s.e.m and statistical analyses were performed using two-way ANOVA with Tukey's multiple-comparison post hoc test or simple linear regression. Figure based on (Geppert, 2021). *p<0.05.

Circulating growth and differentiation factor 15 (GDF15) has recently been shown to be increased in aged individuals (H. Liu, 2021), while also being associated with cancer cachexia. Blocking of GDF15 by antibody treatment was reported to prevent tumor-induced body wasting, and additionally GDF15 was validated as cachexia marker being associated with reduced survival in cancer patients (Rohm, 2020; Suriben, 2020). Circulating GDF15 levels were strongly increased in aged C57BL/6N mice, LLC/J mice, and in C26 tumor-bearing mice irrespective of their age (Figure 67A), implying that there is no common regulation of GDF15 levels across different mouse strains in dependence of age and tumor presence. In line with this observation, a linear regression analysis only revealed significant positive correlations of plasma GDF15 and bodyweight change in BALB/c mice, but not C57BL/6 mice (Figure 67B). Strikingly, circulating GDF15 levels correlated significantly with bodyweight change in young mice (p<0.0001), but not aged mice (p=0.4266) across all mouse strains (Figure 67C), indicating a prominent role of GDF15 in cancer cachexia development only in young mice. Increased levels of

plasma GDF15 might be mediated in part by an upregulation of *Gdf15* expression in skeletal muscle (Chung, 2017). In our models, gene expression levels of *Gdf15* in GC muscles were unchanged between all groups, as indicated in Figure 67D, suggesting other tissues, such as the tumor, to be the major source for increased GDF15 levels in the circulation.
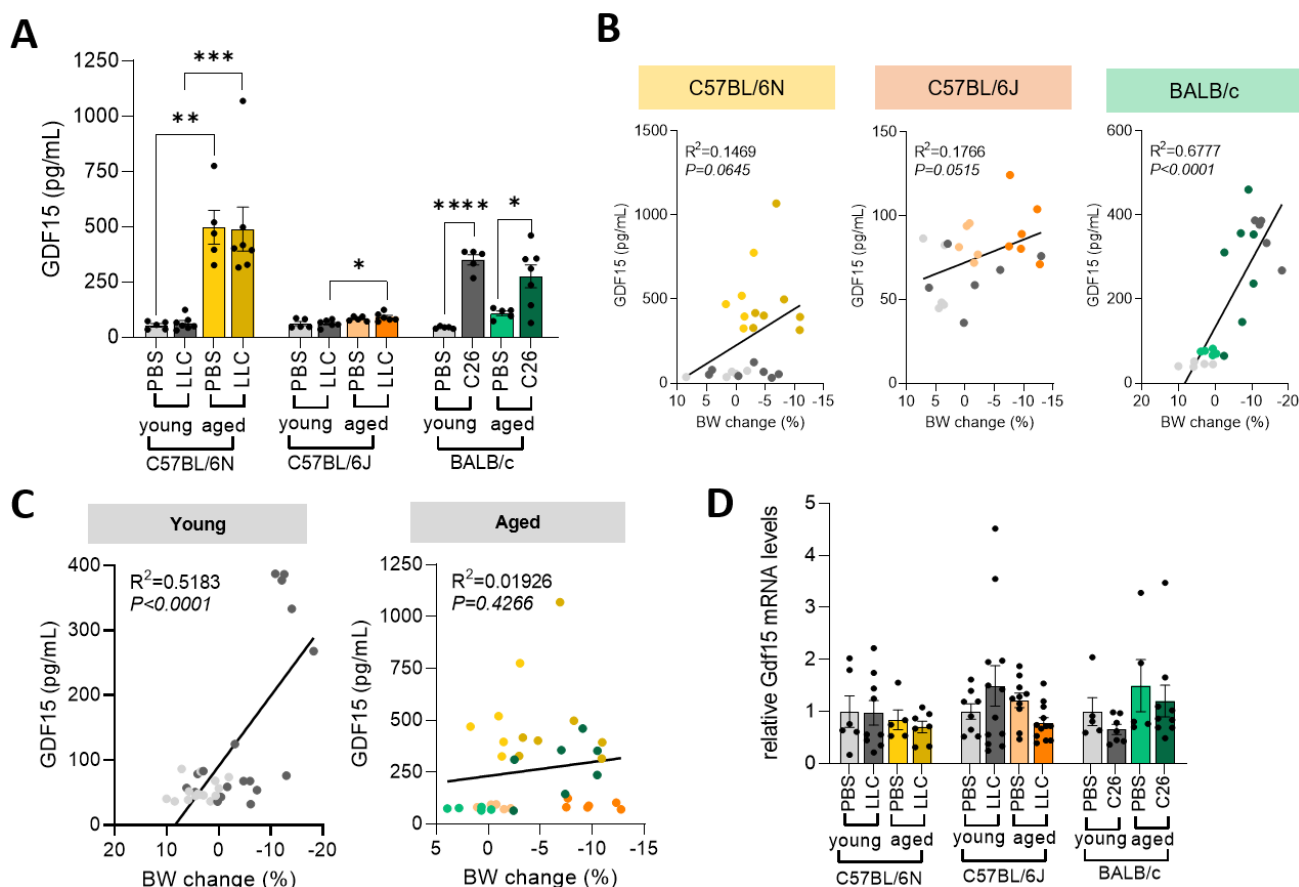
Figure 67. Plasma GDF15 levels are not commonly altered by age or tumor presence between different mouse strains. **(A-D)** Same mice as in Figure 61. **(A)** Circulating GDF15 levels in different mouse strains in young and aged mice. **(B)** Correlations between plasma GDF15 and bodyweight change (final bodyweight minus tumor *vs.* initial bodyweight). **(C)** Correlations comparing circulating GDF15 with bodyweight change in young or aged mice across all mouse models. **(D)** *Gdf15* mRNA levels in GC muscles. Data are mean ± s.e.m and statistical analyses were performed using two-way ANOVA with Tukey's multiple-comparison post hoc test or simple linear regression. Figure based on (Geppert, 2021). **p<0.01, ***p<0.001, ****p<0.0001.

Similar to the C26 model, plasma GDF15 levels tended to increase in both young and aged cachectic cancer patients compared to weight stable cancer and control patients. In addition, there was also a trend for elevated GDF15 levels in aged compared to young patients (Figure 68A). Interestingly, a linear regression analysis revealed only significant correlations between plasma GDF15 and age, but not bodyweight loss (Figure 68B), in accordance with the importance of age when correlating plasma GDF15 or IL6 with bodyweight loss across different mouse strains (as shown in Figure 66C and Figure 67C). Again, these data highlight the crucial influence that age can have on cachexia development and the hint of caution that should be applied.
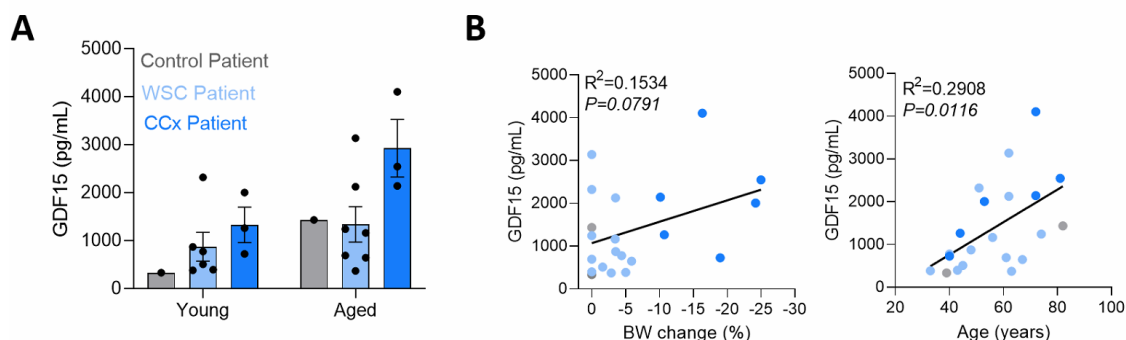
Figure 68. Age but not bodyweight change has a crucial impact on GDF15 levels in patients. Plasma GDF15 levels were assessed in patients suffering from gastrointestinal tumors with (CCx) or without (WSC) weight loss. Control patients did not develop any tumors. **(A)** Circulating GDF15 levels. **(B)** Correlations comparing plasma GDF15 with bodyweight (BW) change or age. Data are mean ± s.e.m. and statistical analyses were performed using two-way ANOVA with Tukey's multiple-comparison post hoc test or simple linear regression. Figure based on (Geppert, 2021).

Similarly to GDF15 and IL6 levels being highly influenced by the age of the mice, also correlations of bodyweight change with different cytokines (IL10, IL1b, IL6) in healthy, weight stable and cachectic cancer patients were only significantly correlated in young patients (≤55 years) (Table 3), but not old ones despite comparable weight loss between the two groups (see patient characteristics in Methods section). Interestingly, plasma IL6 levels also only correlated significantly with bodyweight change in young patients, but not old, in line with the mouse data. The discrepancy between young and old patients in terms of correlating weight loss to circulating cytokines was even more striking for IL10 and IL1b.

Table 3. Important cachexia markers only correlate significantly with BW loss in young patients, but not old. Linear regression analyses between bodyweight change and circulating cytokines and metabolites in control patients without cancer, and gastrointestinal cancer patients with and without bodyweight loss. The number of tested patients is displayed in the table (n) and R^2 as well as significance were calculated using simple linear regression analysis. Significant changes are highlighted in red.

|		Young (≤55y)			Aged (>55y)	
Plasma	**n**	**R^2**	**P value**	**n**	**R^2**	**P value**
Cytokines						
IFNγ	14	0.01020	0.7312	14	0.004835	0.8133
IL10	14	0.5571	0.0022	14	0.003069	0.8508
IL13	14	0.1103	0.2461	14	0.04233	0.4804
IL1b	14	0.4384	0.0099	14	0.006826	0.7789
IL6	14	0.4499	0.0086	14	0.2428	0.0734
IL8	14	0.02732	0.5722	14	0.006336	0.7868
MCP1	14	0.2092	0.1001	14	0.04584	0.4623
Tnfa	14	0.1056	0.2570	14	0.01546	0.6719
Metabolites						
Hemoglobin	14	0.2449	0.1019	14	0.4042	0.0355
CRP	14	0.09554	0.2822	14	0.06038	0.3971
Cholesterol	13	0.1093	0.2698	14	0.02556	0.5851
HDL	14	0.1124	0.2413	14	0.05848	0.4049
LDL	14	0.01040	0.7286	14	0.02746	0.5713
Triglycerides	14	0.06374	0.3839	14	0.1144	0.2369

Overall, age has a crucial influence on phenotypic and developmental characteristics of cancer cachexia in mouse models and patients, including an impact on cachexia severity, the immune system, atrogene expression and circulating cytokines. While the C26 cachexia mouse model seems to be rather independent of age, cachexia development in the LLC model is highly affected and accelerated upon aging. Hence, it is important to choose several experimental models to verify pre-clinical data and enhance good translatability to humans.

2.9   Glucocorticoid signaling in T cells is affected by cancer cachexia

Using RNA sequencing, a general repression of cachectic T cells was noted as several activation pathways were identified to be inhibited (Figure 58, Figure 59). In addition, glucocorticoid receptor signaling was found to be amongst the top 50 pathways being commonly elevated upon cachexia in circulating and tumor-infiltrating CD4^{+} and CD8^{+} T cells, although a clear activation or inhibition pattern based on the z-score could not be discriminated in this analysis (Figure 58), possibly reflecting the two-sided function (activating and inhibitory potential) of glucocorticoids (Timmermans, 2019). Accordingly, an upstream regulator analysis using IPA highlighted the glucocorticoid receptor (GR, encoded by *Nr3c1*) as one of the most prominent activating upstream regulators (Figure 69A), and also dexamethasone, a synthetic steroidal GR ligand (Timmermans, 2019), was identified amongst the most important activated upstream regulators, potentially mediating the observed changes on gene expression level in cachectic T cells. In line, increased expression of many GR target genes (Figure 69B) and subsequent repression of cytokine expression on the molecular level were observed in T cells from cachectic mice (Figure 33). Glucocorticoids are known for their various effects on T cells (Taves, 2021), and have previously been linked to cancer cachexia as drivers of muscle atrophy (Braun, 2013) and suppressors of intra-tumoral immunity in cachectic mice (Flint, 2016). Nevertheless, in their study, Flint *et al.* focused rather on an IL6-induced hepatoketogenesis-glucocorticoid axis than on the immune system; hence, to my knowledge, no detailed mechanistic analysis linking glucocorticoids to T cell repression in cancer cachexia has been conducted so far.
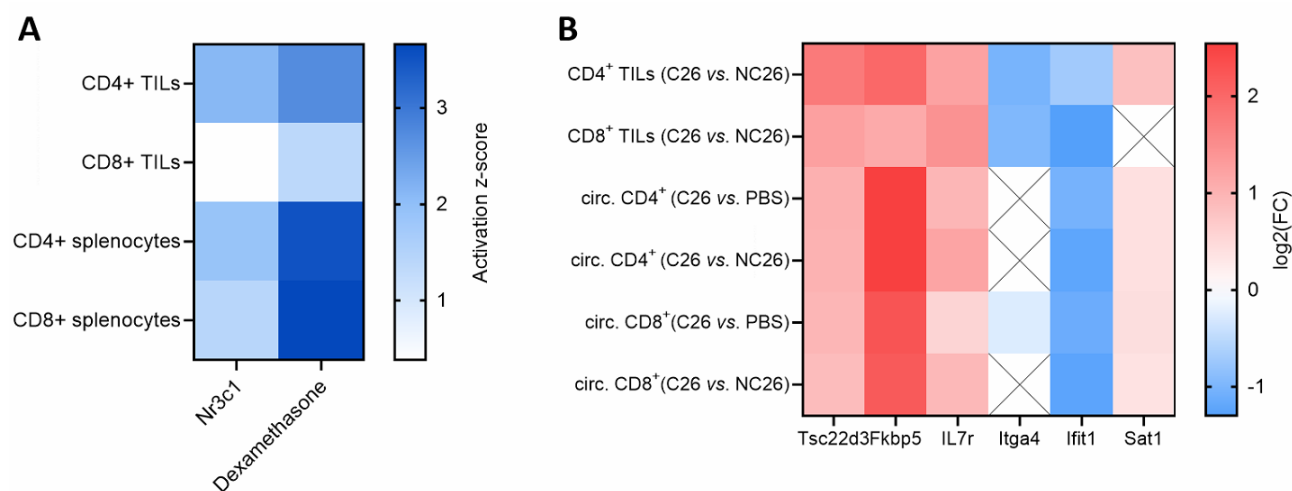
Figure 69. Glucocorticoid signaling strongly affects circulating and tumor-infiltrating T cells in cachectic mice. Heat maps visualizing **(A)** an upstream regulator analysis using IPA, which identified Nr3c1 and dexamethasone as potent regulators in cachectic T cells, and **(B)** regulation of glucocorticoid-associated genes, including *Tsc22d3, Il7r, Itga4, Ifit1, Fkbp5* and *Sat1*.

2.9.1   Circulating glucocorticoid levels are increased in cancer cachexia

Already in the 1990s, it has been shown that cancer cachexia leads to a rise of plasma glucocorticoids in both mouse (Tanaka, 1990) and man (Knapp, 1991). In line, the C26 model used in this study represented a significant increase of corticosterone levels not only upon fully developed cachexia, but already in pre-cachectic mice (Figure 70A). As expected, short-term presence of C26 tumor cells, did not alter corticosterone levels, indicating that the rise of corticosterone is solely dependent on cachexia development and not tumor presence per se. Also in LLC tumor-bearing mice, significantly elevated plasma corticosterone levels were observed, while unexpectedly and contrary to previous reports (Martin, 2022), APC[Min/+] mice displayed no alterations (Figure 70B).
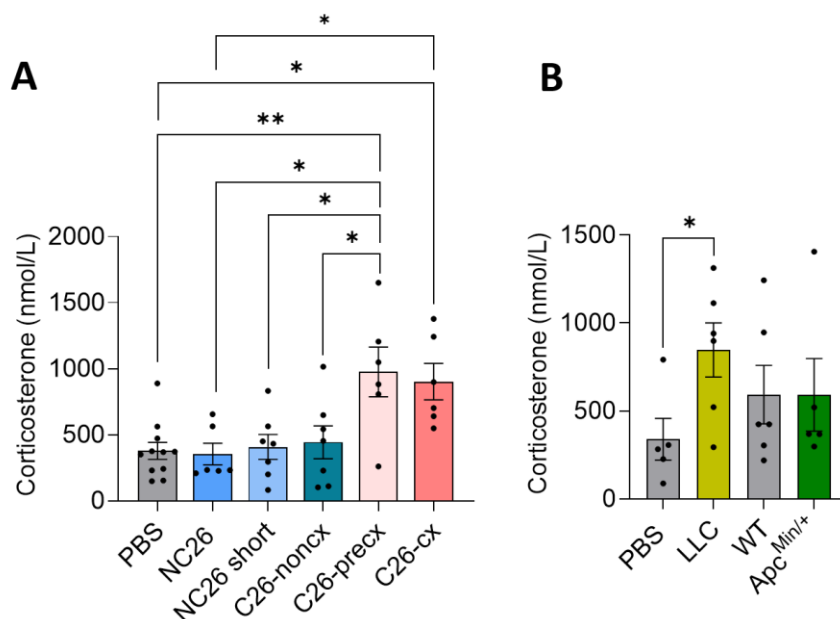
Figure 70. Circulating corticosterone is increased in mouse models of cachexia. (A) Corticosterone concentration in the plasma of BALB/c PBS (n=11), NC26 (n=6), NC26 short (n=7), C26 non-cx (n=7), C26 pre-cx (n=6) and C26 cx (n=6) mice. **(B)** Circulating corticosterone in C57BL/6J mice injected with PBS (n=5), or LLC cells (n=6), APC wildtype (n=6) and APC[Min/+] (n=5) mice. Data are mean ± s.e.m. Statistical analyses were performed using one-way ANOVA or Kruskal-Wallis test with Tukey's or Dunn's multiple-comparison *post hoc* test, respectively. To compare two groups, unpaired t-test was conducted. **(A)** *p<0.05 compared to C26 pre-cx mice, #p<0.05 compared to C26 cx mice. **(B)** *p<0.05 between PBS and LLC mice.

2.9.2   *In vivo* dexamethasone-treatment can mimic low expression of T cell marker genes in eWAT similar to cachexia presence

To assess the effect of high circulating glucocorticoid levels on immune cell presence within the adipose tissue, I investigated the expression of T cell marker genes in eWAT from mice that were long-term treated with dexamethasone in their drinking water (*in vivo* study performed by Manuel Gil Lozano). Strikingly, *Cd8a*, *Cd4* and *Foxp3* gene expression were strongly reduced in eWAT of treated mice (Figure 71) similarly to cachectic mice (Figure 18A). In line with reduced *Gzmb* expression of cachectic T cells, *Gzmb* levels in eWAT tended to be reduced upon dexamethasone treatment as well, but with high variability (Figure 71). Overall, these data highlight glucocorticoids as potential mediators of reduced T cell infiltration into cachectic eWAT.
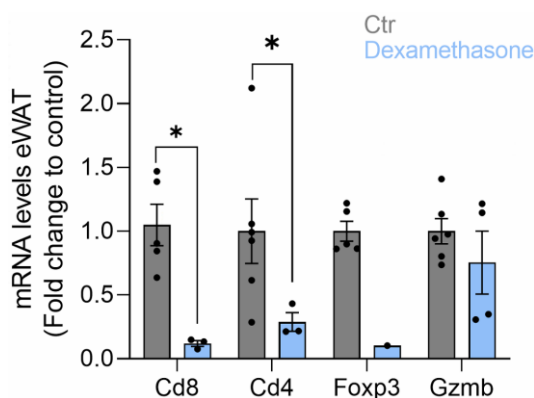
Figure 71. Long-term dexamethasone-treated mice show similar T cell marker mRNA expression in eWAT compared to cachectic mice. *In vivo* study was conducted by Manuel Gil Lozano. Expression of T cell marker (*Cd8a*, *Cd4*, *Foxp3*) and effector (*Gzmb*) genes in eWAT from control (n=5) animals, or mice that were long-term treated with dexamethasone in their drinking water (n=4, if not displayed samples were undetermined). Data are mean ± s.e.m. Statistical analyses were performed using unpaired Mann–Whitney test. *p<0.05.

2.9.3 *In vitro* dexamethasone-treatment of T cells imitates T cell gene expression changes of cachectic T cells

Since *in vivo* long-term treatment of mice with dexamethasone was able to mimic reduced T cell marker gene expression in adipose tissue, similar to cachectic animals, we were wondering if *in vitro* treatment of T cells with dexamethasone could as well imitate the cachectic T cell state. To this end, together with an internship student (Veronika Stadler), I isolated CD8$^+$ splenocytes from wildtype C57BL/6J mice and cultured them for 48 h using 10^{-6} M dexamethasone (Figure 72), which resembled the plasma corticosterone concentration I previously had measured in cachectic C26 tumor-bearing mice (Figure 70A). To mimic T cell stimulation by the tumor, two additional groups were added in which T cells were being activated by CD3/CD28 co-stimulation (Figure 72).
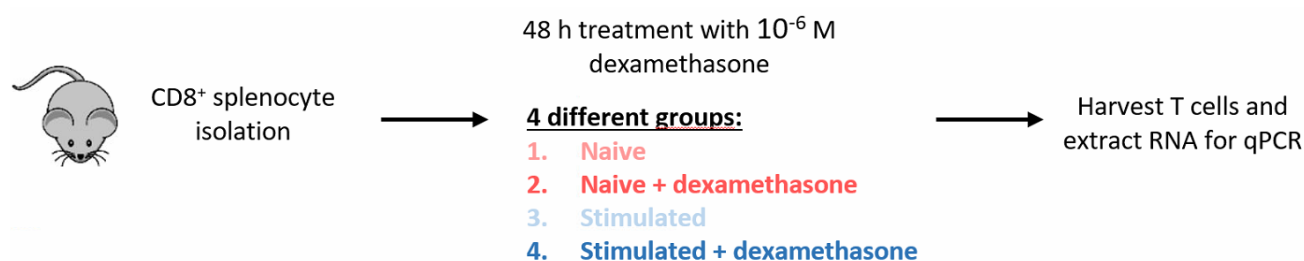
Figure 72. Schematic representation of the experimental setup, aiming to mimic the cachectic T cell phenotype *in vitro* by dexamethasone treatment. CD8$^+$ splenocytes were isolated from C57BL/6J wildtype mice and treated with 10^{-6} M dexamethasone for 48h. To imitate *in vivo* stimulation by the tumor, isolated T cells were simultaneously activated by CD3/CD28 co-stimulation *in vitro*. After 48 h, T cells were harvested, and RNA was extracted for gene expression analysis (naïve ctr n=6; naïve + dex n=6; stimulated ctr n=6; stimulated + dex n=6 biological replicates).

Strikingly, dexamethasone treatment reduced gene expression of T cell effector genes, including *Ifnγ*, *Tnfα* and *Gzmb* and metabolic genes, such as *Slc2a1* (encoding GLUT1) in CD8$^+$ splenocytes (Figure 73A, B), comparably to CD8$^+$ T cells isolated from cachectic mice. Importantly, suppression of effector gene expression and metabolism was much stronger and mimicked the cachectic phenotype better in stimulated compared to naïve T cells treated with dexamethasone (Figure 73), underlining the importance of establishing perfect *in vitro* conditions to mimic the *in vivo* situation.
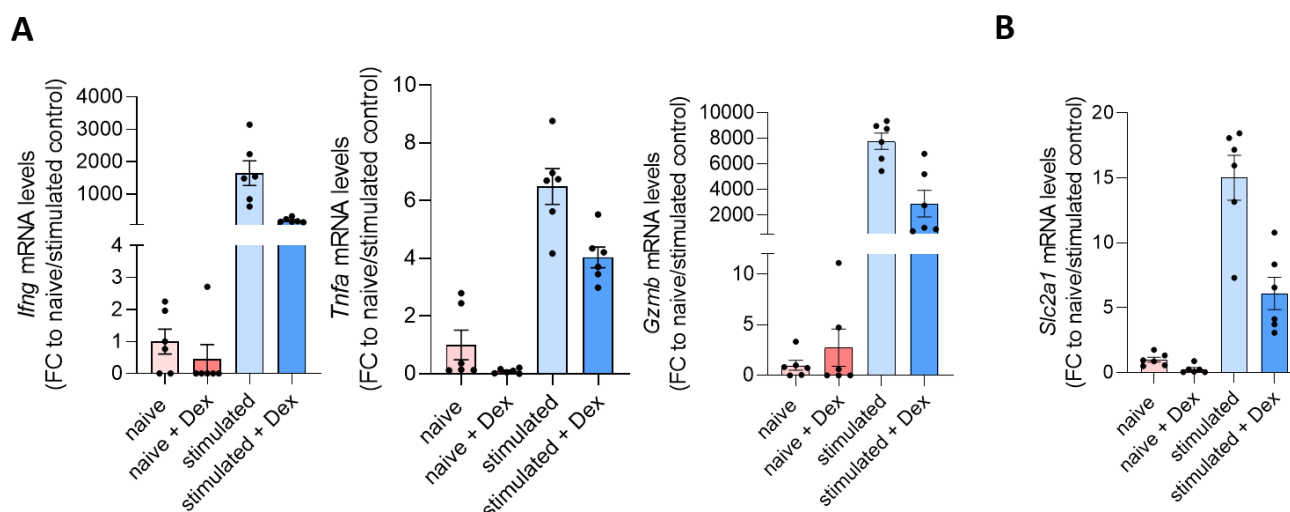
Figure 73. In vitro dexamethasone treatment of stimulated T cells imitates the cachectic T cell phenotype. Expression of **(A)** functional (*Ifnγ, Tnfα,* Gzmb) and **(B)** metabolic (*Slc2a1*, encoding GLUT1) T cell genes in T cells +/- dexamethasone treatment and +/- stimulation. Same samples as in Figure 72. Data are mean ± s.e.m and statistical analyses were performed using Kruskal-Wallist test with Dunn's multiple-comparison *post hoc* test. *p<0.05, **p<0.01.

Verification of the treatment was performed by analyzing gene expression of known glucocorticoid-induced genes. Strikingly, downstream targets of glucocorticoid receptor signaling, like *Sat1*

(Spermidine/Spermine N1-Acetyltransferase 1), Btg1 (B-Cell Translocation Gene 1) or *IL1r2 (Interleukin 1 Receptor Type 2)* (Franchimont, 2002) were regulated similarly between CD8^{+} splenocytes treated *in vitro* with dexamethasone (Figure 74A), and CD4^{+} and CD8^{+} T cells isolated from cachectic mice (Figure 74B, C). Again, stimulated splenocytes mimicked the cachectic phenotype much better compared to naïve T cells, pointing out the importance to imitate tumor stimulation also in an *in vitro* setting.
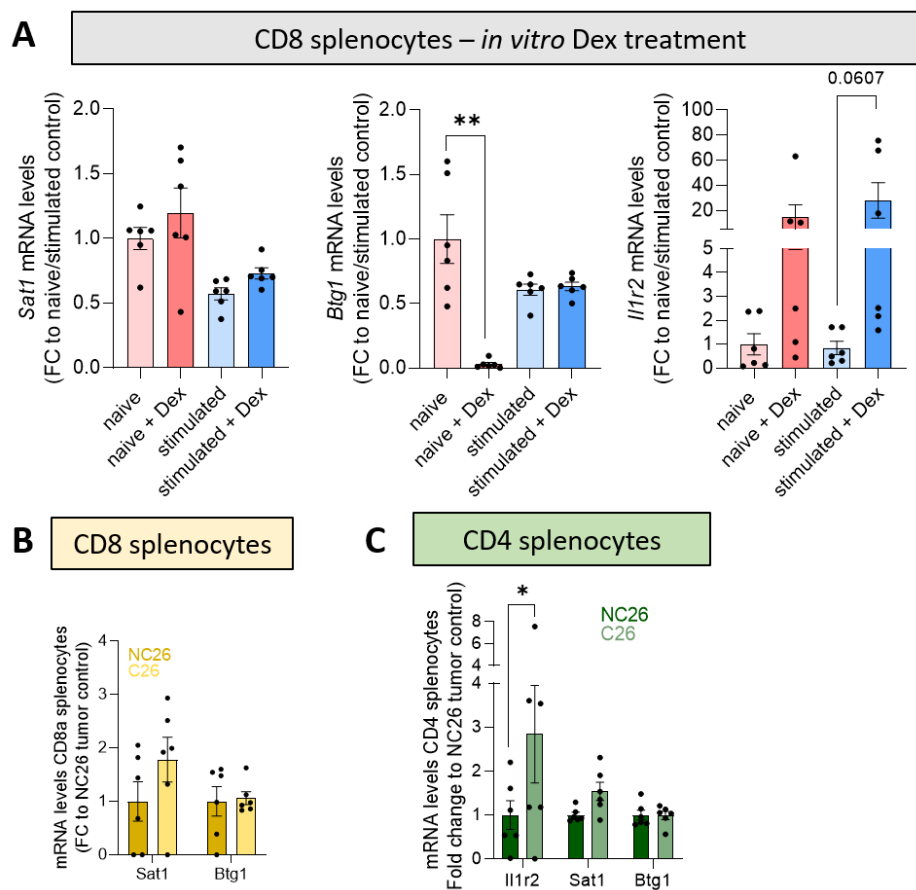
Figure 74. In vitro cultivation of stimulated CD8^{+} T cells with dexamethasone induces similar expression of glucocorticoid-related genes compared to cachectic T cells. (A) mRNA levels of glucocorticoid-associated target genes *Sat1*, *Btg1*, and *Il1r2* in CD8^{+} splenocytes +/- CD3/CD28 co-stimulation +/- dexamethasone treatment. Same samples as in Figure 72. **(B-C)** Gene expression of *Sat1, Btg1* and *Il1r2* in **(B)** CD8^{+} and **(C)** CD4^{+} splenocytes from cachectic C26 (n=6) and non-cachectic NC26 (n=6) tumor-bearing animals. Data are mean ± s.e.m and statistical analyses were performed using Kruskal-Wallist test with Dunn's multiple-comparison *post hoc* test or t test. *$p<0.05$, **$p<0.01$.

Overall, *in vitro* treatment of stimulated CD8^{+} T cells closely resembled the phenotype of T cells isolated from cachectic mice based on the expression of genes associated with effector function, metabolism and glucocorticoid signaling. These data suggest that T cell dysfunction in cachectic mice might be mediated by increased glucocorticoid signaling, thereby repressing T cell function.

2.9.4 Aminoglutethimide treatment does not improve body wasting in cachectic C26 tumor-bearing mice

Since all experiments so far had supported the idea of glucocorticoids as major mediators of T cell suppression in cancer cachexia, we aimed to reduce glucocorticoid levels in mice to attenuate cachexia. To this end, we decided to use the well-known corticosteroid synthesis inhibitor Aminoglutethimide (AG) (Flint, 2016) to effectively decrease circulating glucocorticoid levels in cachectic mice, thereby aiming to improve disease outcome.

Aminoglutethimide injection reduces corticosterone levels with high variabilty

The efficacy of AG to reduce corticosterone levels was first tested in a pilot study (Figure 75). To this end, 0.4 mg AG were injected per mouse and plasma corticosterone levels were measure directly before, and 3h, 8h, 24h, and 48h post injection, which was conducted at 9 am (Figure 75). Reduction of the corticosterone plasma concentration was strongest 3h post AG injection, but rapidly increased again after 8h. 24h post injection corticosterone levels were still non-significantly reduced compared to T0. Based on these pilot results, mice should have been injected twice a day to constantly reduce corticosterone levels in the plasma. Nevertheless, to lower the stress and side-effects of the treatment for the mice, we decided to only inject once a day. Injections would be conducted at 9 am to dampen the continuous rise of corticosterone throughout the day (Teilmann, 2014).

Figure 75. Pilot study to assess efficacy and half-life of Aminoglutethimide (AG) treatment *in vivo*. BALB/c mice (n=4) were treated with 0.4 mg AG per mouse and blood samples were taken before, and 3h, 8h, 24h and 48h post AG injection. Corticosterone levels were assessed using a specific ELISA kit. Data are mean ± s.e.m. Statistical analysis was performed using one-way ANOVA with Tukey's multiple-comparison *post hoc* test. **$p < 0.01$.

Aminoglutethimide did not sufficiently reduce plasma corticosterone in cachectic mice

BALB/c mice were injected with PBS or C26 tumor cells and 8 days post cell injection, when tumors started to be palpable, daily treatment with AG or the vehicle control was initiated (Figure 76).

Figure 76. Schematic figure of aminoglutethimide treatment of PBS- or C26-injected mice over a time course of 20 days. Mice were injected once C26 tumors were palpable. 0.4 mg AG were administered daily via intraperitoneal injection per mouse. The experiment was ended 27 days post PBS-/C26-injection.

Although the pilot experiment had indicated a sufficient inhibition of circulating corticosterone levels after 24 h, AG was not able to reduce corticosterone levels of C26 tumor-bearing mice to normal healthy levels and could only in part decrease circulating corticosterone levels 24 h post injection (T24) or shortly after injection (Figure 77).

Figure 77. Elevated corticosterone levels in cachectic mice could not be sufficiently restored to healthy levels by daily AG injections. To measure circulating corticosterone, blood samples were taken before sacrifice (shortly after AG injection), while T24 samples were taken 24h post AG injection (T24 PBS+vehicle n=4; T24 PBS+AG n=4; T24 C26+vehicle n=1; C26+AG n=1). Unfortunately, a daily injection of 0.4 mg AG per mouse was not sufficient to restore physiological corticosterone levels in cachectic mice (C26+vehicle n=9; C26+AG n=9), as compared to PBS-injected (PBS+vehicle n=5; PBS+AG n=5) animals. Data are mean ± s.e.m. Statistical analysis was performed using ordinary one-way ANOVA with Tukey's multiple-comparison *post hoc* test. *p<0.05.

Aminoglutethimide treatment did not attenuate body wasting in C26 tumor-bearing mice

In line with only slightly altered corticosterone levels, also incidence-free time (used as a proxy for survival) was not affected by AG treatment (Figure 78A). Since all mice were killed once they had developed cachexia, body wasting, indicated by the percentage of bodyweight change of the animals, was not altered by AG (Figure 78B). Importantly, tumor size was similar between both C26 tumor-bearing groups (Figure 78C). In accordance with no changes in bodyweight, organ weights, including GC, WAT, inguinal lymph nodes, and spleen were unaltered, and the expression of atrophy marker genes (*Trim63, Fbxo32*) in GC muscles was unaffected by AG (data not shown). In line, circulating metabolites, such as LDL, HDL, cholesterol, triglycerides, NEFAs and Glucose were also not altered (data not shown). Interestingly, AG treatment induced a strong increase of plasma alanine aminotransferase and aspartate aminotransferase in healthy mice, indicating elevated liver toxicity (Figure 78C). However, alkaline phosphatase levels were significantly reduced, contradicting liver damage mediated by AG treatment. C26 tumor-bearing mice showed in general relatively low levels of these liver toxicity markers, which were also not affected by AG. To sum up, AG treatment seemed to not have induced liver damage, which thus is not a possible explanation for the low efficiency of the drug in our hands.
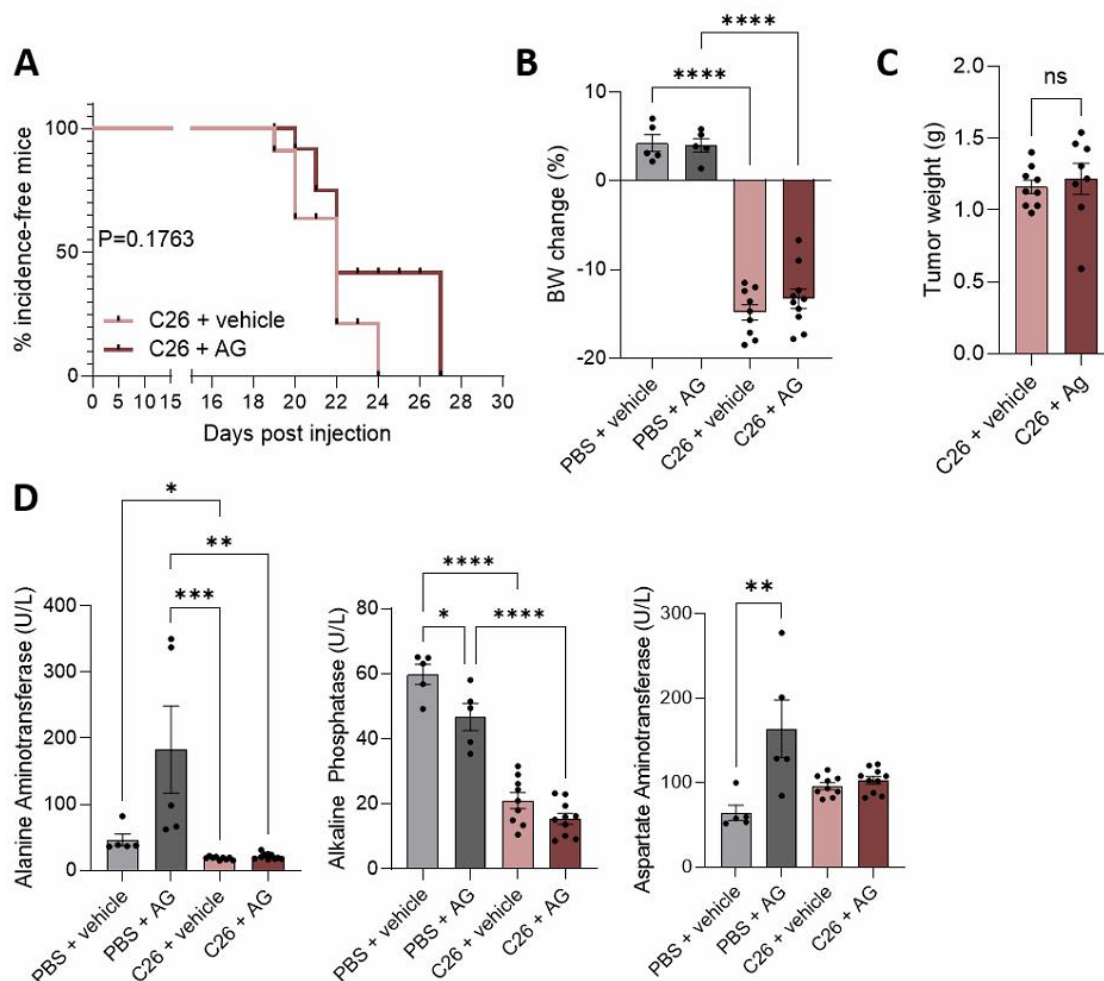
Figure 78. Body wasting upon C26-injection was not attenuated by Aminoglutethimide treatment. Same mice than in Figure 77. **(A)** Percentage of incidence-free C26 tumor-bearing mice over time as a proxy for survival. **(B)** Bodyweight change in percentage at the end of the experiment. **(C)** Tumor weight of C26-injected mice at the end of the experiment. **(D)** Assessment of toxicity, mediated by AG treatment, as measured by circulating levels of Alanine Aminotransferase, Alkaline Phosphatase, and Aspartate Aminotransferase. Data are mean ± s.e.m. Statistical analyses were performed using one-way ANOVA or Kruskal-Wallist test with Tukey's or Dunn's multiple-comparison *post hoc* test, respectively or log-rank (Mantel–Cox) test. *p<0.05, **p<0.01, ***p<0.001, ****p<0.0001.

Expression of genes related to T cell effector function and proliferation is unchanged in AG treated mice

By assessing gene expression of T cell effector function markers, I found no attenuation of the cachexia-mediated repression of *Gzmb*, *Ifnγ,* and *Tnfα* by AG treatment in CD4^{+} (Figure 79A) and CD8^{+} (Figure 79B) T cells isolated from cachectic mice. Importantly, as previously observed, also here effector genes were significantly downregulated in T cells from cachectic C26 tumor-bearing mice compared to healthy PBS mice, underlining the strong T cell repression mediated by cachexia. Only minor changes, such as increased *Slc2a1*, encoding GLUT1, gene expression in CD4^{+} splenocytes (Figure 79C) or reduced *Pdcd1* expression in CD8^{+} T cells, encoding PD1, (Figure 79B) indicated a slight improvement of overall T cell health upon AG treatment. Contrary, *Pdcd1* expression was increased in CD4^{+} T cells from C26 tumor-bearing AG treated mice (Figure 79A), while *Slc2a1* was downregulated in CD8^{+} T cells upon cachexia, and even further due to AG treatment (Figure 79D).
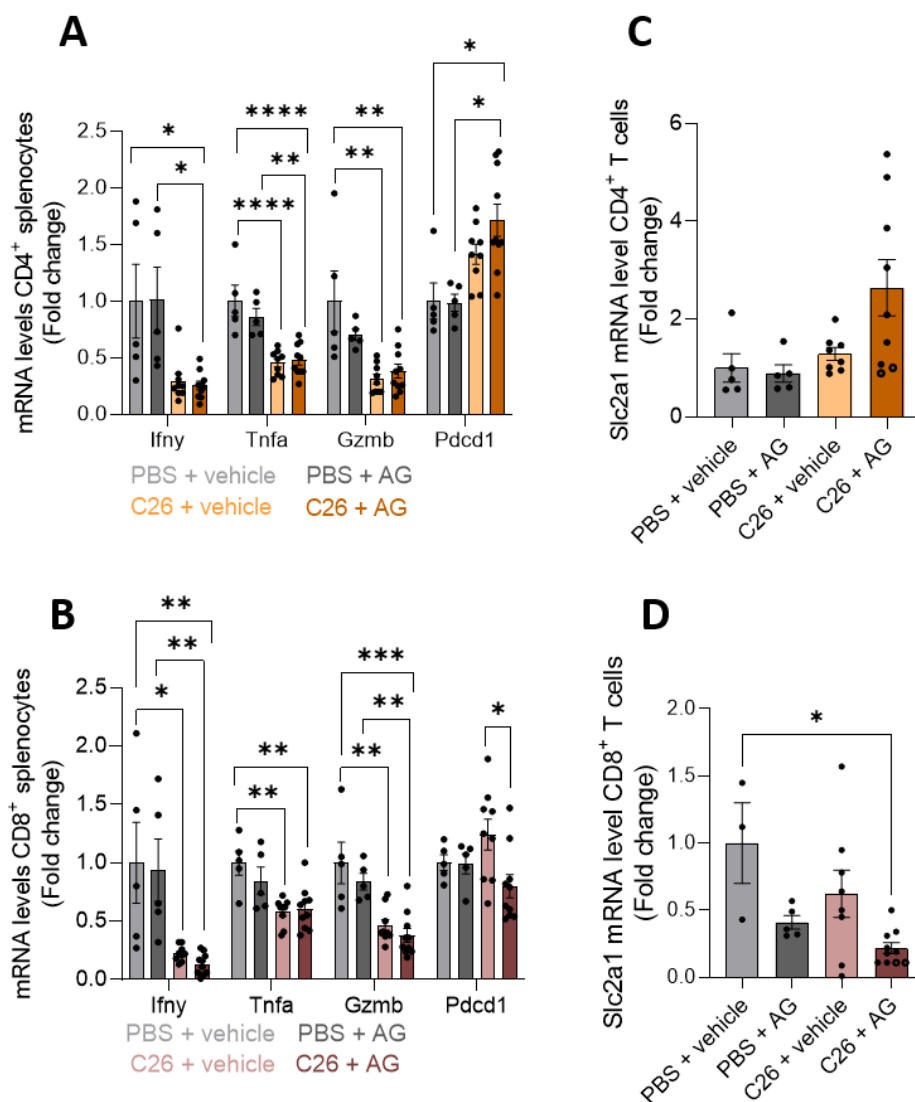
Figure 79. Expression of genes involved in T cell effector function is unchanged upon AG treatment. Same mice than in Figure 77. **(A, C)** mRNA levels of **(A)** *Gzmb*, *Ifnγ*, and *Tnfα* and **(C)** *Slc2a1* in CD4+ splenocytes. **(B, D)** mRNA levels of **(B)** *Gzmb*, *Ifnγ*, and *Tnfα* and **(D)** *Slc2a1* in CD8+ splenocytes. Data are mean ± s.e.m. Statistical analyses were performed using one-way ANOVA or Kruskal-Wallist test with Tukey's or Dunn's multiple-comparison *post hoc* test, respectively. *p<0.05, **p<0.01, ***p<0.001, ****p<0.0001.

Surprisingly, despite AG showing only low efficiency to reduce plasma corticosterone levels, treatment changed glucocorticoid-associated gene expression, especially in CD8+ splenocytes. There was a significant downregulation of the corticosterone-related induction of *Sat1, Tsc22d3* (TSC22 Domain Family Member 3), Itga4 (Integrin Subunit Alpha 4), *Itgal* (Integrin Subunit Alpha L) and *Btg1* (B-Cell Translocation Gene 1), and a non-significant reduction of *Il1r2 (Interleukin 1 Receptor Type 2)*, but only in C26 tumor-bearing mice, indicating that the treatment at least partially affected T cell glucocorticoid signaling upon cachexia (Figure 80B). Healthy mice showed no differences due to AG treatment, with the exception of *Il1r2*, which tended to be upregulated upon treatment (Figure 80B). In CD4+ splenocytes, despite cachexia-mediated changes, only *Il1r2* gene expression was significantly downregulated upon AG treatment, while no changes in the other investigated genes were observed (*Sat1, Tsc22d3, Itgal, Itga4, Btg1*). Overall, AG treatment was not able to efficiently reduce cachexia-induced upregulation of glucocorticoid signaling in T cells on the molecular level.

In summary, aminoglutethimide treatment was not able to reduce high corticosterone levels upon cachexia to physiological levels, in line with no improvements in terms of body wasting, circulating

parameters or atrogene expression. Also, T cell functionality was not restored by the treatment, as AG was not able to fully reduce cachexia-induced repression of T cell effector function and induction of glucocorticoid signaling.
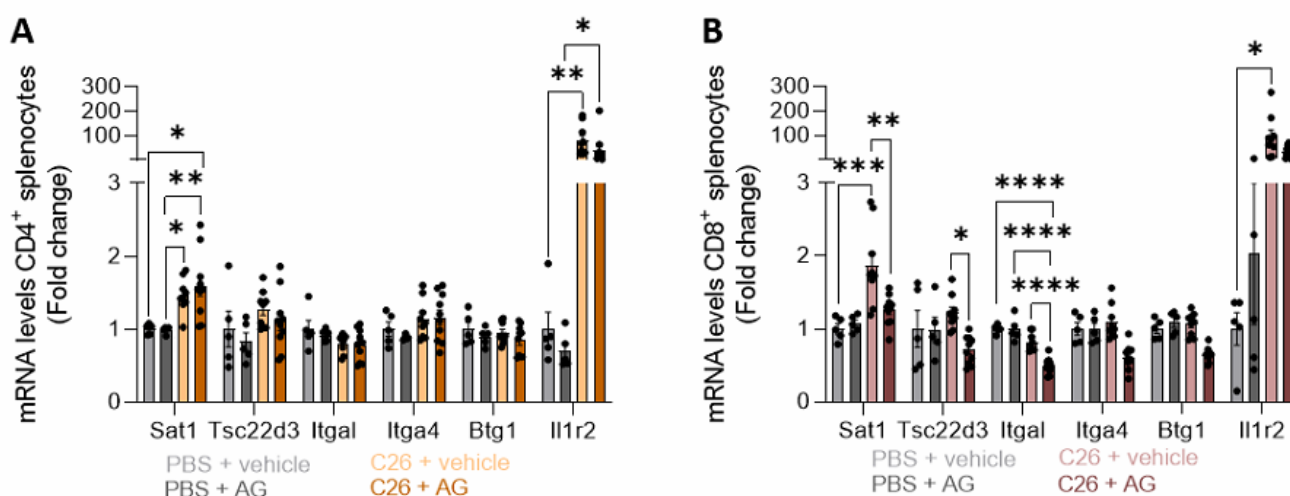
Figure 80. GR-related gene expression is slightly decreased upon AG treatment in CD4⁺ and CD8⁺ T cells. Same mice than in Figure 77. **(A, B)** mRNA levels of *Sat1, Tsc22d3, Itgal, Itga4, Btg1 and Il1r2* in **(A)** CD4⁺ splenocytes and **(B)** CD8⁺ splenocytes. Data are mean ± s.e.m. Statistical analyses were performed using one-way ANOVA or Kruskal-Wallist test with Tukey's or Dunn's multiple-comparison *post hoc* test, respectively. *p<0.05, **p<0.01, ***p<0.001, ****p<0.0001.

2.9.5 T cell specific glucocorticoid receptor knockout

To address the role of T cell intrinsic GR signaling, more specifically, without affecting GR signaling in other tissues, cachexia development was assessed in T cell specific GR knockout mice (CD4cre_GRflox/flox: Tg(Cd4-cre)1Cwi/BfluJ x B6.Cg-Nr3c1tm1.1Jda/J). Glucocorticoids are potent mediators of immunosuppression (Coutinho, 2011). Hence, by knocking out the glucocorticoid receptor on T cells, we aimed to improve T cell dysfunction likely mediated by high corticosterone levels in cachexia. To this end, GR[CD4-Cre] mice were subcutaneously injected with LLC tumor cells, and cachexia development was monitored over a course of 18 days. Unfortunately, all mice had to be sacrificed before cachexia onset, either because of tumor size or tumor ulceration, a well-known problem of the LLC cachexia model (Geppert, 2021). Nevertheless, compared to wildtype LLC tumor-bearing mice, GR[CD4-Cre] LLC mice showed a non-significant increase in bodyweight at the end of the experiment, while importantly, their initial bodyweight was similar (Figure 81A). Accordingly, WT LLC mice showed a lower individual weight gain compared to GR[CD4-Cre] LLC mice (Figure 81A). Tumor size was as well comparable between the two groups (Figure 81B). Although I observed a trend towards higher bodyweight in the GR[CD4-Cre] mice, WAT and GC muscle weight were almost identical between the two groups (Figure 81C), implying that a T cell specific GR knockout could not improve tissue wasting in pre-cachexia. Inguinal lymph node weight was unaffected, while spleen weight seemed to be non-significantly elevated in GR[CD4-Cre] mice (Figure 81D), indicating a stronger immune response (Jiang, 2021).
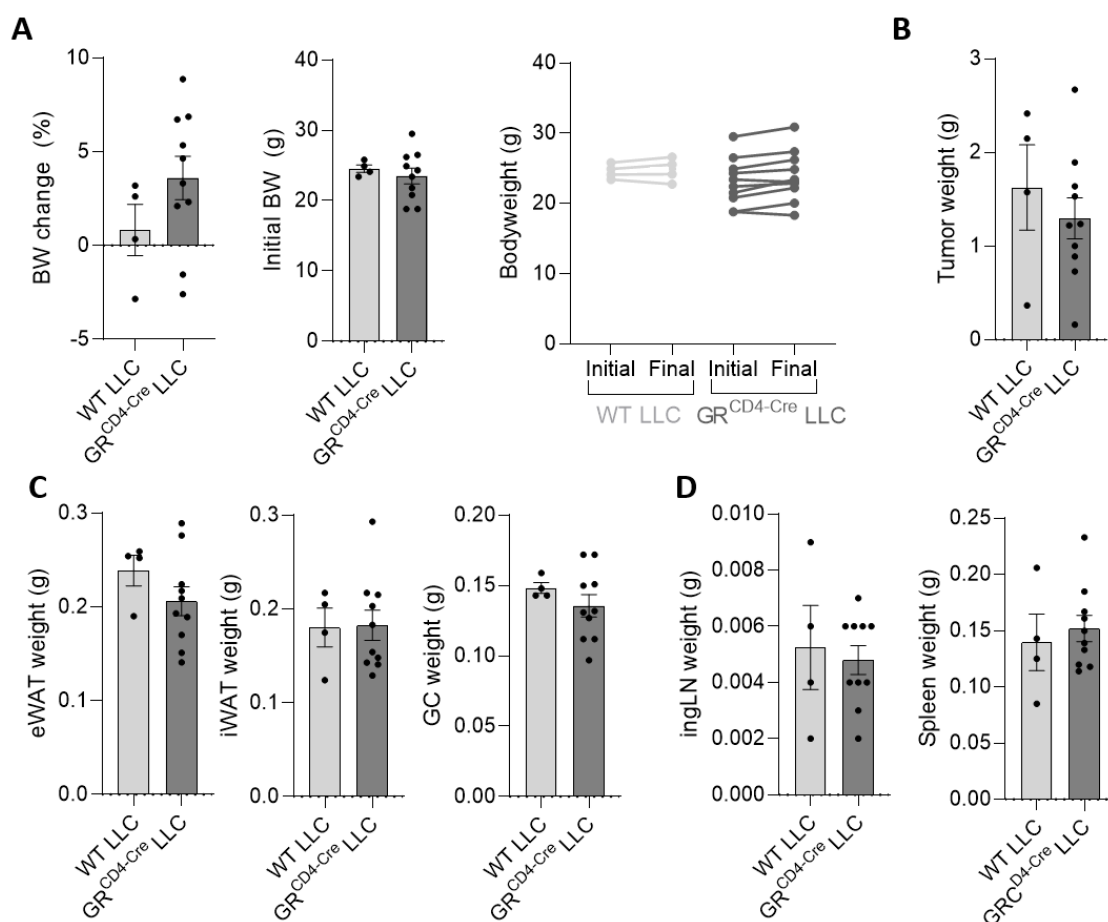
Figure 81. T cell specific glucocorticoid receptor (GR) knockout does not protect from cancer-induced tissue wasting. **(A-D)** CD4-Cre x GRfl/fl knockout mice (n=10) and WT control mice (n=4) were injected with LLC tumor cells. **(A)** Bodyweight (BW) change at the end of the experiment in percent, as measured by comparing final bodyweight minus tumor to initial bodyweight. Initial bodyweight in gram. Comparison of individual initial and final BW (minus tumor). **(B)** Tumor weight at the end of the experiment. **(C)** Tissue weights of eWAT, iWAT and GC muscle. **(D)** Weight of inguinal lymph nodes and spleen. Data are mean ± s.e.m. Statistical analyses were performed using unpaired t test or Mann-Whitney test.

To further assess the impact of the T cell specific GR knockout on cancer cachexia development, muscle atrophy was investigated on the molecular level by expression analysis of atrophy marker genes (Deval, 2001; Rohm, 2019; Sandri, 2004). Despite unaltered GC muscle weight in GR[CD4-Cre] mice, *Trim63*, *FoxO3a* and *Fbxo32* were non-significantly, and *Ctsl* expression significantly reduced in skeletal muscle upon T cell specific GR knockout (Figure 82), although we previously demonstrated that young mice from the C57BL/6J background are not susceptible to LLC-induced expression of atrophy markers (Geppert, 2021). The mild decrease of atrophy marker gene expression suggests that the T cell-specific GR knockout has a beneficial effect on tissue wasting on the gene level, potentially mediated by ameliorating T cell suppression induced by elevated glucocorticoid levels in cancer cachexia (Tanaka, 1990). Indeed, other groups have already shown a link between skeletal muscle repair and T cells, as regulatory T cells were reported to mediate positive effects on muscle tissue repair upon injury (Arpaia, 2015; Burzyn, 2013; Castiglioni, 2015).
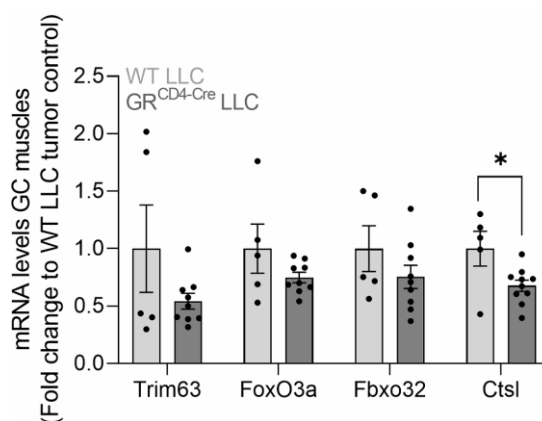
Figure 82. On the molecular level, muscle atrophy is mildly improved by T cell specific GR knockout. Same mice as in Figure 81. Expression of atrophy marker genes in GC muscles, including Trim63, FoxO3a, Fbxo32 and Ctsl. Data are mean ± s.e.m. Statistical analyses were performed using unpaired t test or Mann-Whitney test. *p<0.05.

Based on the mild amelioration of T cell atrophy marker expression upon T cell specific GR knockout, I wanted to assess if T cell infiltration into skeletal muscle was altered. To this end, expression of several T cell marker genes, including *Cd3, Cd8a, Cd4*, and *Foxp3* was determined (Figure 83). No significant changes in T cell marker gene expression were noted, although *Cd8* tended to be upregulated in GC muscles from GR[CD4-Cre] mice. Interestingly, *Gzmb*, encoding one of the most important T cell effector molecules, was significantly upregulated in GC muscle from T cell specific GR knockout mice (Figure 83). In combination with increased *Cd8a* expression, the upregulated *Gzmb* levels imply an increase in CD8^{+} effector T cells due to reduced glucocorticoid-mediated T cell suppression, with potentially beneficial effects protecting from tissue wasting in later stages of cachexia.
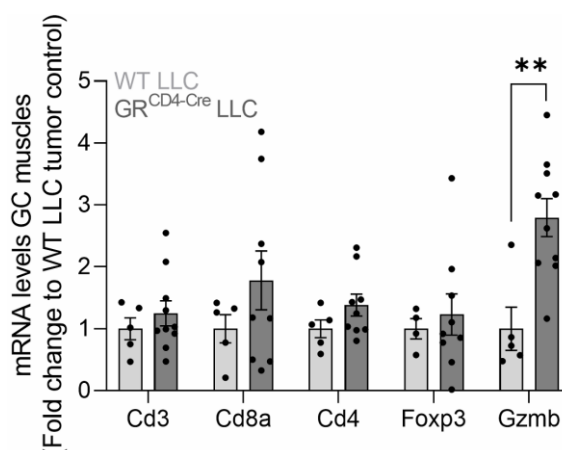
Figure 83. T cell effector function seems to be restored in GR[CD4-Cre] mice upon LLC injection. Same mice as in Figure 81. T cell marker gene expression in GC muscles. T cell specific genes include *Cd3, CD8a, Cd4* and *Foxp3*. *Gzmb* is encoding one of the most important effector proteins. Data are mean ± s.e.m. Statistical analyses were performed using unpaired t test or Mann-Whitney test. **p<0.01.

On the molecular level, T cell effector function was partially improved by GR knockout. Gene expression of *Ifnγ* and *Il2* was significantly upregulated in CD4^{+} splenocytes (Figure 84A) and tended to be increased in CD8^{+} T cells (Figure 84B) upon GR knockout in LLC tumor-bearing mice, suggesting enhanced effector function and overall well-being of the cells. Interestingly, despite increased *Gzmb* levels in GC muscle, *Gzmb* expression in CD4^{+} and CD8^{+} T cells was not affected in GR knockout mice, indicating that elevated *Gzmb* expression in GC muscles in GR[CD4-Cre] mice might be linked to increased Natural Killer (NK) cell infiltration, which are also able to secret GZMB (Y. Wang, 2018). *Tnfα* expression was slightly upregulated in CD8^{+} T cells, and *Pdcd1* seemed to be decreased in CD4^{+} and

CD8^{+} T cells from LLC tumor-bearing mice carrying a T cell-specific GR knockout. Thus, GR knockout seemed to have an overall beneficial effect on T cell in the LLC setting. Importantly, also downstream targets of GR signaling were affected in GR[CD4-Cre] T cells, verifying the functionality of the GR knockout on the molecular level. In that regard, multiple GR taget genes were decreased in T cell-specific GR knockout mice, such as *Tsc22d3, Il1r2, Sat1* and *Itgal* (Figure 84C, D). Interestingly, *Tsc22d3*, encoding the glucocorticoid-induced leucine zipper (GILZ), was shown to inhibit T cell activation by interfering with TCR and NF-κB signaling (Ayroldi, 2001). Hence, reduced *Tsc22d3* expression in GR knockout T cells of LLC tumor-bearing mice, suggest improved potential for T cell activation and thus effector function, in line with the elevated expression of effector genes (Figure 84A, B). Furthermore, glucocorticoids are known to induce expression of the decoy receptor IL-1R2 (Interleukin 1 Receptor Type 2) (Peters, 2013), which can neutralize IL-1 (Van Den Eeckhout, 2020), thereby preventing its effects on CD8^{+} T cell effector function (Ben-Sasson, 2013). Thus, the GR knockout-mediated reduction of *Il1r2* expression indicates beneficial effects on T cell functionality, while similarly being a proof of concept for a functional knockout.
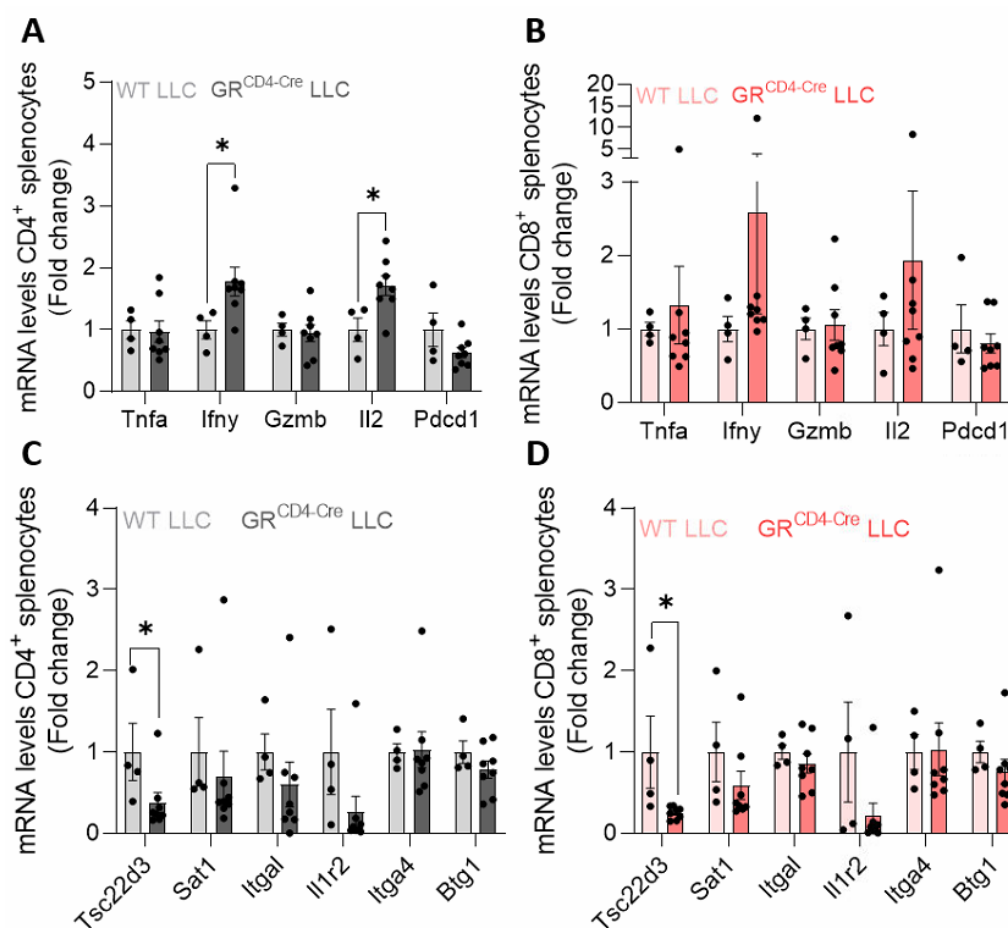
Figure 84. T cell-specific GR knockout improves effector function and reduces expression of GR target genes in T cells upon LLC injection. Same mice as in Figure 81. **(A-B)** Expression of genes associated with T cell functionality in **(A)** CD4^{+} and **(B)** CD8^{+} T cells. **(C-D)** GR target gene expression in **(C)** CD4^{+} and **(D)** CD8^{+} T cells. Data are mean ± s.e.m. Statistical analyses were performed using unpaired t test or Mann-Whitney test. *p<0.05.

In summary, the T cell-specific GR knockout did not significantly affect wasting and bodyweight evolution upon LLC-injection, but showed already a promising trend, However, this was most probably a result of the small group size and the premature sacrifice of the mice. Nevertheless, atrophy marker expression and T cell effector function tended to be improved, in line with decreased expression of GR target genes in GR[CD4-Cre] LLC-injected mice.

2.10 Glucose deprivation may drive diminished T cell signaling and function in cachexia

Activation of naïve T cells through their T cell receptor (TCR) is initiated by antigen/MHC complexes (Rosenthal, 1973; Shevach, 1973), and additional signaling of costimulatory receptors, such as CD28 (Linsley, 1991) (Figure 85). Upon stimulation, several signaling pathways are being activated, including the PI3K/AKT pathway, which is induced by CD28-mediated signaling (Truitt, 1995). Downstream of PI3K/AKT, the serine/threonine kinase mechanistic target of rapamycin (mTOR) becomes activated, which regulates a variety of cellular functions, including apoptosis (Q. Wu, 2011), differentiation (Rao, 2010), growth and metabolism (Düvel, 2010), all functions that were dysregulated in T cells in the cachexia setting. Interestingly, mTOR was also shown to link environmental signals such as glucose availability to different cellular fates of T cells (Chapman, 2014). In addition, the transcription factor forkhead-Box-O-1 (FOXO1) was reported to integrate signals from mTOR and AKT signaling pathways in T cells, and to play an important role in proliferation (Stittrich, 2010), survival (Kerdiles, 2009), DNA repair (Ju, 2014) and glucose metabolism (W. Zhang, 2006).
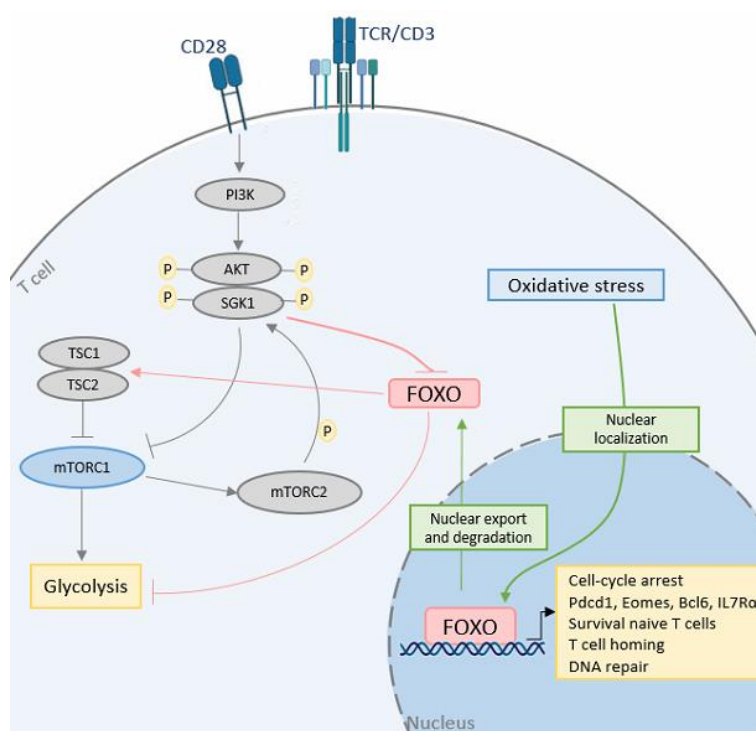
Figure 85. Scheme representing FOXO1 interactions upon T cell activation. T cell stimulation via the TCR/CD3 receptor in combination with CD28-mediated signaling leads to the activation of phosphoinositide 3-kinase (PI3K), which promotes the phosphorylation of AKT and serum/glucocorticoid Regulated Kinase 1 (SGK1) by 3-phosphoinositide-dependent kinase 1 (PDK1), inhibiting mechanistic target of rapamycin (mTOR) complex 1 (mTORC1) and thereby glycolysis. Additionally, mTORC1 phosphorylation can be mediated by the heterodimerized tumor suppressors TSC1 and TSC2. After additional phosphorylation by mTORC2, AKT and SGK1 are capable of directly phosphorylating FoxO transcription factors, thereby inhibiting by causing nuclear export and degradation. Contrary, oxidative stress leads to nuclear localization of FOXO1, leading to cell-cycle arrest, survival of naïve T cells, T cell homing to lymph nodes, DNA repair and expression of T cell exhaustion marker genes, such as *Pdcd1, Eomes, Bcl6* and *IL7Rα*. Figure based on (Hedrick, 2012).

2.10.1 Cachexia affects C28-mediated signaling in CD4⁺ and CD8⁺ T cells

RNA sequencing of circulating and tumor-infiltrating T cells from cachectic mice, highlighted a strong downregulation of the PI3K/AKT/mTOR pathway (Figure 58). Indeed, also several mTOR-associated genes were identified as important upstream regulators in cachectic T cells (Figure 86). In detail, the predicted activation status of rapamycin-insensitive companion of mTOR (Rictor) and Rapamycin were calculated to be activated, while Myc, Mycn and FOXO1 were predicted to be inhibited in T cells upon cachexia, as indicated by their activation z-score (Figure 86). Rapamycin - also known as

Sirolimus - is a natural metabolite produced by bacteria (Sehgal, 1975), with strong immunosuppressive properties (Sehgal, 1993). Hence, the prediction of Rapamycin as important activated upstream regulator, suggests a strong suppression of cachectic T cells, most probably based on alterations in the mTOR pathway. Rictor is part of mTOR complex 2 (mTORC2) (Sarbassov, 2004). Thus, the predicted elevation of activated Rictor in cachectic T cells, implies an increase of mTORC2, and subsequently elevated phosphorylation and activation of AKT (Sarbassov, 2005), which then inhibits mTORC1 and thereby glycolysis (Yang, 2013) (Figure 85). Of note, regulatory associated protein of mTOR (Raptor), being part of the mTORC1 complex (Hara, 2002), was not identified as altered upstream regulator using IPA. Regulation of glucose metabolism by mTOR is in part mediated by HIF (Hypoxia Inducible Factor) and Myc (Iyer, 1998; R. Wang, 2011), the latter being identified as inhibited upstream regulator in cachectic T cells. Additionally, also the Myc family member Mycn, was predicted to be inhibited as identified by IPA upstream regulator analysis (Figure 86). Myc is an oncogenic transcription factor, controlling several important metabolic pathways, including glycolysis, FAO, and glutaminolysis, all being important for T cell proliferation (R. Wang, 2011), and potentially explaining the decreased T cell proliferation we saw upon cachexia. Additionally, Myc is a transcriptional repressor of TSC2 expression (Ravitz, 2007). Upon cachexia, Myc was identified as inhibited upstream regulator, thus indicating that inhibited Myc levels might lead to an increase in TSC2 protein, which then decreases mTORC1 activity (Figure 85). These data further support the hypothesis that repression of the PI3K/AKT/mTOR pathway might be in part the underlying cause for dysfunctional T cells upon cachexia. FOXO1 was also identified as major upstream regulator with predicted inhibited activity in cachectic T cells (Figure 86). FOXO1 has previously been demonstrated to integrate signals from the mTOR/AKT signaling pathway in T cells (Staron, 2014), while also affecting glycolysis (Jeng, 2018; Newton, 2016). Moreover, decreased PI3K/AKT signaling leads to enhanced FOXO1-mediated transcription (Hedrick, 2012) (Figure 85).
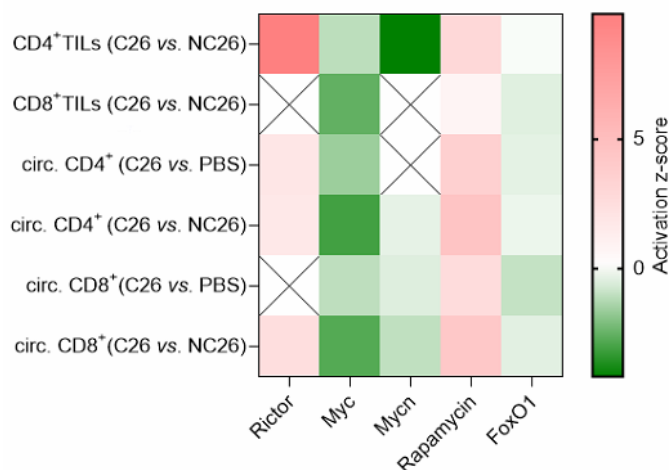
Figure 86. Several mTOR-related factors were identified as potential upstream regulators in cachectic T cells using IPA. Heatmap displaying identified mTOR-associated upstream regulators (Rictor, Myc, Mycn, Rapamycin, FOXO1), and their activation z-score in circulating and tumor-infiltrating CD4^{+} and CD8^{+} T cells.

Importantly, several FOXO1 target genes were regulated by cancer cachexia in T cells (Figure 87). Amongst them, the interleukin 7 receptor *α (Il7rα)* gene, encoding a subunit of the main survival receptor of naïve T cells, and being one of the key FOXO1-regulated genes (Kerdiles, 2009), was upon the most upregulated genes in cachectic T cells (Figure 87), indicating a high activation of the FOXO1 pathway and a higher percentage of naïve *vs.* activated T cells (Kerdiles, 2009). Additional FOXO1 target genes being regulated in cachexia, include Krupple-like factor 2 (*Klf2*), which in turn promotes

the transcription of *Sell* (encoding CD62L, also called L-selectin), Sphingosine-1-phosphate receptor 1 (*S1pr1*), BCL6 transcription repressor (*Bcl6*), Forkhead Box P3 (*Foxp3*), Eomesodermin (*Eomes*), and Cytotoxic T-Lymphocyte associated protein 4 (*Ctla4*) (Figure 87). Both, KLF2 and CD62L are markers for naïve T cells and play an important role in T cell migration and homing (Arbonés, 1994; Kahn, 1994; Sebzda, 2008). Thus, the upregulation of *Klf2* and *Sell* in combination with the strong increase of *IL7rα* further highlights an increase of naïve compared to activated T cells in cachectic mice, in line with our flow cytometry data indicating an increase of CD62L⁺CD8⁺ T cells upon cachexia (Figure 19). In line with aberrant T cell homing, based on irregular *Klf2* and *Sell* expression, *S1pr1* was downregulated in T cells from cachectic mice, additionally indicating altered thymic egress (Matloubian, 2004). *Ctla4*, mediating T cell inhibition (Krummel, 1995), and *Bcl6*, which is essential for Treg repressor function during tumor appearance (Y. Li, 2020), were both increased upon cachexia, suggesting an elevated T cell inhibition and an increased stability of Tregs, potentially leading to less effector T cells and worsened outcome in cachexia. This hypothesis is further supported by the downregulation of the FOXO1 target gene Eomes, a critical regulator of CD8⁺ T cell effector function (Pearce, 2003). Altogether, these data suggest an important role of FOXO1 in T cell metabolism during cachexia. Future studies using T cell-specific FOXO1 knockout mice will aim at clarifying the role of FOXO1 for cachexia development and altered T cell function in cancer-associated wasting.
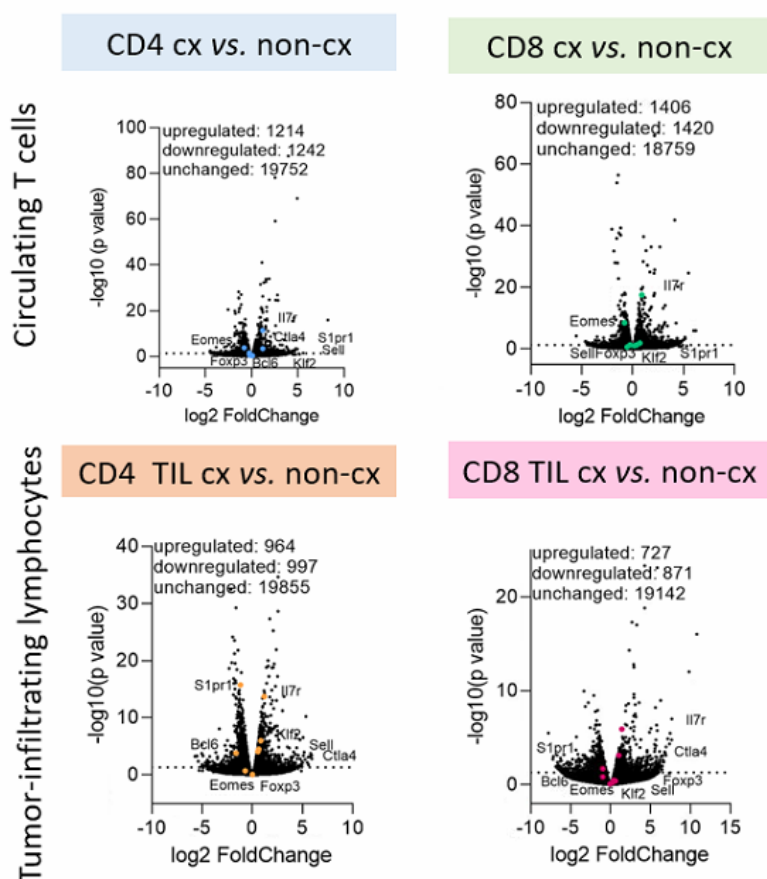
Figure 87. FOXO1 target genes are strongly regulated in cachectic T cells. Volcano plots showing the expression of target genes of FOXO1 signaling in cachectic CD4⁺ and CD8⁺ lymphocytes from spleen and tumor, as measured by RNA sequencing.

2.10.2 Central and local glucose deprivation may drive diminished T cell function in cachexia

Throughout all experiments, cachectic mice of different mouse strains displayed a considerable reduction in blood glucose levels (Figure 88B-E). Importantly, non-cachectic C26 control mice and non-cachectic young APC$^{Min/+}$ mice showed no alterations of circulating glucose levels (Figure 88A, D), linking the presence of cachexia directly to lower systemic glucose levels, despite increased food intake (Figure 11A). Interestingly, also pre-cachectic C26 tumor-bearing mice had no changes in circulating glucose (Figure 88C), again highlighting the connection between refractory cachexia and central glucose deprivation.
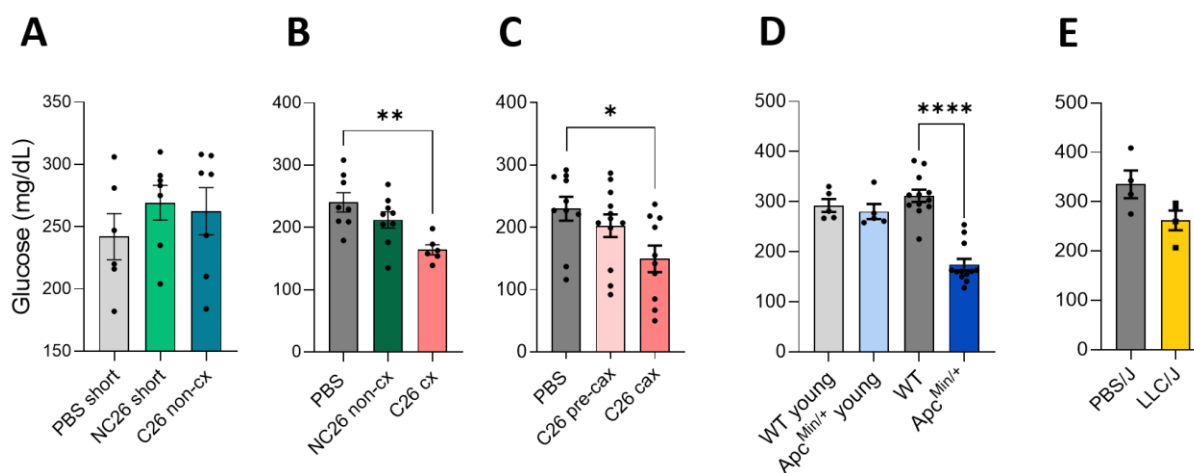
Figure 88. Cachectic mice suffer from central glucose deprivation. Circulating glucose levels in **(A)** PBS short (n=6), NC26 short (n=7), C26 non-cx (n=7), **(B)** PBS (n=8), NC26 non-cx (n=9), C26 cx (n=6), **(C)** PBS (n=10), C26 pre-cx (n=12), C26 cx (n=10), **(D)** APC WT young (n=5), APC$^{Min/+}$ young (n=5), WT (n=12), APC$^{Min/+}$ cx (n=12), and **(E)** PBS/J (n=4) and LLC/J (n=4) mice. Data are mean ± s.e.m. Statistical analyses were performed using one-way ANOVA or Kruskal-Wallis test with Tukey's or Dunn's multiple-comparison *post hoc* test, respectively. To compare two groups, unpaired t test was conducted. *$p < 0.05$, **$p < 0.01$, ****$p < 0.0001$.

Glucose is important for T cell survival, differentiation, and proliferation, mainly mediated through mTOR and AKT signaling (Jacobs, 2008; C. S. Palmer, 2015), both pathways being strongly downregulated in cachectic T cells, as indicated by RNA sequencing. Indeed, correlations of numbers of tumor-infiltrating T cells and circulating glucose levels showed the highest significances in cachectic mice compared to other plasma markers related to metabolism (Figure 89C). This strong positive correlation was only present in cachectic mice, while there were no significances in non-cachectic animals (Figure 89A). Pre-cachectic mice showed an in-between stage (Figure 89B), underlining that cachexia development itself is the key driver, linking T cell dysfunction and central glucose deprivation. Within the cachectic C26 group, numbers of TILs were strongly correlated to cachexia as measured by bodyweight change of the mice (Figure 89D).
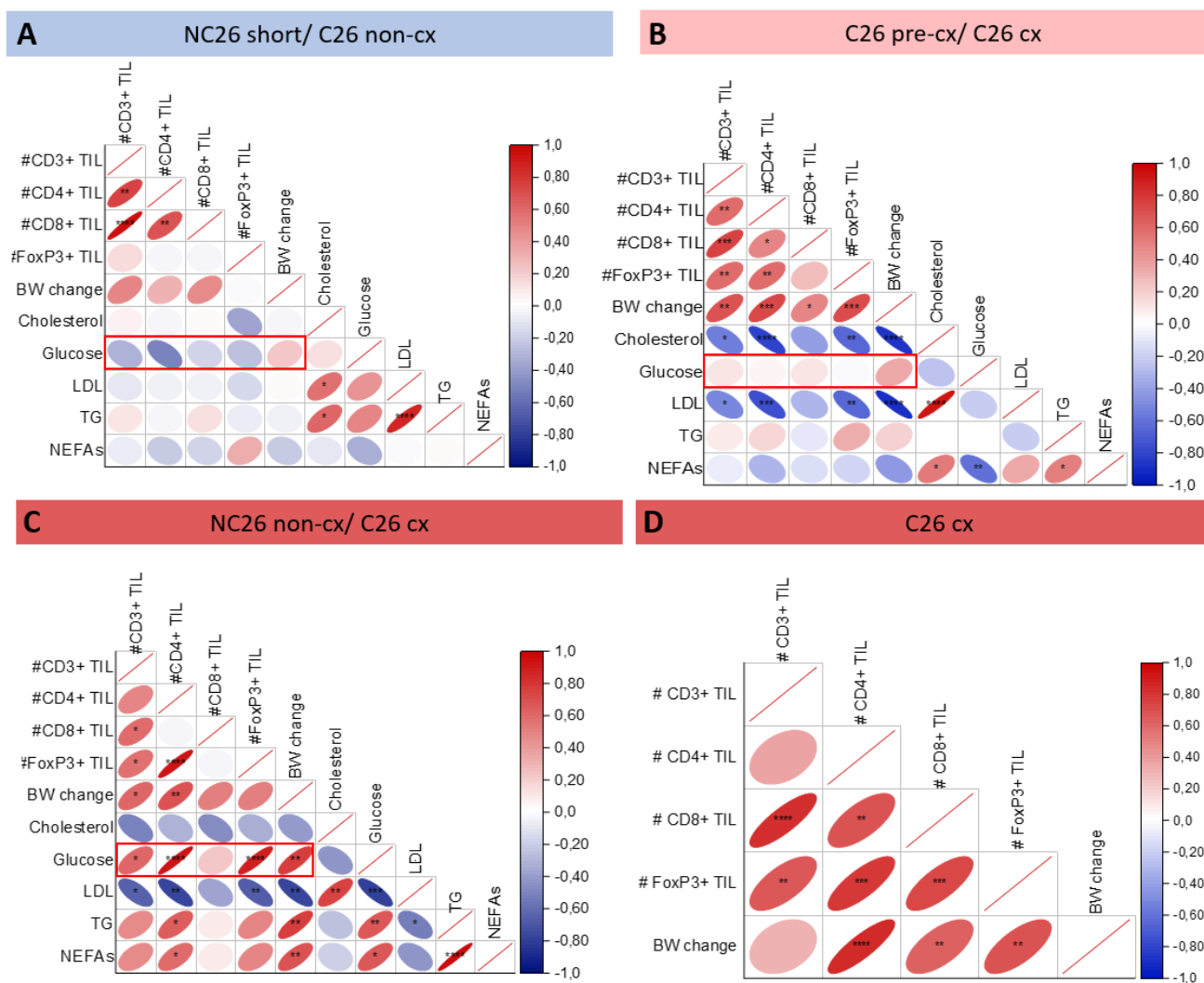
Figure 89. Numbers of tumor-infiltrating T cells and bodyweight change strongly correlate with circulating glucose levels. Pearson correlation matrices of TIL numbers, bodyweight change (in percentage) and circulating markers in **(A)** non-cachectic C26 and NC26 mice from the short-term study, **(B)** pre-cachectic and cachectic C26 mice and **(C)** cachectic C26 and non-cachectic NC26 mice. **(D)** Pearson correlation matrix of TIL numbers and bodyweight change (in percentage) only in cachectic C26 tumor-bearing mice. The angle of the ellipse indicates whether the correlation is positive (1.0) or negative (-1.0) and in addition, the size of the ellipse is associated with the pearson coefficient. The smaller the width of the ellipse, the closer the pearson coefficient was to 1.0/-1.0. Color coding can be looked up at the color scale ranging from -1.0 (blue) to 1.0 (red). Red squares highlight correlations between circulating glucose and numbers of TILs and bodyweight change (in percentage). Significances of the correlations are indicated using *p<0.05, **p<0.01, ***p<0.001, ****p<0.0001

Spatial metabolomics revealed a strong and highly significant enrichment of hexose (including glucose) in the vital parts of C26, but not NC26 tumors (Figure 90), indicating a higher glucose demand of cachexia-inducing tumors compared to non-cachexia-inducing tumors. Altogether, cachectic mice not only suffered from central, but also local glucose deprivation in the tumor microenvironment, potentially leading to impaired T cell function and worsened disease outcome.
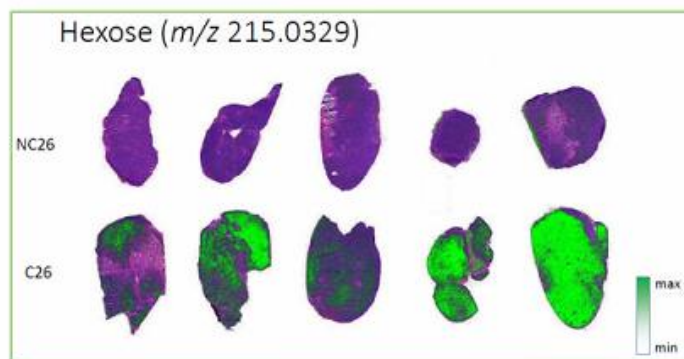
Figure 90. Local glucose deprivation in the tumor microenvironment of cachectic C26 tumors. Metabolomic analysis was performed by the HMGU Core Facility for Pathology and Tissue Analytics. Shown is the hexose concentration in NC26 (n=5) and C26 (n=5) tumors, with high intensity shown in green.

2.10.3 Anorexia or fasting are likely not drivers of T cell dysfunction in cachexia

Glucose deprivation has previously been linked to defects in T cell functional capacity, including dampened cytokine production, defective proliferation and cytolysis (Cham, 2008; Cham, 2005; Jacobs, 2008), all dysfunctional mechanisms observed in cachectic T cells. Indeed, T cells from cachectic mice also seemed to have a fasting signature (low PI3K/AKT, high FKBP5), although compensatory over-eating was frequently observed in our studies to counteract cachexia in C26 mice. Hence, to better understand the metabolic dysregulation of T cells in cachexia, the T cell fasting phenotype was mimicked by either direct fasting of mice for 16 h or 2-Deoxyglucose (2-DG) treatment, an inhibitor of glycolysis. Subsequently, CD4$^+$ and CD8$^+$ splenocytes were isolated and their global gene signatures were compared to those of cachectic T cells. To compare the overall overlap between global gene expression profiles from cachectic and fasted or 2-DG treated mice, the number of differentially expressed genes (DEGs) that are regulated in two RNA sequencing datasets was assessed. The overlapping count was then normalized to the total numbers of DEGs of each dataset, respectively. Table 4 shows the overall overlap in percentage, normalized to the dataset defining the column, i.e. the number of DEGs being present in both RNA sequencing datasets, CD4 TILs and CD8 TILs, exhibited 45% of all DEGs detected in the CD8 TIL dataset, while these commonly altered genes only made up about 20% of the CD4$^+$ TIL dataset. The color code hereby marks high overlap in green, while low overlapping of DEG in percentage is indicated by red color. Without going too much into detail, it can be easily seen that CD4$^+$ T cells from fasted and 2-DG treated mice do not resemble the cachectic phenotype, based on the simultaneous appearance of DEGs. Of note, this analysis did not consider the specific regulation of the genes (up *vs.* down), which could, despite the presence of common DEGs, be contrary between overlapping DEGs. Overall, based on the comparison of regulated DEGs, the dysfunctional T cell phenotype in cachectic mice could not be mimicked by fasting or 2-DG treatment, contradicting previous results by Flint *et al.*, which have shown that caloric deficiency is a central mediator of T cell dysfunction in cancer cachexia (Flint, 2016).

Table 4. Neither fasting nor 2-DG treatment can mimic the dysfunctional T cell state in cancer cachexia based on differentially expressed gene levels (DEGs). Overlapping DEGs between two RNA sequencing data sets were identified, independent of the type of their regulation (up-or downregulated). The count of overlapping DEGs was identified and normalized to the number of total DEGs of each of the two data sets, respectively. The table shows the overall overlap in percentage, normalized to the dataset defining the column. The color code indicates high overlap in green and low overlap in red.

	CD4 TILs NC26 vs C26	CD8 TILs NC26 vs C26	Circ CD4 C26 vs NC26	Circ CD4 C26 vs PBS	Circ CD4 NC26 vs PBS	Circ CD8 C26 vs NC26	Circ CD8 C26 vs PBS	Circ CD8 NC26 vs PBS	CD4 Fast Fast vs ad libitum	CD4 2DG 2-DG vs vehicle
CD4 TILs	100%	45%	30%	27%	27%	28%	30%	29%	26%	20%
CD8 TILs	20%	100%	13%	12%	15%	12%	13%	14%	12%	11%
Circ CD4 C26 vs NC26	20%	20%	100%	61%	35%	46%	38%	29%	21%	19%
Circ CD4 C26 vs PBS	21%	21%	66%	100%	40%	49%	45%	30%	24%	22%
Circ CD4 NC26 vs PBS	3%	3%	5%	6%	100%	3%	3%	10%	3%	2%
Circ CD8 C26 vs NC26	22%	21%	53%	53%	25%	100%	59%	32%	24%	21%
Circ CD8 C26 vs PBS	28%	27%	54%	58%	28%	72%	100%	49%	30%	27%
Circ CD8 NC26 vs PBS	3%	4%	5%	5%	12%	5%	6%	100%	4%	4%
CD4 Fast	11%	11%	13%	14%	13%	13%	13%	13%	100%	19%
CD4 2DG	5%	6%	7%	7%	5%	7%	7%	9%	11%	100%

A similar pattern was also observed when significantly regulated canonical pathways or upstream regulators, identified by IPA, were compared between datasets from cachectic T cells and 2-DG treated or fasted animals (Table 5). In line with the DEG data, these comparisons revealed a low percentual overlap of canonical pathways (Table 5A) or upstream regulators (Table 5B), as indicated by red color coding. Interestingly, all analyses showed also very little overlap between the NC26 *vs.* PBS data set compared to the other data sets from cachectic animals, implying only a minor overlap between DEGs, canonical pathways and upstream regulators, being altered between NC26 *vs*. PBS and all other datasets including cachectic mice, strengthening the reliability of this type of analysis.

Table 5. T cell impairment in cachexia cannot be mimicked by fasting or 2-DG treatment based on canonical pathway or upstream regulator analysis using IPA. (A) Overlapping canonical pathways and **(B)** upstream regulators, as identified by IPA analysis, between two RNA sequencing data sets were assessed, independent of the type of their regulation (up- or downregulated). The count of overlapping canonical pathways was identified and normalized to the number of total DEGs of each of the two data sets, respectively. The table shows the overall overlap in percentage, normalized to the dataset defining the column. The color code indicates high overlap in green and low overlap in red.

A	CD4 TILs NC26 vs C26	CD8 TILs NC26 vs C26	Circ CD4 C26 vs NC26	Circ CD4 C26 vs PBS	Circ CD4 NC26 vs PBS	Circ CD8 C26 vs NC26	Circ CD8 C26 vs PBS	Circ CD8 NC26 vs PBS	CD4 Fast Fast vs ad libitum	CD4 2DG 2-DG vs vehicle
CD4 TILs	100 %	97 %	96 %	96 %	99 %	96 %	94 %	99 %	98 %	98 %
CD8 TILs	89 %	100 %	90 %	89 %	97 %	89 %	88 %	95 %	93 %	97 %
Circ CD4 C26 vs NC26	91 %	94 %	100 %	97 %	98 %	94 %	90 %	99 %	94 %	94 %
Circ CD4 C26 vs PBS	91 %	93 %	97 %	100 %	99 %	94 %	91 %	99 %	95 %	94 %
Circ CD4 NC26 vs PBS	67 %	72 %	70 %	70 %	100 %	69 %	66 %	89 %	74 %	80 %
Circ CD8 C26 vs NC26	92 %	94 %	96 %	95 %	99 %	100 %	93 %	98 %	94 %	95 %
Circ CD8 C26 vs PBS	95 %	97 %	96 %	96 %	99 %	98 %	100 %	99 %	97 %	99 %
Circ CD8 NC26 vs PBS	67 %	70 %	70 %	70 %	89 %	69 %	66 %	100 %	74 %	79 %
CD4 Fast	87 %	90 %	88 %	88 %	97 %	87 %	86 %	97 %	100 %	94 %
CD4 2DG	71 %	78 %	72 %	72 %	86 %	72 %	71 %	85 %	77 %	100 %

B	CD4 TILs NC26 vs C26	CD8 TILs NC26 vs C26	Circ CD4 C26 vs NC26	Circ CD4 C26 vs PBS	Circ CD4 NC26 vs PBS	Circ CD8 C26 vs NC26	Circ CD8 C26 vs PBS	Circ CD8 NC26 vs PBS	CD4 Fast Fast vs ad libitum	CD4 2DG 2-DG vs vehicle
CD4 TILs	100 %	48 %	47 %	48 %	37 %	49 %	48 %	42 %	59 %	46 %
CD8 TILs	59 %	100 %	52 %	52 %	45 %	53 %	51 %	46 %	59 %	16 %
Circ CD4 C26 vs NC26	64 %	58 %	100 %	78 %	51 %	76 %	69 %	55 %	70 %	61 %
Circ CD4 C26 vs PBS	63 %	56 %	74 %	100 %	51 %	74 %	68 %	54 %	69 %	57 %
Circ CD4 NC26 vs PBS	50 %	50 %	50 %	53 %	100 %	49 %	48 %	56 %	54 %	42 %
Circ CD8 C26 vs NC26	57 %	51 %	65 %	66 %	43 %	100 %	68 %	48 %	62 %	54 %
Circ CD8 C26 vs PBS	66 %	57 %	69 %	72 %	50 %	80 %	100 %	57 %	70 %	55 %
Circ CD8 NC26 vs PBS	46 %	42 %	44 %	46 %	46 %	45 %	45 %	100 %	45 %	38 %
CD4 Fast	31 %	25 %	27 %	28 %	21 %	28 %	27 %	21 %	100 %	29 %
CD4 2DG	16 %	4 %	16 %	15 %	11 %	16 %	14 %	12 %	19 %	100 %

Overall, both anorexia and fasting are likely not drivers of T cell dysfunction in cancer cachexia.

2.11 Immune phenotyping of cancer patients

In order to verify the results in our mouse models, we initiated a collaboration with Dr. Olga Prokopchuk, who kindly provides us with whole human blood samples from cachectic and weight stable cancer patients. To this end, I analyzed different immune subsets by isolating peripheral blood mononuclear cells (PBMCs) using flow cytometry. As we were unsure if different tumor cell types would increase the variability of the data too much, I firstly compared samples from patients suffering from colorectal (n=3) and pancreatic (n=3) cancer regarding their immune profiles (Figure 91 and Figure 92). All patients from the colorectal cancer group remained weight stable, while one patient suffering from pancreatic cancer developed 10% bodyweight loss (see patient characteristics in Table 6). There were marked differences between colorectal and pancreatic cancer patients, such as an age difference of about 20 years between the two groups. Regarding serum parameters, cholesterol and triglycerides were strongly increased in pancreatic compared to colon cancer patients, with the cachectic pancreatic cancer patient having the lowest cholesterol (160 mg/dL *versus* 200 mg/dL as lowest value in the colon cancer group) and triglyceride level (113 mg/dL in cachectic sample *versus* 495 mg/dL as highest level in pancreatic cancer group). HDL levels were decreased a lot in pancreatic cancer patients compared to colon cancer patients, with the cachectic patient displaying the highest level (56 mg/dL versus 14 mg/dL as lowest level in pancreatic cancer group). LDL plasma levels were similar between the two groups, but with a very high variability in the pancreatic cancer group and with a very low value in the cachectic patient (87 mg/dL). This reduction in LDL upon cachexia was in line with the strong decrease in LDL that we have observed in all of our mouse models and already other cachectic patient cohorts (Geppert, 2021; Morigny&Zuber, 2020).

Table 6. Human clinical data. Data are mean ± s.e.m.

Clinical parameters	Colorectal cancer patients	Pancreatic cancer patients
Overall number (n)	3	3
Female/ Male (n)	3/0	½
Age (years)	41.33 ± 7.97	62.33 ± 5.93
Weight stable/ cachexia (% weight loss)	3 (0%) / 0	2 (0%) / 1 (10%)
Serum Parameters		
Albumin (g/dL)	4.70 ± 0.21	4.23 ±0.19
Cholesterol (mg/dL)	201.0 ± 1.0	284.7 ± 83.41
HDL (mg/dL)	71.50 ± 11.50	39.0 ± 12.77
LDL (mg/dL)	116.0 ± 8.0	125.5 ± 38.5
Triglycerides (mg/dL)	120.0 ± 34	264.3 ± 117.2

Using flow cytometry, I established a protocol to assess distribution and functionality of different immune cell subtypes, including B cells, dendritic cells (DCs), natural killer (NK) cells, monocytes and T cells. In this context, B cells and Plasmablasts, as well as different memory B cell subsets, were quite similar between the two cancer groups, while the cachectic patient seemed to have an increase in B cells, especially conventional B cells (Figure 91A, B). Monocytes were unchanged between the two different cancer groups, with a slight tendency for increased levels of classical monocytes, while non-classical monocytes were slightly decreased in pancreatic cancer samples (Figure 91C, D). The percentage of dendritic cells seemed to be higher in pancreatic cancer patients compared to colorectal cancer patients, while NK cells were mostly similar between the two groups (Figure 91C). Flow cytometry gating strategies of all immune subtypes can be found in Table 7.
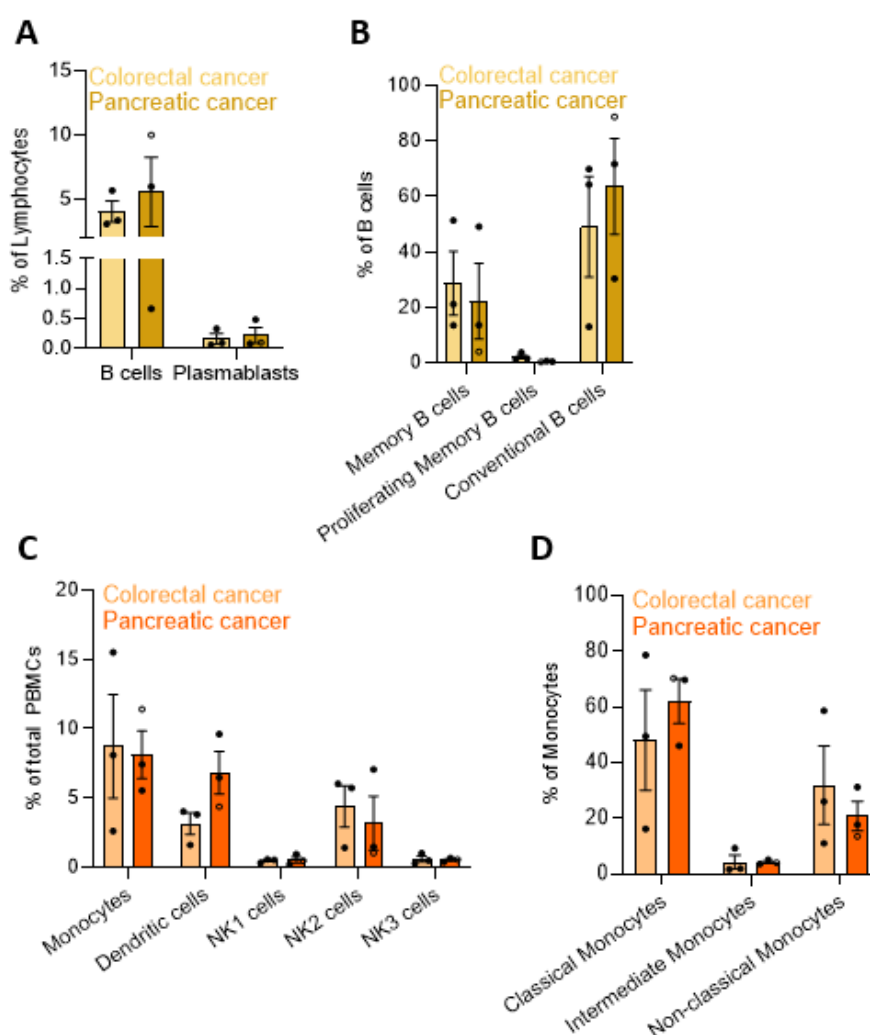
Figure 91. Phenotyping of immune cell subtypes in cachectic cancer patients with two different tumor subtypes with and without weight loss. Patient numbers and metadata are shown in Table 6. **(A)** Percentage of B cells and Plasmablasts of all lymphocytes. **(B)** Analysis of B cell subtypes, including memory B cells, proliferating memory B cells, and conventional B cells, displayed as percentage of B cells. **(C)** Percentage of monocytes, dendritic cells, and natural killer (NK) cells. **(D)** Analysis of monocyte subtypes, including classical, intermediate, and non-classical monocytes. Data are mean ± s.e.m.

Table 7. Flow cytometry gating strategy.

PBMC subtype	Gating
B cells	CD3-CD14-CD19+CD20+
Memory B cells	CD3-CD14-CD19+CD20+IgD-CD27+
Proliferating Memory B cells	CD3-CD14-CD19+CD20+IgD-CD27+KI67+
Conventional B cells	CD3-CD14-CD19+CD20+IgD+CD27-
Plasmablasts	CD3-CD14-CD19+CD20lo/-CD27+CD38+
Monocytes	CD3-CD19-CD20-FSChi SSChi
Classical Monocytes	CD3- CD19- CD20- FSChi SSChi CD14+ CD16-
Intermediate Monocytes	CD3- CD19- CD20- FSChi SSChi CD14+ CD16+
Non-classical Monocytes	CD3- CD19- CD20- FSChi SSChi CD14- CD16+
Dendritic cells	CD3-CD19-CD20-FSClo SSClo CD56- CD16-
NK1 cells	CD3-CD19-CD20-FSClo SSClo CD56+CD16-
NK2 cells	CD3-CD19-CD20-FSClo SSClo CD56+CD16+
NK3 cells	CD3-CD19-CD20-FSClo SSClo CD56-CD16+
CD4+ T cells	CD3+ CD4+ CD8-
Naïve CD4+ T cells	CD3+ CD4+ CD8- CCR7+ CD45RA+ CD28+
Activated CD4+ T cells	CD3+ CD4+ CD8- CD38 + HLA-DR+
Tregs	CD3+ CD4+ CD8- CD127lo CD25hi FoxP3+
Th1 cells	CD3+ CD4+ CD8- CD127+ CD45RA- CXCR5- CCR6- CCR4- CXCR3+
Th2 cells	CD3+ CD4+ CD8- CD127+ CD45RA- CXCR5- CCR6- CCR4+ CXCR3-
Th17 cells	CD3+ CD4+ CD8- CD127+ CD45RA- CXCR5- CCR6+ CXCR3- CCR4+
Tfh1 cells	CD3+ CD4+ CXCR5+ CXCR3+ CCR6-
Tfh2 cells	CD3+ CD4+ CXCR5+ CXCR3- CCR6-
Tfh17 cells	CD3+ CD4+ CXCR5+ CXCR3- CCR6+
CD4+ Central Memory (CM)	CD3+ CD4+ CD8- CCR7+ CD45RA-
CD4+ Temra (Terminal effector)	CD3+ CD4+ CD8- CCR7- CD45RA+ CD28lo/-
CD4+ Tem	CD3+ CD4+ CD8- CCR7- CD45RA- CD28+
CD8+ T cells	CD3+ CD8+ CD4-
Naïve CD8+	CD3+ CD8+ CD4- CD28+ CCR7+ CD45RA+ CD28+
Activated CD8+	CD3+ CD8+ CD4- CD38+ HLA-DR+
CD8+ central memory (CM)	CD3+ CD8+ CD4- CCR7+ CD45RA-
CD8+ Temra	CD3+ CD8+ CD4- CCR7- CD28- CD45RA+
CD8+ Tem	CD3+ CD8+ CD4- CCR7- CD28- CD45RA-

When comparing different T cell subtypes in colorectal and pancreatic cancer patients, I found some parameters being very consistent, while others were strongly altered between the two cancer types (Figure 92). Especially cytokine expression after stimulation seemed to be increased in CD8$^+$ T cells of pancreatic cancer patients, while it was more similar between the two groups in CD4$^+$ T cells (Figure 92A, B). Regarding helper T (Th) cells, I observed an increased percentage of Th1 cells in pancreatic cancer patients compared to colorectal cancer patients, while the other Th cell subtypes, such as Th2 or Th17 cells were similar (Figure 92C). Interestingly, follicular helper T cells tended to be affected by the cancer type, as Tfh1 cells tended to be decreased, while Tfh17 cells seemed to be increased in pancreatic compared to colorectal cancer patients. The general subtype composition of T cells, meaning the percentage of CD4$^+$, CD8$^+$ and regulatory T cells, was mostly similar between the two groups (Figure 92D). Other differences included less KI67$^+$ and naïve T cells in the samples from pancreatic cancer patients, while central memory (CM) cells tended to be increased, all irrespective of cachexia development (Figure 92E, F, G).

Overall, the human samples showed a quite high variability, especially between the two tumor types. Thus, for future investigations, I would suggest deciding on one tumor cell type and rather focus on a weight stable and cachectic group. Importantly, based on the so-far analyzed samples, the cachectic patient displayed a reduced percentage of CD8$^+$ and activated CD8$^+$ T cells compared to weight-stable pancreatic cancer patients, underlining the great translatability of the murine data and the impaired T cell function in cancer cachexia. More samples need to be analyzed in the future to verify these results.
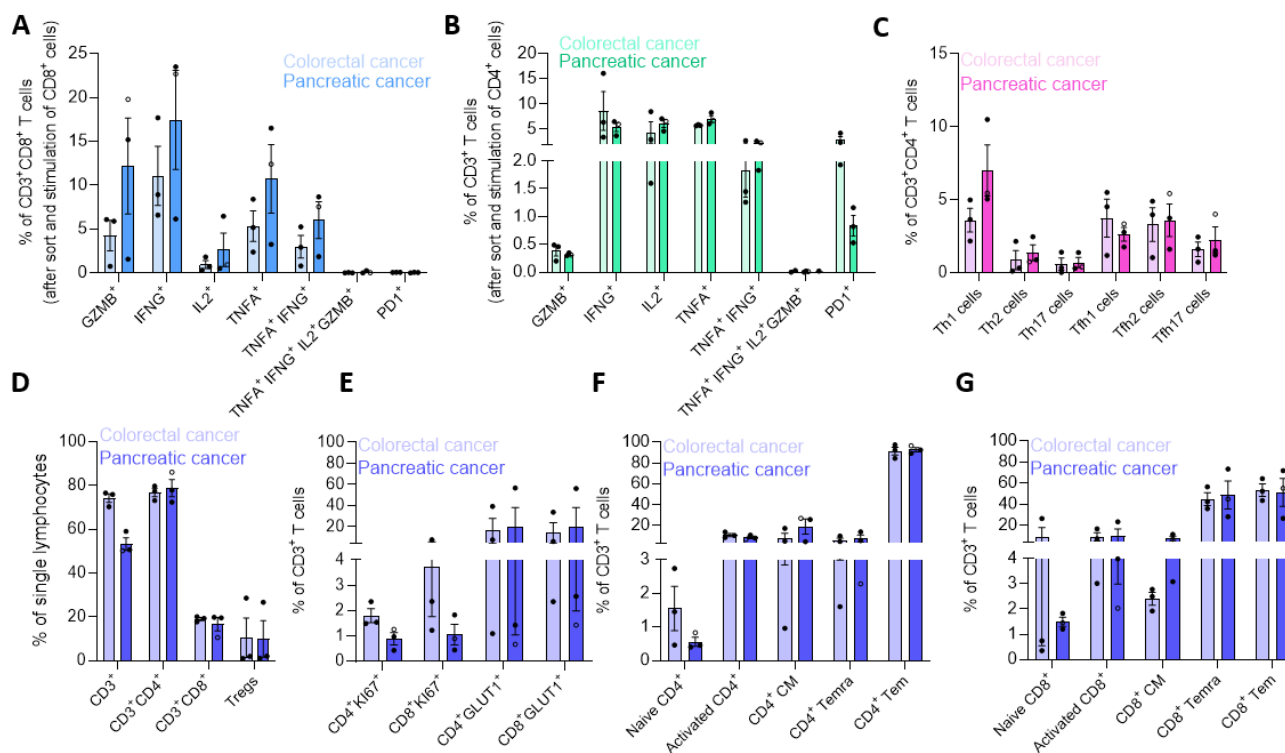
Figure 92. T cell phenotyping in human PBMCs from colorectal and pancreatic cancer patients with and without weight loss. Patient numbers and metadata are shown in Table 6. Analyses from the cachectic patient sample are displayed using an empty circle. **(A)** CD8$^+$ T cell effector function as assessed by cytokine (GZMB, IFNG, IL2, TNFA) and PD1 expression after PMA/Ionomycin stimulation. **(B)** Expression of same cytokines as in (A) in CD4$^+$ T cells after sort and stimulation by PMA/Ionomycin. **(C)** Helper T (Th) cell phenotyping, i.e. Th1, Th2, Th17 cells and follicular Th (Tfh) cells such as Tfh1, Tfh2 and Tfh17. **(D)** General T cell subtype assessment in PBMCs (CD3$^+$, CD4$^+$, CD8$^+$ and Tregs). **(E)** Percentage of proliferating and GLUT1-expressing T cells as % of CD3$^+$ T cells. **(F)** Percentage of CD4$^+$ T cell subtypes, including activated, central memory (CM), effector memory re-expressing CD45RA (Temra) T cells and effector memory (Tem) T cells. **(G)** Percentage of CD8$^+$ T cell subtypes such as activated, CM, Temra and Tem T cells. Data are mean ± s.e.m.

3   DISCUSSION

3.1   Cancer cachexia influences T cell proliferation and recruitment

Cancer cachexia is a multifactorial wasting disorder that is accompanied by drastic weight loss and poor overall survival (K. Fearon, 2011). Many of the negative effects mediated by cancer cachexia can be attributed to systemic inflammation, one of its most prominent hallmarks (Deans, 2005). In this context, several cytokines have already been associated with cachexia, including IL6 and TNFα. Nevertheless, therapeutic approaches, aiming to block these cytokines, were not or only in part capable to improve cancer-associated tissue wasting (Costelli, 1995; Hickish, 2017; Jatoi, 2010; Rupert, 2021). Thus, to date there is no efficient routine therapy available to counteract cachexia. Interestingly, chronic systemic inflammation – as it is present in cachectic mice and patients – has previously been linked to compromised immune cell function (Isomäki, 2001). Yet, only a small number of studies has investigated the link between the immune system and cachexia and thereby has suggested the involvement of several immune cell types in cachexia progression (Barker, 2020; Batista, 2016; Cuenca, 2014; Petruzzelli, 2022) (Flint, 2016; C. Zhao, 2008); however, there is a clear knowledge gap concerning the role of T cells in cancer cachexia. A recent report demonstrated a strong correlation between cancer cachexia and a reduced efficacy of immune checkpoint inhibitors in patients with advanced non-small cell lung cancer (Miyawaki, 2020), strengthening the close association between cachexia and the immune system. In this context, low numbers of tumor-infiltrating lymphocytes (TILs) were shown to be a limiting factor for immunotherapy (Zappasodi, 2018). In line with this, I observed reduced numbers of TILs in cachectic Colon26 (C26), or Lewis Lung Cancer (LLC) but not non-cachectic or pre-cachectic tumor-bearing mice. Moreover, these TIL numbers correlated significantly with the degree of wasting, strengthening the idea that cachexia onset strongly affects T cell presence. Reduced expression of the T cell marker *CD3* was also observed in tumor samples from weight-losing compared to weight-stable colon cancer patients, showing great translational potential from animal studies to clinical practice. In line with our data, Flint *et al.* have previously reported a reduction of TILs in cachectic C26 and pancreatic tumors, mediated by altered CXCR3 chemokine signaling (Flint, 2016). Indeed, I also observed a significant downregulation of chemokines that are associated with T cell migration into solid tumors (Kohli, 2022), such as *Ccl4*, *Cxcl9*, *Cxcl11* and *Cx3cl1*. Increased levels of all four of these chemokines have already been associated with better prognosis in colorectal cancer, a cancer type that is very susceptible to induce wasting; however, cachexia has not been assessed in these studies (Cao, 2021; Ohta, 2005; Shamoun, 2021; Z. Wu, 2016).

Moreover, reduced T cell infiltration into skeletal muscle and epididymal white adipose tissue, as well as a trend for decreased T cell numbers in spleen and lymph nodes suggested a link between cachexia and T cell lymphopenia in peripheral tissues, circulation and tumor. In line, strong positive correlations between muscle-infiltrating T cells and skeletal muscle mass were noted in cancer patients – independent of cachexia development (Anoveros-Barrera, 2019).

Intriguingly, also tissue-infiltration of macrophages, in line with (Inaba, 2018), and natural killer cells, seemed to be decreased in cachectic mice, implying not only T cell specific changes upon cancer-induced weight loss, but also a cachexia-mediated repression of the innate immune system.

Overall, the systemic depletion of T cells and other immune cell types indicates a strong decline of the immune system associated with cachexia, which likely contributes not only to worsened tumor but also cachexia outcome.

3.2   Cancer cachexia alters the circulating lipidome

Previous studies have extensively investigated the link between adipose tissue-infiltrating immune cells and their potential contribution to metabolic dysfunction (Mauro, 2012; Rocha, 2009). In this context, Han *et al.* have shown that a pathogen-dependent increase of immune cells in WAT suppresses pathways linked to lipid metabolism, thereby altering the physiological metabolic adipose tissue function (S. J. Han, 2017). In this context, we hypothesized that the cachexia-dependent reduction of WAT-infiltrating T cells might induce changes in adipose tissue lipid metabolism, thereby altering the cachectic plasma lipidome. Indeed, alterations in the quality of free fatty acids (FFA) and reduced plasma levels of lysophosphatidylcholine (LPC) have previously been associated with cachexia onset in patients and mice (Cala, 2018; Riccardi, 2020; L. A. Taylor, 2007), but a detailed and broad lipidomic screen comparing different mouse models of cachexia and cachectic and weight-stable cancer patients was still missing until our publication (Morigny&Zuber, 2020). We found marked alterations of the plasma lipidome induced by cancer cachexia, with a strong reduction in LPCs and an increase in sphingolipids, including ceramides (CERs), hexosyl-ceramides (HCERs) and sphingomyelins (SMs). These changes were also confirmed in human weight-losing cancer patients. In addition, we found eight lipid species with consistent regulation in the different mouse experiments and cachectic cancer patients, namely SM(16:0), SM(24:1), CER(16:0),CER(24:1), HCER(16:0), and HCER(24:1) being upregulated and LPC(16:1) and LPC(20:3) being downregulated upon wasting. Importantly, there were close correlations between the circulating levels of these eight lipid species with body wasting in mice and humans, again implying great translational potential and even more important, their possible link and contribution to cancer-associated wasting.

Strengthening our results, a reduction in several LPC species, including LPC(20:3), has been previously associated with cancer-induced wasting (Cala, 2018; L. A. Taylor, 2007) and sepsis, a disease which is prone to be accompanied by cachexia (Drobnik, 2003). Notably, low plasma LPC species, especially LPC(16:1) and LPC(20:3), both also being strongly decreased upon cancer cachexia, have previously been linked to reduced mitochondrial oxidative capacity in skeletal muscle of adults (Semba, 2019), a process also being dysregulated in cachectic mice (Carson, 2016). LPCs are an important energy source for solid tumors, which hydrolyze LPCs with high activity, and subsequently take up remaining free fatty acids for energy supply (Raynor, 2015). In T cells, uptake of LPC species was reported to be essential for the evolvement of memory CD8^{+} T cells (Piccirillo, 2019), a T cell subtype whose presence positively correlates with disease outcome in a variety of cancer types, including non-small cell lung cancer (Djenidi, 2015), breast cancer (Egelston, 2019; Savas, 2018), and melanomas (Edwards, 2018). Additionally, LPCs have chemoattractant properties for T cells, mediated through G2A receptor expression on lymphocytes (Radu, 2004). Hypothetically, extensive LPC hydrolysis by cachectic tumors could decrease the amount of LPCs not only in the circulation but also in the tumor microenvironment (TME), leading to impaired memory CD8^{+} T cell formation and reduced chemoattraction of immune cells to cachectic tumors, in line with the observed decrease of TILs in cachectic mice. Hence, a reduction of LPC levels not only likely accelerates tissue wasting by reducing mitochondrial oxidative capacity, but also might have detrimental effects on the immune system, leading to an impaired anti-tumor T cell response.

We have observed a consistent increase of plasma sphingolipids, most importantly CERs, in cachectic mice and cancer patients, in line with the identification of six commonly upregulated sphingolipid species. Strikingly, the progressive changes from a weight-stable tumor-bearing condition to late-stage cachexia, was accompanied by a gradual increase in these lipid species, supporting the use of

sphingolipids as potential biomarkers in cancer cachexia. In line, sphingolipids including ceramides have recently been proposed as valuable biomarkers in different cancer types, including ovarian cancer and advanced stage colorectal cancer, both being very prone to induce cachexia, as well as other diseases such as type 2 diabetes, cardiovascular diseases and sepsis (Kurz, 2019; Matanes, 2019; Pakiet, 2019). In breast cancer patients, high tumor expression of enzymes involved in ceramide metabolism has already been linked to worsened disease outcome, but although breast cancer has been associated with cachexia in the past (Q. Wu, 2019), weight loss was not investigated in this report (Moro, 2018). In our study, we highlighted different mechanisms describing how increased CER levels might contribute to cancer-induced wasting (Morigny&Zuber, 2020). In detail, by promoting lipid uptake and hepatic steatosis (Chaurasia, 2019; J. Y. Xia, 2015), CERs might in part contribute to the development of liver steatosis in cachexia (Berriel Diaz, 2008). Second, elevated synthesis and degradation of CERs in the liver, as assessed by increased gene expression of CER-related enzymes, might induce a highly energy-demanding futile cycle, wasting a large proportion of energy, thereby contributing to cachexia. Moreover, in obesity, liver-derived CERs strongly contribute to the development of insulin resistance (Chaurasia, 2019; J. Y. Xia, 2015). Through direct activation of protein phosphatase 2A and atypical protein kinase Cζ, CERs were demonstrated to prevent AKT membrane translocation and activation due to inhibitory phosphorylation, thereby inducing insulin resistance in several metabolic organs including liver, skeletal muscle and adipose tissue (Aburasayn, 2016; Lipina, 2017). In addition, HCERs and LCERs are precursors of a class called gangliosides, which can directly impair insulin receptor function (Lipina, 2015, 2017). Hence, increased levels of circulating ceramides but also their accumulation in tissues could potentially mediate insulin resistance upon cancer cachexia, a phenomenon that has been associated with cancer-induced wasting in mice and humans in the past (Masi, 2021). In line, CER-treatment of L6 myotubes induced atrophy *in vitro*, and *in vivo* treatment of C26-injected mice with the *de novo* CER synthesis pathway inhibitor myriocin, partially inhibited the cachexia-dependent increase of atrophy markers and muscle wasting (De Larichaudy, 2012), suggesting the possible contribution of CERs to muscle wasting in cancer cachexia.

With respect to T cells, gangliosides have been demonstrated to be present at high levels in the TME (Bernhard, 1989) and display immunosuppressive properties, including promotion of T cell apoptosis (Biswas, 2009), as well as inhibition of cytotoxic CD8^{+} T cell function (H. C. Lee, 2012), T cell proliferation (Ladisch, 1983) and cytokine production (Rayman, 2004). Hence, potentially elevated levels of gangliosides in the circulation but also in the TME could in part mediate T cell dysfunction in cachexia. However, the unaltered rate of apoptotic TILs in cachectic tumors suggests that a more complex mechanism, probably involving additional factors, mediates T cell impairment upon cachexia.

Initially, we hypothesized that altered adipose tissue-infiltration by T cells would lead to changes in the cachectic lipidome. Since we saw this marked rise in sphingolipids, we investigated the expression of enzymes related to different ceramide pathways in several metabolic tissues including skeletal muscle, adipose tissue, liver and tumor. Contrary to our hypothesis, we did not observe an increase, but either unaltered or even decreased gene expression levels of these enzymes in white adipose tissue, skeletal muscle and tumor. In contrast, strong expressional changes were present in the liver, including a marked upregulation of enzymes of CER synthesis pathways. Hence, liver seems to be the main contributor to increased CER levels upon cachexia. Of note, expression of CER-associated enzymes was not uniformly altered in splenic and tumor-infiltrating T cells, suggesting that T cell-intrinsic CER synthesis was not altered by cachexia onset.

3.3   T cell repression aggravates cancer cachexia

Glucose metabolism is dampened in cachectic T cells

Using a broad lipidomic screen, we found prominent alterations of the cachectic plasma lipidome, including changed levels of free fatty acids (FFAs) and sphingolipids (Morigny&Zuber, 2020). With regard to T cells, sphingomyelin and ceramides have previously been linked to T cell dysfunction in cancer (Tallima, 2021; Vaena, 2021), and also elevated uptake of long chain fatty acids and oxidized low density lipoprotein (oxLDL), mediated by CD36, have shown to dampen T cell function (Endemann, 1993; Manzo, 2020; Xu, 2021). Indeed, in line with other studies (Ma, 2021; Xu, 2021), I found a tumor-dependent upregulation of *Cd36* in CD8^{+} T cells. Furthermore, expression of *Cpt1a* (Carnitine palmitoyltransferase 1A), which is the limiting and rate-controlling factor for long chain fatty acid oxidation within mitochondria (Raud, 2018), was upregulated in a tumor-dependent manner, together indicating that the overall increase in fatty acid metabolism is rather tumor-dependent and not cachexia-specific.

To meet their demands during activation, T cells rapidly switch their metabolism to aerobic glycolysis – similar to the Warburg effect – by activating pyruvate dehydrogenase kinase 1 (PDHK1) downstream of the T cell receptor (TCR), which blocks mitochondrial import of pyruvate and thereby promotes its conversion to lactate through lactate dehydrogenase (LDHA). In line, T cell stimulation acutely initiates a decrease in oxidative phosphorylation (OXPHOS), while simultaneously increasing avid glycolysis despite ample oxygen supply (Bental, 1993). This switch was shown to be independent of glucose uptake and has above all the purpose to support rapid cytokine synthesis to immediately eliminate identified targets (Menk, 2018; Peng, 2016). Contrary, on the long-term (hours to days), T cells increase their glucose uptake through upregulation of glucose transporter 1 (GLUT1) to meet their high energy demands upon expansion (Frauwirth, 2002; Menk, 2018), and in line, remain high OXPHOS and glycolysis levels to sustain rapid proliferation (Frauwirth, 2002; Sena, 2013).

In cachectic T cells, I observed a decreased expression of *Slc2a1* (Solute Carrier Family 2 Member 1), encoding the main glucose transporter GLUT1 of T lymphocytes (Cretenet, 2016), while *Ldha* expression was markedly increased in a tumor-dependent manner. Hence, short-term effector function of T cells is likely still functional, while on the long-term glucose supply might be the limiting factor for an effective T cell expansion, possibly leading to insufficient proliferation and dampened effector function in cachexia. In line, cachexia development induced a decrease in the glycolysis rate and oxygen consumption rate (OCR) of CD8^{+} T cells, with a tendency for a reduced basal and maximal respiration compared to T cells from non-cachectic tumor-bearing and control mice in different cachexia mouse models. Upon pre-cachexia, CD8^{+} T cells tended to have an enhanced metabolic response compared to T cells from cachectic mice, as they showed a trend for an elevated basal respiration and less reduction of glycolysis, underlining the gradual transition from a functional to a repressed T cell state induced by cachexia progression. Importantly, *Slc2a1* expression was elevated in T cells from non-cachectic C26 mice compared to PBS mice, implying sufficient glucose uptake of still non-cachectic T cells, thereby probably meeting all energy demands of the cell. However, neither OXPHOS levels nor glycolysis were elevated in CD8^{+} T cells from non-cachectic C26 and NC26 mice, implying that despite marked upregulation of several enzymes related to metabolism (*Ldha, Abca1, Cpt1α, Slc2a1*), T cell activation by the tumor was not present on the metabolic level. In non-cachectic C26 and short NC26 mice, this might be due to the early sacrifice seven days post tumor cell injection, thereby giving the T cell response not the amount of time it needed to properly develop, while it also could be in general a result of the method itself, as all Seahorse measurements showed a high

variability. Nevertheless, T cell metabolism seems to adapt a dysfunctional state as cachexia progresses, which is most likely also linked to an impaired effector function. Strikingly, reduced metabolism in cachectic T cells was revoked upon overnight stimulation, indicating that cachectic T cells do not suffer from an intrinsic stimulation/metabolism defect per se, but rather an immunosuppressive or nutrient depleted environment must be the underlying cause for the defective T cell metabolism upon cachexia.

Interestingly, throughout all of my experiments, cachectic mice of different models and strains displayed a significant reduction in circulating glucose levels, in accordance with other studies (Cui, 2019; O'Connell, 2021). Importantly, of all circulating parameters assessed, T cell numbers in cachectic tumors, but also the circulation (data not shown) correlated the most strongly with circulating glucose levels. In addition, spatial metabolomics revealed a strong and highly significant enrichment of hexose (including glucose) in the vital parts of C26, but not NC26, tumors, indicating a higher glucose demand of cachexia-inducing tumors compared to non-cachexia-inducing tumors. Hence, further investigations (i.e. by using labelled glucose derivatives to determine T cell-specific glucose uptake) should be made to identify whether this central and local glucose deprivation leads to reduced glucose uptake in cachectic T cells (also implied by reduced *Slc2a1* expression), thereby potentially leading to impaired T cell metabolism and worsened disease outcomes.

Of note, glucose starvation was reported to induce metabolic reprogramming of effector T cells by upregulation of genes associated with glutamine uptake (e.g. *Snat1, Snat2*) and glutaminolysis (i.e. *Gls*) for sufficient adenosine triphosphate (ATP) production (Blagih, 2015). However, *Snat1* and *Snat2* were not regulated in cachectic T cells, while *Gls* was downregulated upon cachexia, indicating decreased glutaminolysis (data not shown). Hence, additional repressive mechanisms must mediate dampening of T cell function.

Cachexia is associated with repressed signaling of T cell activation and effector function pathways

In T cells, metabolism and function are tightly coupled (Blachère, 2006; Chang, 2013). Accordingly, induction of aerobic glycolysis upon antigen stimulation is required for the expression of nuclear factor of activated T cells (NFAT), an essential transcription factor for T cell activation (Cereghetti, 2008) and subsequently for the upregulation of important effector cytokines such as IFNγ (Kouidhi, 2017). Hence, an optimal nutrient environment in combination with functional signaling cascades downstream of the TCR and co-stimulatory receptors are of utmost importance for the development of a functional T cell (see Figure 5). Upon cachexia, functional impairments of T cell activation were highlighted by both ingenuity pathway analysis and Kyoto Encyclopedia of Genes and Genomes (KEGG) pathway analysis of whole-transcriptome data from cachectic and non-cachectic T cells from tumor and spleen. Hereby, dampening of pathways related to T cell activation and effector function was linked to cachexia onset, with almost all of the top regulated pathways being downregulated in both CD4+ and CD8+ T cells from spleen and tumor of cachectic C26 *vs.* NC26 mice, implying strong T cell repression in cachexia. In detail, decreased activation and effector function pathways included PI3K/AKT signaling, JAK/STAT signaling, NFκB signaling, CD28 signaling, T cell receptor (TCR) signaling, and interferon signaling, while STAT3 signaling was the only one being increased in cachectic CD8+ TILs. However, STAT3 has already been associated with impaired T cell function, and its ablation from adoptively transferred CD8+ T cells has previously been shown to improve T cell infiltration into tumors, proliferation and anti-tumor effector function (Kujawski, 2010). Accordingly, elevated STAT3 signaling in cachectic CD8+ TILs, could in part mediate reduced tumor infiltration, proliferation, and anti-tumor effector function, all of which I have previously observed upon cachexia.

The JAK/STAT pathway mediates signaling of specific cytokines from transmembrane receptors to the nucleus, where STAT dimers or higher-order tetramers bind to DNA and act as classical transcription factors (Villarino, 2015). Typical cytokines which induce JAK/STAT signaling include IL6, IFNγ and IL2 (Morris, 2018), which all have previously been associated with cancer cachexia (Noguchi, 1996). Contrary to my expectations, the marked systemic inflammation upon cancer cachexia, did not lead to elevated JAK/STAT signaling, but instead to a reduction, suggesting that immunosuppressive conditions must predominate TCR and cytokine signaling in T cells.

T cell activation requires two distinct signals, of which the first is mediated *via* the TCR, induced by antigen-major histocompatibility complex (MHC) stimulation, while the second signal is – in the case of CD4$^+$ T cells – induced by costimulatory receptors, such as the CD28 receptor (Figure 4) (Linsley, 1991; F. Xia, 2018). Downstream of TCR and CD28 signaling, NFκB becomes activated (Kane, 1999), and translocates into the nucleus, where it regulates a myriad of different factors and processes, including IL2 production (Los, 1995), T cell differentiation (Corn, 2003) and apoptosis (Kasibhatla, 1998). Its importance for T cell function becomes even clearer as NFκB blockage can prevent anti-tumor function of T cells by reducing effector cytokine production and cytotoxic ability, ultimately leading to insufficient tumor rejection (Barnes, 2015). Additionally to NFκB, NFAT, mediating Il2 expression (Blachère, 2006; Rooney, 1995), and mTOR as one of the key downstream targets of TCR or CD28/PI3K/AKT signaling (L. X. Wu, 2005), become activated. mTOR regulates several cellular processes in T cells, including cell cycle progression (Appleman, 2002), survival (L. X. Wu, 2005), differentiation (Delgoffe, 2011; K. Lee, 2010) and development of effector and memory T cells (Araki, 2009; Delgoffe, 2009). The overall reduction in the TCR/CD28 mediated signaling cascade, including PI3K/AKT/mTOR and NFκB repression in cachexia, highlights the detrimental effects cachexia has on T cells, leading to a marked repression with major impairments in the activation mechanism, metabolism, and effector functionality, such as dampened cytokine expression. In line, I also observed a reduced expression of several NFAT genes, including *Nfatc3* (data not shown) which is required for *Il2* gene expression and cell proliferation (Urso, 2011).

T cell effector function was also dampened on the molecular level by cachexia onset. Reduced expression of important effector cytokines, including *Il2, Tnfa, Gzmb* and *Ifnγ,* was specifically associated with cachexia in circulating and tumor-infiltrating T cells in different mouse models of cancer cachexia. Pre-cachectic C26, APC$^{Min/+}$ and LLC mice highlighted the gradual progression of cancer cachexia as they displayed intermediate stages between cachectic and control mice. However, not only defective TCR and CD28 signaling might have caused reduced expression of important T cell effector cytokines mediated through dampened NFAT and NFκB signaling, but also insufficient metabolic adaptations of T cells most likely mediated impaired T cell effector cytokine expression. In this context, upon antigen stimulation, the initiation of a metabolic switch towards increased aerobic glycolysis was noted to be of high importance for the rapid induction of cytokine synthesis by blocking the moonlighting function of LDHA, which connects metabolism and effector function in T cells. LDHA and in addition also GAPDH (glyceraldehyde-3-phosphate dehydrogenase) can regulate cytokine expression by binding to AU-rich elements within the 3' untranslated region (UTR) of cytokine transcripts, including those of *Il2* and *Ifnγ,* thereby inhibiting their translation. Hence, GAPDH and LDHA work as energy sensors connecting translation of inflammatory cytokines to glucose availability (Chang, 2013; Menk, 2018; Peng, 2016). Additionally, by preserving high levels of acetyl-coenzyme A to enhance histone acetylation, LDHA was shown to induce *Ifnγ* transcription, independent of binding to the 3' UTR of the IFNγ mRNA (Peng, 2016). Despite high *Ldha* expression in cachectic T cells, *Ifnγ* levels were decreased, probably due to the prominent glucose deprivation in cachectic mice which

engages LDHA rather in its prominent moonlighting function to repress *Ifnγ* translation, than in the aerobic glycolysis pathway, which would lead to the production of acetyl-coenzyme A. In the future, it would be interesting to assess the percentage of LDHA or GAPDH bound to *Ifnγ* or *Il2* transcripts in cachectic T cells using RNA immunoprecipitation.

An important study by Jacobs *et al.* has demonstrated that glucose availability and more importantly CD28-mediated glucose uptake limit T cell activation and subsequent effector cytokine expression. In detail, glucose was required to promote cell growth and induce IL2 production and proliferation upon stimulation despite the presence of other nutrients (Jacobs, 2008). Hence, strong local and systemic glucose deprivation in combination with decreased CD28 signaling, are likely mediators of dampened T cell proliferation and cytokine expression in cachexia. The anti-tumor activity of cytotoxic T lymphocytes (CTLs) is mediated *via* the secretion of cytotoxic granules, carrying perforin and granzymes, with the serine protease GZMB being the most important among them (Voskoboinik, 2015). Accordingly, GZMB expression positively correlated with improved survival in colorectal cancer patients (Prizment, 2017). In CD8$^+$ T cells, IL2 signaling was shown to strongly induce GZMB mRNA and protein expression (Janas, 2005). The strong downregulation of *Il2* expression in cachectic T cells, most likely resulted in a reduced autocrine re-stimulation (Ross, 2018), thereby dampening *Gzmb* expression, leading to impaired T cell effecter function (Janas, 2005).

In summary, cachexia induced a mild dampening of T cell metabolism, but a strong repression of TCR and co-stimulatory receptor signaling on the molecular level, leading to a marked reduction of effector cytokine expression, thereby potentially worsening T cell effector function and disease outcome.

In theory, impaired T cell activation and effector cytokine expression could be either mediated by defective antigen presentation and stimulation by APCs, an intrinsic defect impairing the T cell activation potential, or an intrinsic suppression of signaling pathways mediated by a repressive environment (nutrient deprivation, immunosuppressive components, etc.). However, reduced effector function in cachectic T cells was revoked upon *ex vivo* overnight stimulation, indicating that cachectic T cells did not suffer from an intrinsic stimulation/functional defect *per se.* Hence, rather defective antigen presentation by APCs or an immunosuppressive or nutrient depleted environment must have been the underlying cause for the alterations in T cell metabolism upon cachexia. *In vitro* treatment of T cells with tumor cell conditioned media highlighted that T cell repression was not mediated by tumor-secreted factors. To identify if defective antigen presentation might be the underlying cause for impaired T cell functionality, maturation of dendritic cells should be further investigated. To assess if nutrient depletion could induce the strong T cell impairment, *in vitro* studies could be applied treating T cells with plasma from cachectic and non-cachectic mice with or without T cell stimulation.

Cachectic T cells are neither classically exhausted nor fully senescent

Exhaustion is one of the best studied dysfunctional conditions in T cell biology. It describes a state in which T cells – as a response to chronic antigen stimulation – progressively lose their function. Several inhibitory pathways were shown to induce T cell suppression, of which PD1/PD-L1 (programmed cell death 1/ programmed death-ligand 1) signaling is the most important (Butte, 2007). Exhausted T cells show impaired activation, proliferation and effector cytokine expression (TNFα, IL2,IFNγ) (Wherry, 2015), all characteristics of a cachectic T cell. In the healthy state, inhibitory receptors are transiently expressed to regulate the strength of the immune response and prevent autoimmunity; upon cancer burden, however, prolonged and high expression of several inhibitory receptors is typical for T cell

exhaustion, as tumors use these T cell suppression pathways to escape immune surveillance (Wherry, 2015). Especially PD1/PD-L1 signaling has a potent function in the tumor microenvironment, as it dampens T cell activation, proliferation, and secretion of effector cytokines, thereby suppressing the anti-tumor T cell response (Figure 5) (Patsoukis, 2012; Shi, 2011). Hence, preventing the activation of these dysregulated pathways by targeting inhibitory receptors using blockade therapies, has been a revolutionary breakthrough in cancer immunotherapy. In this context, several immunological checkpoint inhibitors (ICIs) have been investigated to target PD1/PD-L1 signaling and in a notable number of cancer patients anti-PD1 has shown promising results (Colombo, 2021; Gandhi, 2018; Kelly, 2021; Motzer, 2015; Reck, 2016; Robert, 2015). Thus, it was a setback when Miyawaki *et al.* recently linked pre-treatment diagnosis of cancer cachexia to reduced efficacy of PD1/PD-L1 inhibitors in patients with advanced non-small cell lung cancer (Miyawaki, 2020). Interestingly, based on RNA sequencing data, PD1/PD-L1 signaling was strongly reduced in CD8^{+} TILs from cachectic mice. This unexpected reduction of inhibitory signaling is at first sight contrary to the observed T cell repression in cachexia, but at second glance is in line with Miyawaki *et al.* (Miyawaki, 2020) as it implies that unchanged PD1/PD-L1 signaling is not the underlying cause for T cell repression in cachexia, and thus also targeting of this pathway is predetermined to fail. Accordingly, the expression of target genes such as PD1 and their complementary receptors in tumor has been associated with the efficacy of ICI therapy (Taube, 2014). Of note, PD1 expression in splenic T cells tended to be increased upon C26 injection, while it was unchanged in LLC or APC[Min/+] mice. However, a recent study has identified that only numbers of intra-tumoral, but not circulating CD8^{+} T cells can predict treatment outcomes of ICI therapy in cancer patients (F. Li, 2021), indicating that presence and functionality of tumor-infiltrating T cells predominates over circulating T cells. Hence, the cachexia-associated failure of ICI therapy – despite increased PD1 expression in splenic T cells – is likely to be dependent on reduced intra-tumoral numbers of T cells with reduced PD1/PD-L1 signaling, while systemic lymphopenia of cachectic mice and probably also patients might in addition promote failure. Another explanation for the failure of ICI therapy in cachectic patients was demonstrated by Castillo and colleagues who showed that increased catabolic clearance of monoclonal antibodies, observed in cachectic mice and patients might dampen the efficacy of ICI therapy (Castillo, 2021; D. C. Turner, 2018).

In line, in a comparison of the global gene signature and phenotype of cachectic T cells with a set of markers that were specific for either exhausted or senescent T cells (Y. Zhao, 2020), cachectic T lymphocytes neither displayed a classically exhausted nor fully senescent state, meaning that cachexia is not clearly linked to exhaustion nor senescence and hence, further repressive mechanisms must interfere mediating the overall loss of functionality. However, based on the many promising studies using ICI therapy to boost T cell functionality, it is of utmost importance to improve T cell effector function to attenuate disease outcome. The lack of PD1/PD-L1 signaling suggests that other suppressive mechanisms predominate in cachexia, and their identification might be crucial for future therapeutic strategies.

CD8^{+} T cell depletion aggravates cancer-associated wasting
To unravel the direct causal relationship between cancer cachexia and T cell dampening, I injected mice with cachexia-inducing C26 tumor cells and depleted CD4^{+} and CD8^{+} T cells alone or in combination from peripheral tissues, circulation and the tumor using antibodies. Absence of CD8^{+} T cells, alone or in combination with CD4^{+} cells, accelerated weight loss and cachexia development, and shortened survival of the mice. In line, weight of metabolic tissues such as iWAT, eWAT and GC

was strongly decreased in $CD8^+$ and $CD4^+/CD8^+$ depleted mice, with increased expression of atrophy markers and altered lipolysis marker expression. Importantly, tumor growth and size were not altered. In contrast, $CD4^+$ depleted mice showed slower cachexia development, but also significantly reduced tumor growth due to a compensatory effect of cytotoxic $CD8^+$ T cells in response to $CD4^+$ Treg depletion (X. Li, 2010; Yu, 2005). However, postponing anti-CD4 injections to a later time point, when tumors were already bigger in size, led to similar tumor growth in $CD4^+$ depleted mice, and similar cachexia development compared to the isotype control group. Hence, despite similar tumor sizes, absence of $CD8^+$ T cells had detrimental effects on cachexia outcome, while $CD4^+$ T cell depletion had no influence on disease outcome.

Zhao *et al.* have previously noted a marked reduction of a specific $CD4^+$ T cell subpopulation that has a very low expression of CD44 and a high expression of CD62L, namely $CD4^+CD44^{v.low}$ T cells, in non-obese diabetic mice that developed cachexia (C. Zhao, 2008). The group also verified the cachexia-specific depletion of $CD4^+CD4^{v.low}$ cells in a classical cancer cachexia model using LL2 implantation (Z. Wang, 2008). Supplementation of $CD4^+CD44^{v.low}$, but not $CD4^+$ T cells that were depleted of $CD44^{v.low}$, delayed disease onset and attenuated wasting. However, in their study, Wang *et al.* have not addressed effects of the treatment on tumor size, tissue-infiltration of T cells or the $CD8^+$ T cell subset (Z. Wang, 2008). Mechanistically, $CD4^+CD44^{v.low}$ T cells were shown to counteract lymphopenia by maintaining a large $CD4^+$ T cell pool with balanced numbers of naïve, memory and regulatory T cells (Z. Wang, 2008; C. Zhao, 2015). Overall, the authors claim an association between lymphopenia and cachexia, as they demonstrated that protection from lymphopenia by increasing the $CD4^+CD44^{v.low}$ population is linked to an attenuation of cachexia. However, in the present work $CD4^+$ T cell depletion did not worsen cachexia outcome in the C26 model; instead, absence of $CD8^+$ T cells, alone or in combination, accelerated weight loss. Hence, the presence of $CD8^+$ T cells seems to be favorable for disease outcome. In line, the positive outcome in $CD4^+$ T cell depleted mice may be attributed to a compensatory increase of $CD8^+$ T cells, which are under normal circumstance being partially inhibited by $CD4^+$ Tregs. Therefore, $CD8^+$ lymphopenia - as observed in cachexia - might be a crucial determinant contributing to wasting. Accordingly, cachexia can be also induced in immunodeficient nude and SCID (severe combined immune deficiency) mice, highlighting that T cell presence is not required for disease development (Murray, 1997; Yasumoto, 1995). Importantly, high circulating cytokine levels in SCID mice were linked to cachexia onset, underlining that T cells do not contribute to elevated cytokines in cachexia (Murray, 1997), as implied by the decreased T cell effector cytokine expression presented in this work.

Interestingly, in virus-associated cachexia, $CD8^+$ T cells were recently shown to contribute to wasting. Through T cell-intrinsic type 1 interferon signaling and antigen priming, $CD8^+$ T cells induced morphological and molecular changes in adipose tissue, resulting in the depletion of lipid stores. Accordingly, $CD8^+$ T cell depletion protected mice from chronic viral infection-associated cachexia (Baazim, 2019). Even though $CD8^+$ T cell depletion upon virus-associated cachexia had a contradictory effect to cancer-induced cachexia, this study shows the important potential of T cells as metabolic regulators influencing cachexia development associated with different diseases. Of note, contrary to cancer cachexia, infection-associated cachexia was not triggered by high levels of circulating cytokines, suggesting that different mechanisms initiate wasting in those two diseases.

In summary, depletion of various T cell subsets, highlighted the detrimental link between $CD8^+$ T cell absence and accelerated body wasting, and in line, cancer cachexia was associated with a marked systemic depletion of T cells, underlining their role as systemic metabolic regulators. These results

imply that restoring the CD8^{+} T cell subset likely attenuates wasting and is hence a promising strategy to counteract cachexia.

3.4   Aging aggravates cachexia in tumor-bearing mice

The functionality of the adaptive immune system declines with age, leading to an accumulation of senescent terminally differentiated effector T cells (Foster, 2011). Also upon cancer cachexia, T cells displayed a dysfunctional state with senescent characteristics. Since the absence of CD8^{+} T cells was potent to accelerate cachexia, we were interested to assess whether the decline in immune cell function linked to aging has an impact on cachexia development. To this end, a comprehensive study involving different mouse models of cancer cachexia (LLC, C26) with several age groups was conducted. A detailed description of all results can be found in Geppert *et al.* (Geppert, 2021). Aging did not have an impact on C26-induced wasting in BALB/c mice despite smaller tumor size, in line with a previous report (Talbert, 2014). However, LLC-mediated onset and progression of cancer cachexia was specifically regulated by age in the C57BL/6 substrains. Aging aggravated weight loss in C57BL/6J mice, and induced cachexia in aged C57BL/6N mice, while young C57BL/6N mice did not develop cancer cachexia upon LLC injection. Expression of atrophy and stress markers in skeletal muscle and adipose tissue reflected cachexia development in the different models and strains.

T cells are more susceptible to cachexia-induced repression upon aging

Aged individuals are prone to develop cancer (Yancik, 1997), with an impaired immune system being a potent factor contributing to disease development. Especially T cells are highly impacted by aging, which induces for instance thymic involution (S. Palmer, 2018), leading to reduced T cell output, altered effector function (Elyahu, 2019), and a shift in T cell subsets with a marked decrease in naïve T cells and an accumulation of late-differentiated non-proliferative effector T cells (Koch, 2008). Since I have previously noted that cancer cachexia induced partial T cell senescence, we were interested if T cell functionality was further decreased in the aged stage and thereby might have promoted wasting. To investigate T cell functionality and the state of senescence, I determined effector cytokine expression and the CD4^{+}/CD8^{+} T cell ratio, with a low ratio being indicative of aging (Turner, 2016). Interestingly, upon HIV (human immunodeficiency virus) infection, which is also closely associated with cachexia development, an age-dependent link between frailty and the CD4/CD8 ratio has already been observed (Guaraldi, 2019). However, apart from strain- and age-specific differences, I observed no alterations that were dependent on tumor or cachexia presence. Hence, changes in the subtype composition of T cells, meaning an imbalance in the percentage of CD4^{+} and CD8^{+} T cells, are unlikely to mediate accelerated cachexia onset upon high age. A more in depth analysis revealed an increased percentage of Tregs in aged C57BL/6N and BALB/c mice, in line with Garg *et al.* (Garg, 2014), but also here no further tumor-specific changes were observed. With respect to effector cytokine expression, in line with Zanni and colleagues (Zanni, 2003), expression of type 1 (TNFα, INFγ, IL2) cytokines tended to be increased in T cells from aged *vs.* young C57BL/6N and BALB/c mice, suggesting increased numbers of effector T cells upon aging. Accordingly, a higher frequency of effector CD4^{+} and CD8^{+} T cells has been reported in older adults (Alberti, 2006; Zanni, 2003), with an enhanced secretion of inflammatory cytokines likely contributing to a state of low-grade chronic inflammation in aged individuals, termed inflammaging (Macaulay, 2013). Especially IL2 was shown to be reduced in activated T cells from aged individuals (Whisler, 1996) and importantly, its expression recapitulated cachexia severity in the different mouse models and age groups. Hence, there was a strong repression of *Il2* expression in T cells from aged LLC/N *vs.* PBS mice, which was not present in young LLC/N mice,

while *Il2* was equivalently downregulated in T cells of young and aged C26 tumor-bearing mice, reflecting comparable bodyweight loss between these two groups. Overall, the reduction of *Il2* implies that aging in the C57BL/6 model potentiated T cell dysfunction, probably as a result of decreased NFAT and AP1 signaling (Urso, 2011; Whisler, 1996).

Apart from exhausted T cells, also specific subtypes of aged T cells have been shown to express high levels of PD1 (Channappanavar, 2009; Decman, 2012; Shimada, 2009), such as highly activated Tregs (Elyahu, 2019). In aged mice, independent of tumor presence, I observed an elevated expression of *Pdcd1* and *Tox* in CD4$^+$ T cells, implying either an elevated amount of highly active Tregs (in line with the observed increased percentage in Tregs upon aging), potentially inhibiting CD8$^+$ T cells; or a general increase in exhausted CD4$^+$ T cells, either of them potentially worsening disease outcome in LLC tumor-bearing mice. In line, aging was associated with a better response to anti-PD1 therapy in mice and cancer patients (Kugel, 2018).Moreover, increased effector cytokine expression may in addition contribute to strong systemic inflammation, thereby promoting disease onset. Thus, it would be intriguing to investigate if depletion of Tregs in aged animals could attenuate potentiated cachexia onset, especially in LLC tumor-bearing mice.

IL6 and GDF15 cachexia-induced secretion is altered by high age

Aging is linked to chronic low-grade inflammation and increased levels of circulating cytokines such as GDF15 or IL6, both being associated with frailty and unfavorable outcomes in aged individuals (Ershler, 1993; Osawa, 2020). Also cancer cachexia is linked to chronic systemic inflammation and increased circulating IL6 and GDF15 levels, both with therapeutic potential as their blocking was linked to improved cachexia outcome in animals (Rupert, 2021; Suriben, 2020). In C57BL/6 and BALB/c mice, aging led to elevated plasma GDF15 levels, although no alterations in *Gdf15* expression in skeletal muscle were observed, implying that other sources, such as the tumor, heart, liver, spleen, lung or gut must be important contributors to increased GDF15 plasma levels (Böttner, 1999; Koopmann, 2004). Moreover, cachectic mice displayed an (additional) increase in circulating GDF15 levels, which was only pronounced in BALB/c but not C57BL/6 mice. In line, in cancer patients GDF15 levels tended to be increased in cachectic patients, and even more so upon aging. Unexpectedly, high plasma IL6 levels were absent in the LLC cachexia models, although these mice had developed considerable bodyweight loss. Of note, transfection of LLC cells with IL6 cDNA and subsequent implantation into syngeneic C57BL/6 mice induced accelerated cachexia onset, despite unaltered levels of IL1α and TNFα (Ohe, 1993), underlining that the presence of IL6 is necessary to develop a strong and drastic wasting phenotype, but it is not required for cachexia development *per se*. This result is in contrast to a study by Flint *et al.*, who claim an essential role of high IL6 levels for cachexia development (Flint, 2016); however, based on our results cancer cachexia also can be induced in absence of high circulating IL6 levels.

With respect to patients, we found significant correlations between weight loss and the concentration of important cachexia-associated cytokines in young patients, which became non-significant upon aging. Although these results show great translation to the clinical setting, more studies are needed to assess age differences in cachexia in a bigger patient cohort to gain more insight into the interrelation of wasting metabolism and aging in cancer patients.

Based on these results, a hint of caution is warranted when choosing models to study cancer cachexia, as disease onset seems to be regulated by different circulating factors in distinct mouse models. Hence, when exclusively using the C26 model an overrepresentation of specific factors such as IL6 but also others might occur, as BALB/c mice were reported to induce an excessive systemic

inflammation with increased amounts of circulating and hepatic cytokines (Watanabe, 2004). Since the C26 cachexia model implied to be unaffected by aging, this implies its important function as preclinical model in cachexia studies; however, using different mouse models and distinct mouse strains to improve translatability of animal to clinical studies, irrespective of age, is highly recommended.

3.5   Glucocorticoid signaling in T cells is affected by cancer cachexia

Already in the 1990s, it has been shown that cancer cachexia leads to a rise of plasma glucocorticoids in mouse models (Tanaka, 1990) and human patients (Knapp, 1991). In line, I observed significantly elevated corticosterone levels in mice from different cachexia models, including the C26 and LLC model. Glucocorticoids are known for their various effects on T cells (Taves, 2021), and have previously been linked to cancer cachexia as drivers of muscle atrophy (Braun, 2013) and suppressors of intra-tumoral immunity in cachectic mice (Flint, 2016). Importantly, in pancreatic cancer patients, which are very prone to develop cancer cachexia, tumor cell-intrinsic glucocorticoid receptor (GR) signaling was shown to activate PD-L1 expression, while simultaneously preventing MHC-I expression, ultimately leading to immunosuppression and non-responsiveness to immune checkpoint inhibitory therapy (Deng, 2021).

With respect to the prominent role of glucocorticoids in cachexia and their potent immunosuppressive functions, I found GR signaling to be strongly elevated in circulating and tumor-infiltrating T cells from cachectic C26 tumor-bearing mice. Additionally, the glucocorticoid receptor itself and dexamethasone were identified as potent upstream regulators in cachectic T cells, while increased expression of many GR target genes and subsequent repression of cytokine expression were present. *In vivo* and *in vitro* dexamethasone treatment of T cells mimicked the cachectic T cell phenotype to a great extent, further underlining the repressive potential of glucocorticoids in cancer cachexia. Hence, elevated plasma glucocorticoid levels might induce T cell repression upon cachexia. Indeed, Flint and colleagues have already shown a suppression of multiple intra-tumoral immune pathways, including anti-tumor T cell function, due to a marked increase in glucocorticoids upon cachexia (Flint, 2016). Of note, in their study, Flint *et al.* claimed that increased glucocorticoid levels are induced by an IL6-mediated reduction of the hepatic ketogenic potential, which triggers upon caloric deficiency a strong rise in glucocorticoids. However, although cachexia in patients is indeed often associated with anorexia, this phenomenon is only partially observed in animal models, and importantly not seen in the C26 model. Instead, I have frequently observed compensatory over-eating in C26 mice. Moreover, the absence of increased IL6 levels in cachectic LLC tumor-bearing animals (Geppert, 2021), indicates that additional mechanisms must mediate the marked rise in glucocorticoid levels upon cachexia. However, in their study, Flint *et al.* rather focused on this IL6-induced hepatoketogenesis-glucocorticoid axis than on the immune system. Hence, to my knowledge, no detailed mechanistic analysis linking glucocorticoids to T cell repression in cancer cachexia has been conducted so far.

To attenuate cachexia in tumor-bearing mice, we aimed to improve T cell functionality by reducing glucocorticoid levels. Indeed, also other researchers have come to similar conclusions about the devastating effects of glucocorticoids on cachexia progression and have tried to counteract body wasting by using the glucocorticoid receptor antagonist RU486 (also Mifepriston or RU38486). However, the outcomes of these studies were contradictory (Llovera, 1996; Rivadeneira, 1999; Russell, 2005), and most of them failed to improve cancer-associated wasting. In addition to its function as glucocorticoid receptor antagonist, RU486 has a relatively wide spectrum of action,

impacting other steroid hormone receptors, such as the progesterone (Heikinheimo, 1990) and androgen (Song, 2004) receptor. Additionally, high levels of glucocorticoids remain in the circulation of cachectic animals that are treated with RU486 (Llovera, 1996), potentially inducing signaling of the mineralocorticoid receptor (Kino, 2004), thereby introducing further effects that might impact cachexia development. Altogether, the additional involvement of these receptors might weaken possible anticatabolic effects of glucocorticoid signaling inhibition, thereby explaining the rather negative outcomes of the aforementioned studies. To avoid the drawbacks of RU486, but still be able to pharmacologically reduce corticosterone levels in cachectic mice, I treated C26 tumor-bearing animals with the well-known corticosteroid synthesis inhibitor Aminoglutethimide (AG) (Flint, 2016). Unfortunately, AG treatment was not sufficient to restore corticosterone levels in cachectic mice to normal levels, and hence disease outcome was unaltered. As major side effects of AG treatment include loss of appetite and lethargy (Santen, 1977), which could both have unfavorable effects on cachexia development, we decided to apply a dose that was known to be tolerable in long-term treatment and injected the mice only once a day to reduce overall stress. However, daily injection was not sufficient to restore the enormously high corticosterone levels that were associated with cachexia. Thus, for future purposes, the implantation of a slow-releasing pellet containing AG could be applied to continuously decrease glucocorticoid levels over time, while additionally reducing the induction of injection-related stress.

Nevertheless, to address the specific role of T cell-intrinsic GR signaling, cachexia development was assessed in T cell-specific GR knockout mice, which were injected with LLC cells. Cachexia onset and progression were assessed over the course of the experiment. Despite a small group size and premature sacrifice of the mice due to tumor ulceration, I observed a promising trend for an improvement in bodyweight loss and atrogene expression in skeletal muscle of pre-cachectic mice, which was accompanied by improved T cell-associated gene expression in muscle as well as enhanced T cell effector cytokine expression.

In detail, the T cell-specific GR knockout improved *Ifnγ* and *Il2* expression in T cells, probably as a result of reduced NFκB, AP1 and STAT4 inhibition, which might in cachectic mice have been induced by elevated glucocorticoid signaling (Franchimont, 2000; Helmberg, 1995; Scheinman, Gualberto, , 1995; Vacca, 1992). In this context, the GR downstream target *Tsc22d3*, encoding the glucocorticoid-induced leucine zipper (GILZ), was shown to inhibit T cell activation by interfering with the TCR and NFκB signaling (Ayroldi, 2001). Furthermore, glucocorticoids are known to induce expression of the decoy receptor IL-1R2 (Interleukin 1 Receptor Type 2) (Peters, 2013), which can neutralize IL-1 (Van Den Eeckhout, 2020), thereby preventing its enhancing effects on CD8^{+} T cell effector function (Ben-Sasson, 2013). Thus, the reduced expression of *Tsc22d3* and *Il1r2* in GR knockout T cells of LLC mice suggests improved potential for T cell activation and hence effector function, in line with the elevated expression of effector genes. Moreover, a recent study has demonstrated that presence of GCs during TCR activation causes a state of low glycolytic activity with reduced glucose uptake, dampening subsequent development of effector CD8^{+} T cells and their anti-tumor function (Konishi, 2022); in line with the decreased *Slc2a1* and effector cytokine expression of cachectic T cells. Furthermore, it has been recently noted that high glucocorticoid levels in the TME induce the expression of T cell dysfunctional genes (Acharya, 2020). In their study, Acharya *et al.* found that the transition from naïve to dysfunctional CD8^{+} TILs was accompanied by a progressive increase in GR expression and signaling in T cells, a phenomenon that could potentially also reflect the continuous increase of glucocorticoid levels upon cachexia, leading to T cell dysfunction. Hence, inhibition of GR signaling could theoretically be sufficient to improve the cachexia-associated dampening of glucose metabolism and

thereby improve T cell effector cytokine expression and functionality. To this end, further studies involving RNA sequencing of T cells from LLC tumor-bearing GR$^{CD4-Cre}$ knockout and control mice as well as metabolic studies using the Seahorse analyzer are needed to elucidate underlying mechanisms in greater detail.

Importantly, many downstream targets of GR signaling like *Tsc22d3, Il1r2, Sat1* and *Itgal* were reduced in GR$^{CD4-Cre}$ T cells from LLC tumor-bearing mice, verifying the functionality of the GR knockout on the molecular level. Nevertheless, the additional confirmation of absent *Nr3c1* expression indispensable to confirm the GR knockout.

So far, I have only focused on the effects of endogenous corticosterone in cachectic mice; however, glucocorticoids are among the most prescribed drugs administered to cancer patients (Herr, 2006; McNamara, 2018; K. M. Taylor, 2016). Glucocorticoids are still used as appetite stimulants to counteract cachexia-induced anorexia in cancer patients (Dev, 2017). Additionally, in the past few years, exogenous glucocorticoid administration has been routinely applied to counteract immune-related adverse effects (irAEs) induced by ICI therapy (Kumar, 2017). Hereby, initial studies implied that glucocorticoid administration to ICI therapy patients did not negatively affect therapeutic outcome (Beck, 2006; Downey, 2007; D. B. Johnson, 2015; Weber, 2008). However, a recent report noted that patients receiving a high dose of glucocorticoids as first-line treatment for irAEs, showed a significantly shortened overall survival and time to treatment failure compared to low-dose glucocorticoid administration (Faje, 2018). In line, use of baseline corticosteroids at time of treatment start was linked to impaired response to anti-PD-L1 ICI therapy and reduced progression-free survival in patients with non-small-cell lung cancer (Arbour, 2018). To date, there are different and contradictory points of view for the therapeutic use of glucocorticoids in oncology. Thus, it is ever more important to understand the effects of glucocorticoid administration (low vs. high dose, time point of treatment start, weight-stable *vs.* cachectic patient), in order to efficiently use the beneficial characteristics of GR signaling in cancer patients. So far, my findings do not support the exogenous use of glucocorticoids in cachectic cancer patients, as high endogenous steroid amounts already imply to repress T cell functionality, contributing to cachexia and failure of ICI therapy.

3.6 Glucose deprivation may drive diminished T cell function in cachexia

As discussed above, cachectic mice developed central and local glucose deprivation, thereby probably inhibiting T cell functionality. In detail, local glucose deprivation in the TME may inhibit other cell types than tumor cells as these outcompete for instance T cells in glucose uptake. Recently, also a marked increase in neutrophils displaying an enhanced aerobic glycolytic profile was observed in mouse models of cachexia (Petruzzelli, 2022), adding a further cell type despite the tumor, which highly metabolizes glucose in cachexia. Importantly, inhibition of glycolysis in cachectic C26 mice through repression of GAPDH by heptelidic acid, which is expected to only act on tumor and immune cells, resulted in tumor regression but accelerated death, underlining that the detrimental effects of GAPDH inhibition in immune cells prevails its attenuating effect on tumor growth (Petruzzelli, 2022). In this study, Petruzzelli only focused on the interaction of neutrophils and cancer cachexia progression; nevertheless, GAPDH inhibition but also strong glucose deprivation might have also impaired T cell functionality, thereby contributing to disease worsening.

Hence, central and local glucose deprivation might be a potential mechanism, contributing to reduced T cell effector function in cachexia, as T cells do not meet the cells energy demand, subsequently resulting in impaired T cell function and worsened disease outcomes. Of note, although I frequently

observed compensatory over-eating in C26 mice to counteract body wasting, T cells of cachectic mice still seemed to have a fasting signature (low PI3K/AKT, high FKBP5). However, neither fasting nor 2-deoxyglucose treatment of wildtype mice could mimic the global gene signature of T cells from cachectic animals, indicating that anorexia of cachectic mice is likely not the underlying cause for T cell repression upon cachexia.

Glucose deprivation might lead to a severely changed glycosylation pattern of T cell receptors upon cachexia without affecting receptor transcription or translation. T cell glycosylation has previously been shown to be important for a myriad of functions, including T cell migration (Hobbs, 2017), development (Swamy, 2016) and activation (Dennis, 2009). Importantly, glycosylation was noted to affect strength and speed of ligand binding. For instance, glycosylation of the IL7Rα enhances binding of IL7 by 300-fold (McElroy, 2009). Hence, altered T cell receptor glycosylation upon cachexia, may potentially impair T cell activation and co-stimulation, thereby preventing a proper induction of the activation signaling cascade. To unravel if defective glycosylation might mediate T cell repression upon cachexia, *in vitro* studies using plasma from cachectic mice as well as different glucose concentrations in combination with western blot analyses will be applied.

In T cells, glucose is a key regulator of survival, differentiation, and proliferation, all mediated through PI3K/AKT/mTOR signaling (Jacobs, 2008; C. S. Palmer, 2015) in combination with other pathways or factors, like ERK (Marko, 2010), or STAT5 signaling (Wofford, 2008). In this context, mTOR links environmental signals such as glucose availability to T cell fate decisions (Chapman, 2014). Hence, local or central glucose deprivation may be responsible for decreased T cell activation based on reduced PI3K/AKT/mTOR signaling and subsequently impaired T cell functionality in the cachexia setting. Indeed, all of the aforementioned pathways (PI3K/AKT/mTOR, ERK/MAPK and JAK/STAT) were strongly downregulated, and several mTOR-associated factors (such as Rapamycin, Rictor, Myc and FOXO1) were identified as important upstream regulators in cachectic T cells. All of the aforementioned upstream regulators have important immuno-regulating properties, and are thereby involved in T cell activation, metabolism, and proliferation (Iyer, 1998; Jeng, 2018; Sehgal, 1993; R. Wang, 2011; Yang, 2013). Of note, muscle-specific mTORC1 signaling was shown to be impaired in C26-, APC[Min/+] and LLC-induced cancer cachexia (Geremia, 2022; White, 2011), and very recently, Geremia *et al.* have shown that restoring AKT-mTORC1 signaling specifically in the muscle, completely reverted muscle wasting, hampered protein degradation and normalized the skeletal muscle transcriptome (Geremia, 2022).

FOXO1 has previously been demonstrated to integrate signals from the mTOR/AKT signaling pathway in T cells (Staron, 2014), while also affecting glycolysis (Jeng, 2018; Newton, 2016). Moreover, decreased PI3K/AKT signaling leads to enhanced FOXO1-mediated transcription, since triple phosphorylation of FOXO by AKT, leading to nuclear export and degradation, is reduced (Hedrick, 2012). Despite a strong induction of several FOXO1 target genes, FOXO1 mRNA levels were slightly downregulated in cachectic T cells; however, the strong reduction of AKT signaling still suggests an increase in activated FOXO1 protein levels inducing transcription of downstream targets, such as *Il7rα*, *Klf2*, *Sell*, *S1pr1*, *Bcl6*, *Foxp3*, *Eomes*, and *Ctla4*. Interestingly, glucocorticoids were noted to upregulate FOXO1 in myotubes (W. Zhao, 2009) and IL7Rα expression (Franchimont, 2002), highlighting the possibility that also in T cells, glucocorticoid signaling might be linked to FOXO1 expression. IL7Rα, being part of the main survival receptor of naïve T cells and one of the key FOXO1-regulated genes (Kerdiles, 2009), was amongst the most upregulated genes in cachectic T cells. In combination with KLF2 and CD62L (encoded by *Sell*), which are prominent markers for naïve T cells

and important mediators of T cell migration and homing (Arbonés, 1994; Kahn, 1994; Sebzda, 2008), the upregulation of these three genes highlights an increase of naïve compared to activated T cells in cachectic mice, in line with my flow cytometry data indicating an increase in CD62L⁺CD8⁺ T cells upon cachexia. Additionally, induction of FOXO1 downstream targets such as S1pr1, Ctla4 or Bcl6 was linked to thymic egress (Matloubian, 2004), T cell inhibition (Krummel, 1995) and Treg suppressor function (Y. Li, 2020), while FOXO1-dependent downregulation of Eomes is associated with reduced CD8⁺ lymphocyte effector function (Pearce, 2003). Hence, inhibition of FOXO1 in T cells might improve expression of FOXO1 downstream targets, thereby enhancing the development of effector T cells instead of naïve T cells. Importantly, inhibition of FOXO1 in T cells has been noted to improve glucose uptake and overall glucose metabolism, and simultaneously enhanced expression of *Gzmb*, while *Cd62L* and *Il7r* were downregulated (Roux, 2019); thus a T cell-specific FOXO1 knockout might improve chances for glucose uptake in the already glucose-deficient milieu.

3.7   Summary and Outlook

In summary, these data suggest that cancer cachexia mediates strong T cell repression, most likely arbitrated by elevated glucocorticoid signaling, alone or in combination with glucose deprivation. Moreover, reduced CD8⁺ T cell presence and functionality contribute to cachexia development and accelerate disease onset (Figure 93). T cell numbers, proliferation, metabolism and effector function were gradually impaired with cachexia progression.
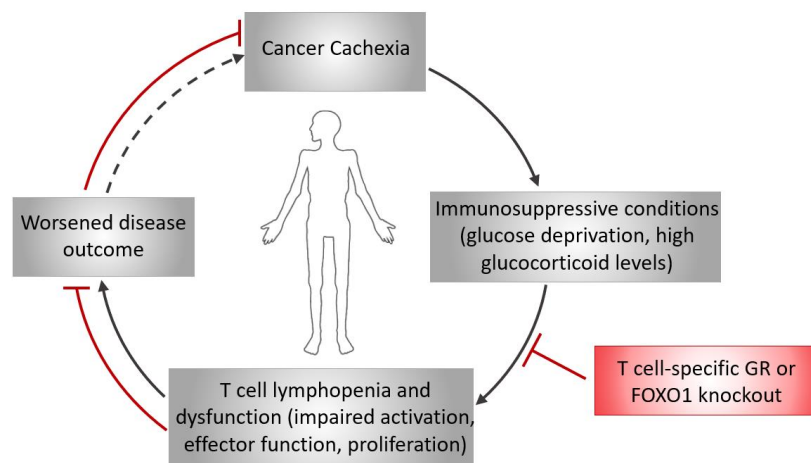
Figure 93. Cancer-induced metabolic reprogramming dampens T cell function and contributes to wasting in cachexia. Cancer cachexia is associated with an immunosuppressive environment that dampens T cell functionality, leading to worsened disease outcomes by accelerating cachexia progression. Created with BioRender.com.

Since T cells displayed reduced cytokine expression, they do not likely contribute to the elevated systemic inflammation in cachexia, nor the local inflammation within the tumor microenvironment. In accordance, cachexia onset with its prominent rise in systemic inflammation, was reported to develop in immunocompromised SCID mice, which lack functional T cells (Murray, 1997). Importantly, T cell repression in cachectic mice was not directly linked to tumor-secreting factors but rather a general immunosuppressive environment (like increased glucocorticoid levels or glucose deprivation). Despite a small sample size, partial restoration of T cell effector function in pre-cachectic mice by a T cell-specific GR knockout showed a promising trend for reduced body wasting in line with decreased atrogene expression in skeletal muscle, independent of direct effects on tumor growth. However, due to an overall small group size and pre-mature sacrifice of the mice (as a result of tumor

ulceration), this experiment needs to be repeated to verify the positive impact of blocking T cell intrinsic GR signaling on cachexia outcome.

With respect to glucose deprivation, the possible deleterious role of FOXO1 activation in cachectic T cells needs to be further elucidated. Hereby, FOXO1 could either mediate compromised T cell functionality by itself, as downstream factor of dampened PI3K/AKT signaling, or in combination with elevated GR signaling. Using T cell-specific FOXO1 knockout mice, overall survival, cachexia progression, and molecular changes associated with cancer cachexia will be assessed.

The ultimate goal of this study was to better understand and characterize underlying mechanisms that mediate cancer cachexia by performing an in-depth phenotyping of cachectic T cells, and to identify novel regulators in T cells that can be used to improve T cell functionality and subsequently cancer-associated wasting. At the moment there is still a knowledge gap regarding the interaction of the immune system (especially T cells) and its potential contribution to cachexia onset. However, it becomes ever more important to unravel the functional contribution of lymphocytes to cachexia development, as their clear relationship was already noted by Miyawaki and colleagues, who reported a strong correlation between the failure of ICI therapy and pre-diagnosis of cachexia in cancer patients (Miyawaki, 2020). Hence, by preventing T cell deterioration, we hope to improve disease outcome, either by the sole enhancement of T cell functionality per se or by boosting therapeutic approaches such as ICI therapy. To this end, additional experiments using ICI drugs such as anti-PD1/PD-L1 could be tested in our knockout models.

Importantly, to prove the translatability of my data, a comprehensive analysis of the immune profile of cachectic and weight-stable cancer patients will be conducted. To this end, I have already started to establish a protocol for the detailed investigation of peripheral blood mononuclear cells, including T cells, B cells, dendritic cells, natural killer cells, and monocytes. Pilot samples have already pointed out the need to decrease sample variability by focusing on one specific cachexia-inducing cancer type, while simultaneously increasing group size.

Overall, there is a clear need to better characterize the impact of cancer-associated wasting on T cells and *vice versa*, with the ultimate aim to improve or even find new therapeutical approaches to counteract cachexia.

4   METHODS

4.1   Cell Biology

T cell isolation

A) T cell isolation from spleen using magnetic activated cell sorting (MACS)

Murine spleens were collected and stored in RPMI+ (RPMI supplemented with 10% heat inactivated fetal calf serum [FCS]) on ice until use. Single cell suspensions were obtained by straining tissues with the plunger of a syringe through 70 µm cell strainers into RPMI+ provided. Cells were centrifuged for 5 min at 400 xg, 4 °C and red blood cells (RBC) were removed by treating spleen solutions with Ammonium-chloride-potassium (ACK) lysis buffer (see Material section) for 2 min at RT. Lysis was stopped by adding 10 mL of RMPI+ and the cells were pelleted at 400 xg, 4 °C for 5 min. $CD4^+$ or $CD8^+$ T cells were separated by magnetic negative selection using Miltenyi Biotec's $CD4^+$ T Cell Isolation Kit, mouse or $CD8a^+$ T Cell Isolation Kit, mouse, following the manufacturer's instructions. Cells were either immediately lysed in 500 µL TRIzol for subsequent gene expression analysis or RNA-sequencing, plated in 96 well plates for further cell culture experiments or used for metabolic analysis using Agilent's Seahorse Extracellular Flux Analyzer.

B) T cell isolation from secondary lymphoid organs for flow cytometry

Murine lymph nodes and spleens were collected and stored in HBSS+ (hanks balanced salt solution supplemented with 5% FCS and 10 mM HEPES [4-(2-hydroxyethyl)- 1-piperazineethanesulfonic acid]) on ice until use. Single cell suspensions were obtained by straining tissues with the plunger of a syringe through 70 µm cell strainers into RPMI+ or HBSS+ provided. Cells were centrifuged for 5 min at 400 xg, 4 °C. When spleen samples were applied to flow cytometric analyses, RBCs were depleted using ACK lysis buffer as described above and only 1/10 of the spleen suspension was used for further flow cytometric analysis. Cells were resuspended in HBSS+ and stored on ice until staining of the samples.

C) T cell isolation from adipose, muscle and tumor tissue

Adipose tissue was harvested and stored on ice in Dulbecco's phosphate buffered saline (PBS) supplemented with 0.5% bovine serum albumin (BSA). Epididymal and inguinal white adipose tissue (eWAT and iWAT) were digested in HBSS supplemented with 10 mM $CaCl_2$ using Collagenase II and continuous rotation in a 37 °C incubator. Digestion was stopped after 8-15 min by adding cold MACS-PBS buffer (PBS supplemented with 0.5% BSA and 2 mM EDTA) and the stromal vascular fraction was filtered through a 200 µm nylon mesh. Cells were centrifuged at 400 xg, 4 °C, for 5 min and adipocytes and free fatty acids were immediately removed to avoid T cell damaging by oxidative stress. Cells were stored in HBSS+ on ice until subsequent flow cytometric staining.

Both gastrocnemius (GC) muscles from a mouse were harvested, pooled and stored on ice in HBSS+. GC muscles were cut into small pieces using scissors and digested in 2 mL of digestion solution containing PBS+ supplemented with 0.18 mg/mL $CaCl_2$ and 0.5 mg/mL Collagenase II. The mixture was incubated for 25-30 min at 37 °C on a rotator. Digestion was stopped using cold MACS-PBS and everything was filtered through a 100 µm mesh using a plunger to disrupt still undigested tissue. Cells were centrifuged for 5 min at 400 xg, 4°C and washed once with HBSS+. Until further flow cytometric processing, cells were resuspended in HBSS+ and kept on ice.

Tumor tissue was harvested and stored on ice in RPMI supplemented with 1% FCS. Tumors were minced using scissors and digested for 30 - 60 min at 37 °C on a rotator in RPMI supplemented with 1% FCS, 200 µg/mL DNase I, 0.5 µg/mL Collagenase IV, and 5 mM $MgCl_2$. The digestion mixture was

passed through a 70 µm cell strainer and centrifuged for 8 min at 2000 xg, RT. Subsequently leukocytes were isolated by density centrifugation over Ficoll Paque PLUS (GE Healthcare). In brief, the tumor suspension was resuspended in 4 mL of RPMI+GlutaMAX and carefully layered on top of 3 mL Ficoll Paque PLUS. To separate leukocytes, samples were centrifuged for 40 min at 400 xg, RT (acceleration: 1, deceleration: 1) and the cloudy interphase carrying leukocytes was collected and diluted in HBSS+. Leukocytes were pelleted at 400 xg, 4 °C for 5 min and stored in HBSS+ on ice until flow cytometric staining.

D) T cell isolation from murine peripheral blood

Venous peripheral blood was collected by puncturing the vena cava or nicking the tail, mixed with 50 µL of Heparin (1:15 dilution, stock 2 mg/mL) and stored at RT until further use. Peripheral blood mononuclear cells (PBMCs) were isolated by density centrifugation over Ficoll Paque PLUS (GE Healthcare) by 20 min centrifugation at 400 xg, RT, acceleration: 1, deceleration: 1. PBMCs were isolated from the interphase, pelleted for 5 min at 400 xg, 4°C and stored on ice in HBSS+ until staining for flow cytometry.

E) T cell isolation from human peripheral blood

Venous peripheral blood was collected in heparinized tubes (S-Monovette® Lithium-Heparin) and PBMCs were isolated by density gradient centrifugation over Ficoll Paque PLUS (GE Healthcare). In brief, blood was diluted 1:1 with PBS and 20 mL of blood-PBS solution were layered on top of 20 mL Ficoll Paque PLUS. PBMCs were separated by 40 min centrifugation at 400 xg, RT, acceleration: 1, deceleration: 1, isolated from the interphase and washed for 10 min in 30 mL HBSS+ at 400 xg, RT.

Cells were counted and at least 2 Mio PBMCs were frozen in CryoStor CS10 cell cryopreservation medium for future analysis. A minimum of 0.5 Mio PBMCs was directly lysed in TRIzol for further gene expression analysis and remaining PBMCs were processed for immune phenotyping, including the sort of CD4+ and CD8+ T cells for RNA and T cell stimulation using PMA and Ionomycin, and the characterization of different immune cell subtypes in cancer patients.

Stimulation of T cells

In order to stimulate murine T cells, 96 well plates were coated either for 3 h at 37 °C or at 4 °C overnight with 5 µg/mL α-CD3e and 5 µg/mL α-CD28 antibodies per well in 50 µL PBS. CD4$^+$ and CD8$^+$ splenocytes were isolated as described in the magnetic activated cell sorting (MACS) protocol above and 150 000 cells were plated in 150 µL RPMI+ on α-CD3/ α-CD28 coated plates. Cells were incubated for 48 h, and cell metabolism and gene expression were assessed afterwards.

Human PBMCs isolated from peripheral blood, were enriched by MACS using human CD3 MicroBeads (Miltenyi Biotec) according to the manufacturer's instructions. Subsequently, CD4$^+$ and CD8$^+$ T cells were sorted for purity from the CD3$^+$ cell mix using a FACS AriaIII (BD). CD4$^+$ and CD8$^+$ T cells were stimulated for 2 h with PMA (1:2000) and Ionomycin (1:20 000) at 37 °C, with the lid of the falcon open. To block intracellular protein transport, GolgiPlug (BD) was added, and cells were incubated for another 2 h at 37 °C before flow cytometric staining.

Flow cytometry

To prevent unspecific binding of antibodies, single cell suspensions were incubated with Fc block (BioLegend) for 10 min on ice. Afterwards, flow cytometric surface staining was conducted for 30 min on ice in the dark and dead cells were excluded using the viability stains Sytox Blue/Red Live Dead Stain (Invitrogen) for unfixed cells or fixable viability dye eFluor450 (Invitrogen) for fixed cells. To detect intracellular protein expression, T cells were fixed and permeabilized using the Foxp3 Staining

Buffer Kit (eBioscience) with a slightly modified protocol. In brief, cells were fixated for 30-40 min on ice in the dark, and after centrifugation for 5 min at 400 xg, 4 °C, resuspended in Perm buffer (diluted to 1X with PBS). Intracellular antibodies were added, and staining was conducted for 30-40 min in the dark. Cells were washed twice with 1X Perm buffer and twice with HBSS+.

After sort and stimulation of human CD4$^+$ and CD8$^+$ T cells, the Cytofix/Cytoperm Plus Kit with BD GolgiP (Beckton Dickinson) was used according to the manufacturers protocol to stain and detect intracellular cytokines. To this end, cells were incubated overnight with Cytofix buffer. The next day, cells were washed once with Cytoperm and stained in 50 µL Cytoperm for 30 min at 4 °C. Before acquisiton in the FACS, cells were washed three times with Cytoperm and twice with HBSS+.

Finally, cells were passed through a 40 µm nylon mesh to remove large debris. Cells were acquired or sorted for purity on a BD FACS AriaIII flow cytometer using FACSDiva software V6.1.3 with optimal compensation and gain settings based on unstained cells and single-color stained cells or beads. All antibodies that were used for analysis are listed in the material section. Doublets were excluded from analysis based on SSC-A vs. SSC-W and FSC-A vs. FSC-W plots. Dead cells were excluded based on live/dead staining. All samples were analyzed using FlowJo Software (V10.8.0; TreeStar Inc.) and data was further processed with Prism 6,7 and 8 (GraphPad) for statistical analyses.

Sorting of T cells

In order to enrich CD4+ and CD8+ T cell simultaneously, samples were applied to fluorescence-activated cell sorting (FACS). To this end, single cell suspensions from murine splenocytes were produced by straining tissues with the plunger of a syringe through 70 µm cell strainers into RPMI+ provided. Samples were centrifuged for 5 min at 400 xg, 4 °C and resuspended in 500 µL HBSS+. To prevent unspecific antibody binding, cells were incubated with FC block (1:50) for 10 min on ice, before staining antibodies were added (CD3-Biotin, CD4, CD8a) and samples were incubated for 30 min on ice in the dark. Cells were washed with 5 mL HBSS+ and centrifuged at 400 xg, 4 °C for 5 min. The pellet was resuspended in 300 µL MACS-PBS per mouse and 25 µL Streptavidin MicroBeads were added to mixture to bind to CD3-bound Biotin for subsequent MACS enrichment of CD3$^+$ cells. After 5 min incubation at 4 °C, 1 µL Streptavidin-PE Antibody was added and samples were incubated for an additional 10 min at 4 °C. Cells were washed with 5 mL of MACS-PBS and CD3$^+$ cells were enriched via positive selection using LS Columns and magnetic enrichment. CD3$^+$ cells were centrifuged for 5 min at 400 xg, 4 min, and filtered through a 40 µm mesh in FACS tubes with a total volume of 200 µL. To differentiate between dead and alive cells, samples were incubated with SytoxRed (dilution of 1:1000) for 5 min at RT in the dark. Before acquisition, the cell suspension was diluted to a volume of 2 mL and CD4$^+$ and CD8$^+$ T cells were sorted for purity into supplied cold HBSS+ with a BD FACS AriaIII using an 85 µm nozzle. Sorted T cells were immediately lysed in TRIzol for subsequent gene expression analysis and RNA-sequencing.

For analyses of human T cells, PBMCs from cancer patients were isolated as described above and enriched for CD3$^+$ cells using CD3 Microbeads (Miltenyi Biotec), following the manufacturer's instructions. In brief, PBMCs were centrifuged for 10 min at 300 xg, 4 °C and resuspended in 80 µL of MACS-PBS and 20 µL human CD3 MicroBeads per 10^7 total cells. Samples were incubated for 15 min at 4 °C, before staining antibodies (CD4, CD8, CD3, dump including CD19, CD14, CD11b) were added and samples were incubated for 20 min at 4 °C. Cells were washed by adding 10 mL MACS-PBS and centrifuged for 10 min at 300 xg, 4 °C. The pellet was resuspended in 500 µL MACS-PBS and cells were applied through a 200 µM mesh to LS columns placed in a magnetic field. After positive selection, CD3$^+$ cells were prepared for further enrichment of CD4$^+$ and CD8$^+$ T cells using FACS by incubating

cells with SytoxBlue viability dye (1:1000) for 5 min at RT in dark. Cells were sorted for purity using a BD FACS AriaIII with an 85 µm nozzle. Sorted T cells were either immediately lysed in TRIzol for subsequent gene expression analysis or stimulated with PMA/Ionomycin for further flow cytometric analyses.

Immunohistochemistry and Metabolomics of Tumors

All immunohistochemical stainings and quantification of CD3-, CD8-, CD4- and FoxP3-positive cells in tumors were assessed by the Core Facility Pathology & Tissue Analytics at the Helmholtz Center in Munich. Statistical analyses and data plotting were performed by me. To assess apoptosis and proliferation of tumor-infiltrating T cells, co-staining of CD3$^+$ cells with Ki67 or terminal deoxynucleotidyl transferase dUTP nick end labeling (TUNEL) was applied. Using the TUNEL assay, apoptotic cells can be detected by labeling double-strand DNA breaks that occur during the late stages of apoptosis.

Metabolomic analysis of cachectic C26 and non-cachectic NC26 tumors was performed in collaboration with the HMGU Core Facility for Pathology and Tissue Analytics. Exemplary pictures were also provided by the core facility.

Lipidomic analysis using the Lipidyzer™ platform

Untargeted analysis of circulating lipids was performed by the HMGU core facility Metabolomics & Proteomics. A detailed description of the methodology can be found in (Morigny&Zuber, 2020).

Thawing of murine cancer cell lines

Murine cancer cell lines (Colon26, NC26, Lewis Lung Carcinoma) were thawed at 37 °C in a water bath, and immediately diluted with 10 mL of tumor cell medium, consisting of Dulbecco's Modified Eagle's Medium (DMEM) + 4.5 g/L D-glucose + L-Glutamine (Gibco; supplemented with 10% FCS, 1% Penicillin/ Streptomycin, 1 mM sodium pyruvate) to avoid cell damage by DMSO. Cells were pelleted for 5 min at 400 xg, RT and seeded on 15 cm tissue culture plates for further cultivation.

Cultivation and subcultivation of murine cancer cell lines

Cells were cultured under sterile conditions in an incubator at 37 °C, 5% CO_2 and 95% air atmosphere. Media and trypsin were warmed to 37 °C prior to usage. Murine cancer cell lines were cultured in tumor cell medium containing the same supplements as described above. When cells reached 80% confluence, passaging was carried out. Medium was removed, cells were washed with PBS, detached with Trypsin-EDTA (Invitrogen) and incubated for 2-5 min at 37 °C. To stop the detaching process, 10 mL of DMEM+ were added and cells were pelleted at 400 xg for 5 min. After counting in a Neubauer counting chamber, 1 x 10^6 cells were passaged onto a new 15 cm tissue culture plate containing 20 mL medium. Cell lines were regularly tested for mycoplasma contamination by PCR according to the manufacturer's instructions (Promokine).

Preparation of conditioned media

To determine the impact of tumor-derived factors on specific cell types in greater detail, conditioned medium (CM) can be used to mimic the secretion of tumor-derived factors into the circulation (J. Guo, 2017). To prepare conditioned medium (CM), tumor cells were cultured in T cell medium (RPMI+) to ensure growing of CM-treated T cell afterwards. When reaching 70% confluency, cells were washed once with PBS and fresh medium was supplied to the cells. As a control, 25 mL of RPMI+ medium were added to a plate without any cells (no cell conditioned medium, NCCM). After 48 h, cell supernatant was collected and dead cells were removed by centrifugation at 2000 xg, 4 °C for 2 min.

The CM was then aliquoted and stored at -80 °C until further processing. To avoid any effects as a consequence of nutrient depletion, CM was concentrated by centrifugation for 1 h at 4000 xg, 4 °C in 3K Amicon Ultra Centrifugal Filter Units (Merck) and the CM concentrate, containing secreted proteins, was replenished with serum-free tumor cell medium to reach the initial volume.

Cryopreservation of murine cancer cell lines
In order to enable long-term storage of murine cancer cell lines in liquid nitrogen, cells were detached from culture plates by 2 min incubation with Trypsin-EDTA (Invitrogen). After centrifugation, 1 million cells were resuspended in 1 mL of cryomedium (70% FCS; 20 % tumor cell medium; and 10% DMSO) and the cell suspension was slowly cooled down (1 °C per minute) to -80 °C using a Mr. Frosty^{TM} Freezing container. After 1 week at -80 °C, cells were transferred to liquid nitrogen tanks for long-term storage.

Cultivation of murine T cells
After isolation from spleen (protocol see above), murine CD4$^+$ and CD8$^+$ T cells were cultured in RPMI 1640 with L-glutamine supplemented with 10 % FBS, 1% Penicillin-Streptomycin and 50 µM β mercaptoethanol. For treatment with CM, either naïve or stimulated (using 5 µg/mL anti-CD3/anti-CD28 coating) T cells were used, and CM treatment was applied for 48 h. 400 000 cells were seeded in 200 µL CM onto 96 well plates per condition and after 48 h T cells were harvested by vigorous pipetting and subsequent washing of the plate using PBS. The cell suspension was centrifuged, the supernatant removed, and the pellet resuspended in 500 µL TRIzol (Invitrogen). Cells were vortexed for 30 seconds to increase lysis and stored at -80°C until further processing.

To investigate whether the effects of high glucocorticoid levels on T cells upon cachexia can be mimicked by *in vitro*, CD8$^+$ T cells were isolated from wildtype mice and treated with 1 x 10^{-6} M dexamethasone. To imitate tumor stimulation *in vitro*, culture plates were coated with anti-CD3e and anti-CD28 antibodies to induce T cell activation. A total of 0.6 x 10^6 CD8$^+$ splenocytes was plated per well and the following conditions were tested: stimulation plus dexamethasone treatment, stimulation without dexamethasone treatment, dexamethasone treatment without stimulation and neither stimulation nor dexamethasone treatment. Cells were seeded in duplicated or triplicates per biological sample. CD8$^+$ T cells were incubated for 48 h before harvest by vigorous pipetting and lysis using TRIzol. Samples were stored at -80°C until RNA extraction.

Measurement of cellular oxygen consumption and extracellular acidification rates
Cellular oxygen consumption rate (OCR) and extracellular acidification rate (ECAR) were measured using a Seahorse XFe96 Extracellular Flux Analyzer (Agilent Technologies). In order to ensure proper attachment of the cells to the plate, a 96 well Seahorse cell plate was precoated for 2 h at RT with Poly-D-Lysin (Sigma Aldrich) before seeding of T cells. After T cell isolation from spleen using magnetic separation, 2x10^5 CD4$^+$ or CD8$^+$ T cells were plated as monolayer culture on precoated Seahorse plates in a volume of 180 µL XF RPMI Seahorse Medium (Agilent; supplemented with 2mM L-Glut, 1 mM Sodium-Pyruvate and 10 mM Glucose). To ameliorate cell adhesion and distribution within a well, culture plates were centrifuged for 2 min at 100 xg, with acceleration and deceleration set to 1. At least 3 technical replicates were plated per biological sample. A mitochondrial stress test was performed by injection of 1 µM Oligomycin (Sigma-Aldrich), 1.5 µM FCCP (Carbonyl cyanide 4-[trifluoromethoxy]phenylhydrazone; Sigma-Aldrich), 1 µM antimycin A (Sigma-Aldrich) + 1µM rotenone (Sigma-Aldrich). Glycolysis was measured by additional injection of 100 mM 2-deoxy-D-glucose (Sigma-Aldrich). Baseline levels were measured three times before first drug injection and

each cycle after injection comprised three repetitions of 3 min mixing and subsequent measurement of OCR and ECAR for 3 min.

To normalize OCR and ECAR values to the cell amount per well, remaining assay medium was removed carefully from each well without disturbing the cell layer once the analysis was finished, plates were sealed with parafilm and stored at -20 °C at least for one day. DNA amount was measured using the CyQUANT Cell Proliferation Assay Kit (Invitrogen), following the manufacturer's instructions.

Normalized Seahorse data were then analyzed as follows: Injection of antimycin A and rotenone, which are complex III and complex I inhibitors of the electron transport chain (ETC), resulted in the shutdown of the ETC, revealing the value for non-mitochondrial respiration. Basal respiration was then calculated as the difference between baseline OCR and non-mitochondrial respiration. Using the complex V (ATP synthase) inhibitor oligomycin, Proton leak-linked respiration was assessed as the minimum of measurements after oligomycin injection but prior to FCCP injection minus non-mitochondrial respiration. Subsequently, ATP-linked respiration was calculated as the difference between baseline OCR and proton leak-linked respiration. In order to investigate maximal respiration, the uncoupler FCCP was added to the cells during the assay to boost ETC function to its maximal capacity. Maximal respiration was then calculated by subtracting non-mitochondrial respiration from the maximal measurement after FCCP injection. Spare respiratory capacity was calculated as the difference between maximal respiration and basal respiration. The rate of glycolysis was derived from the difference of basal ECAR and 2-DG rate. Figure 94 visualizes calculation of different parameters.
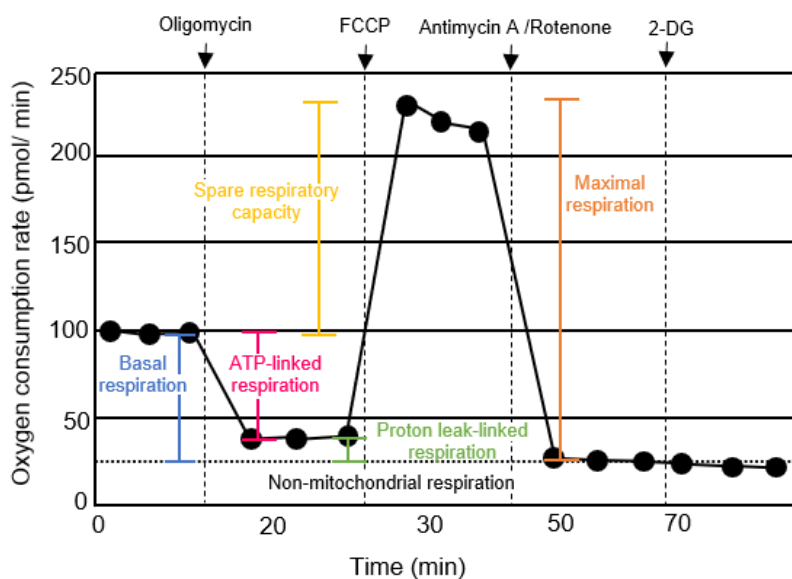
Figure 94. Scheme illustrating calculation of parameters associated with oxygen consumption. Based on (Divakaruni, 2014)

4.2   Molecular Biology

RNA isolation

A) From T cells

Following T cell isolation from spleen, lymph nodes or tumor, RNA was extracted using Qiagen's RNeasy Micro Plus kit for up to 5×10^5 cells or RNeasy Mini Plus kit for 5×10^5 to 4×10^6 cells. T cells were lysed in 500 µL TRIzol (Invitrogen) and incubated for 5 min at room temperature (RT). 150 µL of chloroform were added, samples were mixed by shaking for 2 min, incubated for 5 min at RT and then centrifuged for 20 min at 12,000 xg, 4 °C. The upper aqueous solution containing the RNA was

transferred to a gDNA Eliminator spin column and RNA was purified following the manufacturer's instructions. RNA was eluted in 20 µL (RNeasy Micro Plus Kit) or 30 µL (RNeasy Mini Plus Kit) RNase-free H_2O and stored at -80°C until further use.

<u>B) From tissue</u>

For total RNA extraction, frozen organ or tissue pieces were transferred into a 2 mL RNase/DNase-free Eppendorf tube containing a pre-cooled stainless-steel bead. 1mL TRIzol (Invitrogen) was added, and the samples were immediately homogenized using Qiagen's TissueLyser II (Qiagen) for 2 min at a frequency of 30 Hz. When white adipose tissue was processed, an additional incubation step of 5 min at room temperature (RT) was performed to clear out the fatty layer. RNA was then isolated by adding 200 µL chloroform, samples were mixed by shaking for 2 min, incubated for 5 min at RT and then centrifuged for 20 min at 12,000 xg, 4 °C. The upper aqueous solution containing the RNA was transferred into a fresh 1.5 mL tube and precipitated with 500 µL of isopropanol. After an incubation time of 10 min at RT, samples were centrifuged for 20 min at 12,000 xg, 4 °C. The supernatant was discarded, and the pellet was washed 3 times with 75% ethanol for 6 min at 7500 xg, 4 °C. The pellet was dried for 10 min at RT using a Vacuum-Dryer (Eppendorf), followed by another 30 min drying at RT under the fume hood. RNA was re-solubilized in 30 -100 µL RNase/DNase free water depending on the tissue and incubated for 10 min at 55 °C, 300 rpm using an Eppendorf ThermoMixer. RNA samples were stored at -80 °C until further use.

Determination of RNA concentration

RNA concentration was quantified spectrophotometrically at 260 nm using a NanoDrop2000 spectrophotometer (Thermo Fisher). Sample purity was assessed using both the 260 nm/ 280 nm and the 230 nm/260 nm ratio to measure protein impurities and nucleic acid purity.

RNA-Sequencing

CD4^{+} and CD8^{+} T cells were sorted for purity using a FACS AriaIII (BD), immediately lysed in 500 µL TRIzol (Invitrogen) and stored at -80 °C until sample preparation. RNA extraction and quantification of concentration and purity were conducted as described above. Samples were sent to Novogene (UK) Company Limited for RNA-sequencing. In brief, after quality control procedures, mRNAs were enriched using oligo(dT) beads, and fragmented randomly. The first cDNA was synthesized by using random hexamers primers, after which a customized second-strand synthesis buffer (Illumina), dNTPs, RNase H and DNA polymerase I were added to initiate the second-strand synthesis. The final library was ready after end repair, A-tailing, adaptor ligation, size selection and PCR enrichment. Due to low cell numbers, tumor-infiltrating T cells were processed using SMARTer sequencing with the SMARTSeq V4 Ultra low input RNA kit (Takara Bio) for amplification before polyA library preparation. Circulating T cells were analyzed using low-input sequencing, with kits and optimized reagents that are property to Novogene. Sequencing was performed using NovaSeq6000 (Illumina) with 150 bp read-lengths in paired-end mode. Data were analyzed using Qiagen's ingenuity pathway analysis (IPA) program.

Synthesis of complementary DNA (cDNA)

Complementary DNA (cDNA) was synthesized using 100-1000 ng of RNA. When RNA was extracted using TRIzol, genomic DNA (gDNA) was removed using DNase I (Life Technologies) before reverse transcription, following manufacturer's instructions. For production of cDNA Life Technologies' high-Capacity cDNA Reverse Transcription cDNA synthesis kit was used following the manufacturer's

instructions. After completion, cDNA samples were diluted to a concentration of 2.5- 5 ng/µL using RNase/DNase free water and stored at -20 °C.

Quantitative PCR

Real-time quantitative PCR was conducted using between 2.5 or 20 ng of diluted cDNA obtained from reverse transcription. When 2.5 ng cDNA were used, a master mix containing 3.5 µL Takyon™ Low Rox Probe MasterMix dTTP Blue (Eurogentec), 0.2 µL TaqMan probe (Applied Biosystems) and 2.8 µL of DNase/RNase-free H_2O per individual reaction were used. The final reaction volume of 20 µL was reached by filling up the missing volume using RNase/DNase-free H_2O. When 20 ng cDNA were used, 6 µL Takyon™ Low Rox Probe MasterMix dTTP Blue (Eurogentec), 0.3 µL TaqMan probe (Applied Biosystems) and 0.7 µL of DNase/RNase-free H_2O were used per individual reaction. All TaqMan probes were obtained from Applied Biosystems and are listed in the material section. To control for genomic DNA contamination, samples containing no reverse transcriptase during cDNA synthesis, were included. In addition, water was used as a negative control. All samples were run in technical duplicates. Reactions with a volume of 7-12 µL were run in 384 well reaction plates using Applied Biosystems' QuantStudio 6 or 7 Flex Real-Time PCR System (Applied Biosystems). RNA expression data were quantified according to the ΔCt method (Livak, 2001) and normalized to levels of TATA-box binding protein RNA (*Tbp*).

Genotyping

Ear snips were digested in 50 µL of 50 mM NaOH and incubated for 20 min at 95 °C, 550 rpm. Digestion was stopped using 400 µL of 12.5 mM TRIS HCl (pH8) and samples were stored at -20 °C until further processing. DNA was amplified by polymerase chain reaction (PCR) using a thermocycler and DreamTaq (Thermo Fisher) polymerase. Used primers are listed in the material section and were diluted 1:40 in H_2O. For PCR reaction, 6.5 µL of water, 10 µL DreamTaq, and 2 µL of each primer were mixed with 1.5 µL of DNA and amplified using the following program: 5 min at 95 °C, 35 cycles of 1 min at 95 °C, 1 min at 56 °C, 1 min at 72°C, followed by a 10 min incubation at 72°C.

In order to assess the floxed status of the mice, DNA fragments were separated by agarose gel electrophoresis using a 2% agarose gel containing 1:10 000 SYBR Safe (APExBIO) in TAE buffer. DNA samples were mixed with 1x purple loading dye and separated at 80 V for 20-40 min. DNA bands were visualized using the GelDoc (BioRad). T cell specific knockout of FOXO1 led to a 300 bp long DNA fragment, while wildtype mice showed a band size of 247 bp. T cell specific knockout of the glucocorticoid receptor resulted in a band length of 250 bp, while wildtype mice showed a 200 bp band.

To investigate if mice were Cre+ or Cre-, DNA fragments were separated using Qiagen's QIAcxel Advanced system according to the manufacturer's instructions.

4.3   Animal Experiments

Mouse studies were performed using male BALB/cAnNCrl, C57BL/6J, or C57BL6/N mice, all obtained from Charles River Laboratories. Male C57BL/6J-APC[Min/+] mice were purchased from the Jackson Laboratory (JAX stock #002020) and bred on a C57BL/6J background. They were originally described by Moser and colleagues (Moser, 1990) and later established as model of cancer cachexia (Puppa, 2011). All mice were housed according to international standards under specific pathogen-free conditions on a 12 h light-dark cycle at 22 °C +/- ad libitum access to regular rodent chow diet (Provimi Kliba AG) and water if not stated otherwise. For aging studies, aged mice were either obtained by

Charles River Laboratories or aged in-house. Experiments were initiated when young adult mice had reached an age of 2-4 months, and aged mice an age of 15-20 months. Animal handling and experimentation were performed in accordance with the institutional animal welfare officer, and the necessary licenses were obtained from the state ethics committee and government of Upper Bavaria (nos. ROB-55.2-2532.Vet_02-16-136 and ROB-55.2-2532.Vet_02-18-93). In each animal experiment, mice were assigned to groups in a way that body weight was similar between groups of same age as confirmed by non-significant statistical analysis. The number of mice used for each experiment is indicated in the respective figure legends. Tumors and organs including epididymal and inguinal white adipose tissue (WAT), gastrocnemius (GC) muscles, liver, heart, spleen, inguinal lymph nodes (ingLNs), BAT, thymus and TA, EDL, Sol were collected, snap frozen, and stored at -80 °C until further analysis.

Cachexia models

Systemic effects involved in cancer cachexia were investigated using different mouse models of cachexia. Thus, either the genetic APC min (Puppa, 2011) model or tumor implantation models using subcutaneous implantation of either Colon26 (C26) or Lewis Lung Cancer (LLC) cells into syngeneic mice (Bonetto, 2016; Sherry, 1989; Tanaka, 1990), leading to tumor growth and subsequently cachexia within 3 weeks. To this end, mice were injected subcutaneously into the right flank with either 2 million Lewis lung cancer (LLC) or 1 million Colon26 (C26) cells, resuspended in 50 µL of of Dulbecco's phosphate-buffered saline (DPBS). 1 million NC26 cells were injected as tumor control, while non-tumor healthy control mice were injected with 50 µL DPBS (Thermo Fisher). Mice were monitored for 2-4 weeks after tumor cell implantation, and body weight, tumor growth, food intake and water intake were recorded daily. Tumor growth was monitored by caliper measurement, and tumor volume was calculated using the formula $V = \pi/6 \times 1.69 \times (L \times W)^{3/2}$ (Feldman, 2009), where L is the largest tumor diameter and W is the perpendicular tumor diameter. If not stated otherwise, mice were sacrificed in the morning without previous fasting. When one or more of the following four termination criteria were fulfilled, mice were sacrificed by an overdose of ketamine/xylazine: time after injection > 28 days, ulceration, tumor diameter > 1.5 cm, or cachexia as defined by body weight loss > 15% or body condition score (BCS) < 2 (Ullman-Culleré, 1999). The BC scoring technique was used to assess the overall health status of the mice during the course of the experiment as growing tumors can mask body weight changes as a result of their extensive growth. To this end, the amount of flesh covering bony protuberances of the mice was monitored and transformed into a score ranging from 1 to 5. While obese mice are defined with a BCS=5, mice with a BCS=1 are underconditioned and emaciated. Mice with a BCS=3 are categorized as being in an optimal condition, whereas a BCS= 2 already indicates undernourishment with segmentation of the vertebral column and distinct dorsal pelvic bones. In the C26 non-cachectic vs. NC26 non-cachectic experiment, mice were sacrificed 1 week post PBS/ tumor cell- injection to investigate if differences between NC26 and C26 tumor-bearing mice rely on cachexia development or are rather an artefact of the different cell lines used. In the C26 pre-cachexia vs. C26 cachexia study, the cachectic C26 tumor-bearing group was defined by a 10-15% body weight loss, whereas mice from the C26 pre-cachectic group had a similar tumor size to the cachectic mice but a non-significant loss of body weight at the moment of sacrifice. Thus, mice from both groups had a similar tumor size but suffered from a different degree of body weight loss. A C26 pre-cachectic control with a matching tumor size was euthanized on the same day as a cachectic C26 tumor-bearing mouse. A schematic overview of all mouse models can be found the results section.

T cell specific glucocorticoid receptor (GR) knockout mice

To assess the role of glucocorticoid signaling in T cells upon cancer cachexia, T cell specific glucocorticoid receptor (GR) knockout mice were generated. Male B6.Cg-Tg(Cd4-cre)1Cwi/BfluJ mice (JAX stock #022071) and female B6.129P2-Nr3c1tm2Gsc were kind gifts from Prof. Dr. Daniel and Prof. Dr. Uhlenhaut, respectively. Male CD4-Cre mice were on C57BL/6J background, while the exact substrain of the GR-flox mice is unknown. T cell specific GR knockout was assessed using specific primers for genotyping (see material section).

T cell specific FOXO1 knockout mice

To assess the role of FOXO1 signaling in T cells in cancer cachexia, T cell specific FOXO1 knockout mice were generated. Male B6.Cg-Tg(Cd4-cre)1Cwi/BfluJ mice (JAX stock #022071) and female FOXO1$^{tm1RdP/J}$ (JAX stock #024756) mice were kind gifts from Prof. Dr. Daniel and Prof. Dr. Uhlenhaut, respectively. Male CD4-Cre mice were on C57BL/6J background, while the substrain of female FOXO1 floxed mice was unknown. T cell specific FOXO1 knockout was confirmed by genotyping using specific primers for Cre and FOXO1 (see material section).

Fasting and 2-deoxy-D-glucose treatment

To investigate if T cell impairment upon cancer cachexia was a result of low circulating glucose levels due to fasting or anorexia, mice were fasted or treated with 2-deoxy-D-Glucose (2-DG) to mimic glucose deprivation. To this end, mice were either fasted for 16 h over night or injected two times at a 48 h interval intraperitoneally (i.p.) with 1000 mg/kg 2-DG diluted in PBS. Mice were deprived of food for 2 h after 2-DG injection and after final injection/ before sacrifice. Control mice were i.p. injected with 100 µL PBS and fasted for 2 h before sacrifice.

Reduction of plasma corticosterone levels using Aminoglutethimide (AG)

To effectively decrease circulating glucocorticoid levels in cachectic mice, the well-known corticosteroid synthesis inhibitor Aminoglutethimide (AG) was used. To this end, once tumors were palpable, C26 tumor-bearing and PBS control mice were i.p. injected with 0.4 mg/kg Aminoglutethimide (AG). Injections were conducted in the morning on a daily basis, with the aim to avoid the rise of glucocorticoids throughout the day (Teilmann, 2014). Aminoglutethimide was ordered from Santa Cruz, diluted to a 40 mg/mL stock solution using DMSO and aliquots were stored at -20°C until further use. Shortly before injection, AG was diluted with PBS, so that finally 0.4 mg AG in a volume of 100 µL were injected per mouse.

Body composition analysis using EchoMRI

Body weight of mice was determined directly before start, during the course and at the end of an experiment. To this end, body composition including fat and lean mass was assessed using magnetic resonance (EchoMRI; Zinsser Analytic GmbH).

Blood Plasma

After sacrificing mice by an overdose of ketamin/xylazine, blood was withdrawn from the vena cava, transferred into EDTA tubes (Kabe Labortechnik), and incubated for 15-30 min at room temperature. After centrifugation for 5 min at 2000 xg, 4 °C, plasma was divided into 50 µL aliquots, immediately snap frozen in liquid nitrogen and stored at -80 °C until further use.

Glucose Tolerance Test

A glucose tolerance test (GTT) was conducted to assess how quickly glucose, injected into the peritoneum of fasted mice, can be cleared from the blood, as functional insulin signaling leads to a

quicker lowering of glucose levels due to better glucose clearance from the blood stream. Mice were fasted for 6 h starting from 8 am in fresh cages without food before intraperitoneal injections (i.p.). Blood glucose was measured with a glucometer strip by nicking the tail with a razor blade. Mice were i.p. injected with 2 g D-glucose per kg body weight and blood glucose was assessed before and 15, 30, 60, 90 and 120 min post injection.

Mice for T cell isolation
Male wt BALB/c or C57BL/6J mice were purchased from Charles River and used for isolation of T cells from spleen at the age of 9-12 weeks.

Insulin Tolerance Test
An insulin tolerance test (ITT) was performed to assess if mice were insulin resistant. Mice were fasted 6 h for 6 h starting from 8 am before injection and body weight and basal blood glucose levels were measured with a glucometer stripe by nicking the tail with a razor blade. Mice were i.p. injected with 0.8 U of insulin per kg body weight, dissolved in 0.9% sodium chloride (VWR). Blood glucose levels were monitored before injection and 15, 30, 45, 60, 90 and 120 min post injection.

T cell Depletion
To analyze the impact of T cell functional responses on the development of cancer cachexia, BALB/c mice were injected with C26 tumor cells or PBS as a control and once tumors were palpable (after 8 days), $CD4^+$ and $CD8^+$ T cells were depleted using anti-mouse CD4 and CD8 antibodies (Bio X cell). Since $CD4^+$ T cell depletion reduced tumor growth in C26 tumor-bearing mice, a late anti-CD4 injection group was introduced, in which mice received their first anti-CD4 antibody 13 days post tumor cell injection. Thereby, we wanted to minimize effects on tumor growth that could influence cachexia development. To account for antibody injections, 200 μg of an isotype control antibody (Bio X cell), diluted in 200 μL pH7 dilution buffer were injected in the control group. 200 μg of anti-CD4 or anti-CD8 were i.p. injected in a volume of 200 μL of pH6.5 or pH7 dilution buffer, respectively. When a combination of both antibodies was injected, 200 μg of each antibody were diluted in 100 μL of the appropriate buffer and both solutions were mixed directly before injection. Antibodies were injected every third day and depletion was confirmed by flow cytometric analysis of blood samples collected from the tail vein using antibodies against CD3, CD4 and CD8 (see Material section for antibodies).

4.4   Biochemistry

Determination of Blood Glucose Levels
Blood glucose levels were determined in a drop of blood obtained from the tail vein using an automatic glucose monitor.

Determination of Plasma Parameters using Serum Analyzer
Total alanine aminotransferase, alkaline phosphatase, aspartate aminotransferase, cholesterol, LDL, glucose, NEFA, albumin, total protein, and triacylclycerol (TAG) plasma levels of mice were measured using a Beckman Coulter AU480 Chemistry Analyzer (Beckman Coulter).

Glucocorticoid Enzyme-linked-immunosorbent assay (ELISA)
Murine plasma corticosterone levels were determined using the Corticosterone ELISA kit (TECAN, IBL International GmbH) following the manufacturer's instructions. In brief, plasma samples were diluted 1:5 using standard 0 and 20 μL of each standard, control and sample were pipetted into the microtiter

wells, and 200 μL enzyme conjugate were added to each. The wells were mixed at 300 rpm and incubated for 60 min at RT wrapped in aluminium foil. The wells were washed three times with 200 mL wash solution per well and 100 μL of substrate solution were added. The plate was incubated for 15 min in the dark and the enzymatic reaction was stopped by adding 50 μL of stop solution to each well. The optical density (OD) was read at 450 nm using a plate reader. Corticosterone levels were then calculated according to the measured standard curve.

GDF15 ELISA

Human and murine circulating GDF15 levels were determined using specific ELISA kits (R&D Systems # DGD150 and MGD150, respectively) according to the manufacturer's instructions. Dilution of plasma samples for mouse and human GDF15 detection was optimized to 1/2 and 1/4, respectively.

IL6 ELISA

Murine plasma levels of IL6 were assessed using a specific ELISA kit (R&D Systems #M6000B) according to the manufacturer's instructions. Dilution of plasma samples for mouse IL6 detection was optimized to 2/5.

4.5   Human subjects

Gastrointestinal cancer patients (stages I-IV) were enrolled at the Surgical Clinic of the University Hospital of São Paulo, Brazil after signature of the fully informed consent. This study has been approved by the Ethics Committee on Research involving Human Subjects of the University of the São Paulo Biomedical Sciences Institute (CEP 1151/13 CAAE n 5493116.6.0000467) and by the University Hospital (CEP1390/14 CAAE n 54930116.6.3001.0076) and is in accordance with the Declaration of Helsinki. Patients that had a BMI > 29.9 kg/m^2, chronic anti-inflammatory therapy, AIDS, liver or kidney failure, chemotherapy treatment (at the time or recent past 5 years) or suffered from chronic inflammatory processes not being related to cachexia, were excluded from the study. Cancer patients were classified as weight stable or cachectic following Evans et al. (Evans, 2008). For plasma analysis, approximately 20 mL of blood were collected in a pre-surgical fast at the hospital. This study was conducted by M. Seelaender and her group at the University of São Paulo. Gene expression analysis of patient tumor samples was performed as described above.

A detailed description of the clinical meta-data and patient characteristics for the lipidomics and aging study can be found in (Morigny&Zuber, 2020) and (Geppert, 2021), respectively.

4.6   Statistical Analysis

Results from biological replicates were expressed as mean ± standard error of the mean (s.e.m.). All statistical analyses were performed using GraphPad Prism 9.2. Normality was tested using D'Agostino-Pearson and Shapiro–Wilk normality tests. Unpaired Student's t-tests or Mann-Whitney tests were performed to compare two conditions. Paired two-way analysis of variance (ANOVA) with Tukey's and Bonferroni post hoc tests were used to compare two variables. Statistical tests were two-sided. Linear regression analysis was performed to test the association between two variables. Log-rank (Mantel-Cox) test was used to compare time curves of cachexia development between groups. Pearson correlation matrices were conducted using ©OriginLab (Northampton, Massachusetts, USA). $p < 0.05$ was considered statistically significant.

5 MATERIAL

5.1 Buffer, Media and supplements

Buffer or Medium	Component	Concentration
Ammonium-Chloride-Potassium (ACK) lysis buffer	Ammonium chloride	0.15 M
	Potassium bicarbonate	1 mM
	Na_2-EDTA	0.1 mM
	Fill up to 1 L with water and sterile filter	
Cryopreservation Medium	RPMI + Medium	20%
	FCS	70%
	DMSO	10%
HBSS+	hanks balanced salt solution (HBSS)	
	heat inactivated FCS	5%
	HEPES (4-(2-hydroxyethyl)- 1-piperazineethanesulfonic acid)	10 mM
MACS-PBS	PBS	
	BSA	0.5%
	EDTA	2 mM
RPMI+ Medium	RPMI 1640, no glutamine	
	FCS	10%
	L-Glutamine	2 mM
	Penicillin/Streptomycin	1%
	β-Mercaptoethanol	50 µM
Seahorse Assay Medium	Seahorse XF RPMI Medium, pH 7.4	
	L-Glutamate	2 mM
	Sodium pyruvate	1 mM
	Glucose	25 mM
TBE buffer (10x)	Tris base	100 mM
	EDTA	1 mM
	Boric acid	90 mM
	pH 8.0	
Tumor Cell Medium	DMEM + 4.5 g/L D-Glucose + L-Glutamate	
	Fetal calf serum	10%
	Penicillin/Streptomycin	1%
	Sodium pyruvate	1mM
Tumor digestion medium	RPMI 1640	
	FCS	1%
	DNase I	200 µg/mL
	Collagenase IV	1.5 µg/mL
	$MgCl_2$	5 mM

5.2 Oligonucleotides and TaqMan probes

Oligonucleotide	Sequence 5' → 3'
Ccl4 fw	CATGAAGCTCTGCGTGTCT
Ccl4 rv	CTGCCGGGAGGTGTAA
Cre fw	ATGTTTAGCTGGCCCAAATGT
Cre rv	ACGAGTGATGAGGTTCGCA

Cx3cl1 fw	GCCGCGTTCTTCCATTTG
Cx3cl1 rv	TGGGATTCGTGAGGTCATCTT
Cxcl11 fw	AGGAAGGTCACAGCCATAGC
Cxcl11 rv	CGATCTCTGCCATTTTGACG
Cxcl9 fw	TGT GGA GTT CGA GGA ACC CT
Cxcl9 rv	TGC CTT GGC TGG TGC TG
FOXO1 fw	ACCACTCTGGACGGCATACT
FOXO1 rv	TGAGTCTGGGGCTAGTTTGA
GR 1	GGC ATG CAC ATT ACT GGC CTT CT
GR2	GTG TAG CAG CCA GCT TAC AGG A
GR3	CCT TCT CAT TCC ATG TCA GCA TGT

All TaqMan probes were purchased from Applied Biosystems.

Target species: Mouse					
TaqMan probe	**Assay ID**		**TaqMan probe**	**Assay ID**	
Abca1	Mm00442646_m1		**Hsl**	Mm00495359_m1	
Asah1	Mm00480021_m1		**Hspa5**	Mm00517691_m1	
Atf3	Mm00476032_m1		**Ifnγ**	Mm01168134_m1	
Atg12	Mm00503201_m1		**IL1b**	Mm00434228_m1	
Atg4	Mm04214755_s1		**Il1r2**	Mm00439629_m1	
Atg5	Mm01187303_m1		**Il2**	Mm00434256_m1	
Atgl	Mm00503040_m1		**IL6**	Mm00446190_m1	
Bcl2	Mm00477631_m1		**Itga4**	Mm01277951_m1	
Bnip3	Mm01275600_g1		**Itgal**	Mm00801807_m1	
Btg1	Mm02391761_m1		**Kdsr**	Mm01290268_m1	
Casp3	Mm01195085_m1		**Ki67**	Mm01278617_m1	
Casp9	Mm00516563_m1		**Ldha**	Mm01612132_g1	
Ccl2	Mm00441242_m1		**Mff**	Mm01273401_m1	
Cd161	Mm00824341_m1		**Mgl**	Mm00449274_m1	
Cd19	Mm00515420_m1		**Nos2**	Mm00440502_m1	
Cd205	Mm00522144_m1		**Nrf1**	Mm00447996_m1	
Cd3e	Mm01179194_m1		**Nrf2**	Mm00477784_m1	
Cd335	Mm01337324_g1		**Opa1**	Mm00453879_m1	
Cd36	Mm00432403_m1		**p62**	Mm00448091_m1	
Cd4	Mm00442754_m1		**Pcna**	Mm00448100_g1	
Cd68	Mm03047343_m1		**Pdcd1**	Mm00435532_m1	
Cd8a	Mm01188922_m1		**Pgc1**	Mm01208835_m1	
Cdkn1a	Mm00432448_m1		**Plin4**	Mm00491061_m1	
CerS2	Mm00504086_m1		**Sat1**	Mm00485911_g1	
Cers5	Mm00510998_m1		**Slc2a1**	Mm00441480_m1	
Cers6	Mm00556165_m1		**Smpd1**	Mm00448871_m1	

Cpt1α	Mm00550438_m1		**Sod2**	Mm01313000_m1
Ctsl	Mm00515597_m1		**Sptlc1**	Mm00447343_m1
Ddb1	Mm00497159_m1		**Sptlc2**	Mm00448871_m1
Ddit3	Mm00492097_m1		**St3gal5**	Mm00488237_m1
Degs1	Mm00492146_m1		**Tbp**	Mm01277042_m1
Degs2	Mm00510313_m1		**Tfam**	Mm00447485_m1
Adgre1	Mm00802529_m1		**Tnfα**	Mm00443258_m1
Fbxo32	Mm00499523_m1		**Tox**	Mm00455231_m1
FoxO3a	Mm01185722_m1		**Trim63**	Mm01185221_m1
Foxp3	Mm00475162_m1		**Tsc22d3**	Mm00726417_s1
Gadd34	Mm00435119_m1		**Ugcg**	Mm00495925_m1
Gdf15	Mm00442228_m1		**Xbp1**	Mm00457357_m1
Gzmb	Mm00442834_m1			

Target species: Human				
TaqMan probe	**Assay ID**		**TaqMan probe**	**Assay ID**
CD3E	Hs01062241_m1		**CD8a**	Hs00233520_m1
CD4	Hs01058407_m1		**FOXP3**	Hs01085834_m1

5.3   Antibodies

Antibodies for Flow Cytometry (target species: mouse)

Reactivity	Fluorochrome	Clone	Concentration	Manufacturer
Biotin anti-mouse CD3e		145-2C11	1:100	BioLegend, San Diego
CD3	PE-CF594	145-2C11	1:100	BioLegend, San Diego
CD4	A700	RM4-5	1:200	eBioscience, San Diego
CD62L	PE-Cy7	MEL-14	1:1000	BioLegend, San Diego
CD8	Qdot605	53-6.7	1:200	BioLegend, San Diego
CD8a	Pacific Blue	53-6.7	1:200	BioLegend, San Diego
eFluor450				Invitrogen, Karlsruhe
FC block mouseTruStain FcX™			1:50	BioLegend, San Diego
FOXP3	FITC	FJK-16s	1:200	eBioscience, San Diego
KI67	PE	16A8	1:200	BioLegend, San Diego
Streptavidin	PE		1:400	Invitrogen, Waltham
Streptavidin MicroBeads				Miltenyi Biotec, Bergisch Gladbach
Sytox Blue			1:1000	Invitrogen, Karlsruhe
Sytox Red			1:1000	Invitrogen, Karlsruhe

Antibodies for flow cytometry (target species: human)

Reactivity	Fluorochrome	Clone	Concentration	Manufacturer
CCR10	PE	6588-5	1:20	BioLegend, San Diego
CD10	APC-Cy7	HI10a	1:20	BioLegend, San Diego
CD11b	Pacific Blue	ICRF44	1:50	BioLegend, San Diego
CD11c	APC-Cy7	Bu15	1:50	BioLegend, San Diego
CD123	A700	6H6	1:50	BioLegend, San Diego
CD127	PE-Cy7	A019D5	1:20	BioLegend, San Diego
CD127	BV711	A019D5	1:20	BioLegend, San Diego
CD14	Pacific Blue	HCD14	1:50	BioLegend, San Diego
CD14	FITC	HCD14	1:50	BioLegend, San Diego
CD152 (CTLA4)	APC-Cy7	BNI3	1:20	BioLegend, San Diego
CD16	BV510	3G8	1:20	BioLegend, San Diego
CD19	Pacific Blue	HIB19	1:50	BioLegend, San Diego
CD19	BV500	HIB19	1:50	BioLegend, San Diego
CD19	PerCP-Cy5.5	HIB19	1:50	BioLegend, San Diego
CD194 (CCR4)	BV605	L291H4	1:20	BioLegend, San Diego
CD194 (CCR4)	R718	1G1	1:20	BD Bioscience, Franklin Lakes
CD196 (CCR6)	PE-Cy7	G034E3	1:20	BioLegend, San Diego
CD197 (CCR7)	BV711	150503	1:20	BD Biosciences, Franklin Lakes
CD20	FITC	2H7	1:20	BioLegend, San Diego
CD20	PE-Cy7	2H7	1:20	BioLegend, San Diego
CD24	PE-Cy7	ML5	1:20	BioLegend, San Diego
CD25	BV711	PC61	1:20	BioLegend, San Diego
CD27	APC	M-T271	1:20	BioLegend, San Diego
CD279 (PD1)	BV711	EH12.2H7	1:20	BioLegend, San Diego
CD28	FITC	CD28.2	1:20	BioLegend, San Diego
CD3	PerCP-Cy5.5	HIT3a	1:20	BioLegend, San Diego
CD3	Pacific Blue	HIT3a	1:20	BioLegend, San Diego
CD3 MicroBeads, human				Miltenyi Biotec, Bergisch Gladbach, # 130-050-101
CD38	A700	HIT2	1:20	BioLegend, San Diego
CD4	V500	RPA-T4	1:10	BD Bioscience, Franklin Lakes
CD45RA	BV605	HI100	1:20	BioLegend, San Diego
CD45RO	APC-H7	UCHL1	1:20	BD Bioscience, Franklin Lakes
CD56	APC	HCD56	1:50	BioLegend, San Diego
CD8	PE-Cy7	RPA-T8	1:50	BioLegend, San Diego
CD8A	FITC	RPA-T8	1:50	BioLegend, San Diego
CXCR3	APC-Cy7	G025H7	1:20	BioLegend, San Diego
CXCR5	APC	J252D4	1:20	BioLegend, San Diego
eFluor450				Invitrogen, Karlsruhe

FOXP3	A700	PCH101	1:100	eBioscience, San Diego
FOXP3	FITC	PCH101	1:20	eBioscience, San Diego
GLUT1	Alexa Fluor 647	EPR3915	1:50	Abcam, Cambridge
GZMB	PE	QA16A02	1:100	BioLegend, San Diego
HLA-DR	PE	L243	1:20	BioLegend, San Diego
HLA-DR	PerCP-Cy5.5	G46-6	1:20	BD Pharmingen™, San Diego
Human TruStain FcX™				BioLegend, San Diego
IFNG	APC	4S.B3	1:20	BioLegend, San Diego
IgD	PE	IA6-2	1:20	BioLegend, San Diego
IL2	PE/Dazzle594	MQ1-17H12	1:100	BioLegend, San Diego
KI67	PE/Dazzle594	Ki-67	1:100	BioLegend, San Diego
Sytox Blue			1:1000	Invitrogen, Karlsruhe
TNFA	PE-Cy7	MAb11	1:100	BioLegend, San Diego

Other Antibodies

Reactivity	Used concentration	Manufacturer
Anti- Mouse CD3e	5 µg/mL in vitro	BD Pharmingen™, San Diego
Anti-MO CD28 stimulation	5 µg/mL in vitro	Invitrogen, Karlsruhe
CD8 *InVivo*MAb, #BE0117	200 µg per mouse	Bio X cell, Lebanon
IgG2b isotype control, #BE0090	200 µg per mouse	Bio X cell, Lebanon
InVivoMAb anti-mouse CD4, # BE0003	200 µg per mouse	Bio X cell, Lebanon

5.4   Software

Software	Distributor
BioRender	BioRender, Toronto
Endnote	Thomson, Carlsbad
FACSDiva™ Software V6.1.3	BD Biosciences, Franklin Lakes
FlowJo Software V10.8.0	TreeStar Inc., Ashland
GraphPad Prism	GraphPad Software Inc., La Jolla, USA
Image Lab Software	Bio-Rad, Hercules
Ingenuity Pathway Analysis	Qiagen, Hilden
Microsoft Office	Microsoft, Unterschleißheim
Origin2021b	OriginLab, Northampton
QuantStudio Real-Time PCR Software	Applied Biosystems, Darmstadt
Seahorse Wave Desktop Software	Agilent Technologies, Santa Clara

5.5   Standard Kits

Kit	Distributor
CD4^{+} T Cell Isolation Kit, mouse	Miltenyi Biotec, Bergisch Gladbach
CD8a^{+} T Cell Isolation Kit, mouse	Miltenyi Biotec, Bergisch Gladbach

Corticosterone ELISA	TECAN, Männedorf
CyQUANT Cell Proliferation Assay Kit	Invitrogen, Karlsruhe
Cytofix/Cytoperm Plus Kit with BD GolgiP, #555028	BD Biosciences, Franklin Lakes
DNase I	Life Technologies, Darmstadt
Dreamtaq polymerase genotyping	Thermo Fisher, Waltham
eBioscience Foxp3 / Transcription Factor Staining Buffer Set	eBioscience, San Diego
Glucocorticoid ELISA	TECAN, IBL International GmbH
High-Capacity cDNA Reverse Transcription	Life Technolgies, Darmstadt
Human GDF15 ELISA kit, #DGD150	R&D Systems, Minneapolis
In Situ Cell Death Detection Kit, TMR Red	Roche, Basel
Murine GDF15 ELISA kit (m/rGDF-15 QKit), #MGD150	R&D Systems, Minneapolis
Murine IL6 ELISA kit (mIL-6 Qkit), #M6000B	R&D Systems, Minneapolis
Mycoplasm kit	Promokine, #PK-CA91-1048
RNeasy Plus Micro Kit	Qiagen, Hilden
RNeasy Plus Mini Kit	Qiagen, Hilden
Seahorse XFe96 FluxPaks (inc. mini)	Agilent Technologies, Santa Clara
Takyon^{TM} Low Rox Probe MasterMix dTTP Blue	Eurogentec, Köln

5.6   Consumables

Name	Distributor
2 mL Syringes, Discardit	BD, Franklin Lakes
3K Amicon Ultra Centrifugal Filter Units	Merck, Darmstadt
70 µM cell strainer, single packed	Fisher Scientific, Waltham
96 well cell culture plate	Thermo Fisher, Waltham
C-chip Neubauer improved	VWR International, Radnor
Cell culture dishes (5, 10 and 15 cm)	Thermo Fisher, Waltham
CombiTips Advanced (2.5, 5 and 10 mL)	Eppendorf, Hamburg
Countess® Cell counting chamer slide	Life Technologies, Darmstadt
DNase/ RNase free water	Invitrogen, Karlsruhe
Einmal-Insulinkanülen Sterican, G 30, 0,30 x 12 mm	B. Braun, Melsungen
Embedding cassette, Macro, white special polymer	Carl Roth, Karlsruhe
Facon^{TM} conical centrifugal Tubes (15 mL, 50 mL) Falcon	Fisher Scientific, Waltham
Filters (0.22 µm)	Millipore, Eschborn
Gloves (Safe Skin Purple Nitrile)	Kimberly Clark, BE
Glucometer Test strips Accu-Chek Inform II	Roche, Basel
Insulin syringes BD Microfine, 0.3 mL, 8mm	BD, Franklin Lakes
LS Columns	Miltenyi Biotec, Bergisch Gladbach
MicroAmp® Optical 384-well Reaction Plate	Applied Biosystems, Darmstadt
MicroAmp® Optical Adhesive Film	Applied Biosystems, Darmstadt
Parafilm	Pechinery Inc., Wisconsin
Pasteurpipettes, PE, sterile	Th. Geyer, Hamburg

SafeLock tubes (0.5, 1.5, 2.0, 5.0 mL)	Eppendorf, Hamburg
Sapphire PCR Tubes	Greiner Bio-One, Frickenhausen
S-Monovette® Lithium-Heparin, 9 ml, Verschluss orange, (LxØ): 92 x 16 mm, mit Kunststoffetikett	Sarstedt 02.1065
Stainless Steel Beads, 5 mm	Qiagen, Hilden
TipOne Filter Tips (10, 20, 100, 200 and 1000 µL)	StarLab, Hamburg

5.7 Chemicals and Reagents

Name	Distributor
2-deoxy-D-glucose	Sigma-Aldrich, St. Louis
Agarose	Sigma-Aldrich, St. Louis
Aminoglutethimide	Santa Cruz Biotechnology, Heidelberg
Ammonium chloride	Sigma-Aldrich, St. Louis
Antimycin A	Sigma-Aldrich, St. Louis
Boric acid	Sigma-Aldrich, St. Louis
Bovine Serum Albumine (BSA)	Sigma-Aldrich, St. Louis
CaCl2	Sigma-Aldrich, St. Louis
Chloroform	VWR International, Radnor
Collagenase II	Thermo Fisher, Waltham
Collagenase IV	Thermo Fisher, Waltham
CryoStor CS10 cell cryopreservation medium	Sigma-Aldrich, St. Louis
Dexamethasone	Sigma-Aldrich, St. Louis
D-Glucose	Sigma-Aldrich, St. Louis
Dimethyl sulfoxide (DMSO), cell culture grade	AppliChem GmbH, Darmstadt
DNase I	Roche, Basel
Dulbecco's Modified Eagle Medium (DMEM)	Thermo Fisher, Waltham
Dulbecco's phosphate buffered saline (DPBS)	Life Technologies, Darmstadt
EDTA	Carl Roth, Karlsruhe
Ethanol absolute	Merck, Darmstadt
FCCP (Carboyl cyanide 4-trifluoromethoxy)phenylhydrazone)	Sigma-Aldrich, St. Louis
Fetal bovine serum (FBS)	Invitrogen, Karlsruhe
Ficoll Paque PLUS	GE Healthcare
Hanks' Balanced Salt Solution	Sigma-Aldrich, St. Louis
Insulin human (recombinant yeast)	Sigma-Aldrich, St. Louis
Ionomycin	Biomol GmbH, Hamburg
L-Glutamine	Thermo Fisher, Waltham
L-Glutamine	Thermo Fisher, Waltham
Magnesium chloride (MgCl$_2$)	Sigma-Aldrich, St. Louis
Oligomycin	Sigma-Aldrich, St. Louis
Penicillin/Streptomycin, Gibco™	Invitrogen, Karlsruhe
pH7 buffer	Bio X cell, Lebanon
Phorbol 12-myristate 13-acetate (PMA), PKC activator	Abcam, Cambridge

Poly-D-lysine	Sigma-Aldrich, St. Louis
Potassium bicarbonate	Sigma-Aldrich, St. Louis
Purple loading dye (6X)	New England Biolabs, Frankfurt am Main
Rotenone	Sigma-Aldrich, St. Louis
Roti-Histofix 4%	Carl Roth, Karlsruhe
RPMI 1640 medium, GlutaMAX	Life Technologies, Darmstadt
Sodium hydroxide (NaOH)	Sigma-Aldrich, St. Louis
Sodium pyruvate	Invitrogen, Karlsruhe
SYBR Safe	APExBIO
SYBR Safe (APE-A8743)	APExBIO, Houston
Tris base	Sigma-Aldrich, St. Louis
Tris HCL (pH8)	Carl Roth, Karlsruhe
TRIzol™ Reagent	Invitrogen, Karlsruhe
XF RPMI Seahorse Medium	Agilent Technologies, Santa Clara
β-Mercaptoethanol	Sigma-Aldrich, St. Louis
2-Propanol, ≥99.5 %, Honeywell™	Thermo Fisher, Waltham
Trypan Blue solution, 0.4%	Sigma-Aldrich, St. Louis
Trypsin 0.05% EDTA	Fisher Scientific, Waltham
0.9% sodium chloride for injection	VWR International, Radnor
Seahorse XF RPMI Medium pH7.4	Agilent Technologies, Santa Clara
pH6.5 buffer	Bio X cell, Lebanon

5.8 Instruments

Name	Distributor
Analytical scales	Sartorius, Göttingen
Countess II Automated Cell Counter	Life Technologies, Darmstadt
EchoMRI Body Composition Analyzer	Zinsser Analytic GmbH, Eschborn
ECLIPSE Ts2-FL Microscope	Nikon, Amsterdam
Eppendorf Concentrator Plus (Vacuum dryer)	Eppendorf, Hamburg
FACS Aria III	BD Biosciences, Franklin Lakes
Freezer, -20 °C	Liebherr, Biberach
Freezer, -80°C	Thermo Fisher, Waltham
Fridge, 4°C	Liebherr, Biberach
GelDoc	Bio-Rad, Hercules
Glucometer Accu-Chek Performa	Roche, Basel
Heat Block (Thermostat Plus), ThermoMixer	Eppendorf, Hamburg
Incubator CO_2	Thermo Fisher, Waltham
Microplate shaker	VWR International, Radnor
Mr Frosty Freezing Container	Thermo Fisher, Waltham
Multichannel Stepper Voyager	INTEGRA Biosciences AG, Biebertal
Multipipette E3	Eppendorf, Hamburg

NanoDrop2000	Thermo Fisher Scientific, Dreieich
Neubauer Counting Chamber	Marienfeld GmbH, Lauda-Königshofen
pH-meter	VWR International, Radnor
Pipettes (10, 20, 100, 200 and 1000 µL)	Eppendorf, Hamburg
QIAxcel Advanced system	Qiagen, Hilden
QuadroMACS Separator	Miltenyi Biotec, Bergisch Gladbach
QuantStudio 6 Flex-Real-Time PCR System	Applied Biosystems, Darmstadt
QuantStudio 7 Flex-Real-Time PCR System	Applied Biosystems, Darmstadt
Seahorse XF Prep Station	Agilent Technologies, Santa Clara
Seahorse XFe96 Extracellular Flux Analyzer	Agilent Technologies, Santa Clara
Table Centrifuge	Thermo Fisher, Waltham
Table Centrifuge 5702 R	Eppendorf, Hamburg
Thermocycler PCR	Applied Biosystems, Darmstadt
TissueLyser II	Qiagen, Hilden
Tube Rotator	VWR International, Radnor
Vacuum pump	Neolab, Heidelberg
Varioskan™ LUX multimode microplate reader	Thermo Fisher, Waltham
Vortex-Genie 2	Scientific Industries Inc., New York
Water bath	Neolab, Heidelberg

6 APPENDIX

6.1 Author contributions

6.1.1 First-author publications

In the following section, my individual contribution to my two peer-reviewed first-author papers will be listed.

Morigny P.*, **Zuber J.***, Haid M., Kaltenecker D., Riols F., Lima J. D. C., Simoes E., Otoch J. P., Schmidt S. F., Herzig S., Adamski J., Seelaender M., Berriel Diaz M., and Rohm M. (2020). High levels of modified ceramides are a defining feature of murine and human cancer cachexia. Journal of Cachexia, Sarcopenia and Muscle, 11, 1459–1475, 10.1002/jcsm.12626

*equal contribution

The aforementioned study was conducted in collaboration with Dr. Pauline Morigny with equal contribution by both of us. In detail, my individual contributions to this paper are as follows:

Major contribution to the conduction of all *in vivo* studies that are shown in the paper with support from Dr. Pauline Morigny and Dr. Doris Kaltenecker, shared analysis of all lipidomics data and visualization of these, shared performance of qPCRs. I performed the analyses of patient characteristics. Finally, drafting and writing of the manuscript was performed by Dr. Pauline Morigny and me. Conceptualization of the manuscript was performed together with Dr. Maria Rohm, Dr. Mauricio Berriel Diaz, Dr. Pauline Morigny and me. All co-authors were involved in aspects of scientific discussion, interpretation of the results and reviewed the manuscript.

Geppert J., Walth A.A., Terrón Expósito R., Kaltenecker D., Morigny P. Machado J., Becker M., Simoes E., Lima J.D.C., Daniel C., Berriel Diaz M., Herzig S., Seelaender M., Rohm M. (2021). Aging Aggravates Cachexia in Tumor-Bearing Mice. *Cancers (Basel), 14*(1). doi:10.3390/cancers14010090

I have contributed to this paper as follows:

I performed the in vivo studies with support from Alina Walth, Dr. Doris Kaltenecker and Dr. Pauline Morigny. Moreover, I performed all experiments that are displayed in the paper except for western blots, which were conducted by Alina Walth and staining of muscle sections and quantification of the cross-sectional area in gastrocnemius muscles, which was performed by Dr. Juliano Machado. Patient data were collected and patient parameters (expect for GDF15 and IL6) assessed by Dr. Estefania Simoes Fernandez, Dr. Joanna D.C.C. Lima and Dr. Marilia Seelaender, while I conducted the analyses for the paper. Data analysis and plotting for all experiments were performed by me. Dr. Maria Rohm and I conceptualized the manuscript and finally, Dr. Rohm wrote the manuscript draft, which was reviewed and edited by Dr. Rohm and me.

6.1.2 Additional publications

Peer-reviewed publications:

Karabid N. M.*, Wiedemann T.*, Gulde S., Mohr H., Segaran R. C., **Geppert J.**, Rohm M., Vitale G., Gaudenzi G., Dicitore A., Ankerst D. P., Chen Y., Braren R., Kaissis G., Schilling F., Schillmaier M., Eisenhofer G., Herzig S., Roncaroli F., Honegger J. B., Pellegata N. S. (2022). Angpt2/Tie2 autostimulatory loop controls tumorigenesis. *EMBO Mol Med*, e14364. doi:10.15252/emmm.202114364

Morigny P., Kaltenecker D., **Zuber J.,** Machado J., Mehr L., Tsokanos F. F., Kuzi H., Hermann C. D., Voelkl M., Monogarov G., Springfeld C., Laurent V., Engelmann B., Friess H., Zörnig I., Krüger A., Krijgsveld J., Prokopchuk O., Fisker Schmidt S., Rohm M., Herzig S., Berriel Diaz M. (2021). Association of circulating PLA2G7 levels with cancer cachexia and assessment of darapladib as a therapy. *J Cachexia Sarcopenia Muscle, 12*(5), 1333-1351. doi:10.1002/jcsm.12758

Fischer K, Rieblinger B, Hein R, Sfriso R, **Zuber J**, Fischer A, Klinger B, Liang W, Flisikowski K, Kurome M, Zakhartchenko V, Kessler B, Wolf E, Rieben R, Schwinzer R, Kind A, Schnieke A. (2020). Viable pigs after simultaneous inactivation of porcine MHC class I and three xenoreactive antigen genes GGTA1, CMAH and B4GALNT2. Xenotransplantation, 27:e12560

Posters presented at international conferences:

Zuber J., Morigny P., Haid M., Seelaender M., Berriel Diaz M., Rohm M. Circulating lipids are defining features of murine and human cancer cachexia. *13th International SCWD Digital Conference on Cachexia, Sarcopenia and Muscle Wasting.* **2020** Dec 11-13; online.

Zuber J., Morigny P., Haid M., Seelaender M., Herzig S., Berriel Diaz M., Rohm M. Circulating lipids are defining features of murine and human cancer cachexia. *6th Cancer Cachexia Conference: Bridging Molecular Advances to Clinical Care*. **2021** Aug 27-29; online.

6.2   Glossary

2-DG	2-Deoxyglucose	CTL	Cytotoxic T lymphocyte
Abca1	ATP Binding Cassette Subfamily A Member 1	CTLA4	cytotoxic T lymphocyte-associated antigen-4
ACTH	adrenocorticotropic hormone	Ctsl	Cathepsin-L
AG	Aminoglutethimide	DAG	diacylglycerol
AKT	protein kinase B	DEGs	differentially expressed genes
AP1	adaptor-related protein complex 1	ECAR	extracellular acidification rate
APC	adenomatous polyposis coli	EchoMRI	Echo magnetic resonance imaging
APCs	antigen-presenting cells	Eomes	Eomesodermin
APPR	acute phase protein response	ERK	extracellular-signal-regulated kinase
APPs	acute phase proteins	ESPEN	European Society of Clinical Nutrition and Metabolism
ATGL	adipose triglyceride lipase	eWAT	epididymal white adipose tissue
ATP	Adenosine triphosphate	FAO	fatty acid oxidation
Bcl6	BCL6 transcription repressor	FasL	Fas ligand
BMI	Body Mass Index	FFAs	free fatty acids
Btg1	B-Cell Translocation Gene 1	FoxO	Forkhead-box O
C26	Colon26	FOXP3	forkhead box P3
cAMP	Cyclic adenosine monophosphate	GAPDH	glyceraldehyde-3-phosphate dehydrogenase
CAR T cell	chimeric antigen receptor T cell	GATA3	GATA binding protein 3
CCR2	C-C motif chemokine receptor 2	GCs	glucocorticoids
CCR7	C-C motif chemokine receptor 7	GDF15	Growth Differentiation Factor 15
CERs	ceramides	GFRAL	GDNF receptor alpha-like
CM	conditioned medium	GILZ	Glucocorticoid-induced leucine zipper
Cpt1a	Carnitine Palmitoyltransferase 1A	GLUT1	Glucose Transporter 1
CRAC	calcium release-activated Ca2+ channels	GR	Glucocorticoid receptor
CRH	corticotropin releasing hormone	GZMB	granzyme B

HSL	hormone sensitive lipase		OCR	oxygen consumption rate
ICI	Immune checkpoint inhibitor		OXPHOS	oxidative phosphorylation
HCERs	hexosyl-ceramides		PD1	Programmed cell death 1
HDL	High density lipoprotein		PKCθ	protein kinase Cθ
HIF	Hypoxia Inducible Factor		PLCγ1	phospholipase C γ1
IFNγ	interferon gamma		Plin4	Perilipin 4
IL	Interleukin		POMC	proopiomelanocortin
IL-1R2	Interleukin 1 Receptor Type 2		PP2A	protein phosphatase 2A
IL2Rα	interleukin 2 receptor α chain		PTHrP	parathyroid hormone-related protein
ImpL2	secreted insulin/IGF antagonist		Raptor	regulatory associated protein of mTOR
IP3	inositol triphosphate		RasGRP1	Ras Guanyl-Releasing Protein 1
IPA	ingenuity pathway analysis		REE	resting energy expenditure
irAEs	Immune-related adverse effects		Rictor	rapamycin-insensitive companion of mTOR
ITAMs	immunoreceptor tyrosine based activation motifs		RORγt	retinoic acid-related orphan receptor γt
Itga4	Integrin Subunit Alpha 4		S1pr1	Sphingosine-1-Phosphate Receptor 1
Itgal	Integrin Subunit Alpha L		Sat1	Spermidine/Spermine N1-Acetyltransferase 1
iWAT	Inguinal white adipose tissue		SCID	Severe combined immune deficiency
JAK	Janus Kinase		SCWD	sarcopenia, cachexia and wasting disorders
KEGG	Kyoto Encyclopedia of Genes and Genomes		Slc2a1	Solute Carrier Family 2 Member 1
Klf2	Krupple-like factor 2		SLP76	SH2 domain containing leukocytes protein 76 kDa
KPC	K-rasLSL.G12D/+; Trp53R172H/+; Pdx-1-Cre mutation		SMs	sphingomyelines
LAG3	lymphocyte activation gene 3		STAT5	signal transducer and activator of transcription 5
LAT	linker of activated T cells		TAG	triacylglycerol
LCK	lymphocyte-specific protein tyrosine kinase		TCM	central memory T cell
Ldha	Lactate Dehydrogenase A		TCR	T cell receptor
LDL	low density lipoprotein		TEM	effector memory T cell
LLC	Lewis Lung Carcinoma		Tfh	follicular helper T cells
LMF	lipid-mobilizing factor		TG	triglyceride
LPCs	Lysophosphatidylcholines		TGFβ	transforming growth factor beta 1
LPL	lipogenic enzyme lipoprotein lipase		Th cell	T helper cell
MAFbx	muscle atrophy F box		TIGIT	T cell immunoglobulin and ITIM domain
MAPK	Mitogen activated protein kinase		TILs	tumor-infiltrating lymphocytes
MDSCs	myeloid-derived suppressor cells		TME	Tumor microenvironment
MGL	monoglyceride lipase		TNFα	tumor necrosis factor alpha
MHC	major histocompatibility complex		TOX	thymocyte selection-associated high mobility group box
Min	multiple intestinal neoplasia		Tregs	regulatory T cells
MKP1	MAP kinase phosphatase-1		Tsc22d3	TSC22 Domain Family Member 3
mTOR	Mechanistic Target Of Rapamycin Kinase		TSC22D4	TSC22 Domain Family Member 4
mTORC2	mTOR complex 2		TUNEL	terminal deoxynucleotidyl transferase dUTP nick end labeling
MuRF1	muscle RING finger 1		Ucp1	uncoupling protein 1
ndLNs	non-draining lymph nodes		UPR	ubiquitin-mediated proteasome degradation
NEFA	non-esterified fatty acid		UTR	untranslated region
NFAT	nuclear factor of activated T cells		VAV1	guanine nucleotide exchange factor 1
NFκB	nuclear factor 'kappa-light-chain-enhancer' of activated B-cells		WAT	White adipose tissue
NK cell	natural killer cell		ZAG	zinc-alpha-2-glycoprotein
NPY	neuropeptide Y		ZAP70	Zeta-chain-associated protein kinase 70
NR4A	nuclear receptor subfamily 4A			

6.3 Figures and Tables

Figures

Tables

6.4 References

Aburasayn, H., Al Batran, R., & Ussher, J. R. (2016). Targeting ceramide metabolism in obesity. *Am J Physiol Endocrinol Metab, 311*(2), E423-435. doi:10.1152/ajpendo.00133.2016

Acharya, N., Madi, A., Zhang, H., Klapholz, M., Escobar, G., Dulberg, S., . . . Anderson, A. C. (2020). Endogenous Glucocorticoid Signaling Regulates CD8(+) T Cell Differentiation and Development of Dysfunction in the Tumor Microenvironment. *Immunity, 53*(3), 658-671.e656. doi:10.1016/j.immuni.2020.08.005

Adams, V., Gußen, V., Zozulya, S., Cruz, A., Moriscot, A., Linke, A., & Labeit, S. (2020). Small-Molecule Chemical Knockdown of MuRF1 in Melanoma Bearing Mice Attenuates Tumor Cachexia Associated Myopathy. *Cells, 9*(10). doi:10.3390/cells9102272

Agustsson, T., Rydén, M., Hoffstedt, J., van Harmelen, V., Dicker, A., Laurencikiene, J., . . . Arner, P. (2007). Mechanism of increased lipolysis in cancer cachexia. *Cancer Res, 67*(11), 5531-5537. doi:10.1158/0008-5472.Can-06-4585

Alberti, S., Cevenini, E., Ostan, R., Capri, M., Salvioli, S., Bucci, L., . . . Monti, D. (2006). Age-dependent modifications of Type 1 and Type 2 cytokines within virgin and memory CD4+ T cells in humans. *Mech Ageing Dev, 127*(6), 560-566. doi:10.1016/j.mad.2006.01.014

Alimonti, J. B., Shi, L., Baijal, P. K., & Greenberg, A. H. (2001). Granzyme B induces BID-mediated cytochrome c release and mitochondrial permeability transition. *J Biol Chem, 276*(10), 6974-6982. doi:10.1074/jbc.M008444200

Allan, S. E., Crome, S. Q., Crellin, N. K., Passerini, L., Steiner, T. S., Bacchetta, R., . . . Levings, M. K. (2007). Activation-induced FOXP3 in human T effector cells does not suppress proliferation or cytokine production. *Int Immunol, 19*(4), 345-354. doi:10.1093/intimm/dxm014

Allavena, P., Germano, G., Marchesi, F., & Mantovani, A. (2011). Chemokines in cancer related inflammation. *Exp Cell Res, 317*(5), 664-673. doi:10.1016/j.yexcr.2010.11.013

Amarnath, S., Mangus, C. W., Wang, J. C., Wei, F., He, A., Kapoor, V., . . . Fowler, D. H. (2011). The PDL1-PD1 axis converts human TH1 cells into regulatory T cells. *Sci Transl Med, 3*(111), 111ra120. doi:10.1126/scitranslmed.3003130

Anderson, L. J., Lee, J., Anderson, B., Lee, B., Migula, D., Sauer, A., . . . Garcia, J. M. (2022). Whole-body and adipose tissue metabolic phenotype in cancer patients. *J Cachexia Sarcopenia Muscle, 13*(2), 1124-1133. doi:10.1002/jcsm.12918

Ando, K., Takahashi, F., Kato, M., Kaneko, N., Doi, T., Ohe, Y., . . . Takahashi, K. (2014). Tocilizumab, a proposed therapy for the cachexia of Interleukin6-expressing lung cancer. *PLoS One, 9*(7), e102436. doi:10.1371/journal.pone.0102436

Anoveros-Barrera, A., Bhullar, A. S., Stretch, C., Dunichand-Hoedl, A. R., Martins, K. J. B., Rieger, A., . . . Mazurak, V. C. (2019). Immunohistochemical phenotyping of T cells, granulocytes, and phagocytes in the muscle of cancer patients: association with radiologically defined muscle mass and gene expression. *Skelet Muscle, 9*(1), 24. doi:10.1186/s13395-019-0209-y

Appleman, L. J., van Puijenbroek, A. A., Shu, K. M., Nadler, L. M., & Boussiotis, V. A. (2002). CD28 costimulation mediates down-regulation of p27kip1 and cell cycle progression by activation of the PI3K/PKB signaling pathway in primary human T cells. *J Immunol, 168*(6), 2729-2736. doi:10.4049/jimmunol.168.6.2729

Araki, K., Turner, A. P., Shaffer, V. O., Gangappa, S., Keller, S. A., Bachmann, M. F., . . . Ahmed, R. (2009). mTOR regulates memory CD8 T-cell differentiation. *Nature, 460*(7251), 108-112. doi:10.1038/nature08155

Arbonés, M. L., Ord, D. C., Ley, K., Ratech, H., Maynard-Curry, C., Otten, G., . . . Tedder, T. F. (1994). Lymphocyte homing and leukocyte rolling and migration are impaired in L-selectin-deficient mice. *Immunity, 1*(4), 247-260. doi:10.1016/1074-7613(94)90076-0

Arbour, K. C., Mezquita, L., Long, N., Rizvi, H., Auclin, E., Ni, A., . . . Hellmann, M. D. (2018). Impact of Baseline Steroids on Efficacy of Programmed Cell Death-1 and Programmed Death-Ligand 1 Blockade in Patients With Non-Small-Cell Lung Cancer. *J Clin Oncol, 36*(28), 2872-2878. doi:10.1200/jco.2018.79.0006

Argiles, J. M., Busquets, S., Stemmler, B., & Lopez-Soriano, F. J. (2014). Cancer cachexia: understanding the molecular basis. *Nat Rev Cancer, 14*(11), 754-762. doi:10.1038/nrc3829

Argilés, J. M., Campos, N., Lopez-Pedrosa, J. M., Rueda, R., & Rodriguez-Mañas, L. (2016). Skeletal Muscle Regulates Metabolism via Interorgan Crosstalk: Roles in Health and Disease. *J Am Med Dir Assoc, 17*(9), 789-796. doi:10.1016/j.jamda.2016.04.019

Argilés, J. M., & López-Soriano, F. J. (1991). The energy state of tumor-bearing rats. *J Biol Chem, 266*(5), 2978-2982.

Arpaia, N., Green, J. A., Moltedo, B., Arvey, A., Hemmers, S., Yuan, S., . . . Rudensky, A. Y. (2015). A Distinct Function of Regulatory T Cells in Tissue Protection. *Cell, 162*(5), 1078-1089. doi:10.1016/j.cell.2015.08.021

Asseman, C., Mauze, S., Leach, M. W., Coffman, R. L., & Powrie, F. (1999). An essential role for interleukin 10 in the function of regulatory T cells that inhibit intestinal inflammation. *J Exp Med, 190*(7), 995-1004. doi:10.1084/jem.190.7.995

Au, E. D., Desai, A. P., Koniaris, L. G., & Zimmers, T. A. (2016). The MEK-Inhibitor Selumetinib Attenuates Tumor Growth and Reduces IL-6 Expression but Does Not Protect against Muscle Wasting in Lewis Lung Cancer Cachexia. *Front Physiol, 7*, 682. doi:10.3389/fphys.2016.00682

Aversa, Z., Pin, F., Lucia, S., Penna, F., Verzaro, R., Fazi, M., . . . Muscaritoli, M. (2016). Autophagy is induced in the skeletal muscle of cachectic cancer patients. *Sci Rep, 6*, 30340. doi:10.1038/srep30340

Ayroldi, E., Migliorati, G., Bruscoli, S., Marchetti, C., Zollo, O., Cannarile, L., . . . Riccardi, C. (2001). Modulation of T-cell activation by the glucocorticoid-induced leucine zipper factor via inhibition of nuclear factor kappaB. *Blood, 98*(3), 743-753. doi:10.1182/blood.v98.3.743

Ayroldi, E., Zollo, O., Bastianelli, A., Marchetti, C., Agostini, M., Di Virgilio, R., & Riccardi, C. (2007). GILZ mediates the antiproliferative activity of glucocorticoids by negative regulation of Ras signaling. *J Clin Invest, 117*(6), 1605-1615. doi:10.1172/jci30724

Baazim, H., Schweiger, M., Moschinger, M., Xu, H., Scherer, T., Popa, A., . . . Bergthaler, A. (2019). CD8(+) T cells induce cachexia during chronic viral infection. *Nat Immunol, 20*(6), 701-710. doi:10.1038/s41590-019-0397-y

Bachmann, M. F., & Oxenius, A. (2007). Interleukin 2: from immunostimulation to immunoregulation and back again. *EMBO Rep, 8*(12), 1142-1148. doi:10.1038/sj.embor.7401099

Baldwin, C., Spiro, A., Ahern, R., & Emery, P. W. (2012). Oral nutritional interventions in malnourished patients with cancer: a systematic review and meta-analysis. *J Natl Cancer Inst, 104*(5), 371-385. doi:10.1093/jnci/djr556

Baltgalvis, K. A., Berger, F. G., Pena, M. M., Davis, J. M., Muga, S. J., & Carson, J. A. (2008). Interleukin-6 and cachexia in ApcMin/+ mice. *Am J Physiol Regul Integr Comp Physiol, 294*(2), R393-401. doi:10.1152/ajpregu.00716.2007

Baniyash, M. (2004). TCR zeta-chain downregulation: curtailing an excessive inflammatory immune response. *Nat Rev Immunol, 4*(9), 675-687. doi:10.1038/nri1434

Barata, J. T., Silva, A., Brandao, J. G., Nadler, L. M., Cardoso, A. A., & Boussiotis, V. A. (2004). Activation of PI3K is indispensable for interleukin 7-mediated viability, proliferation, glucose use, and growth of T cell acute lymphoblastic leukemia cells. *J Exp Med, 200*(5), 659-669. doi:10.1084/jem.20040789

Barker, T., Fulde, G., Moulton, B., Nadauld, L. D., & Rhodes, T. (2020). An elevated neutrophil-to-lymphocyte ratio associates with weight loss and cachexia in cancer. *Sci Rep, 10*(1), 7535. doi:10.1038/s41598-020-64282-z

Barnes, S. E., Wang, Y., Chen, L., Molinero, L. L., Gajewski, T. F., Evaristo, C., & Alegre, M. L. (2015). T cell-NF-κB activation is required for tumor control in vivo. *J Immunother Cancer, 3*(1), 1. doi:10.1186/s40425-014-0045-x

Barry, M., Heibein, J. A., Pinkoski, M. J., Lee, S. F., Moyer, R. W., Green, D. R., & Bleackley, R. C. (2000). Granzyme B short-circuits the need for caspase 8 activity during granule-mediated cytotoxic T-lymphocyte killing by directly cleaving Bid. *Mol Cell Biol, 20*(11), 3781-3794. doi:10.1128/mcb.20.11.3781-3794.2000

Barthlott, T., Moncrieffe, H., Veldhoen, M., Atkins, C. J., Christensen, J., O'Garra, A., & Stockinger, B. (2005). CD25+ CD4+ T cells compete with naive CD4+ T cells for IL-2 and exploit it for the induction of IL-10 production. *Int Immunol, 17*(3), 279-288. doi:10.1093/intimm/dxh207

Bates, G. J., Fox, S. B., Han, C., Leek, R. D., Garcia, J. F., Harris, A. L., & Banham, A. H. (2006). Quantification of regulatory T cells enables the identification of high-risk breast cancer patients and those at risk of late relapse. *J Clin Oncol, 24*(34), 5373-5380. doi:10.1200/jco.2006.05.9584

Batista, M. L., Jr., Henriques, F. S., Neves, R. X., Olivan, M. R., Matos-Neto, E. M., Alcantara, P. S., . . . Seelaender, M. (2016). Cachexia-associated adipose tissue morphological rearrangement in gastrointestinal cancer patients. *J Cachexia Sarcopenia Muscle, 7*(1), 37-47. doi:10.1002/jcsm.12037

Beck, K. E., Blansfield, J. A., Tran, K. Q., Feldman, A. L., Hughes, M. S., Royal, R. E., . . . Yang, J. C. (2006). Enterocolitis in patients with cancer after antibody blockade of cytotoxic T-lymphocyte-associated antigen 4. *J Clin Oncol, 24*(15), 2283-2289. doi:10.1200/jco.2005.04.5716

Beheshti, A., Benzekry, S., McDonald, J. T., Ma, L., Peluso, M., Hahnfeldt, P., & Hlatky, L. (2015). Host age is a systemic regulator of gene expression impacting cancer progression. *Cancer Res, 75*(6), 1134-1143. doi:10.1158/0008-5472.Can-14-1053

Ben-Sasson, S. Z., Hogg, A., Hu-Li, J., Wingfield, P., Chen, X., Crank, M., . . . Paul, W. E. (2013). IL-1 enhances expansion, effector function, tissue localization, and memory response of antigen-specific CD8 T cells. *J Exp Med, 210*(3), 491-502. doi:10.1084/jem.20122006

Bense, R. D., Sotiriou, C., Piccart-Gebhart, M. J., Haanen, J., van Vugt, M., de Vries, E. G. E., . . . Fehrmann, R. S. N. (2017). Relevance of Tumor-Infiltrating Immune Cell Composition and Functionality for Disease Outcome in Breast Cancer. *J Natl Cancer Inst, 109*(1). doi:10.1093/jnci/djw192

Bental, M., & Deutsch, C. (1993). Metabolic changes in activated T cells: an NMR study of human peripheral blood lymphocytes. *Magn Reson Med, 29*(3), 317-326. doi:10.1002/mrm.1910290307

Berardi, E., Aulino, P., Murfuni, I., Toschi, A., Padula, F., Scicchitano, B. M., . . . Adamo, S. (2008). Skeletal muscle is enriched in hematopoietic stem cells and not inflammatory cells in cachectic mice. *Neurol Res, 30*(2), 160-169. doi:10.1179/174313208x281046

Berben, L., Floris, G., Wildiers, H., & Hatse, S. (2021). Cancer and Aging: Two Tightly Interconnected Biological Processes. *Cancers (Basel), 13*(6). doi:10.3390/cancers13061400

Bernhard, H., Meyer zum Büschenfelde, K. H., & Dippold, W. G. (1989). Ganglioside GD3 shedding by human malignant melanoma cells. *Int J Cancer, 44*(1), 155-160. doi:10.1002/ijc.2910440127

Berriel Diaz, M., Krones-Herzig, A., Metzger, D., Ziegler, A., Vegiopoulos, A., Klingenspor, M., . . . Herzig, S. (2008). Nuclear receptor cofactor receptor interacting protein 140 controls hepatic triglyceride metabolism during wasting in mice. *Hepatology, 48*(3), 782-791. doi:10.1002/hep.22383

Besedovsky, H. O., del Rey, A., Klusman, I., Furukawa, H., Monge Arditi, G., & Kabiersch, A. (1991). Cytokines as modulators of the hypothalamus-pituitary-adrenal axis. *J Steroid Biochem Mol Biol, 40*(4-6), 613-618. doi:10.1016/0960-0760(91)90284-c

Bhat, P., Leggatt, G., Waterhouse, N., & Frazer, I. H. (2017). Interferon-γ derived from cytotoxic lymphocytes directly enhances their motility and cytotoxicity. *Cell Death Dis, 8*(6), e2836. doi:10.1038/cddis.2017.67

Bindels, L. B., Neyrinck, A. M., Claus, S. P., Le Roy, C. I., Grangette, C., Pot, B., . . . Delzenne, N. M. (2016). Synbiotic approach restores intestinal homeostasis and prolongs survival in leukaemic mice with cachexia. *Isme j, 10*(6), 1456-1470. doi:10.1038/ismej.2015.209

Bing, C., Bao, Y., Jenkins, J., Sanders, P., Manieri, M., Cinti, S., . . . Trayhurn, P. (2004). Zinc-alpha2-glycoprotein, a lipid mobilizing factor, is expressed in adipocytes and is up-regulated in mice with cancer cachexia. *Proc Natl Acad Sci U S A, 101*(8), 2500-2505. doi:10.1073/pnas.0308647100

Bishop, E. L., Gudgeon, N., & Dimeloe, S. (2021). Control of T Cell Metabolism by Cytokines and Hormones. *Front Immunol, 12*, 653605. doi:10.3389/fimmu.2021.653605

Biswas, S., Biswas, K., Richmond, A., Ko, J., Ghosh, S., Simmons, M., . . . Finke, J. H. (2009). Elevated levels of select gangliosides in T cells from renal cell carcinoma patients is associated with T cell dysfunction. *J Immunol, 183*(8), 5050-5058. doi:10.4049/jimmunol.0900259

Blachère, N. E., Morris, H. K., Braun, D., Saklani, H., Di Santo, J. P., Darnell, R. B., & Albert, M. L. (2006). IL-2 is required for the activation of memory CD8+ T cells via antigen cross-presentation. *J Immunol, 176*(12), 7288-7300. doi:10.4049/jimmunol.176.12.7288

Blagih, J., Coulombe, F., Vincent, E. E., Dupuy, F., Galicia-Vazquez, G., Yurchenko, E., . . . Jones, R. G. (2015). The energy sensor AMPK regulates T cell metabolic adaptation and effector responses in vivo. *Immunity, 42*(1), 41-54. doi:10.1016/j.immuni.2014.12.030

Bodenreider, O., Hayamizu, T. F., Ringwald, M., De Coronado, S., & Zhang, S. (2005). Of mice and men: aligning mouse and human anatomies. *AMIA Annu Symp Proc, 2005*, 61-65.

Bodine, S. C., Latres, E., Baumhueter, S., Lai, V. K., Nunez, L., Clarke, B. A., . . . Glass, D. J. (2001). Identification of ubiquitin ligases required for skeletal muscle atrophy. *Science, 294*(5547), 1704-1708. doi:10.1126/science.1065874

Bonetto, A., Rupert, J. E., Barreto, R., & Zimmers, T. A. (2016). The Colon-26 Carcinoma Tumor-bearing Mouse as a Model for the Study of Cancer Cachexia. *J Vis Exp*(117). doi:10.3791/54893

Böttner, M., Laaff, M., Schechinger, B., Rappold, G., Unsicker, K., & Suter-Crazzolara, C. (1999). Characterization of the rat, mouse, and human genes of growth/differentiation factor-15/macrophage inhibiting cytokine-1 (GDF-15/MIC-1). *Gene, 237*(1), 105-111. doi:10.1016/s0378-1119(99)00309-1

Bradley, L. M., Dalton, D. K., & Croft, M. (1996). A direct role for IFN-gamma in regulation of Th1 cell development. *J Immunol, 157*(4), 1350-1358.

Braun, T. P., Grossberg, A. J., Krasnow, S. M., Levasseur, P. R., Szumowski, M., Zhu, X. X., . . . Marks, D. L. (2013). Cancer- and endotoxin-induced cachexia require intact glucocorticoid signaling in skeletal muscle. *Faseb j, 27*(9), 3572-3582. doi:10.1096/fj.13-230375

Braun, T. P., Zhu, X., Szumowski, M., Scott, G. D., Grossberg, A. J., Levasseur, P. R., . . . Marks, D. L. (2011). Central nervous system inflammation induces muscle atrophy via activation of the hypothalamic-pituitary-adrenal axis. *J Exp Med, 208*(12), 2449-2463. doi:10.1084/jem.20111020

Brown, D. M., Lampe, A. T., & Workman, A. M. (2016). The Differentiation and Protective Function of Cytolytic CD4 T Cells in Influenza Infection. *Front Immunol, 7*, 93. doi:10.3389/fimmu.2016.00093

Bruera, E., Neumann, C. M., Pituskin, E., Calder, K., Ball, G., & Hanson, J. (1999). Thalidomide in patients with cachexia due to terminal cancer: preliminary report. *Ann Oncol, 10*(7), 857-859. doi:10.1023/a:1008329821941

Bruno, G., Saracino, A., Monno, L., & Angarano, G. (2017). The Revival of an "Old" Marker: CD4/CD8 Ratio. *AIDS Rev, 19*(2), 81-88.

Bu, J. Y., Shaw, A. S., & Chan, A. C. (1995). Analysis of the interaction of ZAP-70 and syk protein-tyrosine kinases with the T-cell antigen receptor by plasmon resonance. *Proc Natl Acad Sci U S A, 92*(11), 5106-5110. doi:10.1073/pnas.92.11.5106

Bubeck Wardenburg, J., Pappu, R., Bu, J. Y., Mayer, B., Chernoff, J., Straus, D., & Chan, A. C. (1998). Regulation of PAK activation and the T cell cytoskeleton by the linker protein SLP-76. *Immunity, 9*(5), 607-616. doi:10.1016/s1074-7613(00)80658-5

Burfeind, K. G., Zhu, X., Norgard, M. A., Levasseur, P. R., Huisman, C., Buenafe, A. C., . . . Marks, D. L. (2020). Circulating myeloid cells invade the central nervous system to mediate cachexia during pancreatic cancer. *Elife, 9*. doi:10.7554/eLife.54095

Burzyn, D., Kuswanto, W., Kolodin, D., Shadrach, J. L., Cerletti, M., Jang, Y., . . . Mathis, D. (2013). A special population of regulatory T cells potentiates muscle repair. *Cell, 155*(6), 1282-1295. doi:10.1016/j.cell.2013.10.054

Butte, M. J., Keir, M. E., Phamduy, T. B., Sharpe, A. H., & Freeman, G. J. (2007). Programmed death-1 ligand 1 interacts specifically with the B7-1 costimulatory molecule to inhibit T cell responses. *Immunity, 27*(1), 111-122. doi:10.1016/j.immuni.2007.05.016

Cachot, A., Bilous, M., Liu, Y. C., Li, X., Saillard, M., Cenerenti, M., . . . Jandus, C. (2021). Tumor-specific cytolytic CD4 T cells mediate immunity against human cancer. *Sci Adv, 7*(9). doi:10.1126/sciadv.abe3348

Cai, D., Frantz, J. D., Tawa, N. E., Jr., Melendez, P. A., Oh, B. C., Lidov, H. G., . . . Shoelson, S. E. (2004). IKKbeta/NF-kappaB activation causes severe muscle wasting in mice. *Cell, 119*(2), 285-298. doi:10.1016/j.cell.2004.09.027

Cala, M. P., Agulló-Ortuño, M. T., Prieto-García, E., González-Riano, C., Parrilla-Rubio, L., Barbas, C., . . . Lopez-Martin, J. A. (2018). Multiplatform plasma fingerprinting in cancer cachexia: a pilot observational and translational study. *J Cachexia Sarcopenia Muscle, 9*(2), 348-357. doi:10.1002/jcsm.12270

Campisi, J., & d'Adda di Fagagna, F. (2007). Cellular senescence: when bad things happen to good cells. *Nat Rev Mol Cell Biol, 8*(9), 729-740. doi:10.1038/nrm2233

Cao, Y., Jiao, N., Sun, T., Ma, Y., Zhang, X., Chen, H., . . . Zhang, Y. (2021). CXCL11 Correlates With Antitumor Immunity and an Improved Prognosis in Colon Cancer. *Front Cell Dev Biol, 9*, 646252. doi:10.3389/fcell.2021.646252

Carson, J. A., Hardee, J. P., & VanderVeen, B. N. (2016). The emerging role of skeletal muscle oxidative metabolism as a biological target and cellular regulator of cancer-induced muscle wasting. *Semin Cell Dev Biol, 54*, 53-67. doi:10.1016/j.semcdb.2015.11.005

Castella, B., Kopecka, J., Sciancalepore, P., Mandili, G., Foglietta, M., Mitro, N., . . . Massaia, M. (2017). The ATP-binding cassette transporter A1 regulates phosphoantigen release and Vγ9Vδ2 T cell activation by dendritic cells. *Nat Commun, 8*, 15663. doi:10.1038/ncomms15663

Castiglioni, A., Corna, G., Rigamonti, E., Basso, V., Vezzoli, M., Monno, A., . . . Rovere-Querini, P. (2015). FOXP3+ T Cells Recruited to Sites of Sterile Skeletal Muscle Injury Regulate the Fate of Satellite Cells and Guide Effective Tissue Regeneration. *PLoS One, 10*(6), e0128094. doi:10.1371/journal.pone.0128094

Castillo, A. M. M., Vu, T. T., Liva, S. G., Chen, M., Xie, Z., Thomas, J., . . . Coss, C. C. (2021). Murine cancer cachexia models replicate elevated catabolic pembrolizumab clearance in humans. *JCSM Rapid Commun, 4*(2), 232-244. doi:10.1002/rco2.32

Cederholm, T., Bosaeus, I., Barazzoni, R., Bauer, J., Van Gossum, A., Klek, S., . . . Singer, P. (2015). Diagnostic criteria for malnutrition - An ESPEN Consensus Statement. *Clin Nutr, 34*(3), 335-340. doi:10.1016/j.clnu.2015.03.001

Cereghetti, G. M., Stangherlin, A., Martins de Brito, O., Chang, C. R., Blackstone, C., Bernardi, P., & Scorrano, L. (2008). Dephosphorylation by calcineurin regulates translocation of Drp1 to mitochondria. *Proc Natl Acad Sci U S A, 105*(41), 15803-15808. doi:10.1073/pnas.0808249105

Cham, C. M., Driessens, G., O'Keefe, J. P., & Gajewski, T. F. (2008). Glucose deprivation inhibits multiple key gene expression events and effector functions in CD8+ T cells. *Eur J Immunol, 38*(9), 2438-2450. doi:10.1002/eji.200838289

Cham, C. M., & Gajewski, T. F. (2005). Glucose availability regulates IFN-gamma production and p70S6 kinase activation in CD8+ effector T cells. *J Immunol, 174*(8), 4670-4677. doi:10.4049/jimmunol.174.8.4670

Chan, A. C., Iwashima, M., Turck, C. W., & Weiss, A. (1992). ZAP-70: a 70 kd protein-tyrosine kinase that associates with the TCR zeta chain. *Cell, 71*(4), 649-662. doi:10.1016/0092-8674(92)90598-7

Chan, Y. K., Davis, P. F., Poppitt, S. D., Sun, X., Greenhill, N. S., Krishnamurthi, R., . . . Krissansen, G. W. (2012). Influence of tail versus cardiac sampling on blood glucose and lipid profiles in mice. *Lab Anim, 46*(2), 142-147. doi:10.1258/la.2011.011136

Chang, C. H., Curtis, J. D., Maggi, L. B., Jr., Faubert, B., Villarino, A. V., O'Sullivan, D., . . . Pearce, E. L. (2013). Posttranscriptional control of T cell effector function by aerobic glycolysis. *Cell, 153*(6), 1239-1251. doi:10.1016/j.cell.2013.05.016

Channappanavar, R., Twardy, B. S., Krishna, P., & Suvas, S. (2009). Advancing age leads to predominance of inhibitory receptor expressing CD4 T cells. *Mech Ageing Dev, 130*(10), 709-712. doi:10.1016/j.mad.2009.08.006

Chapman, N. M., & Chi, H. (2014). mTOR Links Environmental Signals to T Cell Fate Decisions. *Front Immunol, 5*, 686. doi:10.3389/fimmu.2014.00686

Chaurasia, B., Tippetts, T. S., Mayoral Monibas, R., Liu, J., Li, Y., Wang, L., . . . Summers, S. A. (2019). Targeting a ceramide double bond improves insulin resistance and hepatic steatosis. *Science, 365*(6451), 386-392. doi:10.1126/science.aav3722

Chen, Z., Laurence, A., & O'Shea, J. J. (2007). Signal transduction pathways and transcriptional regulation in the control of Th17 differentiation. *Semin Immunol, 19*(6), 400-408. doi:10.1016/j.smim.2007.10.015

Cheng, Y., Ma, Z., Kim, B. H., Wu, W., Cayting, P., Boyle, A. P., . . . Snyder, M. P. (2014). Principles of regulatory information conservation between mouse and human. *Nature, 515*(7527), 371-375. doi:10.1038/nature13985

Cheung, W. W., Paik, K. H., & Mak, R. H. (2010). Inflammation and cachexia in chronic kidney disease. *Pediatr Nephrol, 25*(4), 711-724. doi:10.1007/s00467-009-1427-z

Chikuma, S., Terawaki, S., Hayashi, T., Nabeshima, R., Yoshida, T., Shibayama, S., . . . Honjo, T. (2009). PD-1-mediated suppression of IL-2 production induces CD8+ T cell anergy in vivo. *J Immunol, 182*(11), 6682-6689. doi:10.4049/jimmunol.0900080

Childs, B. G., Baker, D. J., Wijshake, T., Conover, C. A., Campisi, J., & van Deursen, J. M. (2016). Senescent intimal foam cells are deleterious at all stages of atherosclerosis. *Science, 354*(6311), 472-477. doi:10.1126/science.aaf6659

Chung, H. K., Ryu, D., Kim, K. S., Chang, J. Y., Kim, Y. K., Yi, H. S., . . . Shong, M. (2017). Growth differentiation factor 15 is a myomitokine governing systemic energy homeostasis. *J Cell Biol, 216*(1), 149-165. doi:10.1083/jcb.201607110

Clark, A. L., Coats, A. J. S., Krum, H., Katus, H. A., Mohacsi, P., Salekin, D., . . . Anker, S. D. (2017). Effect of beta-adrenergic blockade with carvedilol on cachexia in severe chronic heart failure: results from the COPERNICUS trial. *J Cachexia Sarcopenia Muscle, 8*(4), 549-556. doi:10.1002/jcsm.12191

Colombo, N., Dubot, C., Lorusso, D., Caceres, M. V., Hasegawa, K., Shapira-Frommer, R., . . . Monk, B. J. (2021). Pembrolizumab for Persistent, Recurrent, or Metastatic Cervical Cancer. *N Engl J Med, 385*(20), 1856-1867. doi:10.1056/NEJMoa2112435

Cong, H., Sun, L., Liu, C., & Tien, P. (2011). Inhibition of atrogin-1/MAFbx expression by adenovirus-delivered small hairpin RNAs attenuates muscle atrophy in fasting mice. *Hum Gene Ther, 22*(3), 313-324. doi:10.1089/hum.2010.057

Conroy, M. J., & Lysaght, J. (2020). CX3CL1 Signaling in the Tumor Microenvironment. *Adv Exp Med Biol, 1231*, 1-12. doi:10.1007/978-3-030-36667-4_1

Cope, A. P. (2002). Studies of T-cell activation in chronic inflammation. *Arthritis Res, 4 Suppl 3*(Suppl 3), S197-211. doi:10.1186/ar557

Corn, R. A., Aronica, M. A., Zhang, F., Tong, Y., Stanley, S. A., Kim, S. R., . . . Boothby, M. (2003). T cell-intrinsic requirement for NF-kappa B induction in postdifferentiation IFN-gamma production and clonal expansion in a Th1 response. *J Immunol, 171*(4), 1816-1824. doi:10.4049/jimmunol.171.4.1816

Cossarizza, A., Chang, H. D., Radbruch, A., Acs, A., Adam, D., Adam-Klages, S., . . . Zychlinsky, A. (2019). Guidelines for the use of flow cytometry and cell sorting in immunological studies (second edition). *Eur J Immunol, 49*(10), 1457-1973. doi:10.1002/eji.201970107

Costa G, L. W., Vincint RG, Siebold JA, Aragon M, Bewley PT. (1980). Weight loss and Cachexia in lung cancer. *Nutr Cancer, 2*(2), 98-104.

Costelli, P., Llovera, M., Carbó, N., García-Martínez, C., López-Sorianoq, F. J., & Argilés, J. M. (1995). Interleukin-1 receptor antagonist (IL-1ra) is unable to reverse cachexia in rats bearing an ascites hepatoma (Yoshida AH-130). *Cancer Lett, 95*(1-2), 33-38. doi:10.1016/0304-3835(95)03858-t

Cote-Sierra, J., Foucras, G., Guo, L., Chiodetti, L., Young, H. A., Hu-Li, J., . . . Paul, W. E. (2004). Interleukin 2 plays a central role in Th2 differentiation. *Proc Natl Acad Sci U S A, 101*(11), 3880-3885. doi:10.1073/pnas.0400339101

Coutinho, A. E., & Chapman, K. E. (2011). The anti-inflammatory and immunosuppressive effects of glucocorticoids, recent developments and mechanistic insights. *Mol Cell Endocrinol, 335*(1), 2-13. doi:10.1016/j.mce.2010.04.005

Cretenet, G., Clerc, I., Matias, M., Loisel, S., Craveiro, M., Oburoglu, L., . . . Taylor, N. (2016). Cell surface Glut1 levels distinguish human CD4 and CD8 T lymphocyte subsets with distinct effector functions. *Sci Rep, 6*, 24129. doi:10.1038/srep24129

Croft, M., & Dubey, C. (2017). Accessory Molecule and Costimulation Requirements for CD4 T Cell Response. *Crit Rev Immunol, 37*(2-6), 261-290. doi:10.1615/CritRevImmunol.v37.i2-6.60

Cuenca, A. G., Cuenca, A. L., Winfield, R. D., Joiner, D. N., Gentile, L., Delano, M. J., . . . Moldawer, L. L. (2014). Novel role for tumor-induced expansion of myeloid-derived cells in cancer cachexia. *J Immunol, 192*(12), 6111-6119. doi:10.4049/jimmunol.1302895

Cui, P., Huang, C., Guo, J., Wang, Q., Liu, Z., Zhuo, H., & Lin, D. (2019). Metabolic Profiling of Tumors, Sera, and Skeletal Muscles from an Orthotopic Murine Model of Gastric Cancer Associated-Cachexia. *J Proteome Res, 18*(4), 1880-1892. doi:10.1021/acs.jproteome.9b00088

Curiel, T. J., Coukos, G., Zou, L., Alvarez, X., Cheng, P., Mottram, P., . . . Zou, W. (2004). Specific recruitment of regulatory T cells in ovarian carcinoma fosters immune privilege and predicts reduced survival. *Nat Med, 10*(9), 942-949. doi:10.1038/nm1093

Curtsinger, J. M., Agarwal, P., Lins, D. C., & Mescher, M. F. (2012). Autocrine IFN-γ promotes naive CD8 T cell differentiation and synergizes with IFN-α to stimulate strong function. *J Immunol, 189*(2), 659-668. doi:10.4049/jimmunol.1102727

Darmon, A. J., Nicholson, D. W., & Bleackley, R. C. (1995). Activation of the apoptotic protease CPP32 by cytotoxic T-cell-derived granzyme B. *Nature, 377*(6548), 446-448. doi:10.1038/377446a0

Das, S. K., Eder, S., Schauer, S., Diwoky, C., Temmel, H., Guertl, B., . . . Hoefler, G. (2011). Adipose triglyceride lipase contributes to cancer-associated cachexia. *Science, 333*(6039), 233-238. doi:10.1126/science.1198973

De Larichaudy, J., Zufferli, A., Serra, F., Isidori, A. M., Naro, F., Dessalle, K., . . . Némoz, G. (2012). TNF-α- and tumor-induced skeletal muscle atrophy involves sphingolipid metabolism. *Skelet Muscle, 2*(1), 2. doi:10.1186/2044-5040-2-2

Deans, C., & Wigmore, S. J. (2005). Systemic inflammation, cachexia and prognosis in patients with cancer. *Curr Opin Clin Nutr Metab Care, 8*(3), 265-269. doi:10.1097/01.mco.0000165004.93707.88

Deboer, M. D. (2009). Animal models of anorexia and cachexia. *Expert Opin Drug Discov, 4*(11), 1145-1155. doi:10.1517/17460440903300842

Decman, V., Laidlaw, B. J., Doering, T. A., Leng, J., Ertl, H. C., Goldstein, D. R., & Wherry, E. J. (2012). Defective CD8 T cell responses in aged mice are due to quantitative and qualitative changes in virus-specific precursors. *J Immunol, 188*(4), 1933-1941. doi:10.4049/jimmunol.1101098

Delgoffe, G. M., Kole, T. P., Zheng, Y., Zarek, P. E., Matthews, K. L., Xiao, B., . . . Powell, J. D. (2009). The mTOR kinase differentially regulates effector and regulatory T cell lineage commitment. *Immunity, 30*(6), 832-844. doi:10.1016/j.immuni.2009.04.014

Delgoffe, G. M., Pollizzi, K. N., Waickman, A. T., Heikamp, E., Meyers, D. J., Horton, M. R., . . . Powell, J. D. (2011). The kinase mTOR regulates the differentiation of helper T cells through the selective activation of signaling by mTORC1 and mTORC2. *Nat Immunol, 12*(4), 295-303. doi:10.1038/ni.2005

Deng, Y., Xia, X., Zhao, Y., Zhao, Z., Martinez, C., Yin, W., . . . Ma, L. (2021). Glucocorticoid receptor regulates PD-L1 and MHC-I in pancreatic cancer cells to promote immune evasion and immunotherapy resistance. *Nat Commun, 12*(1), 7041. doi:10.1038/s41467-021-27349-7

Dennis, J. W., Lau, K. S., Demetriou, M., & Nabi, I. R. (2009). Adaptive regulation at the cell surface by N-glycosylation. *Traffic, 10*(11), 1569-1578. doi:10.1111/j.1600-0854.2009.00981.x

Dessí, S., Batetta, B., Anchisi, C., Pani, P., Costelli, P., Tessitore, L., & Baccino, F. M. (1992). Cholesterol metabolism during the growth of a rat ascites hepatoma (Yoshida AH-130). *Br J Cancer, 66*(5), 787-793. doi:10.1038/bjc.1992.361

Dessì, S., Batetta, B., Pulisci, D., Spano, O., Anchisi, C., Tessitore, L., . . . Pani, P. (1994). Cholesterol content in tumor tissues is inversely associated with high-density lipoprotein cholesterol in serum in patients with gastrointestinal cancer. *Cancer, 73*(2), 253-258. doi:10.1002/1097-0142(19940115)73:2<253::aid-cncr2820730204>3.0.co;2-f

Dev, R., Wong, A., Hui, D., & Bruera, E. (2017). The Evolving Approach to Management of Cancer Cachexia. *Oncology (Williston Park), 31*(1), 23-32.

Deval, C., Mordier, S., Obled, C., Bechet, D., Combaret, L., Attaix, D., & Ferrara, M. (2001). Identification of cathepsin L as a differentially expressed message associated with skeletal muscle wasting. *Biochem J, 360*(Pt 1), 143-150. doi:10.1042/0264-6021:3600143

Dewys, W. D., Begg, C., Lavin, P. T., Band, P. R., Bennett, J. M., Bertino, J. R., . . . Tormey, D. C. (1980). Prognostic effect of weight loss prior to chemotherapy in cancer patients. Eastern Cooperative Oncology Group. *Am J Med, 69*(4), 491-497.

Di Francia, M., Barbier, D., Mege, J. L., & Orehek, J. (1994). Tumor necrosis factor-alpha levels and weight loss in chronic obstructive pulmonary disease. *Am J Respir Crit Care Med, 150*(5 Pt 1), 1453-1455. doi:10.1164/ajrccm.150.5.7952575

Di, W., Zhang, W., Zhu, B., Li, X., Tang, Q., & Zhou, Y. (2021). Colorectal cancer prompted adipose tissue browning and cancer cachexia through transferring exosomal miR-146b-5p. *J Cell Physiol, 236*(7), 5399-5410. doi:10.1002/jcp.30245

Dickmeis, T. (2009). Glucocorticoids and the circadian clock. *J Endocrinol, 200*(1), 3-22. doi:10.1677/joe-08-0415

Divakaruni, A. S., Paradyse, A., Ferrick, D. A., Murphy, A. N., & Jastroch, M. (2014). Analysis and interpretation of microplate-based oxygen consumption and pH data. *Methods Enzymol, 547*, 309-354. doi:10.1016/b978-0-12-801415-8.00016-3

Djenidi, F., Adam, J., Goubar, A., Durgeau, A., Meurice, G., de Montpréville, V., . . . Mami-Chouaib, F. (2015). CD8+CD103+ tumor-infiltrating lymphocytes are tumor-specific tissue-resident memory T cells and a prognostic factor for survival in lung cancer patients. *J Immunol, 194*(7), 3475-3486. doi:10.4049/jimmunol.1402711

Doherty, P. C., Hou, S., & Tripp, R. A. (1994). CD8+ T-cell memory to viruses. *Curr Opin Immunol, 6*(4), 545-552. doi:10.1016/0952-7915(94)90139-2

Dolina, J. S., Van Braeckel-Budimir, N., Thomas, G. D., & Salek-Ardakani, S. (2021). CD8(+) T Cell Exhaustion in Cancer. *Front Immunol, 12*, 715234. doi:10.3389/fimmu.2021.715234

Downey, S. G., Klapper, J. A., Smith, F. O., Yang, J. C., Sherry, R. M., Royal, R. E., . . . Rosenberg, S. A. (2007). Prognostic factors related to clinical response in patients with metastatic melanoma treated by CTL-associated antigen-4 blockade. *Clin Cancer Res, 13*(22 Pt 1), 6681-6688. doi:10.1158/1078-0432.Ccr-07-0187

Drobnik, W., Liebisch, G., Audebert, F. X., Frohlich, D., Gluck, T., Vogel, P., . . . Schmitz, G. (2003). Plasma ceramide and lysophosphatidylcholine inversely correlate with mortality in sepsis patients. *J Lipid Res, 44*(4), 754-761. doi:10.1194/jlr.M200401-JLR200

Duffaut, C., Zakaroff-Girard, A., Bourlier, V., Decaunes, P., Maumus, M., Chiotasso, P., . . . Bouloumié, A. (2009). Interplay between human adipocytes and T lymphocytes in obesity: CCL20 as an adipochemokine and T lymphocytes as lipogenic modulators. *Arterioscler Thromb Vasc Biol, 29*(10), 1608-1614. doi:10.1161/atvbaha.109.192583

Dunne, R. F., Loh, K. P., Williams, G. R., Jatoi, A., Mustian, K. M., & Mohile, S. G. (2019). Cachexia and Sarcopenia in Older Adults with Cancer: A Comprehensive Review. *Cancers (Basel), 11*(12). doi:10.3390/cancers11121861

Düvel, K., Yecies, J. L., Menon, S., Raman, P., Lipovsky, A. I., Souza, A. L., . . . Manning, B. D. (2010). Activation of a metabolic gene regulatory network downstream of mTOR complex 1. *Mol Cell, 39*(2), 171-183. doi:10.1016/j.molcel.2010.06.022

Dwarkasing, J. T., van Dijk, M., Dijk, F. J., Boekschoten, M. V., Faber, J., Argilès, J. M., . . . van Norren, K. (2014). Hypothalamic food intake regulation in a cancer-cachectic mouse model. *J Cachexia Sarcopenia Muscle, 5*(2), 159-169. doi:10.1007/s13539-013-0121-y

Ebinu, J. O., Stang, S. L., Teixeira, C., Bottorff, D. A., Hooton, J., Blumberg, P. M., . . . Stone, J. C. (2000). RasGRP links T-cell receptor signaling to Ras. *Blood, 95*(10), 3199-3203.

Edinger, A. L., & Thompson, C. B. (2002). Akt maintains cell size and survival by increasing mTOR-dependent nutrient uptake. *Mol Biol Cell, 13*(7), 2276-2288. doi:10.1091/mbc.01-12-0584

Edwards, J., Wilmott, J. S., Madore, J., Gide, T. N., Quek, C., Tasker, A., . . . Palendira, U. (2018). CD103(+) Tumor-Resident CD8(+) T Cells Are Associated with Improved Survival in Immunotherapy-Naïve Melanoma Patients and Expand Significantly During Anti-PD-1 Treatment. *Clin Cancer Res, 24*(13), 3036-3045. doi:10.1158/1078-0432.Ccr-17-2257

Egelston, C. A., Avalos, C., Tu, T. Y., Rosario, A., Wang, R., Solomon, S., . . . Lee, P. P. (2019). Resident memory CD8+ T cells within cancer islands mediate survival in breast cancer patients. *JCI Insight, 4*(19). doi:10.1172/jci.insight.130000

Elftman, M. D., Norbury, C. C., Bonneau, R. H., & Truckenmiller, M. E. (2007). Corticosterone impairs dendritic cell maturation and function. *Immunology, 122*(2), 279-290. doi:10.1111/j.1365-2567.2007.02637.x

Elstrom, R. L., Bauer, D. E., Buzzai, M., Karnauskas, R., Harris, M. H., Plas, D. R., . . . Thompson, C. B. (2004). Akt stimulates aerobic glycolysis in cancer cells. *Cancer Res, 64*(11), 3892-3899. doi:10.1158/0008-5472.Can-03-2904

Elyahu, Y., Hekselman, I., Eizenberg-Magar, I., Berner, O., Strominger, I., Schiller, M., . . . Monsonego, A. (2019). Aging promotes reorganization of the CD4 T cell landscape toward extreme regulatory and effector phenotypes. *Sci Adv, 5*(8), eaaw8330. doi:10.1126/sciadv.aaw8330

Endemann, G., Stanton, L. W., Madden, K. S., Bryant, C. M., White, R. T., & Protter, A. A. (1993). CD36 is a receptor for oxidized low density lipoprotein. *J Biol Chem, 268*(16), 11811-11816.

Erdem, M., Möckel, D., Jumpertz, S., John, C., Fragoulis, A., Rudolph, I., . . . Cramer, T. (2019). Macrophages protect against loss of adipose tissue during cancer cachexia. *J Cachexia Sarcopenia Muscle, 10*(5), 1128-1142. doi:10.1002/jcsm.12450

Ershler, W. B., Sun, W. H., Binkley, N., Gravenstein, S., Volk, M. J., Kamoske, G., . . . Weindruch, R. (1993). Interleukin-6 and aging: blood levels and mononuclear cell production increase with advancing age and in vitro production is modifiable by dietary restriction. *Lymphokine Cytokine Res, 12*(4), 225-230.

Evans, W. J., Morley, J. E., Argiles, J., Bales, C., Baracos, V., Guttridge, D., . . . Anker, S. D. (2008). Cachexia: a new definition. *Clin Nutr, 27*(6), 793-799. doi:10.1016/j.clnu.2008.06.013

Faje, A. T., Lawrence, D., Flaherty, K., Freedman, C., Fadden, R., Rubin, K., . . . Sullivan, R. J. (2018). High-dose glucocorticoids for the treatment of ipilimumab-induced hypophysitis is associated with reduced survival in patients with melanoma. *Cancer, 124*(18), 3706-3714. doi:10.1002/cncr.31629

Farrell, C. J., & Carter, A. C. (2016). Serum indices: managing assay interference. *Ann Clin Biochem, 53*(Pt 5), 527-538. doi:10.1177/0004563216643557

Fearon, K., Strasser, F., Anker, S. D., Bosaeus, I., Bruera, E., Fainsinger, R. L., . . . Baracos, V. E. (2011). Definition and classification of cancer cachexia: an international consensus. *Lancet Oncol, 12*(5), 489-495. doi:10.1016/s1470-2045(10)70218-7

Fearon, K. C., Glass, D. J., & Guttridge, D. C. (2012). Cancer cachexia: mediators, signaling, and metabolic pathways. *Cell Metab, 16*(2), 153-166. doi:10.1016/j.cmet.2012.06.011

Fecher, L. A., Agarwala, S. S., Hodi, F. S., & Weber, J. S. (2013). Ipilimumab and its toxicities: a multidisciplinary approach. *Oncologist, 18*(6), 733-743. doi:10.1634/theoncologist.2012-0483

Feldman, J. P. G., R.; Mark, S.; Schwartz, J.; Orion, I.A. (2009). A mathematical model for tumor volume evaluation using two-dimensions. *J. Appl. Quant. Methods, 4*, 455–462.

Feuerer, M., Herrero, L., Cipolletta, D., Naaz, A., Wong, J., Nayer, A., . . . Mathis, D. (2009). Lean, but not obese, fat is enriched for a unique population of regulatory T cells that affect metabolic parameters. *Nat Med, 15*(8), 930-939. doi:10.1038/nm.2002

Figueroa-Clarevega, A., & Bilder, D. (2015). Malignant Drosophila tumors interrupt insulin signaling to induce cachexia-like wasting. *Dev Cell, 33*(1), 47-55. doi:10.1016/j.devcel.2015.03.001

Flaherty, S. E., 3rd, Grijalva, A., Xu, X., Ables, E., Nomani, A., & Ferrante, A. W., Jr. (2019). A lipase-independent pathway of lipid release and immune modulation by adipocytes. *Science, 363*(6430), 989-993. doi:10.1126/science.aaw2586

Flint, T. R., Janowitz, T., Connell, C. M., Roberts, E. W., Denton, A. E., Coll, A. P., . . . Fearon, D. T. (2016). Tumor-Induced IL-6 Reprograms Host Metabolism to Suppress Anti-tumor Immunity. *Cell Metab, 24*(5), 672-684. doi:10.1016/j.cmet.2016.10.010

Fontenot, J. D., Gavin, M. A., & Rudensky, A. Y. (2003). Foxp3 programs the development and function of CD4+CD25+ regulatory T cells. *Nat Immunol, 4*(4), 330-336. doi:10.1038/ni904

Foster, A. D., Sivarapatna, A., & Gress, R. E. (2011). The aging immune system and its relationship with cancer. *Aging health, 7*(5), 707-718. doi:10.2217/ahe.11.56

Franchimont, D., Galon, J., Gadina, M., Visconti, R., Zhou, Y., Aringer, M., . . . O'Shea, J. J. (2000). Inhibition of Th1 immune response by glucocorticoids: dexamethasone selectively inhibits IL-12-induced Stat4 phosphorylation in T lymphocytes. *J Immunol, 164*(4), 1768-1774. doi:10.4049/jimmunol.164.4.1768

Franchimont, D., Galon, J., Vacchio, M. S., Fan, S., Visconti, R., Frucht, D. M., . . . O'Shea, J. J. (2002). Positive effects of glucocorticoids on T cell function by up-regulation of IL-7 receptor alpha. *J Immunol, 168*(5), 2212-2218. doi:10.4049/jimmunol.168.5.2212

Frauwirth, K. A., Riley, J. L., Harris, M. H., Parry, R. V., Rathmell, J. C., Plas, D. R., . . . Thompson, C. B. (2002). The CD28 signaling pathway regulates glucose metabolism. *Immunity, 16*(6), 769-777. doi:10.1016/s1074-7613(02)00323-0

Fridman, W. H., Pagès, F., Sautès-Fridman, C., & Galon, J. (2012). The immune contexture in human tumours: impact on clinical outcome. *Nat Rev Cancer, 12*(4), 298-306. doi:10.1038/nrc3245

Fried, S. K., & Zechner, R. (1989). Cachectin/tumor necrosis factor decreases human adipose tissue lipoprotein lipase mRNA levels, synthesis, and activity. *J Lipid Res, 30*(12), 1917-1923.

Friesen, D. E., Baracos, V. E., & Tuszynski, J. A. (2015). Modeling the energetic cost of cancer as a result of altered energy metabolism: implications for cachexia. *Theor Biol Med Model, 12*, 17. doi:10.1186/s12976-015-0015-0

Fu, J., Xu, D., Liu, Z., Shi, M., Zhao, P., Fu, B., . . . Wang, F. S. (2007). Increased regulatory T cells correlate with CD8 T-cell impairment and poor survival in hepatocellular carcinoma patients. *Gastroenterology, 132*(7), 2328-2339. doi:10.1053/j.gastro.2007.03.102

Fukawa, T., Yan-Jiang, B. C., Min-Wen, J. C., Jun-Hao, E. T., Huang, D., Qian, C. N., . . . Shyh-Chang, N. (2016). Excessive fatty acid oxidation induces muscle atrophy in cancer cachexia. *Nat Med, 22*(6), 666-671. doi:10.1038/nm.4093

Gabrilovich, D. I., & Nagaraj, S. (2009). Myeloid-derived suppressor cells as regulators of the immune system. *Nat Rev Immunol, 9*(3), 162-174. doi:10.1038/nri2506

Gabrilovich, D. I., Ostrand-Rosenberg, S., & Bronte, V. (2012). Coordinated regulation of myeloid cells by tumours. *Nat Rev Immunol, 12*(4), 253-268. doi:10.1038/nri3175

Gandhi, L., Rodríguez-Abreu, D., Gadgeel, S., Esteban, E., Felip, E., De Angelis, F., . . . Garassino, M. C. (2018). Pembrolizumab plus Chemotherapy in Metastatic Non-Small-Cell Lung Cancer. *N Engl J Med, 378*(22), 2078-2092. doi:10.1056/NEJMoa1801005

Garcia, J. M., Garcia-Touza, M., Hijazi, R. A., Taffet, G., Epner, D., Mann, D., . . . Marcelli, M. (2005). Active ghrelin levels and active to total ghrelin ratio in cancer-induced cachexia. *J Clin Endocrinol Metab, 90*(5), 2920-2926. doi:10.1210/jc.2004-1788

Garçon, F., Patton, D. T., Emery, J. L., Hirsch, E., Rottapel, R., Sasaki, T., & Okkenhaug, K. (2008). CD28 provides T-cell costimulation and enhances PI3K activity at the immune synapse independently of its capacity to interact with the p85/p110 heterodimer. *Blood, 111*(3), 1464-1471. doi:10.1182/blood-2007-08-108050

Garg, S. K., Delaney, C., Toubai, T., Ghosh, A., Reddy, P., Banerjee, R., & Yung, R. (2014). Aging is associated with increased regulatory T-cell function. *Aging Cell, 13*(3), 441-448. doi:10.1111/acel.12191

Gault, C. R., Obeid, L. M., & Hannun, Y. A. (2010). An overview of sphingolipid metabolism: from synthesis to breakdown. *Adv Exp Med Biol, 688*, 1-23. doi:10.1007/978-1-4419-6741-1_1

Geppert, J., Walth, A. A., Terrón Expósito, R., Kaltenecker, D., Morigny, P., Machado, J., . . . Rohm, M. (2021). Aging Aggravates Cachexia in Tumor-Bearing Mice. *Cancers (Basel), 14*(1). doi:10.3390/cancers14010090

Geremia, A., Sartori, R., Baraldo, M., Nogara, L., Balmaceda, V., Dumitras, G. A., . . . Blaauw, B. (2022). Activation of Akt-mTORC1 signalling reverts cancer-dependent muscle wasting. *J Cachexia Sarcopenia Muscle, 13*(1), 648-661. doi:10.1002/jcsm.12854

Gisterå, A., Klement, M. L., Polyzos, K. A., Mailer, R. K. W., Duhlin, A., Karlsson, M. C. I., . . . Hansson, G. K. (2018). Low-Density Lipoprotein-Reactive T Cells Regulate Plasma Cholesterol Levels and Development of Atherosclerosis in Humanized Hypercholesterolemic Mice. *Circulation, 138*(22), 2513-2526. doi:10.1161/circulationaha.118.034076

Goldberg, R. M., Loprinzi, C. L., Mailliard, J. A., O'Fallon, J. R., Krook, J. E., Ghosh, C., . . . Shanahan, T. G. (1995). Pentoxifylline for treatment of cancer anorexia and cachexia? A randomized, double-blind, placebo-controlled trial. *J Clin Oncol, 13*(11), 2856-2859. doi:10.1200/jco.1995.13.11.2856

Gomes, M. D., Lecker, S. H., Jagoe, R. T., Navon, A., & Goldberg, A. L. (2001). Atrogin-1, a muscle-specific F-box protein highly expressed during muscle atrophy. *Proc Natl Acad Sci U S A, 98*(25), 14440-14445. doi:10.1073/pnas.251541198

Gondek, D. C., Lu, L. F., Quezada, S. A., Sakaguchi, S., & Noelle, R. J. (2005). Cutting edge: contact-mediated suppression by CD4+CD25+ regulatory cells involves a granzyme B-dependent, perforin-independent mechanism. *J Immunol, 174*(4), 1783-1786. doi:10.4049/jimmunol.174.4.1783

Gordon, J. N., Trebble, T. M., Ellis, R. D., Duncan, H. D., Johns, T., & Goggin, P. M. (2005). Thalidomide in the treatment of cancer cachexia: a randomised placebo controlled trial. *Gut, 54*(4), 540-545. doi:10.1136/gut.2004.047563

Goswami, R., Jabeen, R., Yagi, R., Pham, D., Zhu, J., Goenka, S., & Kaplan, M. H. (2012). STAT6-dependent regulation of Th9 development. *J Immunol, 188*(3), 968-975. doi:10.4049/jimmunol.1102840

Grabenbauer, G. G., Lahmer, G., Distel, L., & Niedobitek, G. (2006). Tumor-infiltrating cytotoxic T cells but not regulatory T cells predict outcome in anal squamous cell carcinoma. *Clin Cancer Res, 12*(11 Pt 1), 3355-3360. doi:10.1158/1078-0432.Ccr-05-2434

Green, E. A., Gorelik, L., McGregor, C. M., Tran, E. H., & Flavell, R. A. (2003). CD4+CD25+ T regulatory cells control anti-islet CD8+ T cells through TGF-beta-TGF-beta receptor interactions in type 1 diabetes. *Proc Natl Acad Sci U S A, 100*(19), 10878-10883. doi:10.1073/pnas.1834400100

Greenberg, A. S., Nordan, R. P., McIntosh, J., Calvo, J. C., Scow, R. O., & Jablons, D. (1992). Interleukin 6 reduces lipoprotein lipase activity in adipose tissue of mice in vivo and in 3T3-L1 adipocytes: a possible role for interleukin 6 in cancer cachexia. *Cancer Res, 52*(15), 4113-4116.

Grivennikov, S. I., & Karin, M. (2011). Inflammatory cytokines in cancer: tumour necrosis factor and interleukin 6 take the stage. *Ann Rheum Dis, 70 Suppl 1*, i104-108. doi:10.1136/ard.2010.140145

Guaraldi, G., Zona, S., Silva, A. R., Menozzi, M., Dolci, G., Milic, J., . . . Mussini, C. (2019). The dynamic association between Frailty, CD4 and CD4/CD8 ratio in people aging with HIV. *PLoS One, 14*(2), e0212283. doi:10.1371/journal.pone.0212283

Guo, J., Liu, C., Zhou, X., Xu, X., Deng, L., Li, X., & Guan, F. (2017). Conditioned Medium from Malignant Breast Cancer Cells Induces an EMT-Like Phenotype and an Altered N-Glycan Profile in Normal Epithelial MCF10A Cells. *Int J Mol Sci, 18*(8). doi:10.3390/ijms18081528

Guo, Y., Xu, F., Lu, T., Duan, Z., & Zhang, Z. (2012). Interleukin-6 signaling pathway in targeted therapy for cancer. *Cancer Treat Rev, 38*(7), 904-910. doi:10.1016/j.ctrv.2012.04.007

Han, J., Meng, Q., Shen, L., & Wu, G. (2018). Interleukin-6 induces fat loss in cancer cachexia by promoting white adipose tissue lipolysis and browning. *Lipids Health Dis, 17*(1), 14. doi:10.1186/s12944-018-0657-0

Han, S. J., Glatman Zaretsky, A., Andrade-Oliveira, V., Collins, N., Dzutsev, A., Shaik, J., . . . Belkaid, Y. (2017). White Adipose Tissue Is a Reservoir for Memory T Cells and Promotes Protective Memory Responses to Infection. *Immunity, 47*(6), 1154-1168.e1156. doi:10.1016/j.immuni.2017.11.009

Hara, K., Maruki, Y., Long, X., Yoshino, K., Oshiro, N., Hidayat, S., . . . Yonezawa, K. (2002). Raptor, a binding partner of target of rapamycin (TOR), mediates TOR action. *Cell, 110*(2), 177-189. doi:10.1016/s0092-8674(02)00833-4

Harlin, H., Meng, Y., Peterson, A. C., Zha, Y., Tretiakova, M., Slingluff, C., . . . Gajewski, T. F. (2009). Chemokine expression in melanoma metastases associated with CD8+ T-cell recruitment. *Cancer Res, 69*(7), 3077-3085. doi:10.1158/0008-5472.Can-08-2281

Hasenkrug, K. J., & Myers, L. M. (2011). In vitro and in vivo analyses of regulatory T cell suppression of CD8+ T cells. *Methods Mol Biol, 707*, 45-54. doi:10.1007/978-1-61737-979-6_4

Hassin, D., Garber, O. G., Meiraz, A., Schiffenbauer, Y. S., & Berke, G. (2011). Cytotoxic T lymphocyte perforin and Fas ligand working in concert even when Fas ligand lytic action is still not detectable. *Immunology, 133*(2), 190-196. doi:10.1111/j.1365-2567.2011.03426.x

He, W. A., Calore, F., Londhe, P., Canella, A., Guttridge, D. C., & Croce, C. M. (2014). Microvesicles containing miRNAs promote muscle cell death in cancer cachexia via TLR7. *Proc Natl Acad Sci U S A, 111*(12), 4525-4529. doi:10.1073/pnas.1402714111

Heck, S., Kullmann, M., Gast, A., Ponta, H., Rahmsdorf, H. J., Herrlich, P., & Cato, A. C. (1994). A distinct modulating domain in glucocorticoid receptor monomers in the repression of activity of the transcription factor AP-1. *Embo j, 13*(17), 4087-4095.

Hedrick, S. M., Hess Michelini, R., Doedens, A. L., Goldrath, A. W., & Stone, E. L. (2012). FOXO transcription factors throughout T cell biology. *Nat Rev Immunol, 12*(9), 649-661. doi:10.1038/nri3278

Heikinheimo, O., Ylikorkala, O., & Lähteenmäki, P. (1990). Antiprogesterone RU 486--a drug for non-surgical abortion. *Ann Med, 22*(2), 75-84. doi:10.3109/07853899009147247

Helmberg, A., Auphan, N., Caelles, C., & Karin, M. (1995). Glucocorticoid-induced apoptosis of human leukemic cells is caused by the repressive function of the glucocorticoid receptor. *Embo j, 14*(3), 452-460.

Herr, I., & Pfitzenmaier, J. (2006). Glucocorticoid use in prostate cancer and other solid tumours: implications for effectiveness of cytotoxic treatment and metastases. *Lancet Oncol, 7*(5), 425-430. doi:10.1016/s1470-2045(06)70694-5

Hetzler, K. L., Hardee, J. P., Puppa, M. J., Narsale, A. A., Sato, S., Davis, J. M., & Carson, J. A. (2015). Sex differences in the relationship of IL-6 signaling to cancer cachexia progression. *Biochim Biophys Acta, 1852*(5), 816-825. doi:10.1016/j.bbadis.2014.12.015

Hickish, T., Andre, T., Wyrwicz, L., Saunders, M., Sarosiek, T., Kocsis, J., . . . de Gramont, A. (2017). MABp1 as a novel antibody treatment for advanced colorectal cancer: a randomised, double-blind, placebo-controlled, phase 3 study. *Lancet Oncol, 18*(2), 192-201. doi:10.1016/s1470-2045(17)30006-2

Hillen, F., Baeten, C. I., van de Winkel, A., Creytens, D., van der Schaft, D. W., Winnepenninckx, V., & Griffioen, A. W. (2008). Leukocyte infiltration and tumor cell plasticity are parameters of aggressiveness in primary cutaneous melanoma. *Cancer Immunol Immunother, 57*(1), 97-106. doi:10.1007/s00262-007-0353-9

Hingorani, S. R., Wang, L., Multani, A. S., Combs, C., Deramaudt, T. B., Hruban, R. H., . . . Tuveson, D. A. (2005). Trp53R172H and KrasG12D cooperate to promote chromosomal instability and widely metastatic pancreatic ductal adenocarcinoma in mice. *Cancer Cell, 7*(5), 469-483. doi:10.1016/j.ccr.2005.04.023

Hirai, K., Hussey, H. J., Barber, M. D., Price, S. A., & Tisdale, M. J. (1998). Biological evaluation of a lipid-mobilizing factor isolated from the urine of cancer patients. *Cancer Res, 58*(11), 2359-2365.

Hirai, K., Ishiko, O., & Tisdale, M. (1997). Mechanism of depletion of liver glycogen in cancer cachexia. *Biochem Biophys Res Commun, 241*(1), 49-52. doi:10.1006/bbrc.1997.7732

Hobbs, S. J., & Nolz, J. C. (2017). Regulation of T Cell Trafficking by Enzymatic Synthesis of O-Glycans. *Front Immunol, 8*, 600. doi:10.3389/fimmu.2017.00600

Hodi, F. S., O'Day, S. J., McDermott, D. F., Weber, R. W., Sosman, J. A., Haanen, J. B., . . . Urba, W. J. (2010). Improved survival with ipilimumab in patients with metastatic melanoma. *N Engl J Med, 363*(8), 711-723. doi:10.1056/NEJMoa1003466

Homann, D., Teyton, L., & Oldstone, M. B. (2001). Differential regulation of antiviral T-cell immunity results in stable CD8+ but declining CD4+ T-cell memory. *Nat Med, 7*(8), 913-919. doi:10.1038/90950

Hori, S., Nomura, T., & Sakaguchi, S. (2003). Control of regulatory T cell development by the transcription factor Foxp3. *Science, 299*(5609), 1057-1061. doi:10.1126/science.1079490

Hwang, J. R., Byeon, Y., Kim, D., & Park, S. G. (2020). Recent insights of T cell receptor-mediated signaling pathways for T cell activation and development. *Exp Mol Med, 52*(5), 750-761. doi:10.1038/s12276-020-0435-8

Inaba, S., Hinohara, A., Tachibana, M., Tsujikawa, K., & Fukada, S. I. (2018). Muscle regeneration is disrupted by cancer cachexia without loss of muscle stem cell potential. *PLoS One, 13*(10), e0205467. doi:10.1371/journal.pone.0205467

Ishiko, O., Nishimura, S., Yasui, T., Sumi, T., Hirai, K., Honda, K., & Ogita, S. (1999). Metabolic and morphologic characteristics of adipose tissue associated with the growth of malignant tumors. *Jpn J Cancer Res, 90*(6), 655-659. doi:10.1111/j.1349-7006.1999.tb00797.x

Isomäki, P., Panesar, M., Annenkov, A., Clark, J. M., Foxwell, B. M., Chernajovsky, Y., & Cope, A. P. (2001). Prolonged exposure of T cells to TNF down-regulates TCR zeta and expression of the TCR/CD3 complex at the cell surface. *J Immunol, 166*(9), 5495-5507. doi:10.4049/jimmunol.166.9.5495

Iyer, N. V., Kotch, L. E., Agani, F., Leung, S. W., Laughner, E., Wenger, R. H., . . . Semenza, G. L. (1998). Cellular and developmental control of O2 homeostasis by hypoxia-inducible factor 1 alpha. *Genes Dev, 12*(2), 149-162. doi:10.1101/gad.12.2.149

J. R. Rigas , M. S., S. V. Orlov , B. Milovanovic , K. Prabhash , J. T. Smith. (2010). Efect of ALD518, a humanized anti-IL-6 antibody, on lean body mass loss and symptoms in patients with advanced non-small cell lung cancer (NSCLC): Results of a phase II randomized, double-blind safety and efficacy trial. *Journal of Clinical Oncology, 28*(15), Abstract 7622.

Jacobs, S. R., Herman, C. E., Maciver, N. J., Wofford, J. A., Wieman, H. L., Hammen, J. J., & Rathmell, J. C. (2008). Glucose uptake is limiting in T cell activation and requires CD28-mediated Akt-dependent and independent pathways. *J Immunol, 180*(7), 4476-4486. doi:10.4049/jimmunol.180.7.4476

Janas, M. L., Groves, P., Kienzle, N., & Kelso, A. (2005). IL-2 regulates perforin and granzyme gene expression in CD8+ T cells independently of its effects on survival and proliferation. *J Immunol, 175*(12), 8003-8010. doi:10.4049/jimmunol.175.12.8003

Jatoi, A., Ritter, H. L., Dueck, A., Nguyen, P. L., Nikcevich, D. A., Luyun, R. F., . . . Loprinzi, C. L. (2010). A placebo-controlled, double-blind trial of infliximab for cancer-associated weight loss in elderly and/or poor performance non-small cell lung cancer patients (N01C9). *Lung Cancer, 68*(2), 234-239. doi:10.1016/j.lungcan.2009.06.020

Jeevanandam, M., Horowitz, G. D., Lowry, S. F., & Brennan, M. F. (1984). Cancer cachexia and protein metabolism. *Lancet, 1*(8392), 1423-1426. doi:10.1016/s0140-6736(84)91929-9

Jeng, M. Y., Hull, P. A., Fei, M., Kwon, H. S., Tsou, C. L., Kasler, H., . . . Ott, M. (2018). Metabolic reprogramming of human CD8(+) memory T cells through loss of SIRT1. *J Exp Med, 215*(1), 51-62. doi:10.1084/jem.20161066

Jiang, W., Li, Y., Zhang, S., Kong, G., & Li, Z. (2021). Association between cellular immune response and spleen weight in mice with hepatocellular carcinoma. *Oncol Lett, 22*(2), 625. doi:10.3892/ol.2021.12886

Johnen, H., Lin, S., Kuffner, T., Brown, D. A., Tsai, V. W., Bauskin, A. R., . . . Breit, S. N. (2007). Tumor-induced anorexia and weight loss are mediated by the TGF-beta superfamily cytokine MIC-1. *Nat Med, 13*(11), 1333-1340. doi:10.1038/nm1677

Johnson, D. B., Friedman, D. L., Berry, E., Decker, I., Ye, F., Zhao, S., . . . Lovly, C. M. (2015). Survivorship in Immune Therapy: Assessing Chronic Immune Toxicities, Health Outcomes, and Functional Status among Long-term Ipilimumab Survivors at a Single Referral Center. *Cancer Immunol Res, 3*(5), 464-469. doi:10.1158/2326-6066.Cir-14-0217

Johnson, T. A., Paakinaho, V., Kim, S., Hager, G. L., & Presman, D. M. (2021). Genome-wide binding potential and regulatory activity of the glucocorticoid receptor's monomeric and dimeric forms. *Nat Commun, 12*(1), 1987. doi:10.1038/s41467-021-22234-9

Jones, A., Friedrich, K., Rohm, M., Schäfer, M., Algire, C., Kulozik, P., . . . Herzig, S. (2013). TSC22D4 is a molecular output of hepatic wasting metabolism. *EMBO Mol Med, 5*(2), 294-308. doi:10.1002/emmm.201201869

Ju, Y., Xu, T., Zhang, H., & Yu, A. (2014). FOXO1-dependent DNA damage repair is regulated by JNK in lung cancer cells. *Int J Oncol, 44*(4), 1284-1292. doi:10.3892/ijo.2014.2269

June, C. H., O'Connor, R. S., Kawalekar, O. U., Ghassemi, S., & Milone, M. C. (2018). CAR T cell immunotherapy for human cancer. *Science, 359*(6382), 1361-1365. doi:10.1126/science.aar6711

Kägi, D., Ledermann, B., Bürki, K., Seiler, P., Odermatt, B., Olsen, K. J., . . . Hengartner, H. (1994). Cytotoxicity mediated by T cells and natural killer cells is greatly impaired in perforin-deficient mice. *Nature, 369*(6475), 31-37. doi:10.1038/369031a0

Kahn, J., Ingraham, R. H., Shirley, F., Migaki, G. I., & Kishimoto, T. K. (1994). Membrane proximal cleavage of L-selectin: identification of the cleavage site and a 6-kD transmembrane peptide fragment of L-selectin. *J Cell Biol, 125*(2), 461-470. doi:10.1083/jcb.125.2.461

Kalantaridou, S., Makrigiannakis, A., Zoumakis, E., & Chrousos, G. P. (2007). Peripheral corticotropin-releasing hormone is produced in the immune and reproductive systems: actions, potential roles and clinical implications. *Front Biosci, 12*, 572-580. doi:10.2741/2083

Kälin, S., Becker, M., Ott, V. B., Serr, I., Hosp, F., Mollah, M. M. H., . . . Daniel, C. (2017). A Stat6/Pten Axis Links Regulatory T Cells with Adipose Tissue Function. *Cell Metab, 26*(3), 475-492.e477. doi:10.1016/j.cmet.2017.08.008

Kanamori, M., Nakatsukasa, H., Ito, M., Chikuma, S., & Yoshimura, A. (2018). Reprogramming of Th1 cells into regulatory T cells through rewiring of the metabolic status. *Int Immunol, 30*(8), 357-373. doi:10.1093/intimm/dxy043

Kanasi, E., Ayilavarapu, S., & Jones, J. (2016). The aging population: demographics and the biology of aging. *Periodontol 2000, 72*(1), 13-18. doi:10.1111/prd.12126

Kane, L. P., Shapiro, V. S., Stokoe, D., & Weiss, A. (1999). Induction of NF-kappaB by the Akt/PKB kinase. *Curr Biol, 9*(11), 601-604. doi:10.1016/s0960-9822(99)80265-6

Karalis, K., Muglia, L. J., Bae, D., Hilderbrand, H., & Majzoub, J. A. (1997). CRH and the immune system. *J Neuroimmunol, 72*(2), 131-136. doi:10.1016/s0165-5728(96)00178-6

Karupiah, G., Xie, Q. W., Buller, R. M., Nathan, C., Duarte, C., & MacMicking, J. D. (1993). Inhibition of viral replication by interferon-gamma-induced nitric oxide synthase. *Science, 261*(5127), 1445-1448. doi:10.1126/science.7690156

Kasibhatla, S., Brunner, T., Genestier, L., Echeverri, F., Mahboubi, A., & Green, D. R. (1998). DNA damaging agents induce expression of Fas ligand and subsequent apoptosis in T lymphocytes via the activation of NF-kappa B and AP-1. *Mol Cell, 1*(4), 543-551. doi:10.1016/s1097-2765(00)80054-4

Katz, A. M., & Katz, P. B. (1962). Diseases of the heart in the works of Hippocrates. *Br Heart J, 24*(3), 257-264. doi:10.1136/hrt.24.3.257

Kawahito, Y., Sano, H., Kawata, M., Yuri, K., Mukai, S., Yamamura, Y., . . . Kondo, M. (1994). Local secretion of corticotropin-releasing hormone by enterochromaffin cells in human colon. *Gastroenterology, 106*(4), 859-865. doi:10.1016/0016-5085(94)90743-9

Kelly, R. J., Ajani, J. A., Kuzdzal, J., Zander, T., Van Cutsem, E., Piessen, G., . . . Moehler, M. (2021). Adjuvant Nivolumab in Resected Esophageal or Gastroesophageal Junction Cancer. *N Engl J Med, 384*(13), 1191-1203. doi:10.1056/NEJMoa2032125

Kerdiles, Y. M., Beisner, D. R., Tinoco, R., Dejean, A. S., Castrillon, D. H., DePinho, R. A., & Hedrick, S. M. (2009). Foxo1 links homing and survival of naive T cells by regulating L-selectin, CCR7 and interleukin 7 receptor. *Nat Immunol, 10*(2), 176-184. doi:10.1038/ni.1689

Khaled, Y. S., Ammori, B. J., & Elkord, E. (2014). Increased levels of granulocytic myeloid-derived suppressor cells in peripheral blood and tumour tissue of pancreatic cancer patients. *J Immunol Res, 2014*, 879897. doi:10.1155/2014/879897

Khan, I. M., Perrard, X. Y., Brunner, G., Lui, H., Sparks, L. M., Smith, S. R., . . . Ballantyne, C. M. (2015). Intermuscular and perimuscular fat expansion in obesity correlates with skeletal muscle T cell and macrophage infiltration and insulin resistance. *Int J Obes (Lond), 39*(11), 1607-1618. doi:10.1038/ijo.2015.104

Khan, O., Giles, J. R., McDonald, S., Manne, S., Ngiow, S. F., Patel, K. P., . . . Wherry, E. J. (2019). TOX transcriptionally and epigenetically programs CD8(+) T cell exhaustion. *Nature, 571*(7764), 211-218. doi:10.1038/s41586-019-1325-x

Khan, Z. H., Simpson, E. J., Cole, A. T., Holt, M., MacDonald, I., Pye, D., . . . Freeman, J. G. (2003). Oesophageal cancer and cachexia: the effect of short-term treatment with thalidomide on weight loss and lean body mass. *Aliment Pharmacol Ther, 17*(5), 677-682. doi:10.1046/j.1365-2036.2003.01457.x

Kino, T., & Chrousos, G. P. (2004). Glucocorticoid and mineralocorticoid receptors and associated diseases. *Essays Biochem, 40*, 137-155. doi:10.1042/bse0400137

Kir, S., Komaba, H., Garcia, A. P., Economopoulos, K. P., Liu, W., Lanske, B., . . . Spiegelman, B. M. (2016). PTH/PTHrP Receptor Mediates Cachexia in Models of Kidney Failure and Cancer. *Cell Metab, 23*(2), 315-323. doi:10.1016/j.cmet.2015.11.003

Kir, S., White, J. P., Kleiner, S., Kazak, L., Cohen, P., Baracos, V. E., & Spiegelman, B. M. (2014). Tumour-derived PTH-related protein triggers adipose tissue browning and cancer cachexia. *Nature, 513*(7516), 100-104. doi:10.1038/nature13528

Klaus, S. (2004). Adipose tissue as a regulator of energy balance. *Curr Drug Targets, 5*(3), 241-250. doi:10.2174/1389450043490523

Kleijn, M., & Proud, C. G. (2002). The regulation of protein synthesis and translation factors by CD3 and CD28 in human primary T lymphocytes. *BMC Biochem, 3*, 11. doi:10.1186/1471-2091-3-11

Klingenberg, R., Gerdes, N., Badeau, R. M., Gisterå, A., Strodthoff, D., Ketelhuth, D. F., . . . Hansson, G. K. (2013). Depletion of FOXP3+ regulatory T cells promotes hypercholesterolemia and atherosclerosis. *J Clin Invest, 123*(3), 1323-1334. doi:10.1172/jci63891

Knapp, M. L., al-Sheibani, S., Riches, P. G., Hanham, I. W., & Phillips, R. H. (1991). Hormonal factors associated with weight loss in patients with advanced breast cancer. *Ann Clin Biochem, 28 (Pt 5)*, 480-486. doi:10.1177/000456329102800510

Koch, S., Larbi, A., Derhovanessian, E., Ozcelik, D., Naumova, E., & Pawelec, G. (2008). Multiparameter flow cytometric analysis of CD4 and CD8 T cell subsets in young and old people. *Immun Ageing, 5*, 6. doi:10.1186/1742-4933-5-6

Kohli, K., Pillarisetty, V. G., & Kim, T. S. (2022). Key chemokines direct migration of immune cells in solid tumors. *Cancer Gene Ther, 29*(1), 10-21. doi:10.1038/s41417-021-00303-x

Komdeur, F. L., Prins, T. M., van de Wall, S., Plat, A., Wisman, G. B. A., Hollema, H., . . . Nijman, H. W. (2017). CD103+ tumor-infiltrating lymphocytes are tumor-reactive intraepithelial CD8+ T cells associated with prognostic benefit and therapy response in cervical cancer. *Oncoimmunology, 6*(9), e1338230. doi:10.1080/2162402x.2017.1338230

Konishi, A., Suzuki, J., Kuwahara, M., Matsumoto, A., Nomura, S., Soga, T., . . . Yamashita, M. (2022). Glucocorticoid imprints a low glucose metabolism onto CD8 T cells and induces the persistent suppression of the immune response. *Biochem Biophys Res Commun, 588*, 34-40. doi:10.1016/j.bbrc.2021.12.050

Koopmann, J., Buckhaults, P., Brown, D. A., Zahurak, M. L., Sato, N., Fukushima, N., . . . Goggins, M. (2004). Serum macrophage inhibitory cytokine 1 as a marker of pancreatic and other periampullary cancers. *Clin Cancer Res, 10*(7), 2386-2392. doi:10.1158/1078-0432.ccr-03-0165

Kouidhi, S., Elgaaied, A. B., & Chouaib, S. (2017). Impact of Metabolism on T-Cell Differentiation and Function and Cross Talk with Tumor Microenvironment. *Front Immunol, 8*, 270. doi:10.3389/fimmu.2017.00270

Koundouros, N., & Poulogiannis, G. (2020). Reprogramming of fatty acid metabolism in cancer. *Br J Cancer, 122*(1), 4-22. doi:10.1038/s41416-019-0650-z

Kruisbeek, A. M., Mond, J. J., Fowlkes, B. J., Carmen, J. A., Bridges, S., & Longo, D. L. (1985). Absence of the Lyt-2-,L3T4+ lineage of T cells in mice treated neonatally with anti-I-A correlates with absence of intrathymic I-A-bearing antigen-presenting cell function. *J Exp Med, 161*(5), 1029-1047. doi:10.1084/jem.161.5.1029

Krummel, M. F., & Allison, J. P. (1995). CD28 and CTLA-4 have opposing effects on the response of T cells to stimulation. *J Exp Med, 182*(2), 459-465. doi:10.1084/jem.182.2.459

Kugel, C. H., 3rd, Douglass, S. M., Webster, M. R., Kaur, A., Liu, Q., Yin, X., . . . Weeraratna, A. T. (2018). Age Correlates with Response to Anti-PD1, Reflecting Age-Related Differences in Intratumoral Effector and Regulatory T-Cell Populations. *Clin Cancer Res, 24*(21), 5347-5356. doi:10.1158/1078-0432.Ccr-18-1116

Kujawski, M., Zhang, C., Herrmann, A., Reckamp, K., Scuto, A., Jensen, M., . . . Yu, H. (2010). Targeting STAT3 in adoptively transferred T cells promotes their in vivo expansion and antitumor effects. *Cancer Res, 70*(23), 9599-9610. doi:10.1158/0008-5472.Can-10-1293

Kumar, V., Chaudhary, N., Garg, M., Floudas, C. S., Soni, P., & Chandra, A. B. (2017). Current Diagnosis and Management of Immune Related Adverse Events (irAEs) Induced by Immune Checkpoint Inhibitor Therapy. *Front Pharmacol, 8*, 49. doi:10.3389/fphar.2017.00049

Kurtulus, S., Sakuishi, K., Ngiow, S. F., Joller, N., Tan, D. J., Teng, M. W., . . . Anderson, A. C. (2015). TIGIT predominantly regulates the immune response via regulatory T cells. *J Clin Invest, 125*(11), 4053-4062. doi:10.1172/jci81187

Kurz, J., Parnham, M. J., Geisslinger, G., & Schiffmann, S. (2019). Ceramides as Novel Disease Biomarkers. *Trends Mol Med, 25*(1), 20-32. doi:10.1016/j.molmed.2018.10.009

Kyrylkova, K., Kyryachenko, S., Leid, M., & Kioussi, C. (2012). Detection of apoptosis by TUNEL assay. *Methods Mol Biol, 887*, 41-47. doi:10.1007/978-1-61779-860-3_5

Ladisch, S., Gillard, B., Wong, C., & Ulsh, L. (1983). Shedding and immunoregulatory activity of YAC-1 lymphoma cell gangliosides. *Cancer Res, 43*(8), 3808-3813.

Laird, B. J., McMillan, D., Skipworth, R. J. E., Fallon, M. T., Paval, D. R., McNeish, I., & Gallagher, I. J. (2021). The Emerging Role of Interleukin 1β (IL-1β) in Cancer Cachexia. *Inflammation, 44*(4), 1223-1228. doi:10.1007/s10753-021-01429-8

Lane, S. W., Sykes, S. M., Al-Shahrour, F., Shterental, S., Paktinat, M., Lo Celso, C., . . . Gilliland, D. G. (2010). The Apc(min) mouse has altered hematopoietic stem cell function and provides a model for MPD/MDS. *Blood, 115*(17), 3489-3497. doi:10.1182/blood-2009-11-251728

Lanna, A., Henson, S. M., Escors, D., & Akbar, A. N. (2014). The kinase p38 activated by the metabolic regulator AMPK and scaffold TAB1 drives the senescence of human T cells. *Nat Immunol, 15*(10), 965-972. doi:10.1038/ni.2981

Lau, L. L., Jamieson, B. D., Somasundaram, T., & Ahmed, R. (1994). Cytotoxic T-cell memory without antigen. *Nature, 369*(6482), 648-652. doi:10.1038/369648a0

Laurence, J. Z. (1855). The Diagnosis of Surgical Cancer. *London: John Churchill, The Liston Prize Essay for 1854.*

Lecker, S. H., Jagoe, R. T., Gilbert, A., Gomes, M., Baracos, V., Bailey, J., . . . Goldberg, A. L. (2004). Multiple types of skeletal muscle atrophy involve a common program of changes in gene expression. *Faseb j, 18*(1), 39-51. doi:10.1096/fj.03-0610com

Lee, C. M., & Kang, J. (2020). Prognostic impact of myosteatosis in patients with colorectal cancer: a systematic review and meta-analysis. *J Cachexia Sarcopenia Muscle, 11*(5), 1270-1282. doi:10.1002/jcsm.12575

Lee, H. C., Wondimu, A., Liu, Y., Ma, J. S., Radoja, S., & Ladisch, S. (2012). Ganglioside inhibition of CD8+ T cell cytotoxicity: interference with lytic granule trafficking and exocytosis. *J Immunol, 189*(7), 3521-3527. doi:10.4049/jimmunol.1201256

Lee, K., Gudapati, P., Dragovic, S., Spencer, C., Joyce, S., Killeen, N., . . . Boothby, M. (2010). Mammalian target of rapamycin protein complex 2 regulates differentiation of Th1 and Th2 cell subsets via distinct signaling pathways. *Immunity, 32*(6), 743-753. doi:10.1016/j.immuni.2010.06.002

Lerner, L., Hayes, T. G., Tao, N., Krieger, B., Feng, B., Wu, Z., . . . Garcia, J. M. (2015). Plasma growth differentiation factor 15 is associated with weight loss and mortality in cancer patients. *J Cachexia Sarcopenia Muscle, 6*(4), 317-324. doi:10.1002/jcsm.12033

Ley, K., & Kansas, G. S. (2004). Selectins in T-cell recruitment to non-lymphoid tissues and sites of inflammation. *Nat Rev Immunol, 4*(5), 325-335. doi:10.1038/nri1351

Li, C., Wang, X., Casal, I., Wang, J., Li, P., Zhang, W., . . . Zhang, H. (2016). Growth differentiation factor 15 is a promising diagnostic and prognostic biomarker in colorectal cancer. *J Cell Mol Med, 20*(8), 1420-1426. doi:10.1111/jcmm.12830

Li, F., Li, C., Cai, X., Xie, Z., Zhou, L., Cheng, B., . . . Liang, W. (2021). The association between CD8+ tumor-infiltrating lymphocytes and the clinical outcome of cancer immunotherapy: A systematic review and meta-analysis. *EClinicalMedicine, 41*, 101134. doi:10.1016/j.eclinm.2021.101134

Li, L., Liu, X., Sanders, K. L., Edwards, J. L., Ye, J., Si, F., . . . Peng, G. (2019). TLR8-Mediated Metabolic Control of Human Treg Function: A Mechanistic Target for Cancer Immunotherapy. *Cell Metab, 29*(1), 103-123.e105. doi:10.1016/j.cmet.2018.09.020

Li, T., Wu, B., Yang, T., Zhang, L., & Jin, K. (2020). The outstanding antitumor capacity of CD4(+) T helper lymphocytes. *Biochim Biophys Acta Rev Cancer, 1874*(2), 188439. doi:10.1016/j.bbcan.2020.188439

Li, X., Kostareli, E., Suffner, J., Garbi, N., & Hämmerling, G. J. (2010). Efficient Treg depletion induces T-cell infiltration and rejection of large tumors. *Eur J Immunol, 40*(12), 3325-3335. doi:10.1002/eji.201041093

Li, Y., Wang, Z., Lin, H., Wang, L., Chen, X., Liu, Q., . . . Xu, L. (2020). Bcl6 Preserves the Suppressive Function of Regulatory T Cells During Tumorigenesis. *Front Immunol, 11*, 806. doi:10.3389/fimmu.2020.00806

Li, Y. P., Schwartz, R. J., Waddell, I. D., Holloway, B. R., & Reid, M. B. (1998). Skeletal muscle myocytes undergo protein loss and reactive oxygen-mediated NF-kappaB activation in response to tumor necrosis factor alpha. *Faseb j, 12*(10), 871-880. doi:10.1096/fasebj.12.10.971

Lighvani, A. A., Frucht, D. M., Jankovic, D., Yamane, H., Aliberti, J., Hissong, B. D., . . . O'Shea, J. J. (2001). T-bet is rapidly induced by interferon-gamma in lymphoid and myeloid cells. *Proc Natl Acad Sci U S A, 98*(26), 15137-15142. doi:10.1073/pnas.261570598

Lima, J., Simoes, E., de Castro, G., Morais, M., de Matos-Neto, E. M., Alves, M. J., . . . Seelaender, M. (2019). Tumour-derived transforming growth factor-β signalling contributes to fibrosis in patients with cancer cachexia. *J Cachexia Sarcopenia Muscle, 10*(5), 1045-1059. doi:10.1002/jcsm.12441

Linsley, P. S., Brady, W., Grosmaire, L., Aruffo, A., Damle, N. K., & Ledbetter, J. A. (1991). Binding of the B cell activation antigen B7 to CD28 costimulates T cell proliferation and interleukin 2 mRNA accumulation. *J Exp Med, 173*(3), 721-730. doi:10.1084/jem.173.3.721

Lipina, C., & Hundal, H. S. (2015). Ganglioside GM3 as a gatekeeper of obesity-associated insulin resistance: Evidence and mechanisms. *FEBS Lett, 589*(21), 3221-3227. doi:10.1016/j.febslet.2015.09.018

Lipina, C., & Hundal, H. S. (2017). Lipid modulation of skeletal muscle mass and function. *J Cachexia Sarcopenia Muscle, 8*(2), 190-201. doi:10.1002/jcsm.12144

Liston, C., Cichon, J. M., Jeanneteau, F., Jia, Z., Chao, M. V., & Gan, W. B. (2013). Circadian glucocorticoid oscillations promote learning-dependent synapse formation and maintenance. *Nat Neurosci, 16*(6), 698-705. doi:10.1038/nn.3387

Liu, H., Huang, Y., Lyu, Y., Dai, W., Tong, Y., & Li, Y. (2021). GDF15 as a biomarker of ageing. *Exp Gerontol, 146*, 111228. doi:10.1016/j.exger.2021.111228

Liu, R., & Nikolajczyk, B. S. (2019). Tissue Immune Cells Fuel Obesity-Associated Inflammation in Adipose Tissue and Beyond. *Front Immunol, 10*, 1587. doi:10.3389/fimmu.2019.01587

Liu, W., Putnam, A. L., Xu-Yu, Z., Szot, G. L., Lee, M. R., Zhu, S., . . . Bluestone, J. A. (2006). CD127 expression inversely correlates with FoxP3 and suppressive function of human CD4+ T reg cells. *J Exp Med, 203*(7), 1701-1711. doi:10.1084/jem.20060772

Liu, X., Mo, W., Ye, J., Li, L., Zhang, Y., Hsueh, E. C., . . . Peng, G. (2018). Regulatory T cells trigger effector T cell DNA damage and senescence caused by metabolic competition. *Nat Commun, 9*(1), 249. doi:10.1038/s41467-017-02689-5

Liu, Y., Zhou, N., Zhou, L., Wang, J., Zhou, Y., Zhang, T., . . . Huang, B. (2021). IL-2 regulates tumor-reactive CD8(+) T cell exhaustion by activating the aryl hydrocarbon receptor. *Nat Immunol, 22*(3), 358-369. doi:10.1038/s41590-020-00850-9

Livak, K. J., & Schmittgen, T. D. (2001). Analysis of relative gene expression data using real-time quantitative PCR and the 2(-Delta Delta C(T)) Method. *Methods, 25*(4), 402-408. doi:10.1006/meth.2001.1262

Ljunggren, H. G., & Thorpe, C. J. (1996). Principles of MHC class I-mediated antigen presentation and T cell selection. *Histol Histopathol, 11*(1), 267-274.

Llovera, M., García-Martínez, C., Costelli, P., Agell, N., Carbó, N., López-Soriano, F. J., & Argilés, J. M. (1996). Muscle hypercatabolism during cancer cachexia is not reversed by the glucocorticoid receptor antagonist RU38486. *Cancer Lett, 99*(1), 7-14. doi:10.1016/0304-3835(95)04026-9

Lopez, J. A., Susanto, O., Jenkins, M. R., Lukoyanova, N., Sutton, V. R., Law, R. H., . . . Voskoboinik, I. (2013). Perforin forms transient pores on the target cell plasma membrane to facilitate rapid access of granzymes during killer cell attack. *Blood, 121*(14), 2659-2668. doi:10.1182/blood-2012-07-446146

Lorite, M. J., Thompson, M. G., Drake, J. L., Carling, G., & Tisdale, M. J. (1998). Mechanism of muscle protein degradation induced by a cancer cachectic factor. *Br J Cancer, 78*(7), 850-856. doi:10.1038/bjc.1998.592

Los, M., Schenk, H., Hexel, K., Baeuerle, P. A., Dröge, W., & Schulze-Osthoff, K. (1995). IL-2 gene expression and NF-kappa B activation through CD28 requires reactive oxygen production by 5-lipoxygenase. *Embo j, 14*(15), 3731-3740.

Lu, Y., Wang, Q., Xue, G., Bi, E., Ma, X., Wang, A., . . . Yi, Q. (2018). Th9 Cells Represent a Unique Subset of CD4(+) T Cells Endowed with the Ability to Eradicate Advanced Tumors. *Cancer Cell, 33*(6), 1048-1060.e1047. doi:10.1016/j.ccell.2018.05.004

Ma, X., Xiao, L., Liu, L., Ye, L., Su, P., Bi, E., . . . Yi, Q. (2021). CD36-mediated ferroptosis dampens intratumoral CD8(+) T cell effector function and impairs their antitumor ability. *Cell Metab, 33*(5), 1001-1012.e1005. doi:10.1016/j.cmet.2021.02.015

Macaulay, R., Akbar, A. N., & Henson, S. M. (2013). The role of the T cell in age-related inflammation. *Age (Dordr), 35*(3), 563-572. doi:10.1007/s11357-012-9381-2

Macintyre, A. N., Gerriets, V. A., Nichols, A. G., Michalek, R. D., Rudolph, M. C., Deoliveira, D., . . . Rathmell, J. C. (2014). The glucose transporter Glut1 is selectively essential for CD4 T cell activation and effector function. *Cell Metab, 20*(1), 61-72. doi:10.1016/j.cmet.2014.05.004

Mahmoud, S. M., Paish, E. C., Powe, D. G., Macmillan, R. D., Lee, A. H., Ellis, I. O., & Green, A. R. (2011). An evaluation of the clinical significance of FOXP3+ infiltrating cells in human breast cancer. *Breast Cancer Res Treat, 127*(1), 99-108. doi:10.1007/s10549-010-0987-8

Malyshkina, A., Littwitz-Salomon, E., Sutter, K., Zelinskyy, G., Windmann, S., Schimmer, S., . . . Dittmer, U. (2017). Fas Ligand-mediated cytotoxicity of CD4+ T cells during chronic retrovirus infection. *Sci Rep, 7*(1), 7785. doi:10.1038/s41598-017-08578-7

Maneechotesuwan, K., Yao, X., Ito, K., Jazrawi, E., Usmani, O. S., Adcock, I. M., & Barnes, P. J. (2009). Suppression of GATA-3 nuclear import and phosphorylation: a novel mechanism of corticosteroid action in allergic disease. *PLoS Med, 6*(5), e1000076. doi:10.1371/journal.pmed.1000076

Mangan, P. R., Harrington, L. E., O'Quinn, D. B., Helms, W. S., Bullard, D. C., Elson, C. O., . . . Weaver, C. T. (2006). Transforming growth factor-beta induces development of the T(H)17 lineage. *Nature, 441*(7090), 231-234. doi:10.1038/nature04754

Manzo, T., Prentice, B. M., Anderson, K. G., Raman, A., Schalck, A., Codreanu, G. S., . . . Nezi, L. (2020). Accumulation of long-chain fatty acids in the tumor microenvironment drives dysfunction in intrapancreatic CD8+ T cells. *J Exp Med, 217*(8). doi:10.1084/jem.20191920

Märkl, B., Rößle, J., Arnholdt, H. M., Schaller, T., Krammer, I., Cacchi, C., . . . Anthuber, M. (2012). The clinical significance of lymph node size in colon cancer. *Mod Pathol, 25*(10), 1413-1422. doi:10.1038/modpathol.2012.92

Marko, A. J., Miller, R. A., Kelman, A., & Frauwirth, K. A. (2010). Induction of glucose metabolism in stimulated T lymphocytes is regulated by mitogen-activated protein kinase signaling. *PLoS One, 5*(11), e15425. doi:10.1371/journal.pone.0015425

Martignoni, M. E., Dimitriu, C., Bachmann, J., Krakowski-Rosen, H., Ketterer, K., Kinscherf, R., & Friess, H. (2009). Liver macrophages contribute to pancreatic cancer-related cachexia. *Oncol Rep, 21*(2), 363-369.

Martin, A., Castells, J., Allibert, V., Emerit, A., Zolotoff, C., Cardot-Ruffino, V., . . . Freyssenet, D. (2022). Hypothalamic-pituitary-adrenal axis activation and glucocorticoid-responsive gene expression in skeletal muscle and liver of Apc mice. *J Cachexia Sarcopenia Muscle*. doi:10.1002/jcsm.12939

Martinez, G. J., Pereira, R. M., Äijö, T., Kim, E. Y., Marangoni, F., Pipkin, M. E., . . . Rao, A. (2015). The transcription factor NFAT promotes exhaustion of activated CD8^{+} T cells. *Immunity, 42*(2), 265-278. doi:10.1016/j.immuni.2015.01.006

Masi, T., & Patel, B. M. (2021). Altered glucose metabolism and insulin resistance in cancer-induced cachexia: a sweet poison. *Pharmacol Rep, 73*(1), 17-30. doi:10.1007/s43440-020-00179-y

Matanes, F., Twal, W. O., & Hammad, S. M. (2019). Sphingolipids as Biomarkers of Disease. *Adv Exp Med Biol, 1159*, 109-138. doi:10.1007/978-3-030-21162-2_7

Matloubian, M., Lo, C. G., Cinamon, G., Lesneski, M. J., Xu, Y., Brinkmann, V., . . . Cyster, J. G. (2004). Lymphocyte egress from thymus and peripheral lymphoid organs is dependent on S1P receptor 1. *Nature, 427*(6972), 355-360. doi:10.1038/nature02284

Matthys, P., Dijkmans, R., Proost, P., Van Damme, J., Heremans, H., Sobis, H., & Billiau, A. (1991). Severe cachexia in mice inoculated with interferon-gamma-producing tumor cells. *Int J Cancer, 49*(1), 77-82. doi:10.1002/ijc.2910490115

Mauro, C., & Marelli-Berg, F. M. (2012). T cell immunity and cardiovascular metabolic disorders: does metabolism fuel inflammation? *Front Immunol, 3*, 173. doi:10.3389/fimmu.2012.00173

McElroy, C. A., Dohm, J. A., & Walsh, S. T. (2009). Structural and biophysical studies of the human IL-7/IL-7Ralpha complex. *Structure, 17*(1), 54-65. doi:10.1016/j.str.2008.10.019

McNamara, K. M., Kannai, A., & Sasano, H. (2018). Possible roles for glucocorticoid signalling in breast cancer. *Mol Cell Endocrinol, 466*, 38-50. doi:10.1016/j.mce.2017.07.004

Meiraz, A., Garber, O. G., Harari, S., Hassin, D., & Berke, G. (2009). Switch from perforin-expressing to perforin-deficient CD8(+) T cells accounts for two distinct types of effector cytotoxic T lymphocytes in vivo. *Immunology, 128*(1), 69-82. doi:10.1111/j.1365-2567.2009.03072.x

Menk, A. V., Scharping, N. E., Moreci, R. S., Zeng, X., Guy, C., Salvatore, S., . . . Delgoffe, G. M. (2018). Early TCR Signaling Induces Rapid Aerobic Glycolysis Enabling Distinct Acute T Cell Effector Functions. *Cell Rep, 22*(6), 1509-1521. doi:10.1016/j.celrep.2018.01.040

Michaelis, K. A., Zhu, X., Burfeind, K. G., Krasnow, S. M., Levasseur, P. R., Morgan, T. K., & Marks, D. L. (2017). Establishment and characterization of a novel murine model of pancreatic cancer cachexia. *J Cachexia Sarcopenia Muscle, 8*(5), 824-838. doi:10.1002/jcsm.12225

Mills, R. E., & Jameson, J. M. (2009). T cell dependence on mTOR signaling. *Cell Cycle, 8*(4), 545-548. doi:10.4161/cc.8.4.7625

Misra, N., Bayry, J., Lacroix-Desmazes, S., Kazatchkine, M. D., & Kaveri, S. V. (2004). Cutting edge: human CD4+CD25+ T cells restrain the maturation and antigen-presenting function of dendritic cells. *J Immunol, 172*(8), 4676-4680. doi:10.4049/jimmunol.172.8.4676

Mittelstadt, P. R., & Ashwell, J. D. (2001). Inhibition of AP-1 by the glucocorticoid-inducible protein GILZ. *J Biol Chem, 276*(31), 29603-29610. doi:10.1074/jbc.M101522200

Miyawaki, T., Naito, T., Kodama, A., Nishioka, N., Miyawaki, E., Mamesaya, N., . . . Takahashi, T. (2020). Desensitizing effect of cancer cachexia on immune checkpoint inhibitors in patients with advanced non-small-cell lung cancer. *JTO Clinical and Research Reports, 1*, 100020. doi:10.1016/j.jtocrr.2020.100020

Mizukami, Y., Kono, K., Kawaguchi, Y., Akaike, H., Kamimura, K., Sugai, H., & Fujii, H. (2008). Localisation pattern of Foxp3+ regulatory T cells is associated with clinical behaviour in gastric cancer. *Br J Cancer, 98*(1), 148-153. doi:10.1038/sj.bjc.6604149

Mognol, G. P., Spreafico, R., Wong, V., Scott-Browne, J. P., Togher, S., Hoffmann, A., . . . Trifari, S. (2017). Exhaustion-associated regulatory regions in CD8(+) tumor-infiltrating T cells. *Proc Natl Acad Sci U S A, 114*(13), E2776-e2785. doi:10.1073/pnas.1620498114

Montes, C. L., Chapoval, A. I., Nelson, J., Orhue, V., Zhang, X., Schulze, D. H., . . . Gastman, B. R. (2008). Tumor-induced senescent T cells with suppressor function: a potential form of tumor immune evasion. *Cancer Res, 68*(3), 870-879. doi:10.1158/0008-5472.Can-07-2282

Moran, T. H., & Dailey, M. J. (2011). Intestinal feedback signaling and satiety. *Physiol Behav, 105*(1), 77-81. doi:10.1016/j.physbeh.2011.02.005

Morgan, M. E., van Bilsen, J. H., Bakker, A. M., Heemskerk, B., Schilham, M. W., Hartgers, F. C., . . . Toes, R. E. (2005). Expression of FOXP3 mRNA is not confined to CD4+CD25+ T regulatory cells in humans. *Hum Immunol, 66*(1), 13-20. doi:10.1016/j.humimm.2004.05.016

Morigny&Zuber, Haid, M., Kaltenecker, D., Riols, F., Lima, J. D. C., Simoes, E., . . . Rohm, M. (2020). High levels of modified ceramides are a defining feature of murine and human cancer cachexia. *J Cachexia Sarcopenia Muscle, 11*(6), 1459-1475. doi:10.1002/jcsm.12626

Moro, K., Kawaguchi, T., Tsuchida, J., Gabriel, E., Qi, Q., Yan, L., . . . Nagahashi, M. (2018). Ceramide species are elevated in human breast cancer and are associated with less aggressiveness. *Oncotarget, 9*(28), 19874-19890. doi:10.18632/oncotarget.24903

Morris, R., Kershaw, N. J., & Babon, J. J. (2018). The molecular details of cytokine signaling via the JAK/STAT pathway. *Protein Sci, 27*(12), 1984-2009. doi:10.1002/pro.3519

Moser, A. R., Pitot, H. C., & Dove, W. F. (1990). A dominant mutation that predisposes to multiple intestinal neoplasia in the mouse. *Science, 247*(4940), 322-324. doi:10.1126/science.2296722

Moses, A. G., Maingay, J., Sangster, K., Fearon, K. C., & Ross, J. A. (2009). Pro-inflammatory cytokine release by peripheral blood mononuclear cells from patients with advanced pancreatic cancer: relationship to acute phase response and survival. *Oncol Rep, 21*(4), 1091-1095. doi:10.3892/or_00000328

Mosmann, T. R., Li, L., & Sad, S. (1997). Functions of CD8 T-cell subsets secreting different cytokine patterns. *Semin Immunol, 9*(2), 87-92. doi:10.1006/smim.1997.0065

Motzer, R. J., Escudier, B., McDermott, D. F., George, S., Hammers, H. J., Srinivas, S., . . . Sharma, P. (2015). Nivolumab versus Everolimus in Advanced Renal-Cell Carcinoma. *N Engl J Med, 373*(19), 1803-1813. doi:10.1056/NEJMoa1510665

Murray, S., Schell, K., McCarthy, D. O., & Albertini, M. R. (1997). Tumor growth, weight loss and cytokines in SCID mice. *Cancer Lett, 111*(1-2), 111-115. doi:10.1016/s0304-3835(96)04519-3

Narsale, A., Moya, R., Ma, J., Anderson, L. J., Wu, D., Garcia, J. M., & Davies, J. D. (2019). Cancer-driven changes link T cell frequency to muscle strength in people with cancer: a pilot study. *J Cachexia Sarcopenia Muscle, 10*(4), 827-843. doi:10.1002/jcsm.12424

Newton, R., Priyadharshini, B., & Turka, L. A. (2016). Immunometabolism of regulatory T cells. *Nat Immunol, 17*(6), 618-625. doi:10.1038/ni.3466

Nishimura, S., Manabe, I., Nagasaki, M., Eto, K., Yamashita, H., Ohsugi, M., . . . Nagai, R. (2009). CD8+ effector T cells contribute to macrophage recruitment and adipose tissue inflammation in obesity. *Nat Med, 15*(8), 914-920. doi:10.1038/nm.1964

Noguchi, Y., Makino, T., Yoshikawa, T., Nomura, K., Fukuzawa, K., Matsumoto, A., & Yamada, T. (1996). The possible role of TNF-alpha and IL-2 in inducing tumor-associated metabolic alterations. *Surg Today, 26*(1), 36-41. doi:10.1007/bf00311989

Norment, A. M., Salter, R. D., Parham, P., Engelhard, V. H., & Littman, D. R. (1988). Cell-cell adhesion mediated by CD8 and MHC class I molecules. *Nature, 336*(6194), 79-81. doi:10.1038/336079a0

Norton, J. A., Moley, J. F., Green, M. V., Carson, R. E., & Morrison, S. D. (1985). Parabiotic transfer of cancer anorexia/cachexia in male rats. *Cancer Res, 45*(11 Pt 1), 5547-5552.

O'Connell, T. M., Golzarri-Arroyo, L., Pin, F., Barreto, R., Dickinson, S. L., Couch, M. E., & Bonetto, A. (2021). Metabolic Biomarkers for the Early Detection of Cancer Cachexia. *Front Cell Dev Biol, 9*, 720096. doi:10.3389/fcell.2021.720096

Ohe, Y., Podack, E. R., Olsen, K. J., Miyahara, Y., Miura, K., Saito, H., . . . et al. (1993). Interleukin-6 cDNA transfected Lewis lung carcinoma cells show unaltered net tumour growth rate but cause weight loss and shortened survival in syngeneic mice. *Br J Cancer, 67*(5), 939-944. doi:10.1038/bjc.1993.174

Ohira, T., Nishio, K., Ohe, Y., Arioka, H., Nishio, M., Funayama, Y., . . . Saijo, N. (1996). Improvement by eicosanoids in cancer cachexia induced by LLC-IL6 transplantation. *J Cancer Res Clin Oncol, 122*(12), 711-715. doi:10.1007/bf01209117

Ohki, S., Shibata, M., Gonda, K., Machida, T., Shimura, T., Nakamura, I., . . . Takenoshita, S. (2012). Circulating myeloid-derived suppressor cells are increased and correlate to immune suppression, inflammation and hypoproteinemia in patients with cancer. *Oncol Rep, 28*(2), 453-458. doi:10.3892/or.2012.1812

Ohta, M., Tanaka, F., Yamaguchi, H., Sadanaga, N., Inoue, H., & Mori, M. (2005). The high expression of Fractalkine results in a better prognosis for colorectal cancer patients. *Int J Oncol, 26*(1), 41-47.

Oliff, A., Defeo-Jones, D., Boyer, M., Martinez, D., Kiefer, D., Vuocolo, G., . . . Socher, S. H. (1987). Tumors secreting human TNF/cachectin induce cachexia in mice. *Cell, 50*(4), 555-563. doi:10.1016/0092-8674(87)90028-6

Olson, B., Diba, P., Korzun, T., & Marks, D. L. (2021). Neural Mechanisms of Cancer Cachexia. *Cancers (Basel), 13*(16). doi:10.3390/cancers13163990

Osawa, Y., Semba, R. D., Fantoni, G., Candia, J., Biancotto, A., Tanaka, T., . . . Ferrucci, L. (2020). Plasma proteomic signature of the risk of developing mobility disability: A 9-year follow-up. *Aging Cell, 19*(4), e13132. doi:10.1111/acel.13132

Pakiet, A., Kobiela, J., Stepnowski, P., Sledzinski, T., & Mika, A. (2019). Changes in lipids composition and metabolism in colorectal cancer: a review. *Lipids Health Dis, 18*(1), 29. doi:10.1186/s12944-019-0977-8

Palmer, C. S., Ostrowski, M., Balderson, B., Christian, N., & Crowe, S. M. (2015). Glucose metabolism regulates T cell activation, differentiation, and functions. *Front Immunol, 6*, 1. doi:10.3389/fimmu.2015.00001

Palmer, S., Albergante, L., Blackburn, C. C., & Newman, T. J. (2018). Thymic involution and rising disease incidence with age. *Proc Natl Acad Sci U S A, 115*(8), 1883-1888. doi:10.1073/pnas.1714478115

Pardo, J., Wallich, R., Martin, P., Urban, C., Rongvaux, A., Flavell, R. A., . . . Simon, M. M. (2008). Granzyme B-induced cell death exerted by ex vivo CTL: discriminating requirements for cell death and some of its signs. *Cell Death Differ, 15*(3), 567-579. doi:10.1038/sj.cdd.4402289

Park, I. K., Shultz, L. D., Letterio, J. J., & Gorham, J. D. (2005). TGF-beta1 inhibits T-bet induction by IFN-gamma in murine CD4+ T cells through the protein tyrosine phosphatase Src homology region 2 domain-containing phosphatase-1. *J Immunol, 175*(9), 5666-5674. doi:10.4049/jimmunol.175.9.5666

Parkin, J., & Cohen, B. (2001). An overview of the immune system. *Lancet, 357*(9270), 1777-1789. doi:10.1016/s0140-6736(00)04904-7

Parry, R. V., Chemnitz, J. M., Frauwirth, K. A., Lanfranco, A. R., Braunstein, I., Kobayashi, S. V., . . . Riley, J. L. (2005). CTLA-4 and PD-1 receptors inhibit T-cell activation by distinct mechanisms. *Mol Cell Biol, 25*(21), 9543-9553. doi:10.1128/mcb.25.21.9543-9553.2005

Patsalos, O., Dalton, B., Leppanen, J., Ibrahim, M. A. A., & Himmerich, H. (2020). Impact of TNF-α Inhibitors on Body Weight and BMI: A Systematic Review and Meta-Analysis. *Front Pharmacol, 11*, 481. doi:10.3389/fphar.2020.00481

Patsoukis, N., Sari, D., & Boussiotis, V. A. (2012). PD-1 inhibits T cell proliferation by upregulating p27 and p15 and suppressing Cdc25A. *Cell Cycle, 11*(23), 4305-4309. doi:10.4161/cc.22135

Pearce, E. L. (2010). Metabolism in T cell activation and differentiation. *Curr Opin Immunol, 22*(3), 314-320. doi:10.1016/j.coi.2010.01.018

Pearce, E. L., Mullen, A. C., Martins, G. A., Krawczyk, C. M., Hutchins, A. S., Zediak, V. P., . . . Reiner, S. L. (2003). Control of effector CD8+ T cell function by the transcription factor Eomesodermin. *Science, 302*(5647), 1041-1043. doi:10.1126/science.1090148

Pearce, E. L., Poffenberger, M. C., Chang, C. H., & Jones, R. G. (2013). Fueling immunity: insights into metabolism and lymphocyte function. *Science, 342*(6155), 1242454. doi:10.1126/science.1242454

Peeters, L. M., Vanheusden, M., Somers, V., Van Wijmeersch, B., Stinissen, P., Broux, B., & Hellings, N. (2017). Cytotoxic CD4+ T Cells Drive Multiple Sclerosis Progression. *Front Immunol, 8*, 1160. doi:10.3389/fimmu.2017.01160

Peng, M., Yin, N., Chhangawala, S., Xu, K., Leslie, C. S., & Li, M. O. (2016). Aerobic glycolysis promotes T helper 1 cell differentiation through an epigenetic mechanism. *Science, 354*(6311), 481-484. doi:10.1126/science.aaf6284

Penna, F., Costamagna, D., Pin, F., Camperi, A., Fanzani, A., Chiarpotto, E. M., . . . Costelli, P. (2013). Autophagic degradation contributes to muscle wasting in cancer cachexia. *Am J Pathol, 182*(4), 1367-1378. doi:10.1016/j.ajpath.2012.12.023

Perlman, R. L. (2016). Mouse models of human disease: An evolutionary perspective. *Evol Med Public Health, 2016*(1), 170-176. doi:10.1093/emph/eow014

Peters, V. A., Joesting, J. J., & Freund, G. G. (2013). IL-1 receptor 2 (IL-1R2) and its role in immune regulation. *Brain Behav Immun, 32*, 1-8. doi:10.1016/j.bbi.2012.11.006

Petruzzelli, M., Ferrer, M., Schuijs, M. J., Kleeman, S. O., Mourikis, N., Hall, Z., . . . Janowitz, T. (2022). Early Neutrophilia Marked by Aerobic Glycolysis Sustains Host Metabolism and Delays Cancer Cachexia. *Cancers (Basel), 14*(4). doi:10.3390/cancers14040963

Petruzzelli, M., Schweiger, M., Schreiber, R., Campos-Olivas, R., Tsoli, M., Allen, J., . . . Wagner, E. F. (2014). A switch from white to brown fat increases energy expenditure in cancer-associated cachexia. *Cell Metab, 20*(3), 433-447. doi:10.1016/j.cmet.2014.06.011

Piccirillo, A. R., Hyzny, E. J., Beppu, L. Y., Menk, A. V., Wallace, C. T., Hawse, W. F., . . . D'Cruz, L. M. (2019). The Lysophosphatidylcholine Transporter MFSD2A Is Essential for CD8(+) Memory T Cell Maintenance and Secondary Response to Infection. *J Immunol, 203*(1), 117-126. doi:10.4049/jimmunol.1801585

Postow, M. A., Chesney, J., Pavlick, A. C., Robert, C., Grossmann, K., McDermott, D., . . . Hodi, F. S. (2015). Nivolumab and ipilimumab versus ipilimumab in untreated melanoma. *N Engl J Med, 372*(21), 2006-2017. doi:10.1056/NEJMoa1414428

Prado, B. L., & Qian, Y. (2019). Anti-cytokines in the treatment of cancer cachexia. *Ann Palliat Med, 8*(1), 67-79. doi:10.21037/apm.2018.07.06

Prizment, A. E., Vierkant, R. A., Smyrk, T. C., Tillmans, L. S., Nelson, H. H., Lynch, C. F., . . . Limburg, P. J. (2017). Cytotoxic T Cells and Granzyme B Associated with Improved Colorectal Cancer Survival in a Prospective Cohort of Older Women. *Cancer Epidemiol Biomarkers Prev, 26*(4), 622-631. doi:10.1158/1055-9965.Epi-16-0641

Puppa, M. J., White, J. P., Sato, S., Cairns, M., Baynes, J. W., & Carson, J. A. (2011). Gut barrier dysfunction in the Apc(Min/+) mouse model of colon cancer cachexia. *Biochim Biophys Acta, 1812*(12), 1601-1606. doi:10.1016/j.bbadis.2011.08.010

Purwar, R., Schlapbach, C., Xiao, S., Kang, H. S., Elyaman, W., Jiang, X., . . . Kupper, T. S. (2012). Robust tumor immunity to melanoma mediated by interleukin-9-producing T cells. *Nat Med, 18*(8), 1248-1253. doi:10.1038/nm.2856

Qian, X., Chen, H., Wu, X., Hu, L., Huang, Q., & Jin, Y. (2017). Interleukin-17 acts as double-edged sword in anti-tumor immunity and tumorigenesis. *Cytokine, 89*, 34-44. doi:10.1016/j.cyto.2015.09.011

Quigley, M., Pereyra, F., Nilsson, B., Porichis, F., Fonseca, C., Eichbaum, Q., . . . Haining, W. N. (2010). Transcriptional analysis of HIV-specific CD8+ T cells shows that PD-1 inhibits T cell function by upregulating BATF. *Nat Med, 16*(10), 1147-1151. doi:10.1038/nm.2232

Radu, C. G., Yang, L. V., Riedinger, M., Au, M., & Witte, O. N. (2004). T cell chemotaxis to lysophosphatidylcholine through the G2A receptor. *Proc Natl Acad Sci U S A, 101*(1), 245-250. doi:10.1073/pnas.2536801100

Rao, R. R., Li, Q., Odunsi, K., & Shrikant, P. A. (2010). The mTOR kinase determines effector versus memory CD8+ T cell fate by regulating the expression of transcription factors T-bet and Eomesodermin. *Immunity, 32*(1), 67-78. doi:10.1016/j.immuni.2009.10.010

Raud, B., Roy, D. G., Divakaruni, A. S., Tarasenko, T. N., Franke, R., Ma, E. H., . . . Berod, L. (2018). Etomoxir Actions on Regulatory and Memory T Cells Are Independent of Cpt1a-Mediated Fatty Acid Oxidation. *Cell Metab, 28*(3), 504-515.e507. doi:10.1016/j.cmet.2018.06.002

Rausch, M. E., Weisberg, S., Vardhana, P., & Tortoriello, D. V. (2008). Obesity in C57BL/6J mice is characterized by adipose tissue hypoxia and cytotoxic T-cell infiltration. *Int J Obes (Lond), 32*(3), 451-463. doi:10.1038/sj.ijo.0803744

Raval, A., Puri, N., Rath, P. C., & Saxena, R. K. (1998). Cytokine regulation of expression of class I MHC antigens. *Exp Mol Med, 30*(1), 1-13. doi:10.1038/emm.1998.1

Ravitz, M. J., Chen, L., Lynch, M., & Schmidt, E. V. (2007). c-myc Repression of TSC2 contributes to control of translation initiation and Myc-induced transformation. *Cancer Res, 67*(23), 11209-11217. doi:10.1158/0008-5472.Can-06-4351

Ray, A., & Prefontaine, K. E. (1994). Physical association and functional antagonism between the p65 subunit of transcription factor NF-kappa B and the glucocorticoid receptor. *Proc Natl Acad Sci U S A, 91*(2), 752-756. doi:10.1073/pnas.91.2.752

Rayman, P., Wesa, A. K., Richmond, A. L., Das, T., Biswas, K., Raval, G., . . . Finke, J. (2004). Effect of renal cell carcinomas on the development of type 1 T-cell responses. *Clin Cancer Res, 10*(18 Pt 2), 6360s-6366s. doi:10.1158/1078-0432.Ccr-050011

Raynor, A., Jantscheff, P., Ross, T., Schlesinger, M., Wilde, M., Haasis, S., . . . Massing, U. (2015). Saturated and mono-unsaturated lysophosphatidylcholine metabolism in tumour cells: a potential therapeutic target for preventing metastases. *Lipids Health Dis, 14*, 69. doi:10.1186/s12944-015-0070-x

Reck, M., Rodríguez-Abreu, D., Robinson, A. G., Hui, R., Csőszi, T., Fülöp, A., . . . Brahmer, J. R. (2016). Pembrolizumab versus Chemotherapy for PD-L1-Positive Non-Small-Cell Lung Cancer. *N Engl J Med, 375*(19), 1823-1833. doi:10.1056/NEJMoa1606774

Reid, M. B., & Li, Y. P. (2001). Tumor necrosis factor-alpha and muscle wasting: a cellular perspective. *Respir Res, 2*(5), 269-272. doi:10.1186/rr67

Revu, S., Wu, J., Henkel, M., Rittenhouse, N., Menk, A., Delgoffe, G. M., . . . McGeachy, M. J. (2018). IL-23 and IL-1β Drive Human Th17 Cell Differentiation and Metabolic Reprogramming in Absence of CD28 Costimulation. *Cell Rep, 22*(10), 2642-2653. doi:10.1016/j.celrep.2018.02.044

Riccardi, D., das Neves, R. X., de Matos-Neto, E. M., Camargo, R. G., Lima, J., Radloff, K., . . . Seelaender, M. (2020). Plasma Lipid Profile and Systemic Inflammation in Patients With Cancer Cachexia. *Front Nutr, 7*, 4. doi:10.3389/fnut.2020.00004

Rice, D. A., Mouw, A. R., Bogerd, A. M., & Parker, K. L. (1991). A shared promoter element regulates the expression of three steroidogenic enzymes. *Mol Endocrinol, 5*(10), 1552-1561. doi:10.1210/mend-5-10-1552

Rivadeneira, D. E., Naama, H. A., McCarter, M. D., Fujita, J., Evoy, D., Mackrell, P., & Daly, J. M. (1999). Glucocorticoid blockade does not abrogate tumor-induced cachexia. *Nutr Cancer, 35*(2), 202-206. doi:10.1207/s15327914nc352_16

Robert, C. (2020). A decade of immune-checkpoint inhibitors in cancer therapy. *Nat Commun, 11*(1), 3801. doi:10.1038/s41467-020-17670-y

Robert, C., Schachter, J., Long, G. V., Arance, A., Grob, J. J., Mortier, L., . . . Ribas, A. (2015). Pembrolizumab versus Ipilimumab in Advanced Melanoma. *N Engl J Med, 372*(26), 2521-2532. doi:10.1056/NEJMoa1503093

Rocha, V. Z., & Libby, P. (2009). Obesity, inflammation, and atherosclerosis. *Nat Rev Cardiol, 6*(6), 399-409. doi:10.1038/nrcardio.2009.55

Roche, P. A., & Furuta, K. (2015). The ins and outs of MHC class II-mediated antigen processing and presentation. *Nat Rev Immunol, 15*(4), 203-216. doi:10.1038/nri3818

Roeland, E. J., Bohlke, K., Baracos, V. E., Bruera, E., Del Fabbro, E., Dixon, S., . . . Loprinzi, C. L. (2020). Management of Cancer Cachexia: ASCO Guideline. *J Clin Oncol, 38*(21), 2438-2453. doi:10.1200/jco.20.00611

Roggero, E., Pérez, A. R., Tamae-Kakazu, M., Piazzon, I., Nepomnaschy, I., Besedovsky, H. O., . . . del Rey, A. (2006). Endogenous glucocorticoids cause thymus atrophy but are protective during acute Trypanosoma cruzi infection. *J Endocrinol, 190*(2), 495-503. doi:10.1677/joe.1.06642

Rohm, M., & Herzig, S. (2020). An Antibody Attack against Body Wasting in Cancer. *Cell Metab, 32*(3), 331-333. doi:10.1016/j.cmet.2020.08.003

Rohm, M., Schafer, M., Laurent, V., Ustunel, B. E., Niopek, K., Algire, C., . . . Herzig, S. (2016). An AMP-activated protein kinase-stabilizing peptide ameliorates adipose tissue wasting in cancer cachexia in mice. *Nat Med, 22*(10), 1120-1130. doi:10.1038/nm.4171

Rohm, M., Zeigerer, A., Machado, J., & Herzig, S. (2019). Energy metabolism in cachexia. *EMBO Rep, 20*(4). doi:10.15252/embr.201847258

Rooney, J. W., Sun, Y. L., Glimcher, L. H., & Hoey, T. (1995). Novel NFAT sites that mediate activation of the interleukin-2 promoter in response to T-cell receptor stimulation. *Mol Cell Biol, 15*(11), 6299-6310. doi:10.1128/mcb.15.11.6299

Roose, J. P., Mollenauer, M., Gupta, V. A., Stone, J., & Weiss, A. (2005). A diacylglycerol-protein kinase C-RasGRP1 pathway directs Ras activation upon antigen receptor stimulation of T cells. *Mol Cell Biol, 25*(11), 4426-4441. doi:10.1128/mcb.25.11.4426-4441.2005

Rosenthal, A. S., & Shevach, E. M. (1973). Function of macrophages in antigen recognition by guinea pig T lymphocytes. I. Requirement for histocompatible macrophages and lymphocytes. *J Exp Med, 138*(5), 1194-1212. doi:10.1084/jem.138.5.1194

Ross, S. H., & Cantrell, D. A. (2018). Signaling and Function of Interleukin-2 in T Lymphocytes. *Annu Rev Immunol, 36*, 411-433. doi:10.1146/annurev-immunol-042617-053352

Rossjohn, J., Gras, S., Miles, J. J., Turner, S. J., Godfrey, D. I., & McCluskey, J. (2015). T cell antigen receptor recognition of antigen-presenting molecules. *Annu Rev Immunol, 33*, 169-200. doi:10.1146/annurev-immunol-032414-112334

Roux, A., Leroy, H., De Muylder, B., Bracq, L., Oussous, S., Dusanter-Fourt, I., . . . Mangeney, M. (2019). FOXO1 transcription factor plays a key role in T cell-HIV-1 interaction. *PLoS Pathog, 15*(5), e1007669. doi:10.1371/journal.ppat.1007669

Rupert, J. E., Narasimhan, A., Jengelley, D. H. A., Jiang, Y., Liu, J., Au, E., . . . Zimmers, T. A. (2021). Tumor-derived IL-6 and trans-signaling among tumor, fat, and muscle mediate pancreatic cancer cachexia. *J Exp Med, 218*(6). doi:10.1084/jem.20190450

Russell, S. T., & Tisdale, M. J. (2005). The role of glucocorticoids in the induction of zinc-alpha2-glycoprotein expression in adipose tissue in cancer cachexia. *Br J Cancer, 92*(5), 876-881. doi:10.1038/sj.bjc.6602404

Ruzek, M. C., Pearce, B. D., Miller, A. H., & Biron, C. A. (1999). Endogenous glucocorticoids protect against cytokine-mediated lethality during viral infection. *J Immunol, 162*(6), 3527-3533.

Rydén, M., Agustsson, T., Laurencikiene, J., Britton, T., Sjölin, E., Isaksson, B., . . . Arner, P. (2008). Lipolysis--not inflammation, cell death, or lipogenesis--is involved in adipose tissue loss in cancer cachexia. *Cancer, 113*(7), 1695-1704. doi:10.1002/cncr.23802

Saito, T., Nishikawa, H., Wada, H., Nagano, Y., Sugiyama, D., Atarashi, K., . . . Sakaguchi, S. (2016). Two FOXP3(+)CD4(+) T cell subpopulations distinctly control the prognosis of colorectal cancers. *Nat Med, 22*(6), 679-684. doi:10.1038/nm.4086

Sakaguchi, S., Sakaguchi, N., Asano, M., Itoh, M., & Toda, M. (1995). Immunologic self-tolerance maintained by activated T cells expressing IL-2 receptor alpha-chains (CD25). Breakdown of a single mechanism of self-tolerance causes various autoimmune diseases. *J Immunol, 155*(3), 1151-1164.

Sakaguchi, S., Yamaguchi, T., Nomura, T., & Ono, M. (2008). Regulatory T cells and immune tolerance. *Cell, 133*(5), 775-787. doi:10.1016/j.cell.2008.05.009

Sallusto, F., Geginat, J., & Lanzavecchia, A. (2004). Central memory and effector memory T cell subsets: function, generation, and maintenance. *Annu Rev Immunol, 22*, 745-763. doi:10.1146/annurev.immunol.22.012703.104702

Sallusto, F., Lenig, D., Förster, R., Lipp, M., & Lanzavecchia, A. (1999). Two subsets of memory T lymphocytes with distinct homing potentials and effector functions. *Nature, 401*(6754), 708-712. doi:10.1038/44385

Salmond, R. J. (2018). mTOR Regulation of Glycolytic Metabolism in T Cells. *Front Cell Dev Biol, 6*, 122. doi:10.3389/fcell.2018.00122

Samelson, L. E., Patel, M. D., Weissman, A. M., Harford, J. B., & Klausner, R. D. (1986). Antigen activation of murine T cells induces tyrosine phosphorylation of a polypeptide associated with the T cell antigen receptor. *Cell, 46*(7), 1083-1090. doi:10.1016/0092-8674(86)90708-7

Sandri, M., Sandri, C., Gilbert, A., Skurk, C., Calabria, E., Picard, A., . . . Goldberg, A. L. (2004). Foxo transcription factors induce the atrophy-related ubiquitin ligase atrogin-1 and cause skeletal muscle atrophy. *Cell, 117*(3), 399-412. doi:10.1016/s0092-8674(04)00400-3

Santen, R. J., Samojlik, E., Lipton, A., Harvey, H., Ruby, E. B., Wells, S. A., & Kendall, J. (1977). Kinetic, hormonal and clinical studies with aminoglutethimide in breast cancer. *Cancer, 39*(6 Suppl), 2948-2958. doi:10.1002/1097-0142(197706)39:6<2948::aid-cncr2820390681>3.0.co;2-9

Sapolsky, R. M., Romero, L. M., & Munck, A. U. (2000). How do glucocorticoids influence stress responses? Integrating permissive, suppressive, stimulatory, and preparative actions. *Endocr Rev, 21*(1), 55-89. doi:10.1210/edrv.21.1.0389

Sarbassov, D. D., Ali, S. M., Kim, D. H., Guertin, D. A., Latek, R. R., Erdjument-Bromage, H., . . . Sabatini, D. M. (2004). Rictor, a novel binding partner of mTOR, defines a rapamycin-insensitive and raptor-independent pathway that regulates the cytoskeleton. *Curr Biol, 14*(14), 1296-1302. doi:10.1016/j.cub.2004.06.054

Sarbassov, D. D., Guertin, D. A., Ali, S. M., & Sabatini, D. M. (2005). Phosphorylation and regulation of Akt/PKB by the rictor-mTOR complex. *Science, 307*(5712), 1098-1101. doi:10.1126/science.1106148

Savas, P., Virassamy, B., Ye, C., Salim, A., Mintoff, C. P., Caramia, F., . . . Loi, S. (2018). Single-cell profiling of breast cancer T cells reveals a tissue-resident memory subset associated with improved prognosis. *Nat Med, 24*(7), 986-993. doi:10.1038/s41591-018-0078-7

Schäfer, M., Oeing, C. U., Rohm, M., Baysal-Temel, E., Lehmann, L. H., Bauer, R., . . . Herzig, S. (2016). Ataxin-10 is part of a cachexokine cocktail triggering cardiac metabolic dysfunction in cancer cachexia. *Mol Metab, 5*(2), 67-78. doi:10.1016/j.molmet.2015.11.004

Scheinman, R. I., Cogswell, P. C., Lofquist, A. K., & Baldwin, A. S., Jr. (1995). Role of transcriptional activation of I kappa B alpha in mediation of immunosuppression by glucocorticoids. *Science, 270*(5234), 283-286. doi:10.1126/science.270.5234.283

Scheinman, R. I., Gualberto, A., Jewell, C. M., Cidlowski, J. A., & Baldwin, A. S., Jr. (1995). Characterization of mechanisms involved in transrepression of NF-kappa B by activated glucocorticoid receptors. *Mol Cell Biol, 15*(2), 943-953. doi:10.1128/mcb.15.2.943

Schmidt, S. F., Rohm, M., Herzig, S., & Berriel Diaz, M. (2018). Cancer Cachexia: More Than Skeletal Muscle Wasting. *Trends Cancer, 4*(12), 849-860. doi:10.1016/j.trecan.2018.10.001

Schwartz, R. H. (2003). T cell anergy. *Annu Rev Immunol, 21*, 305-334. doi:10.1146/annurev.immunol.21.120601.141110

Sebzda, E., Zou, Z., Lee, J. S., Wang, T., & Kahn, M. L. (2008). Transcription factor KLF2 regulates the migration of naive T cells by restricting chemokine receptor expression patterns. *Nat Immunol, 9*(3), 292-300. doi:10.1038/ni1565

Sehgal, S. N. (1993). Immunosuppressive profile of rapamycin. *Ann N Y Acad Sci, 696*, 1-8. doi:10.1111/j.1749-6632.1993.tb17136.x

Sehgal, S. N., Baker, H., & Vézina, C. (1975). Rapamycin (AY-22,989), a new antifungal antibiotic. II. Fermentation, isolation and characterization. *J Antibiot (Tokyo), 28*(10), 727-732. doi:10.7164/antibiotics.28.727

Semba, R. D., Zhang, P., Adelnia, F., Sun, K., Gonzalez-Freire, M., Salem, N., Jr., . . . Ferrucci, L. (2019). Low plasma lysophosphatidylcholines are associated with impaired mitochondrial oxidative capacity in adults in the Baltimore Longitudinal Study of Aging. *Aging Cell, 18*(2), e12915. doi:10.1111/acel.12915

Sena, L. A., Li, S., Jairaman, A., Prakriya, M., Ezponda, T., Hildeman, D. A., . . . Chandel, N. S. (2013). Mitochondria are required for antigen-specific T cell activation through reactive oxygen species signaling. *Immunity, 38*(2), 225-236. doi:10.1016/j.immuni.2012.10.020

Shamoun, L., Landerholm, K., Balboa Ramilo, A., Andersson, R. E., Dimberg, J., & Wågsäter, D. (2021). Association of gene and protein expression and genetic polymorphism of CC chemokine ligand 4 in colorectal cancer. *World J Gastroenterol, 27*(30), 5076-5087. doi:10.3748/wjg.v27.i30.5076

Shen, Y., Tolić, N., Liu, T., Zhao, R., Petritis, B. O., Gritsenko, M. A., . . . Smith, R. D. (2010). Blood peptidome-degradome profile of breast cancer. *PLoS One, 5*(10), e13133. doi:10.1371/journal.pone.0013133

Sheppard, B. C., Venzon, D., Fraker, D. L., Langstein, H. N., Jensen, J. C., & Norton, J. A. (1990). Prolonged survival of tumor-bearing rats with repetitive low-dose recombinant tumor necrosis factor. *Cancer Res, 50*(13), 3928-3933.

Sheppard, K. A., Fitz, L. J., Lee, J. M., Benander, C., George, J. A., Wooters, J., . . . Chaudhary, D. (2004). PD-1 inhibits T-cell receptor induced phosphorylation of the ZAP70/CD3zeta signalosome and downstream signaling to PKCtheta. *FEBS Lett, 574*(1-3), 37-41. doi:10.1016/j.febslet.2004.07.083

Sherry, B. A., Gelin, J., Fong, Y., Marano, M., Wei, H., Cerami, A., . . . Moldawer, L. L. (1989). Anticachectin/tumor necrosis factor-alpha antibodies attenuate development of cachexia in tumor models. *Faseb j, 3*(8), 1956-1962. doi:10.1096/fasebj.3.8.2721856

Shevach, E. M., & Rosenthal, A. S. (1973). Function of macrophages in antigen recognition by guinea pig T lymphocytes. II. Role of the macrophage in the regulation of genetic control of the immune response. *J Exp Med, 138*(5), 1213-1229. doi:10.1084/jem.138.5.1213

Shi, F., Shi, M., Zeng, Z., Qi, R. Z., Liu, Z. W., Zhang, J. Y., . . . Wang, F. S. (2011). PD-1 and PD-L1 upregulation promotes CD8(+) T-cell apoptosis and postoperative recurrence in hepatocellular carcinoma patients. *Int J Cancer, 128*(4), 887-896. doi:10.1002/ijc.25397

Shim, E. K., Jung, S. H., & Lee, J. R. (2011). Role of two adaptor molecules SLP-76 and LAT in the PI3K signaling pathway in activated T cells. *J Immunol, 186*(5), 2926-2935. doi:10.4049/jimmunol.1001785

Shimada, Y., Hayashi, M., Nagasaka, Y., Ohno-Iwashita, Y., & Inomata, M. (2009). Age-associated up-regulation of a negative co-stimulatory receptor PD-1 in mouse CD4+ T cells. *Exp Gerontol, 44*(8), 517-522. doi:10.1016/j.exger.2009.05.003

Shukla, S. K., Markov, S. D., Attri, K. S., Vernucci, E., King, R. J., Dasgupta, A., . . . Mehla, K. (2020). Macrophages potentiate STAT3 signaling in skeletal muscles and regulate pancreatic cancer cachexia. *Cancer Lett, 484*, 29-39. doi:10.1016/j.canlet.2020.04.017

Shyer, J. A., Flavell, R. A., & Bailis, W. (2020). Metabolic signaling in T cells. *Cell Res, 30*(8), 649-659. doi:10.1038/s41422-020-0379-5

Sim, B. C., Aftahi, N., Reilly, C., Bogen, B., Schwartz, R. H., Gascoigne, N. R., & Lo, D. (1998). Thymic skewing of the CD4/CD8 ratio maps with the T-cell receptor alpha-chain locus. *Curr Biol, 8*(12), 701-704. doi:10.1016/s0960-9822(98)70276-3

Simon, M. M., Greenaway, S., White, J. K., Fuchs, H., Gailus-Durner, V., Wells, S., . . . Brown, S. D. (2013). A comparative phenotypic and genomic analysis of C57BL/6J and C57BL/6N mouse strains. *Genome Biol, 14*(7), R82. doi:10.1186/gb-2013-14-7-r82

Singer, M., Wang, C., Cong, L., Marjanovic, N. D., Kowalczyk, M. S., Zhang, H., . . . Anderson, A. C. (2016). A Distinct Gene Module for Dysfunction Uncoupled from Activation in Tumor-Infiltrating T Cells. *Cell, 166*(6), 1500-1511.e1509. doi:10.1016/j.cell.2016.08.052

Śledzińska, A., Vila de Mucha, M., Bergerhoff, K., Hotblack, A., Demane, D. F., Ghorani, E., . . . Quezada, S. A. (2020). Regulatory T Cells Restrain Interleukin-2- and Blimp-1-Dependent Acquisition of Cytotoxic Function by CD4(+) T Cells. *Immunity, 52*(1), 151-166.e156. doi:10.1016/j.immuni.2019.12.007

Slominski, A., Wortsman, J., Luger, T., Paus, R., & Solomon, S. (2000). Corticotropin releasing hormone and proopiomelanocortin involvement in the cutaneous response to stress. *Physiol Rev, 80*(3), 979-1020. doi:10.1152/physrev.2000.80.3.979

Slominski, A. T., Zmijewski, M. A., Zbytek, B., Tobin, D. J., Theoharides, T. C., & Rivier, J. (2013). Key role of CRF in the skin stress response system. *Endocr Rev, 34*(6), 827-884. doi:10.1210/er.2012-1092

Smith, B. D., Smith, G. L., Hurria, A., Hortobagyi, G. N., & Buchholz, T. A. (2009). Future of cancer incidence in the United States: burdens upon an aging, changing nation. *J Clin Oncol, 27*(17), 2758-2765. doi:10.1200/jco.2008.20.8983

Solheim, T. S., & Laird, B. J. (2012). Evidence base for multimodal therapy in cachexia. *Curr Opin Support Palliat Care, 6*(4), 424-431. doi:10.1097/SPC.0b013e328359b668

Song, L. N., Coghlan, M., & Gelmann, E. P. (2004). Antiandrogen effects of mifepristone on coactivator and corepressor interactions with the androgen receptor. *Mol Endocrinol, 18*(1), 70-85. doi:10.1210/me.2003-0189

Staff, A. C., Bock, A. J., Becker, C., Kempf, T., Wollert, K. C., & Davidson, B. (2010). Growth differentiation factor-15 as a prognostic biomarker in ovarian cancer. *Gynecol Oncol, 118*(3), 237-243. doi:10.1016/j.ygyno.2010.05.032

Stahl, M., Dijkers, P. F., Kops, G. J., Lens, S. M., Coffer, P. J., Burgering, B. M., & Medema, R. H. (2002). The forkhead transcription factor FoxO regulates transcription of p27Kip1 and Bim in response to IL-2. *J Immunol, 168*(10), 5024-5031. doi:10.4049/jimmunol.168.10.5024

Staron, M. M., Gray, S. M., Marshall, H. D., Parish, I. A., Chen, J. H., Perry, C. J., . . . Kaech, S. M. (2014). The transcription factor FoxO1 sustains expression of the inhibitory receptor PD-1 and survival of antiviral CD8(+) T cells during chronic infection. *Immunity, 41*(5), 802-814. doi:10.1016/j.immuni.2014.10.013

Stathopoulou, C., Gangaplara, A., Mallett, G., Flomerfelt, F. A., Liniany, L. P., Knight, D., . . . Amarnath, S. (2018). PD-1 Inhibitory Receptor Downregulates Asparaginyl Endopeptidase and Maintains Foxp3 Transcription Factor Stability in Induced Regulatory T Cells. *Immunity, 49*(2), 247-263.e247. doi:10.1016/j.immuni.2018.05.006

Stephens, N. A., Skipworth, R. J., Gallagher, I. J., Greig, C. A., Guttridge, D. C., Ross, J. A., & Fearon, K. C. (2015). Evaluating potential biomarkers of cachexia and survival in skeletal muscle of upper gastrointestinal cancer patients. *J Cachexia Sarcopenia Muscle, 6*(1), 53-61. doi:10.1002/jcsm.12005

Stitt, T. N., Drujan, D., Clarke, B. A., Panaro, F., Timofeyva, Y., Kline, W. O., . . . Glass, D. J. (2004). The IGF-1/PI3K/Akt pathway prevents expression of muscle atrophy-induced ubiquitin ligases by inhibiting FOXO transcription factors. *Mol Cell, 14*(3), 395-403. doi:10.1016/s1097-2765(04)00211-4

Stittrich, A. B., Haftmann, C., Sgouroudis, E., Kühl, A. A., Hegazy, A. N., Panse, I., . . . Mashreghi, M. F. (2010). The microRNA miR-182 is induced by IL-2 and promotes clonal expansion of activated helper T lymphocytes. *Nat Immunol, 11*(11), 1057-1062. doi:10.1038/ni.1945

Strassmann, G., Fong, M., Kenney, J. S., & Jacob, C. O. (1992). Evidence for the involvement of interleukin 6 in experimental cancer cachexia. *J Clin Invest, 89*(5), 1681-1684. doi:10.1172/jci115767

Strassmann, G., Masui, Y., Chizzonite, R., & Fong, M. (1993). Mechanisms of experimental cancer cachexia. Local involvement of IL-1 in colon-26 tumor. *J Immunol, 150*(6), 2341-2345.

Strissel, K. J., DeFuria, J., Shaul, M. E., Bennett, G., Greenberg, A. S., & Obin, M. S. (2010). T-cell recruitment and Th1 polarization in adipose tissue during diet-induced obesity in C57BL/6 mice. *Obesity (Silver Spring), 18*(10), 1918-1925. doi:10.1038/oby.2010.1

Su, X., Ye, J., Hsueh, E. C., Zhang, Y., Hoft, D. F., & Peng, G. (2010). Tumor microenvironments direct the recruitment and expansion of human Th17 cells. *J Immunol, 184*(3), 1630-1641. doi:10.4049/jimmunol.0902813

Su, X., Yu, Y., Zhong, Y., Giannopoulou, E. G., Hu, X., Liu, H., . . . Ivashkiv, L. B. (2015). Interferon-γ regulates cellular metabolism and mRNA translation to potentiate macrophage activation. *Nat Immunol, 16*(8), 838-849. doi:10.1038/ni.3205

Sung, H., Ferlay, J., Siegel, R. L., Laversanne, M., Soerjomataram, I., Jemal, A., & Bray, F. (2021). Global cancer statistics 2020: GLOBOCAN estimates of incidence and mortality worldwide for 36 cancers in 185 countries. *CA Cancer J Clin*. doi:10.3322/caac.21660

Suriben, R., Chen, M., Higbee, J., Oeffinger, J., Ventura, R., Li, B., . . . Allan, B. B. (2020). Antibody-mediated inhibition of GDF15-GFRAL activity reverses cancer cachexia in mice. *Nat Med, 26*(8), 1264-1270. doi:10.1038/s41591-020-0945-x

Swamy, M., Pathak, S., Grzes, K. M., Damerow, S., Sinclair, L. V., van Aalten, D. M., & Cantrell, D. A. (2016). Glucose and glutamine fuel protein O-GlcNAcylation to control T cell self-renewal and malignancy. *Nat Immunol, 17*(6), 712-720. doi:10.1038/ni.3439

Talbert, E. E., Metzger, G. A., He, W. A., & Guttridge, D. C. (2014). Modeling human cancer cachexia in colon 26 tumor-bearing adult mice. *J Cachexia Sarcopenia Muscle, 5*(4), 321-328. doi:10.1007/s13539-014-0141-2

Tallima, H., Azzazy, H. M. E., & El Ridi, R. (2021). Cell surface sphingomyelin: key role in cancer initiation, progression, and immune evasion. *Lipids Health Dis, 20*(1), 150. doi:10.1186/s12944-021-01581-y

Tanaka, Y., Eda, H., Tanaka, T., Udagawa, T., Ishikawa, T., Horii, I., . . . Taguchi, T. (1990). Experimental cancer cachexia induced by transplantable colon 26 adenocarcinoma in mice. *Cancer Res, 50*(8), 2290-2295.

Tang, Y., Zhou, J., Hooi, S. C., Jiang, Y. M., & Lu, G. D. (2018). Fatty acid activation in carcinogenesis and cancer development: Essential roles of long-chain acyl-CoA synthetases. *Oncol Lett, 16*(2), 1390-1396. doi:10.3892/ol.2018.8843

Tao, X., Constant, S., Jorritsma, P., & Bottomly, K. (1997). Strength of TCR signal determines the costimulatory requirements for Th1 and Th2 CD4+ T cell differentiation. *J Immunol, 159*(12), 5956-5963.

Tardif, N., Klaude, M., Lundell, L., Thorell, A., & Rooyackers, O. (2013). Autophagic-lysosomal pathway is the main proteolytic system modified in the skeletal muscle of esophageal cancer patients. *Am J Clin Nutr, 98*(6), 1485-1492. doi:10.3945/ajcn.113.063859

Tau, G. Z., Cowan, S. N., Weisburg, J., Braunstein, N. S., & Rothman, P. B. (2001). Regulation of IFN-gamma signaling is essential for the cytotoxic activity of CD8(+) T cells. *J Immunol, 167*(10), 5574-5582. doi:10.4049/jimmunol.167.10.5574

Taube, J. M. (2014). Unleashing the immune system: PD-1 and PD-Ls in the pre-treatment tumor microenvironment and correlation with response to PD-1/PD-L1 blockade. *Oncoimmunology, 3*(11), e963413. doi:10.4161/21624011.2014.963413

Taves, M. D., & Ashwell, J. D. (2020). Glucocorticoids in T cell development, differentiation and function. *Nat Rev Immunol*. doi:10.1038/s41577-020-00464-0

Taves, M. D., & Ashwell, J. D. (2021). Glucocorticoids in T cell development, differentiation and function. *Nat Rev Immunol, 21*(4), 233-243. doi:10.1038/s41577-020-00464-0

Taylor, K. M., Ray, D. W., & Sommer, P. (2016). Glucocorticoid receptors in lung cancer: new perspectives. *J Endocrinol, 229*(1), R17-28. doi:10.1530/joe-15-0496

Taylor, L. A., Arends, J., Hodina, A. K., Unger, C., & Massing, U. (2007). Plasma lyso-phosphatidylcholine concentration is decreased in cancer patients with weight loss and activated inflammatory status. *Lipids Health Dis, 6*, 17. doi:10.1186/1476-511x-6-17

Teilmann, A. C., Kalliokoski, O., Sørensen, D. B., Hau, J., & Abelson, K. S. (2014). Manual versus automated blood sampling: impact of repeated blood sampling on stress parameters and behavior in male NMRI mice. *Lab Anim, 48*(4), 278-291. doi:10.1177/0023677214541438

Teunissen, S. C., Wesker, W., Kruitwagen, C., de Haes, H. C., Voest, E. E., & de Graeff, A. (2007). Symptom prevalence in patients with incurable cancer: a systematic review. *J Pain Symptom Manage, 34*(1), 94-104. doi:10.1016/j.jpainsymman.2006.10.015

Thapa, P., & Farber, D. L. (2019). The Role of the Thymus in the Immune Response. *Thorac Surg Clin, 29*(2), 123-131. doi:10.1016/j.thorsurg.2018.12.001

Thelemann, C., Eren, R. O., Coutaz, M., Brasseit, J., Bouzourene, H., Rosa, M., . . . Acha-Orbea, H. (2014). Interferon-γ induces expression of MHC class II on intestinal epithelial cells and protects mice from colitis. *PLoS One, 9*(1), e86844. doi:10.1371/journal.pone.0086844

Théry, C., & Amigorena, S. (2001). The cell biology of antigen presentation in dendritic cells. *Curr Opin Immunol, 13*(1), 45-51. doi:10.1016/s0952-7915(00)00180-1

Thoma, O. M., Neurath, M. F., & Waldner, M. J. (2021). T Cell Aging in Patients with Colorectal Cancer-What Do We Know So Far? *Cancers (Basel), 13*(24). doi:10.3390/cancers13246227

Thompson, M. P., Cooper, S. T., Parry, B. R., & Tuckey, J. A. (1993). Increased expression of the mRNA for hormone-sensitive lipase in adipose tissue of cancer patients. *Biochim Biophys Acta, 1180*(3), 236-242. doi:10.1016/0925-4439(93)90044-2

Timmermans, S., Souffriau, J., & Libert, C. (2019). A General Introduction to Glucocorticoid Biology. *Front Immunol, 10*, 1545. doi:10.3389/fimmu.2019.01545

Tisdale, M. J. (2002). Cachexia in cancer patients. *Nat Rev Cancer, 2*(11), 862-871. doi:10.1038/nrc927

Tisdale, M. J., & Beck, S. A. (1991). Inhibition of tumour-induced lipolysis in vitro and cachexia and tumour growth in vivo by eicosapentaenoic acid. *Biochem Pharmacol, 41*(1), 103-107. doi:10.1016/0006-2952(91)90016-x

Todorov, P. T., Field, W. N., & Tisdale, M. J. (1999). Role of a proteolysis-inducing factor (PIF) in cachexia induced by a human melanoma (G361). *Br J Cancer, 80*(11), 1734-1737. doi:10.1038/sj.bjc.6690590

Todorov, P. T., McDevitt, T. M., Meyer, D. J., Ueyama, H., Ohkubo, I., & Tisdale, M. J. (1998). Purification and characterization of a tumor lipid-mobilizing factor. *Cancer Res, 58*(11), 2353-2358.

Togashi, Y., Shitara, K., & Nishikawa, H. (2019). Regulatory T cells in cancer immunosuppression - implications for anticancer therapy. *Nat Rev Clin Oncol, 16*(6), 356-371. doi:10.1038/s41571-019-0175-7

Torelli, G. F., Meguid, M. M., Moldawer, L. L., Edwards, C. K., 3rd, Kim, H. J., Carter, J. L., . . . Rossi Fanelli, F. (1999). Use of recombinant human soluble TNF receptor in anorectic tumor-bearing rats. *Am J Physiol, 277*(3), R850-855. doi:10.1152/ajpregu.1999.277.3.R850

Tosolini, M., Kirilovsky, A., Mlecnik, B., Fredriksen, T., Mauger, S., Bindea, G., . . . Galon, J. (2011). Clinical impact of different classes of infiltrating T cytotoxic and helper cells (Th1, th2, treg, th17) in patients with colorectal cancer. *Cancer Res, 71*(4), 1263-1271. doi:10.1158/0008-5472.Can-10-2907

Tracey, K. J., Wei, H., Manogue, K. R., Fong, Y., Hesse, D. G., Nguyen, H. T., . . . et al. (1988). Cachectin/tumor necrosis factor induces cachexia, anemia, and inflammation. *J Exp Med, 167*(3), 1211-1227. doi:10.1084/jem.167.3.1211

Truitt, K. E., Shi, J., Gibson, S., Segal, L. G., Mills, G. B., & Imboden, J. B. (1995). CD28 delivers costimulatory signals independently of its association with phosphatidylinositol 3-kinase. *J Immunol, 155*(10), 4702-4710.

Tsoli, M., Schweiger, M., Vanniasinghe, A. S., Painter, A., Zechner, R., Clarke, S., & Robertson, G. (2014). Depletion of white adipose tissue in cancer cachexia syndrome is associated with inflammatory signaling and disrupted circadian regulation. *PLoS One, 9*(3), e92966. doi:10.1371/journal.pone.0092966

Tsukamoto, H., Senju, S., Matsumura, K., Swain, S. L., & Nishimura, Y. (2015). IL-6-mediated environmental conditioning of defective Th1 differentiation dampens antitumour immune responses in old age. *Nat Commun, 6*, 6702. doi:10.1038/ncomms7702

Tumeh, P. C., Harview, C. L., Yearley, J. H., Shintaku, I. P., Taylor, E. J., Robert, L., . . . Ribas, A. (2014). PD-1 blockade induces responses by inhibiting adaptive immune resistance. *Nature, 515*(7528), 568-571. doi:10.1038/nature13954

Turner, D. C., Kondic, A. G., Anderson, K. M., Robinson, A. G., Garon, E. B., Riess, J. W., . . . Stone, J. A. (2018). Pembrolizumab Exposure-Response Assessments Challenged by Association of Cancer Cachexia and Catabolic Clearance. *Clin Cancer Res, 24*(23), 5841-5849. doi:10.1158/1078-0432.Ccr-18-0415

Turner, J. E. (2016). Is immunosenescence influenced by our lifetime "dose" of exercise? *Biogerontology, 17*(3), 581-602. doi:10.1007/s10522-016-9642-z

Ullman-Culleré, M. H., & Foltz, C. J. (1999). Body condition scoring: a rapid and accurate method for assessing health status in mice. *Lab Anim Sci, 49*(3), 319-323.

Urso, K., Alfranca, A., Martínez-Martínez, S., Escolano, A., Ortega, I., Rodríguez, A., & Redondo, J. M. (2011). NFATc3 regulates the transcription of genes involved in T-cell activation and angiogenesis. *Blood, 118*(3), 795-803. doi:10.1182/blood-2010-12-322701

Vacca, A., Felli, M. P., Farina, A. R., Martinotti, S., Maroder, M., Screpanti, I., . . . Gulino, A. (1992). Glucocorticoid receptor-mediated suppression of the interleukin 2 gene expression through impairment of the cooperativity between nuclear factor of activated T cells and AP-1 enhancer elements. *J Exp Med, 175*(3), 637-646. doi:10.1084/jem.175.3.637

Vaena, S., Chakraborty, P., Lee, H. G., Janneh, A. H., Kassir, M. F., Beeson, G., . . . Ogretmen, B. (2021). Aging-dependent mitochondrial dysfunction mediated by ceramide signaling inhibits antitumor T cell response. *Cell Rep, 35*(5), 109076. doi:10.1016/j.celrep.2021.109076

Van Den Eeckhout, B., Tavernier, J., & Gerlo, S. (2020). Interleukin-1 as Innate Mediator of T Cell Immunity. *Front Immunol, 11*, 621931. doi:10.3389/fimmu.2020.621931

van Panhuys, N., Klauschen, F., & Germain, R. N. (2014). T-cell-receptor-dependent signal intensity dominantly controls CD4(+) T cell polarization In Vivo. *Immunity, 41*(1), 63-74. doi:10.1016/j.immuni.2014.06.003

Vandamme, T. F. (2014). Use of rodents as models of human diseases. *J Pharm Bioallied Sci, 6*(1), 2-9. doi:10.4103/0975-7406.124301

Villarino, A. V., Kanno, Y., Ferdinand, J. R., & O'Shea, J. J. (2015). Mechanisms of Jak/STAT signaling in immunity and disease. *J Immunol, 194*(1), 21-27. doi:10.4049/jimmunol.1401867

von Haehling, S., & Anker, S. D. (2010). Cachexia as a major underestimated and unmet medical need: facts and numbers. *J Cachexia Sarcopenia Muscle, 1*(1), 1-5. doi:10.1007/s13539-010-0002-6

Von Roenn, J. H., Roth, E. L., & Craig, R. (1992). HIV-related cachexia: potential mechanisms and treatment. *Oncology, 49 Suppl 2*, 50-54. doi:10.1159/000227129

Voskoboinik, I., Whisstock, J. C., & Trapani, J. A. (2015). Perforin and granzymes: function, dysfunction and human pathology. *Nat Rev Immunol, 15*(6), 388-400. doi:10.1038/nri3839

Wang, B., Maile, R., Greenwood, R., Collins, E. J., & Frelinger, J. A. (2000). Naive CD8+ T cells do not require costimulation for proliferation and differentiation into cytotoxic effector cells. *J Immunol, 164*(3), 1216-1222. doi:10.4049/jimmunol.164.3.1216

Wang, Q., & Wu, H. (2018). T Cells in Adipose Tissue: Critical Players in Immunometabolism. *Front Immunol, 9*, 2509. doi:10.3389/fimmu.2018.02509

Wang, R., Dillon, C. P., Shi, L. Z., Milasta, S., Carter, R., Finkelstein, D., . . . Green, D. R. (2011). The transcription factor Myc controls metabolic reprogramming upon T lymphocyte activation. *Immunity, 35*(6), 871-882. doi:10.1016/j.immuni.2011.09.021

Wang, T., Marquardt, C., & Foker, J. (1976). Aerobic glycolysis during lymphocyte proliferation. *Nature, 261*(5562), 702-705. doi:10.1038/261702a0

Wang, Y., Chu, J., Yi, P., Dong, W., Saultz, J., Wang, Y., . . . Yu, J. (2018). SMAD4 promotes TGF-β-independent NK cell homeostasis and maturation and antitumor immunity. *J Clin Invest, 128*(11), 5123-5136. doi:10.1172/jci121227

Wang, Z., Zhao, C., Moya, R., & Davies, J. D. (2008). A novel role for CD4+ T cells in the control of cachexia. *J Immunol, 181*(7), 4676-4684. doi:10.4049/jimmunol.181.7.4676

Warburg, O. (1956). On the origin of cancer cells. *Science, 123*(3191), 309-314. doi:10.1126/science.123.3191.309

Watanabe, H., Numata, K., Ito, T., Takagi, K., & Matsukawa, A. (2004). Innate immune response in Th1- and Th2-dominant mouse strains. *Shock, 22*(5), 460-466. doi:10.1097/01.shk.0000142249.08135.e9

Watt, M. J., Barnett, A. C., Bruce, C. R., Schenk, S., Horowitz, J. F., & Hoy, A. J. (2012). Regulation of plasma ceramide levels with fatty acid oversupply: evidence that the liver detects and secretes de novo synthesised ceramide. *Diabetologia, 55*(10), 2741-2746. doi:10.1007/s00125-012-2649-3

Weber, J. S., D'Angelo, S. P., Minor, D., Hodi, F. S., Gutzmer, R., Neyns, B., . . . Larkin, J. (2015). Nivolumab versus chemotherapy in patients with advanced melanoma who progressed after anti-CTLA-4 treatment (CheckMate 037): a randomised, controlled, open-label, phase 3 trial. *Lancet Oncol, 16*(4), 375-384. doi:10.1016/s1470-2045(15)70076-8

Weber, J. S., O'Day, S., Urba, W., Powderly, J., Nichol, G., Yellin, M., . . . Hersh, E. (2008). Phase I/II study of ipilimumab for patients with metastatic melanoma. *J Clin Oncol, 26*(36), 5950-5956. doi:10.1200/jco.2008.16.1927

Webster, J. M. K., Ljap ;Hardy, R. S. ;Langen, R. C. J. (2020). Inflammation and Skeletal Muscle Wasting During Cachexia. *Front Physiol, 11*, 597675. doi:10.3389/fphys.2020.597675

Wherry, E. J., & Kurachi, M. (2015). Molecular and cellular insights into T cell exhaustion. *Nat Rev Immunol, 15*(8), 486-499. doi:10.1038/nri3862

Whisler, R. L., Beiqing, L., & Chen, M. (1996). Age-related decreases in IL-2 production by human T cells are associated with impaired activation of nuclear transcriptional factors AP-1 and NF-AT. *Cell Immunol, 169*(2), 185-195. doi:10.1006/cimm.1996.0109

White, J. P., Baynes, J. W., Welle, S. L., Kostek, M. C., Matesic, L. E., Sato, S., & Carson, J. A. (2011). The regulation of skeletal muscle protein turnover during the progression of cancer cachexia in the Apc(Min/+) mouse. *PLoS One, 6*(9), e24650. doi:10.1371/journal.pone.0024650

Wiedenmann, B., Malfertheiner, P., Friess, H., Ritch, P., Arseneau, J., Mantovani, G., . . . Von Hoff, D. (2008). A multicenter, phase II study of infliximab plus gemcitabine in pancreatic cancer cachexia. *J Support Oncol, 6*(1), 18-25.

Wilkes, E. A., Selby, A. L., Cole, A. T., Freeman, J. G., Rennie, M. J., & Khan, Z. H. (2011). Poor tolerability of thalidomide in end-stage oesophageal cancer. *Eur J Cancer Care (Engl), 20*(5), 593-600. doi:10.1111/j.1365-2354.2011.01255.x

Wofford, J. A., Wieman, H. L., Jacobs, S. R., Zhao, Y., & Rathmell, J. C. (2008). IL-7 promotes Glut1 trafficking and glucose uptake via STAT5-mediated activation of Akt to support T-cell survival. *Blood, 111*(4), 2101-2111. doi:10.1182/blood-2007-06-096297

Wu, H., Ghosh, S., Perrard, X. D., Feng, L., Garcia, G. E., Perrard, J. L., . . . Ballantyne, C. M. (2007). T-cell accumulation and regulated on activation, normal T cell expressed and secreted upregulation in adipose tissue in obesity. *Circulation, 115*(8), 1029-1038. doi:10.1161/circulationaha.106.638379

Wu, L. X., La Rose, J., Chen, L., Neale, C., Mak, T., Okkenhaug, K., . . . Rottapel, R. (2005). CD28 regulates the translation of Bcl-xL via the phosphatidylinositol 3-kinase/mammalian target of rapamycin pathway. *J Immunol, 174*(1), 180-194. doi:10.4049/jimmunol.174.1.180

Wu, Q., Liu, Y., Chen, C., Ikenoue, T., Qiao, Y., Li, C. S., . . . Zheng, P. (2011). The tuberous sclerosis complex-mammalian target of rapamycin pathway maintains the quiescence and survival of naive T cells. *J Immunol, 187*(3), 1106-1112. doi:10.4049/jimmunol.1003968

Wu, Q., Sun, S., Li, Z., Yang, Q., Li, B., Zhu, S., . . . Sun, S. (2019). Breast cancer-released exosomes trigger cancer-associated cachexia to promote tumor progression. *Adipocyte, 8*(1), 31-45. doi:10.1080/21623945.2018.1551688

Wu, T. D., Madireddi, S., de Almeida, P. E., Banchereau, R., Chen, Y. J., Chitre, A. S., . . . Grogan, J. L. (2020). Peripheral T cell expansion predicts tumour infiltration and clinical response. *Nature, 579*(7798), 274-278. doi:10.1038/s41586-020-2056-8

Wu, Z., Huang, X., Han, X., Li, Z., Zhu, Q., Yan, J., . . . Wang, Y. (2016). The chemokine CXCL9 expression is associated with better prognosis for colorectal carcinoma patients. *Biomed Pharmacother, 78*, 8-13. doi:10.1016/j.biopha.2015.12.021

Wysong, A., Couch, M., Shadfar, S., Li, L., Rodriguez, J. E., Asher, S., . . . Willis, M. S. (2011). NF-κB inhibition protects against tumor-induced cardiac atrophy in vivo. *Am J Pathol, 178*(3), 1059-1068. doi:10.1016/j.ajpath.2010.12.009

Xia, F., Qian, C. R., Xun, Z., Hamon, Y., Sartre, A. M., Formisano, A., . . . He, H. T. (2018). TCR and CD28 Concomitant Stimulation Elicits a Distinctive Calcium Response in Naive T Cells. *Front Immunol, 9*, 2864. doi:10.3389/fimmu.2018.02864

Xia, J. Y., Holland, W. L., Kusminski, C. M., Sun, K., Sharma, A. X., Pearson, M. J., . . . Scherer, P. E. (2015). Targeted Induction of Ceramide Degradation Leads to Improved Systemic Metabolism and Reduced Hepatic Steatosis. *Cell Metab, 22*(2), 266-278. doi:10.1016/j.cmet.2015.06.007

Xie, H., Heier, C., Meng, X., Bakiri, L., Pototschnig, I., Tang, Z., . . . Zechner, R. (2022). An immune-sympathetic neuron communication axis guides adipose tissue browning in cancer-associated cachexia. *Proc Natl Acad Sci U S A, 119*(9). doi:10.1073/pnas.2112840119

Xu, S., Chaudhary, O., Rodríguez-Morales, P., Sun, X., Chen, D., Zappasodi, R., . . . Kaech, S. M. (2021). Uptake of oxidized lipids by the scavenger receptor CD36 promotes lipid peroxidation and dysfunction in CD8(+) T cells in tumors. *Immunity, 54*(7), 1561-1577.e1567. doi:10.1016/j.immuni.2021.05.003

Yablonski, D., Kadlecek, T., & Weiss, A. (2001). Identification of a phospholipase C-gamma1 (PLC-gamma1) SH3 domain-binding site in SLP-76 required for T-cell receptor-mediated activation of PLC-gamma1 and NFAT. *Mol Cell Biol, 21*(13), 4208-4218. doi:10.1128/mcb.21.13.4208-4218.2001

Yancik, R. (1997). Cancer burden in the aged: an epidemiologic and demographic overview. *Cancer, 80*(7), 1273-1283.

Yang, K., Shrestha, S., Zeng, H., Karmaus, P. W., Neale, G., Vogel, P., . . . Chi, H. (2013). T cell exit from quiescence and differentiation into Th2 cells depend on Raptor-mTORC1-mediated metabolic reprogramming. *Immunity, 39*(6), 1043-1056. doi:10.1016/j.immuni.2013.09.015

Yasumoto, K., Mukaida, N., Harada, A., Kuno, K., Akiyama, M., Nakashima, E., . . . et al. (1995). Molecular analysis of the cytokine network involved in cachexia in colon 26 adenocarcinoma-bearing mice. *Cancer Res, 55*(4), 921-927.

Ye, J., Huang, X., Hsueh, E. C., Zhang, Q., Ma, C., Zhang, Y., . . . Peng, G. (2012). Human regulatory T cells induce T-lymphocyte senescence. *Blood, 120*(10), 2021-2031. doi:10.1182/blood-2012-03-416040

Ye, J., Ma, C., Hsueh, E. C., Dou, J., Mo, W., Liu, S., . . . Peng, G. (2014). TLR8 signaling enhances tumor immunity by preventing tumor-induced T-cell senescence. *EMBO Mol Med, 6*(10), 1294-1311. doi:10.15252/emmm.201403918

Ye, J., Ma, C., Hsueh, E. C., Eickhoff, C. S., Zhang, Y., Varvares, M. A., . . . Peng, G. (2013). Tumor-derived γδ regulatory T cells suppress innate and adaptive immunity through the induction of immunosenescence. *J Immunol, 190*(5), 2403-2414. doi:10.4049/jimmunol.1202369

Ye, J., & Peng, G. (2015). Controlling T cell senescence in the tumor microenvironment for tumor immunotherapy. *Oncoimmunology, 4*(3), e994398. doi:10.4161/2162402x.2014.994398

You, S., Ohmori, M., Pena, M. M., Nassri, B., Quiton, J., Al-Assad, Z. A., . . . Hrushesky, W. J. (2006). Developmental abnormalities in multiple proliferative tissues of Apc(Min/+) mice. *Int J Exp Pathol, 87*(3), 227-236. doi:10.1111/j.1365-2613.2006.00477.x

Yu, P., Lee, Y., Liu, W., Krausz, T., Chong, A., Schreiber, H., & Fu, Y. X. (2005). Intratumor depletion of CD4+ cells unmasks tumor immunogenicity leading to the rejection of late-stage tumors. *J Exp Med, 201*(5), 779-791. doi:10.1084/jem.20041684

Yue, F., Cheng, Y., Breschi, A., Vierstra, J., Wu, W., Ryba, T., . . . Ren, B. (2014). A comparative encyclopedia of DNA elements in the mouse genome. *Nature, 515*(7527), 355-364. doi:10.1038/nature13992

Zaki, M. H., Nemeth, J. A., & Trikha, M. (2004). CNTO 328, a monoclonal antibody to IL-6, inhibits human tumor-induced cachexia in nude mice. *Int J Cancer, 111*(4), 592-595. doi:10.1002/ijc.20270

Zanni, F., Vescovini, R., Biasini, C., Fagnoni, F., Zanlari, L., Telera, A., . . . Sansoni, P. (2003). Marked increase with age of type 1 cytokines within memory and effector/cytotoxic CD8+ T cells in humans: a contribution to understand the relationship between inflammation and immunosenescence. *Exp Gerontol, 38*(9), 981-987. doi:10.1016/s0531-5565(03)00160-8

Zappasodi, R., Merghoub, T., & Wolchok, J. D. (2018). Emerging Concepts for Immune Checkpoint Blockade-Based Combination Therapies. *Cancer Cell, 33*(4), 581-598. doi:10.1016/j.ccell.2018.03.005

Zhang, H., Li, X., Huang, X., Li, J., Ma, H., & Zeng, R. (2021). Impact of corticosteroid use on outcomes of non-small-cell lung cancer patients treated with immune checkpoint inhibitors: A systematic review and meta-analysis. *J Clin Pharm Ther, 46*(4), 927-935. doi:10.1111/jcpt.13469

Zhang, L., Tang, H., Kou, Y., Li, R., Zheng, Y., Wang, Q., . . . Jin, L. (2013). MG132-mediated inhibition of the ubiquitin-proteasome pathway ameliorates cancer cachexia. *J Cancer Res Clin Oncol, 139*(7), 1105-1115. doi:10.1007/s00432-013-1412-6

Zhang, W., Patil, S., Chauhan, B., Guo, S., Powell, D. R., Le, J., . . . Unterman, T. G. (2006). FoxO1 regulates multiple metabolic pathways in the liver: effects on gluconeogenic, glycolytic, and lipogenic gene expression. *J Biol Chem, 281*(15), 10105-10117. doi:10.1074/jbc.M600272200

Zhang, X., Zhang, H., Chen, L., Feng, Z., Gao, L., & Li, Q. (2019). TIGIT expression is upregulated in T cells and causes T cell dysfunction independent of PD-1 and Tim-3 in adult B lineage acute lymphoblastic leukemia. *Cell Immunol, 344*, 103958. doi:10.1016/j.cellimm.2019.103958

Zhang, Y., Reynolds, J. M., Chang, S. H., Martin-Orozco, N., Chung, Y., Nurieva, R. I., & Dong, C. (2009). MKP-1 is necessary for T cell activation and function. *J Biol Chem, 284*(45), 30815-30824. doi:10.1074/jbc.M109.052472

Zhao, C., & Davies, J. D. (2010). A peripheral CD4+ T cell precursor for naive, memory, and regulatory T cells. *J Exp Med, 207*(13), 2883-2894. doi:10.1084/jem.20100598

Zhao, C., Marrero, I., Narsale, A., Moya, R., & Davies, J. D. (2015). CD4(+) CD44(v.low) cells are unique peripheral precursors that are distinct from recent thymic emigrants and stem cell-like memory cells. *Cell Immunol, 296*(2), 106-114. doi:10.1016/j.cellimm.2015.04.002

Zhao, C., Wang, Z., Robertson, M. W., & Davies, J. D. (2008). Cachexia in the non-obese diabetic mouse is associated with CD4+ T-cell lymphopenia. *Immunology, 125*(1), 48-58. doi:10.1111/j.1365-2567.2008.02819.x

Zhao, W., Qin, W., Pan, J., Wu, Y., Bauman, W. A., & Cardozo, C. (2009). Dependence of dexamethasone-induced Akt/FOXO1 signaling, upregulation of MAFbx, and protein catabolism upon the glucocorticoid receptor. *Biochem Biophys Res Commun, 378*(3), 668-672. doi:10.1016/j.bbrc.2008.11.123

Zhao, Y., Shao, Q., & Peng, G. (2020). Exhaustion and senescence: two crucial dysfunctional states of T cells in the tumor microenvironment. *Cell Mol Immunol, 17*(1), 27-35. doi:10.1038/s41423-019-0344-8

Zheng, C., Zheng, L., Yoo, J. K., Guo, H., Zhang, Y., Guo, X., . . . Zhang, Z. (2017). Landscape of Infiltrating T Cells in Liver Cancer Revealed by Single-Cell Sequencing. *Cell, 169*(7), 1342-1356.e1316. doi:10.1016/j.cell.2017.05.035

Zheng, W., & Flavell, R. A. (1997). The transcription factor GATA-3 is necessary and sufficient for Th2 cytokine gene expression in CD4 T cells. *Cell, 89*(4), 587-596. doi:10.1016/s0092-8674(00)80240-8

Zhou, F. (2009). Molecular mechanisms of IFN-gamma to up-regulate MHC class I antigen processing and presentation. *Int Rev Immunol, 28*(3-4), 239-260. doi:10.1080/08830180902978120

Zou, W., & Restifo, N. P. (2010). T(H)17 cells in tumour immunity and immunotherapy. *Nat Rev Immunol, 10*(4), 248-256. doi:10.1038/nri2742

Zuijdgeest-van Leeuwen, S. D., van den Berg, J. W., Wattimena, J. L., van der Gaast, A., Swart, G. R., Wilson, J. H., & Dagnelie, P. C. (2000). Lipolysis and lipid oxidation in weight-losing cancer patients and healthy subjects. *Metabolism, 49*(7), 931-936. doi:10.1053/meta.2000.6740

7 ACKNOWLEDGEMENTS

Zuallererst möchte ich mich von ganzem Herzen bei Maria Rohm bedanken. Vielen Dank für deine Unterstützung, die Freiheit unkonventionellen Theorien zu folgen, die vielen wissenschaftlichen Diskussionen, dein Vertrauen und vor allem deine inspirierende Art. Ich freue mich schon auf die nächsten unlösbar erscheinenden Fragestellungen, die wir zusammen in Angriff nehmen.

Vielen Dank auch an Mauricio Berriel Diaz für das Engagement und die Unterstützung während meiner Doktorarbeit. Du warst ein super Ersatz-Betreuer – Danke!

Ein großer Dank gebührt auch Prof. Dr. Stephan Herzig. Vielen Dank für die kritischen Fragen und die anregenden Ideen, die zum Erfolg dieses Projektes beigetragen haben.

Auch möchte ich Prof. Dr. Angelika Schnieke für Ihre Unterstützung bei meinen TAC-Meetings, sowie für die Prüfung meiner Doktorarbeit danken. Danke auch, dass ich bei meiner Masterarbeit an Ihrem Lehrstuhl so viel Wichtiges lernen konnte, das mir das Leben als PhD Student leichter gemacht hat (danke hier auch an Beate Rieblinger, Andrea Fischer und Konrad Fischer).

Vielen Dank auch an alle (ehemaligen) Mitglieder des IDC – jeder von euch hat auf seine eigene Art und Weise zu dieser Arbeit beigetragen – DANKE!
Ganz besonderer Dank gilt hier Teresa, Miri und Dani für die unglaublich lustigen Mittagspausen, die vielen Erlebnisse und euer immer offenes Ohr. Elena – danke, dass du mich vor allem am Anfang so stark unterstützt hast, du immer für mich da bist, mich zum Lachen bringst und ich auf dich zählen kann. Das weiß ich sehr zu schätzen. Auch Quirin Rein(H)old möchte ich für die viele Hilfe und die lustigen Diskussionen über Gott und die Welt danken – es war mir eine Freude mit dir zusammen zu arbeiten. Des Weiteren möchte ich mich bei Lisa Mehr, Jeanette Biebl und Andrea Takacs bedanken.

Ein großes Danke geht auch an meine Gruppe TCT sowie an die Gruppe MAC. Danke für die Unterstützung, die vielen Diskussionen und die Hilfe bei schwierigen, langwierigen Experimenten – ohne euch wäre Vieles nicht möglich gewesen. Speziell möchte ich hier Alina danken - für die vielen Diskussionen, meine Lieblingskaffeepausen, die Schokolade, wenn es mal nicht so lief wie geplant und vor allem deine Freundschaft. Special thanks to Raúl Terrón Expósito – thank you for being the organizing fairy in our lab, always knowing everything and most of all for all your support! Gracias my furry cat friend. Also thanks to Pauline for teaching me many things in the lab. Vielen Dank auch an Doris für die vielen gemeinsamen Wochenenden im Labor, deine Hilfsbereitschaft und deine lustige Art.

Vielen Dank auch an meine Studenten Madleen Biggel und Veronika Stadler für eure tatkräftige Unterstützung.

Hiermit möchte ich mich auch noch von ganzem Herzen bei Prof. Dr. Carolin Daniel und ihrem Labor bedanken. Diese Arbeit wäre ohne euch nicht möglich gewesen. Danke Carolin, dass du als T-Zell-Spezialistin mein Projekt kritisch betrachtet und mit spannenden Ideen verbessert hast. Danke auch dir Maike, für die vielen gemeinsamen Stunden am FACS, die Hilfe bei der Umsetzung zahlreicher T-Zell-Experimente, deine Unterstützung als ich mich zum ersten Mal in die Tiefen von FlowJo

Mic Drop.